

# *PSP/IS⊙IS Energetic Particle Data - User Guide*

Prepared by: Bala Poduval, Jonathan Niehof & Wouter de Wet  
Bala.Poduval@unh.edu; Jonathan.Niehof@unh.edu; Wouter.deWet@unh.edu

**Release Version – Release 16**

May 12, 2023

# Contents

<b>1</b>	<b>INTRODUCTION</b>	<b>1</b>
1.1	Terms of Use: IS $\odot$ IS Data	1
1.2	Release Notes	2
1.2.1	Release 1	2
1.2.2	Release 2	2
1.2.3	Release 3	3
1.2.4	Release 4	3
1.2.5	Release 5	4
1.2.6	Release 6	4
1.2.7	Release 7	4
1.2.8	Release 8	5
1.2.9	Release 9	6
1.2.10	Release 10	6
1.2.11	Release 11	7
1.2.12	Release 12	7
1.2.13	Release 13	8
1.2.14	Release 14	8
1.2.15	Release 15	9
1.2.16	Release 16	9
1.2.17	Release 17	9
1.3	Photon Contamination	9
1.3.1	Photons and Dust	10
1.3.2	Look Directions	10
1.3.3	Energy Ranges	10
1.3.4	Proxies	11
1.3.5	Summary	11
<b>2</b>	<b>SUMMARY: SCIENCE DATA</b>	<b>12</b>
2.1	Ephemeris and pointing	12
2.2	EPI-Lo Science Data	13
2.2.1	File: psp_isois-epilo_l2-ic	15
2.2.2	File: psp_isois-epilo_l2-pe	17
2.3	EPI-Hi Science Data	18
2.3.1	File: psp_isois-epihi_l2-het-rates10	18
2.3.2	File: psp_isois-epihi_l2-het-rates300	21
2.3.3	File: psp_isois-epihi_l2-het-rates3600	21
2.3.4	File: psp_isois-epihi_l2-het-rates60	30
2.3.5	File: psp_isois-epihi_l2-let1-rates10	38
2.3.6	File: psp_isois-epihi_l2-let1-rates300	39
2.3.7	File: psp_isois-epihi_l2-let1-rates3600	39
2.3.8	File: psp_isois-epihi_l2-let1-rates60	46
2.3.9	File: psp_isois-epihi_l2-let2-rates10	51
2.3.10	File: psp_isois-epihi_l2-let2-rates300	52

2.3.11	File: psp_isois-epihi_l2-let2-rates3600	52
2.3.12	File: psp_isois-epihi_l2-let2-rates60	57
2.3.13	File: psp_isois-epihi_l2-second-rates	61
2.4	IS $\odot$ IS Science Data	62
2.4.1	File: psp_isois-epihi_l2-second-rates	62
<b>3</b>	<b>DATA QUALITY FLAGS AND FILL</b>	<b>63</b>
3.1	Motivation	63
3.2	Quality flag structure	63
3.3	Existing categories	64
3.3.1	Warm up	64
3.3.2	Livetime	64
3.3.3	Pitch Angle Calculations	64
3.4	Fill values	64
<b>4</b>	<b>EPI-Lo DECODER RING</b>	<b>66</b>
<b>5</b>	<b>GENERAL LIST OF VARIABLES</b>	<b>69</b>
5.1	psp_isois-epihi_l2-het-rates10	69
5.2	psp_isois-epihi_l2-het-rates300	69
5.3	psp_isois-epihi_l2-het-rates3600	70
5.4	psp_isois-epihi_l2-het-rates60	73
5.5	psp_isois-epihi_l2-let1-rates10	76
5.6	psp_isois-epihi_l2-let1-rates300	76
5.7	psp_isois-epihi_l2-let1-rates3600	78
5.8	psp_isois-epihi_l2-let1-rates60	81
5.9	psp_isois-epihi_l2-let2-rates10	84
5.10	psp_isois-epihi_l2-let2-rates300	84
5.11	psp_isois-epihi_l2-let2-rates3600	85
5.12	psp_isois-epihi_l2-let2-rates60	87
5.13	psp_isois-epihi_l2-second-rates	88
5.14	psp_isois-epilo_l2-ic	89
5.15	psp_isois-epilo_l2-pe	91
5.16	psp_isois_l2-ephem	92
5.17	psp_isois_l2-summary	93
<b>6</b>	<b>CDF CONTENTS</b>	<b>94</b>
6.1	psp_isois-epilo_l2-ic	94
6.1.1	Primary variables	94
6.1.2	Other data	95
6.1.3	Other support	107
6.2	psp_isois-epilo_l2-pe	108
6.2.1	Primary variables	108
6.2.2	Other data	108
6.2.3	Other support	115

6.3	psp_isois-epihi_l2-het-rates10	116
6.3.1	Primary variables	116
6.3.2	Other data	117
6.3.3	Other support	121
6.4	psp_isois-epihi_l2-het-rates300	121
6.4.1	Primary variables	121
6.4.2	Other data	121
6.4.3	Other support	125
6.5	psp_isois-epihi_l2-het-rates3600	126
6.5.1	Primary variables	126
6.5.2	Other data	127
6.5.3	Other support	147
6.6	psp_isois-epihi_l2-het-rates60	147
6.6.1	Primary variables	147
6.6.2	Other data	149
6.6.3	Other support	163
6.7	psp_isois-epihi_l2-let1-rates10	163
6.7.1	Primary variables	163
6.7.2	Other data	164
6.7.3	Other support	167
6.8	psp_isois-epihi_l2-let1-rates300	168
6.8.1	Primary variables	168
6.8.2	Other data	168
6.8.3	Other support	175
6.9	psp_isois-epihi_l2-let1-rates3600	175
6.9.1	Primary variables	175
6.9.2	Other data	177
6.9.3	Other support	198
6.10	psp_isois-epihi_l2-let1-rates60	198
6.10.1	Primary variables	198
6.10.2	Other data	200
6.10.3	Other support	216
6.11	psp_isois-epihi_l2-let2-rates10	216
6.11.1	Primary variables	217
6.11.2	Other data	217
6.11.3	Other support	219
6.12	psp_isois-epihi_l2-let2-rates300	219
6.12.1	Primary variables	220
6.12.2	Other data	220
6.12.3	Other support	223
6.13	psp_isois-epihi_l2-let2-rates3600	224
6.13.1	Primary variables	224
6.13.2	Other data	225
6.13.3	Other support	236
6.14	psp_isois-epihi_l2-let2-rates60	236

6.14.1	Primary variables	236
6.14.2	Other data	237
6.14.3	Other support	245
6.15	psp_isois-epihi_l2-second-rates	246
6.15.1	Primary variables	246
6.15.2	Other data	246
6.15.3	Other support	252
6.16	psp_isois_l2-ephem	253
6.16.1	Primary variables	253
6.16.2	Other data	253
6.16.3	Other support	255
6.17	psp_isois_l2-summary	255
6.17.1	Primary variables	256
6.17.2	Other data	256
6.17.3	Other support	256

**7 ACRONYMS** **257**

**REFERENCES** **257**

**List of Tables**

2.2.1	psp_isois-epilo_l2-ic	15
2.2.2	psp_isois-epilo_l2-pe	17
2.3.1	psp_isois-epihi_l2-het-rates10	20
2.3.2	psp_isois-epihi_l2-het-rates300	21
2.3.3	psp_isois-epihi_l2-het-rates3600	22
2.3.4	psp_isois-epihi_l2-het-rates3600 contd	23
2.3.5	psp_isois-epihi_l2-het-rates3600 contd	23
2.3.6	psp_isois-epihi_l2-het-rates3600 contd	24
2.3.7	psp_isois-epihi_l2-het-rates3600 contd	25
2.3.8	psp_isois-epihi_l2-het-rates3600 contd	26
2.3.9	psp_isois-epihi_l2-het-rates3600 contd	27
2.3.10	psp_isois-epihi_l2-het-rates3600 contd	28
2.3.11	psp_isois-epihi_l2-het-rates3600 contd	29
2.3.12	psp_isois-epihi_l2-het-rates60	30
2.3.13	psp_isois-epihi_l2-het-rates60 contd	31
2.3.14	psp_isois-epihi_l2-het-rates60 contd	31
2.3.15	psp_isois-epihi_l2-het-rates60 contd	32
2.3.16	psp_isois-epihi_l2-het-rates60 contd	33
2.3.17	psp_isois-epihi_l2-het-rates60 contd	34
2.3.18	psp_isois-epihi_l2-het-rates60 contd	35
2.3.19	psp_isois-epihi_l2-het-rates60 contd	36
2.3.20	psp_isois-epihi_l2-het-rates60 contd	37
2.3.21	psp_isois-epihi_l2-let1-rates10	38

2.3.22	psp_isois-epihi_l2-let1-rates300	39
2.3.23	psp_isois-epihi_l2-let1-rates3600	40
2.3.24	psp_isois-epihi_l2-let1-rates3600 contd	40
2.3.25	psp_isois-epihi_l2-let1-rates3600 contd	41
2.3.26	psp_isois-epihi_l2-let1-rates3600 contd	42
2.3.27	psp_isois-epihi_l2-let1-rates3600 contd	43
2.3.28	psp_isois-epihi_l2-let1-rates3600 contd	43
2.3.29	psp_isois-epihi_l2-let1-rates3600 contd	44
2.3.30	psp_isois-epihi_l2-let1-rates3600 contd	44
2.3.31	psp_isois-epihi_l2-let1-rates3600 contd	44
2.3.32	psp_isois-epihi_l2-let1-rates3600 contd	45
2.3.33	psp_isois-epihi_l2-let1-rates60	46
2.3.34	psp_isois-epihi_l2-let1-rates60 contd	47
2.3.35	psp_isois-epihi_l2-let1-rates60 contd	47
2.3.36	psp_isois-epihi_l2-let1-rates60 contd	48
2.3.37	psp_isois-epihi_l2-let1-rates60 contd	48
2.3.38	psp_isois-epihi_l2-let1-rates60 contd	49
2.3.39	psp_isois-epihi_l2-let1-rates60 contd	50
2.3.40	psp_isois-epihi_l2-let2-rates10	51
2.3.41	psp_isois-epihi_l2-let2-rates300	52
2.3.42	psp_isois-epihi_l2-let2-rates3600	53
2.3.43	psp_isois-epihi_l2-let2-rates3600 contd	53
2.3.44	psp_isois-epihi_l2-let2-rates3600 contd	54
2.3.45	psp_isois-epihi_l2-let2-rates3600 contd	55
2.3.46	psp_isois-epihi_l2-let2-rates3600 contd	55
2.3.47	psp_isois-epihi_l2-let2-rates3600 contd	56
2.3.48	psp_isois-epihi_l2-let2-rates3600 contd	56
2.3.49	psp_isois-epihi_l2-let2-rates3600 contd	57
2.3.50	psp_isois-epihi_l2-let2-rates60	57
2.3.51	psp_isois-epihi_l2-let2-rates60 contd	58
2.3.52	psp_isois-epihi_l2-let2-rates60 contd	58
2.3.53	psp_isois-epihi_l2-let2-rates60 contd	59
2.3.54	psp_isois-epihi_l2-let2-rates60 contd	59
2.3.55	psp_isois-epihi_l2-let2-rates60 contd	60
2.3.56	psp_isois-epihi_l2-let2-rates60 contd	60
2.3.57	psp_isois-epihi_l2-second-rates	61

## List of Figures

1	EPI-Lo Instrument	14
2	EPI-Lo Skymap	16
3	EPI-Hi Instrument & FOV	19
4	EPI-Lo Decoder Ring for LUT Regime 0 to 5.	67
5	EPI-Lo Decoder Ring for LUT Regime 6 to present.	68

# *PSP/IS⊙IS Energetic Particle Data - User Guide*

August 25, 2023

## **1 INTRODUCTION**

This user guide contains detailed information on the various quantities measured by the Integrated Science Investigation of the Sun (IS⊙IS) instrument suite on board the Parker Solar Probe (PSP) and how to access them from the data repository. These are the Level 2 data from the EPI-Lo (Energetic Particle Instrument - Low Energy) and EPI-Hi (Energetic Particle Instrument - High Energy) instruments. This document is divided into seven sections, including this introduction and references. Also included in the Introduction is an account of photon contamination (§ 1.3). The terms of using the PSP/IS⊙IS data is presented in § 1.1. The various properties of the solar energetic particles detected in a wide range of energies and the associated attributes such as cadence, energy bins, look directions and sectors in each CDF file that are useful for science analysis are tabulated and presented in § 2. All the variables currently available in the data repository for the scientific community are listed in § 5 and § 6 consists of a compilation of all the information of the variables from the metadata in each CDF file. The variables listed in § 5 are dynamically linked to their detailed descriptions in § 6. The EPI-Lo Decoder Ring is presented in § 4 and a list acronyms in § 7, followed by References.

### **1.1 TERMS OF USE: IS⊙IS DATA**

Production of Integrated Science Investigation of the Sun (IS⊙IS) data is funded as part of NASA's Parker Solar Probe mission under contract NNN06AA01C. Use of any IS⊙IS data should include the following acknowledgement and also refer to the publication provided below.

#### **Acknowledgement:**

“Thanks to the Integrated Science Investigation of the Sun (IS⊙IS) Science Team (PI: David McComas, Princeton University).”

#### **Reference Publication:**

McComas, D. J. et al. (2016), Integrated Science Investigation of the Sun (IS⊙IS): Design of the Energetic Particle Investigation, Space Science Reviews, 204, 187–256, doi:10.1007/s11214-014-0059-1.

## 1.2 RELEASE NOTES

### 1.2.1 RELEASE 1

Released 2019-11-15.

Proper analysis of this first release of the data requires knowledge of several caveats and possible instrumental effects.

- Pitch angles are using preliminary calibrations from the FIELDS magnetic field instrument. This may result in errors in pitch angle determination up to about 1.5 degrees.
- EPI-Hi and EPI-Lo data use different units for energies and thus for fluxes. EPI-Hi data are reported MeV for protons and electrons, and MeV/nuc for heavy ions. EPI-Lo uses keV for all species except for time-of-flight only data, which uses keV/nuc. These differences are important when combining data across the two sensors.
- Ions heavier than helium and electrons are likely to have substantial background, including from other species, and are thus provided as count rates only until commissioning of these species can be completed for inclusion in a future release.
- EPI-Hi data below approximately 2MeV may be subject to instrumental effects that are currently being quantified. At these energies, the incident energy may be under reported by as much as 10% and the flux may be underreported by as much as 30%.
- EPI-Hi hourly (3600) data is compiled on the hour according to the spacecraft clock. The first integration after turn-on may be substantially shorter than an hour depending on when turn-on occurred. This may result in poor counting statistics from a short integration and unrealistic spectra for this first integration. The same effect is present, but less apparent, for the first integration of shorter periods.
- Spacecraft position is provided for every timebase in a file. Position is in HCI (variable names starting with HCI\_R, HCI\_Lat, HCI\_Lon for each timebase) and HGC (names starting with HGC\_R, HGC\_Lat, HGC\_Lon). Particle flow direction for each look direction is provided as unit vectors in HCI and RTN, as well as pitch angle, also on every timebase; variable names start with HCI, RTN, and PA.

### 1.2.2 RELEASE 2

Released 2020-01-27.

This release extends the dataset through 2019-10-10 (after third encounter). Files included cover the entire mission; thus it supersedes release 1. Contact the SOC for access to release 1 data if needed for comparison.

- Pitch angles for 2019 use updated FIELDS calibrations. The 2018 pitch angles have not changed from release 1, as FIELDS calibrations from 2018 required no updating.
- The summary product (psp\_isois\_l2-summary) includes a new variable, A\_Heavy\_Rate\_TS. This is a total heavy-ion count rate from the EPI-Hi LET1A telescope.



### 1.2.3 RELEASE 3

Released 2020-04-14.

This release extends the dataset through 2020-01-06. This includes the end of Orbit 3 and beginning of Orbit 4, including Venus Flyby 2, but with no new encounter data. Files included cover the entire mission; thus it supersedes previous releases. Contact the SOC for access to release 1 and 2 data if needed for comparison.

- Much of the CDF metadata has been updated to provide better descriptions and make data easier to find. In particular, pitch angle and related pointing data are tagged as data rather than `support_data` to make them more visible in many tools. Variable names have not been changed.
- Updated calibration tables for EPI-Lo have been applied. This results in small (a few percent) changes in energy channels and fluxes throughout the mission.

### 1.2.4 RELEASE 4

Released 2020-08-04.

This release extends the dataset through 2020-04-29. This includes Encounter 4 and the rest of orbit 4. Files included cover the entire mission; thus this release supersedes all previous releases. Contact the SOC for access to release 1-3 data if needed for comparison.

- The EPI-Hi instrument was off for operational reasons from 2019-10-07 through 2020-02-12.
- Due to a dust impact on 2019-04-03 around 16:45Z, look direction 31 of the EPI-Lo TOF-only products (channel T) is highly susceptible to UV photon contamination after this time (see <http://dx.doi.org/10.3847/1538-4365/ab643d>). Release 3 removed calibrated fluxes for this look direction after this time. In release 4, L31 is also excluded from count rate products that are summed over look direction. This includes `H_CountRate_ChanT_SP` in `psp_isois_12-summary` and related quicklook plots. This exclusion is for all time, so that rates before and after the dust impact can be compared. Look directions 34 and 35, although they retain intact foils, can also be heavily contaminated by UV and are excluded from summed count rate products as well.
- During the EPI-Lo high voltage ramp-up immediately after turn-on (approximately 15 minutes), count rates and fluxes are not accurate measurements of the incident population. These periods have been filtered out from the flux and count rate variables.
- All pitch angle variables now have a corresponding “spiral angle” variable, containing the angle the particle flow direction makes with the outward nominal Parker Spiral. “Nominal” is defined as  $400\text{km/s } v_{sw}$  with corotation breakdown at  $10R_S$ . For EPI-Lo, these variables are named like `SA_ChanX`; for EPI-Hi, names are similar to `LET1_A_SA` and `LET1_A_R1_SECT_SA` (for non-sectored and sectored rates, respectively.)
- Many small metadata updates have been made for greater clarity; variable names remain the same.

- EPI-Hi energy unit labeling is consistent (MeV/nuc for ions heavier than protons; MeV for all else) and all energy labels have consistent formatting.

### **1.2.5 RELEASE 5**

Released 2020-09-24.

This release includes data through 2020-04-29, with no additional dates since release 4. This includes Encounter 4 and the rest of orbit 4. Files included cover the entire mission; thus this release supersedes all previous releases. Contact the SOC for access to release 1-4 data if needed for comparison.

- Release 4 was made using the EPI-Lo calibration data from release 2; release 5 uses the latest calibration data. This results in small (a few percent) changes in energy channels and fluxes throughout the mission, similar to release 3.
- Release 4 also included fluxes for look direction 31 of the time-of-flight products after the dust impact on 2019-04-03; these fluxes are largely from UV photon contamination and should not be used. They are properly filtered from release 5.
- EPI-Hi data are the same as release 4, but the files are reproduced in release 5 to avoid confusion.
- IS $\odot$ IS summary data are largely the same as release 4, but may have small changes in energy channels in the variables related to EPI-Lo.

### **1.2.6 RELEASE 6**

Released 2020-11-16.

This release extends the dataset through 2020-08-13. This includes Encounter 5 and the rest of orbit 5. Files included cover the entire mission; thus this release supersedes all previous releases. Contact the SOC for access to release 1-5 data if needed for comparison.

- Data may include brief periods of counts generated internally to the instrument for calibration purposes. These will be filtered in a future release and are noted in the Data Anomalies & Quality list (<https://spp-isois.sr.unh.edu/Released-Data-Anomalies-and-Quality-Notes.html>).
- Pitch angles for the periods 2019 Jan through Aug and 2020 Jan through Feb were added for this release.

### **1.2.7 RELEASE 7**

Released 2021-04-05.

This release extends the dataset through 2021-01-04. This includes Encounter 6 and the rest of orbit 6. Files included cover the entire mission; thus this release supersedes all previous releases. Contact the SOC for access to release 1-6 data if needed for comparison.

- EPI-Hi LET electron count rate variables are now included. These match the naming scheme for the HET electron variables, e.g. `A_Electrons_Rate` is the count rate for electrons in LET1-A.
- Most quantities that are included as a count rate are now also reported as counts per integration, for those interested in performing their own statistical analysis. These variables have descriptions with simply “counts”, units of “counts”, and variable names with “Counts” or no specific notation. Examples are `A_H` for EPI-Hi A-side protons or `H_Counts_ChanP` for EPI-Lo triple-coincidence protons. Count rate variables have “Rate” or “CountRate” in the name, “count rate” in the description, and units of “counts/s”. Examples `A_H_Rate`; `H_CountRate_ChanP`. Count rates are properly corrected for instrument livetime; counts are not.
- EPI-Lo calibrations were updated based on observations from the large event of 29 November 2020. This is not the final calibration that will result from that event, but it is significant enough of an improvement that we are releasing it now.
  - Updated efficiencies were calculated for H, He, O, and Fe. These incorporate contributions from grid transmission fraction, scattering, and MCP detection efficiency. Updates primarily affect the ion composition triple coincidence channels P and C. The ion composition TOF-only channel T was corrected based on the updated channel P values.
  - Updated instrument geometric factors were calculated, including large-scale instrument geometry, not finer corrections such as grid transmission. Flat fielding corrections were calculated from a period of high isotropy (November 30, 2020 19:00 to December 1, 2020 02:00)
- Due to a dust impact on 2020-12-30 between 02:00 and 07:00Z (while EPI-Lo was off), look direction 35 of the EPI-Lo TOF-only products (channel T) is highly susceptible to UV photon contamination after this time. Release 7 removed calibrated fluxes for this look direction after this time. This look direction was excluded from look-averaged TOF-only products starting in release 3.
- The large event of 2020-11-30 through 2020-12-02 was the first event of the mission where EPI-Hi switched into operational modes for handling high rates. These modes have not been fully calibrated: count rate and flux data for this period should not be used without consulting the EPI-Hi team.

### 1.2.8 RELEASE 8

Released 2021-06-28.

This release extends the dataset through 2021-03-27. This includes Encounter 7 and the rest of orbit 7. Files included cover the entire mission; thus this release supersedes all previous releases. Contact the SOC for access to release 1-7 data if needed for comparison.

- The large event of 2020-11-30 through 2020-12-02 was the first event of the mission where EPI-Hi switched into operational modes for handling high rates. These modes have not been

fully calibrated: count rate and flux data for this period should not be used without consulting the EPI-Hi team.

### **1.2.9 RELEASE 9**

Released 2021-09-20.

This release contains data quality enhancements only and ends on 2021-03-27. Files included cover the entire mission; thus this release supersedes all previous releases. Contact the SOC for access to release 1-8 data if needed for comparison.

- EPI-Hi processing and calibrations have been improved for high rate periods, the most notable of which to date is the large event of 2020-11-30 through 2020-12-02.
  - Count rates and fluxes are corrected to account for the fraction of particle detections which are not fully processed by the flight software. This is described in more detail in the data user guide.
  - Calibrations for high rate operational modes have been updated. HET calibrations for dynamic threshold mode 1 are those used by Cohen et al. (2021, <https://doi.org/10.1051/0004-6361/202140967>). HET modes 2 and 3, and all high rate modes of LET1 and LET2, do not have mature calibrations at this time, so fluxes are not reported for the high rate modes.
- Minor adjustments to EPI-Lo telemetry processing may result in slightly higher (of order one percent) count rates and fluxes during active times.
- EPI-Lo ion composition (IC) files have new count rate variables for N and Ne, in anticipation of refined tracks for these species. These variables contain no records until the refined tracks are implemented on-orbit.
- Due to ongoing dust effects, several more look directions are excluded from the look-averaged TOF-only products in the summary file. The complete list is now 21, 24-29, 31, 34, 35, and 39.

### **1.2.10 RELEASE 10**

Released 2021-10-26.

This release extends the dataset through 2021-07-24. This includes all of orbit 8, including Encounter 8, and part of the inbound leg of orbit 9. Files included cover the entire mission; thus this release supersedes all previous releases. Contact the SOC for access to release 1-9 data if needed for comparison.

No changes have been made to the processing of the data; caveats remain the same.

- EPI-Lo species identification tables were updated on 2021-06-14. Ion composition (IC) files after this day will have records populated in the N and Ne count rate variables added in release 9.

### 1.2.11 RELEASE 11

Released 2022-02-07.

This release extends the dataset through 2021-11-04. This includes the rest of orbit 9, including Encounter 9, and part of the inbound leg of orbit 10, including Venus Flyby 5. Files included cover the entire mission; thus this release supersedes all previous releases. Contact the SOC for access to release 1-10 data if needed for comparison.

No changes have been made to the processing of the EPI-Hi data; caveats remain the same. The following updates have been made to EPI-Lo data.

- Updated EPI-Lo energy channel assignments and efficiencies for all species and energies before 14 June 2021, reflecting the imprecise on-board energy normalization that was in use at that time. The resulting energies are much more strongly dependent on look direction.
- Minor updates to the calculation of EPI-Lo livetimes, resulting in flux increases of order 1% in some circumstances.
- Corrected EPI-Lo energy assignments for electron channels after 14 June 2021 (release 10 erroneously used development tables which were not uploaded).

### 1.2.12 RELEASE 12

Released 2022-04-25.

This release extends the dataset through 2022-01-23. This includes the rest of orbit 10, including Encounter 10, and part of the inbound leg of orbit 11. Files included cover the entire mission; thus this release supersedes all previous releases. Contact the SOC for access to release 1-11 data if needed for comparison.

The following changes and caveats apply to both EPI-Hi and EPI-Lo data, or to IS $\odot$ IS suite products:

- H\_CountRate\_ChanT-related variables have been removed from the psp\_isois\_l2-summary files, as these time-of-flight only rates contain substantial background. They have been replaced with H\_CountRate\_ChanP-derived variables, containing protons with a triple coincidence (TOFxE) requirement. These contain all look directions and a similar energy range to the previous ChanT variables. As a reminder, these summary files are intended to support high-level surveys for periods of interest and should not be used for science analysis.
- Pitch angles are not available after 2021-12-31.

The following changes apply to EPI-Hi:

- Calibrations for high rate operational modes have been updated. HET calibrations H and He for dynamic threshold mode 1 have been updated; initial LET calibrations are included for H and He in dynamic threshold mode 1.

- HET calibrations for H and He in dynamic threshold mode 0 (the normal mode for the lowest count rates) have been updated to account for the non-flat response of the instrument.
- Processing of the data at EPI-Hi dynamic threshold changes has been updated to ensure proper timing of the transition.

No changes have been made to processing of the EPI-Lo data.

### **1.2.13 RELEASE 13**

Release 2022-08-01.

This release extends the dataset through 2022-04-29. This includes the rest of orbit 11, including Encounter 11, and part of the inbound leg of orbit 12. Files included cover the entire mission; thus this release supersedes all previous releases. Contact the SOC for access to release 1-12 data if needed for comparison.

- Pitch angles are included for all times where FIELDS data are available, including times omitted in release 12.
- EPI-Lo calibrations have been updated for apertures with thick entrance foils (L23, L30–L33, L40). The energy binning for these look directions is substantially different from others, particularly at lower energies, and care should be used when combining data from multiple look directions.

### **1.2.14 RELEASE 14**

Release 2022-11-14.

This release extends the dataset through 2022-08-15. This includes the rest of orbit 12, including Encounter 12, and part of the inbound leg of orbit 13. Files included cover the entire mission; thus this release supersedes all previous releases. Contact the SOC for access to release 1-13 data if needed for comparison.

- EPI-Lo livetime calculations have been updated to better account for quadrant-specific dead-time effects. This will have little effect on fluxes averaged over all apertures; however, quadrant 1 (look directions 20–39) fluxes and count rates may be increased with a smaller decrease in all other quadrants. This effect is most pronounced for high-rate periods and may reach a 50% effect in quadrant 1.
- EPI-Lo underwent two tests characterizing instrument performance leading up to and during the first portion of encounter 12. During these tests, the data in quadrant 1 are not entirely of science quality. The fluxes have been replaced with fill values and count rates should not be used. Tests were run 2022-05-24T16:13:09 through 2022-05-29T16:13:09 and 2022-05-30T11:50:08 through 2022-06-04T11:50:08. Future work may recover some quadrant 1 science data from this period.

No changes have been made to the processing of the EPI-Hi data.

### 1.2.15 RELEASE 15

Release 2023-02-20.

This release extends the dataset through 2022-11-14. This includes the rest of orbit 13, including Encounter 13, and part of the inbound leg of orbit 14. Files included cover the entire mission; thus this release supersedes all previous releases. Contact the SOC for access to release 1-14 data if needed for comparison.

No changes have been made to the processing of the IS $\odot$ IS data.

### 1.2.16 RELEASE 16

Release 2023-05-12.

This release extends the dataset through 2023-02-09. This includes the rest of orbit 14, including Encounter 14, and part of the inbound leg of orbit 15. Files included cover the entire mission; thus this release supersedes all previous releases. Contact the SOC for access to release 1-15 data if needed for comparison.

- Relative to release 15, pitch angle tags for the period 2022-09-22 through 2022-11-14 were added; they are included for the entire release (through 2023-02-09).
- To avoid an instrument overcurrent condition, EPI-Lo raised thresholds during periods of high rates. This happened on 2022-12-11 from 8:20:40 through 8:45:40. Data in look directions 40 – 59 are not science quality during this period and fluxes have been replaced with fill.

No other changes have been made to the processing of the IS $\odot$ IS data. There are no updates to the IS $\odot$ IS event list.

### 1.2.17 RELEASE 17

Release 2023-08-27.

This release extends the dataset through 2023-06-04. This includes the rest of orbit 15, including Encounter 15, and part of the inbound leg of orbit 16. Files included cover the entire mission; thus this release supersedes all previous releases. Contact the SOC for access to release 1-16 data if needed for comparison.

- EPI-Lo and EPI-Hi data have new variables with quality flags; these variables and their interpretation are described in section 3.
- EPI-Lo data have been updated with improved geometric factors for the “particle” SSD; this affects the calibration of the TOF-only (T) flux.

## 1.3 PHOTON CONTAMINATION

EPI-Lo was designed to investigate the physics of energetic particles, however in the special lowest-energy “time-of-flight only” product used in this study, it also responds to solar photons in a subset of approximately sunward-looking apertures lacking special light-attenuating foils. This topic is discussed in detail by [Hill et al. \(2019\)](#) but we provide some details here.

### 1.3.1 PHOTONS AND DUST

The EPI-Lo design is robust against the detrimental effects of ambient dust or light entering any of EPI-Lo's eighty apertures. The mitigation for light contamination includes employing thicker start foils in the six look directions dominated by photospheric light that is Thomson scattering off electrons near the Sun, and thus visible away from the solar disk where there is no shielding from PSP's thermal protection system (TPS). In addition to thicker foils, we employ baffles and multiple coincidence logic to cut down photon contamination. Also, to protect against dust and resulting dust-hole-admitted light, an extra "collimator foil" was added to all collimator turrets so that pinholes from dust impacts either penetrate only the collimator foil (for the smallest dust grains  $\leq 100$  nm) or only admit light from very tiny solid angles where these holes line up, resulting in a greatly reduced geometry factor for post-impact light contamination than would occur with only one foil. The first dust impact directly detectable by EPI-Lo (i.e., an impact resulting in noticeable light-admitting damage) took place after the second perihelion on 2019-04-03 (DOY 093) 16:45 in the L31 direction (see Figure 2 for description of EPI-Lo look directions). This L31 hole resulted in elevated photon background in one look direction but at a level that has not diminish EPI-Lo's scientific capabilities. This dust impact is discussed in more detail by [Szalay et al. \(2019\)](#).

A second dust impact occurred in the L35 direction on 2020-12-30 (DOY 365) sometime between 02:00 and 07:00 when the instrument was off. This hole is larger than the L31 hole and is under current investigation.

During Orbit 8, two more dust impacts were detected. L55 on 2021-04-19 12:00 and L21 on 2021-04-27 18:29. TOF-only products have increased in noise, but triple-coincidence products are not impacted by photon contamination.

### 1.3.2 LOOK DIRECTIONS

We divided the field of view (FOV) into three independent sets of look directions: the generally sunward-looking Bright Look directions with very clear photon viewing (composed of the look directions L22, L25, L34-L37, L44, and L46); the Dim Look directions surrounding the bright area, where there are reduced indications of photons (composed of look directions L24, L26, L27, L41, L45, L47); and the Dark Look direction region, where there is no strong sign of photons (composed of the apertures that are neither the bright look direction or the dim look direction lists and which are mostly composed of wedges W0, W1, and W5-W7, which look away from the Sun). Explicitly, the list of dark look directions is L00-L21, L23, L28-L33, L38-L40, L42, L43, and L48-L79, with the sum of the Bright, Dim, and Dark look directions incorporating all 80 apertures. Although the bright look directions are roughly those most directed at the Sun, an important distinction is that the six apertures closest to the Sun with thicker light-blocking start foils (L23, L30-L33, and L40) are not included in the bright FOV or dim FOV because the thick foils effectively block the scattered light.

### 1.3.3 ENERGY RANGES

In addition to the division of the FOV, the energy channels are also split into three independent ranges: Low Energy (channels T030 and T031, 1-4 keV/nuc detected energy, based on the TOF measurement, corresponding to incident energies below 34 keV when H is assumed), where accidentals dominate during quiet times; Medium Energy (channels T016-T029, 4-350 keV/nuc de-



tected and 34–370 keV for incident H), where foreground ion measurements are the strongest; and High Energy (channels T001–T015, 350 keV/nuc – 37 MeV/nuc detected and 370 keV – 39 MeV for incident H), where crosstalk events dominate during quiet times. Although the upper energy limit is high, no ions were detected above a few hundred keV/nuc (confirmed by EPI-Hi observations). The reason that accidental coincidences are associated with lower energy intensifications is because randomly distributed start and stop events that accidentally satisfy the TOF logic result in a flat distribution in TOF-space, but because of the inverse square relationship between energy and TOF, a large fraction of the longer end of the TOF range corresponds to a small, low-energy range of energies.

#### **1.3.4 PROXIES**

With these definitions we found that a good proxy for the clean ion signal is found by combining Low Energy/Dark Look Directions, Medium-Energy/Dim Look Directions, and Medium-Energy/Dark Look Directions and a good proxy for photon contamination is the Low-Energy/Bright Look Direction measurements. That is, Ion Proxy = Low Dark + Medium Dim + Medium Dark and Photon Proxy = Low Bright.

#### **1.3.5 SUMMARY**

EPI-Lo measures ion intensity, energy, composition, and anisotropy, by design, and also responds to photons that are most likely scattered by zodiacal dust. Utilizing thicker start foils to suppress photon contamination unfortunately degrades low–energy ion response, so this mitigation was used sparingly; consequently, there are several generally sunward apertures with thin start foils where photons produce backgrounds, mostly through accidental coincidence of uncorrelated transmitted photon start and stop triggers. The result is that EPI-Lo responds to SEPs and solar photons, and through directional and energy filtering as well as accidental coincidence calculations, the ion signal can be largely separated from the photon backgrounds, as we have detailed.

## 2 SUMMARY: SCIENCE DATA

In this section, the energetic particle measurements of PSP/IS $\odot$ IS that are useful for science investigations are presented. The various quantities measured by the EPI-Lo (Energetic Particle Instrument - Low Energy) and EPI-Hi (Energetic Particle Instrument - High Energy) instruments are tabulated in Tables 2.2.1 – 2.3.57.

### 2.1 EPHEMERIS AND POINTING

A high-level view of the spacecraft position and attitude can be found in the `psp_isois_12-ephem` file. The central attitude question is usually “is the spacecraft in a nominal orientation?”. For this the first variable of concern is `Sun_Angle` (6.16.2.14), the angle between the spacecraft TPS (thermal protection system, heat shield) and the Sun-spacecraft line. Normally this is 0 unless some distance from the Sun; a simple flag to determine this is the variable `Umbra_Pointing` (6.16.2.15). If the spacecraft is in umbra orientation, the `Roll_Angle` (6.16.2.9) variable is a simple rotation around the Sun-spacecraft axis. Nominally IS $\odot$ IS is on the ram-facing side, roll angle is 0, and this is indicated by `Ram_Pointing` (6.16.2.8).

If the spacecraft is not in umbra orientation, the roll angle is still defined but is much less intuitively useful; the ephemeris defines a `Clock_Angle` (6.16.2.1) which describes in which direction the TPS is off-pointing from the Sun. The TPS tilted up out of the ecliptic in the 12 o’clock position is zero clock angle. Down out of the ecliptic, 180/-180 degrees. “Left” when sun-facing (i.e. anti-ram) is 90 degrees; and “right” (TPS into ram), -90.

The ephemeris also includes basic spacecraft location in HGC and HCI and the direction of the main EPI-Lo instrument, LET1A, LET2C, HETA relative to the nominal Parker Spiral. These values are also included in each science data file.

Each science data file, for each cadence included in a file, includes ephemeris and attitude information on the same cadence, i.e. at the point-in-time of the `Epoch` variable. For any quantitative treatment of particle direction, using these variables is *highly recommended* rather than trying to infer direction from the ephemeris files.

Spacecraft position is provided in HGC and HCI spherical polar coordinates after Fränz and Harper, 2002 (<https://www2.mps.mpg.de/homes/fraenz/systems/>). For EPI-Hi, there is only one cadence per file and these are simply named like `HCI_R`, `HCI_Lat`, `HCI_Lon` and similarly for HGC. For EPI-Lo, each channel has its own cadence and set of variables, e.g. `HCI_Lat_ChanP`.

Pointing information is provided in several forms. Each is provided for each aperture of EPI-Lo (all 80 apertures for channels with a valid start pulse and 8 wedges for those without), the main telescope boresight for each EPI-Hi telescope, and a geometrically nominal “center direction” for the EPI-Hi sectorized rates. Note that the angular response of the EPI-Hi sectorized rates is complex and simply assuming all incident particles are coming from the center direction is likely to be highly inaccurate.

For each of these directions, unit vectors are provided representing the direction of travel of an incident particle that is coming straight into the instrument, as represented in the RTN coordinate system. For instrument look direction, multiply each component of the unit vector by -1. No corrections are made for aberration due to spacecraft motion. The variables for these unit vectors include

RTN. For EPI-Lo, there is one variable (containing an array) for each channel, e.g. RTN\_ChanP. For EPI-Hi, there is one for each telescope end, e.g. HET\_A\_RTN as well as an array for sectorized rates, e.g. HET\_A\_R17\_SECT\_RTN. There are similar variables representing the particle motion direction in HCI coordinates (with HCI instead of RTN); again, no aberration corrections are made.

Particle directions are also expressed as a pitch angle, i.e. the angle between particle motion and the ambient magnetic field. The field is taken from the FIELDS instrument and averaged over the IS $\odot$ IS integration period by the FIELDS team. 0 represents particles directed parallel to the field; 180, antiparallel. Only 0-180 is used; there is no gyrophase information. EPI-Lo variables are named like PA\_ChanP; EPI-Hi, like HET\_A\_PA, HET\_A\_R17\_SECT\_PA. In addition to the ambient field, a similar angle is calculated from the nominal Parker Spiral. This is assumed to always point outwards (i.e. no hemispheric or solar cycle polarity is applied) and is derived from a 400km/s constant solar wind with corotation breakdown at 10R $\odot$ . These are named with SA (for “spiral angle”) instead of PA.

## 2.2 EPI-LO SCIENCE DATA

Figure 1 shows the EPI-Lo instrument layout and Figure 2 depicts the view of the sky of the 80 apertures. The files containing the EPI-Lo data are named as: <mission>\_<suite-instrument>\_<data level>\_<file-descriptor> (e.g., psp\_isois-epilo\_l2\_ic). There are four primary science data files corresponding to the four modes (depicted by <file-descriptor>) of observation: ion composition (ic), ion energy (ie), particle composition (pc) and particle energy (pe). The tables in this section summarize the science data available for the following EPI-Lo data files:

psp\_isois-epilo\_l2-ic (ion composition)  
psp\_isois-epilo\_l2-pe (particle energy)

Species without energy ranges specified are measured in this mode but are not yet commissioned. They will be included in future releases.

EPI-Lo constantly (eight times per second) cycles between “modes” with slightly different techniques for measuring the ambient plasma; the effective result is an apparent simultaneous measurement with all four modes. Modes with “composition” in the name trigger off a valid measurement from the TOF system; in these modes, a simultaneous valid measurement in a SSD may also be present (and is used if so), but is not required. Modes named “energy” trigger off a valid energy signal in a solid state detector; in these modes, a valid TOF measurement (or at least the corresponding start signals) may be used if present, but is not required. There are two sets of SSDs: the “particle” detectors have an aluminum flashing that rejects low-energy ions (improving the fraction of counts which are electrons); the “ion” detectors lack this flashing. Which SSD is checked for a signal depends on the current instrument mode. Thus the four modes: ion composition, particle energy, particle composition, ion energy. Only ion composition and particle composition have calibrated data at this time.

EPI-Lo products are integrated over different periods by “channel” (described below). These integration periods usually change a few times per orbit: upon encounter entrance and exit, and when updates are made to manage data allocation. For this reason, each channel has its own Epoch variable (and associated DELTA) which should always be used rather than assuming a cadence.

Similarly, EPI-Lo energies may vary by look direction, and vary occasionally in time when new tables are uploaded. The actual energy value recorded in the file should be examined rather than making assumptions about the energy channels. The energy labels thus also vary in look direction and time. Because these variables *may* change in time and look, they are included as fully-populated arrays for every time and look direction. The most notable change with look direction is the higher minimum energy (and resulting changes to the lowest bins) for the look directions with thick foils: L23, L30–L33, and L40.

The size of the energy variables reflects the maximum possible number of energy bins for that species and channel; the actual number of bins used may be smaller. Bins which are not used are given fill values for energy, and should be ignored. Similarly, bins which are not fully calibrated may be included. Fluxes corresponding to these bins are populated with fill but there may be count rates and best current evaluation of incident energy. This may include bins of zero width. Most science users should ignore any energy bins where the flux is entirely fill.

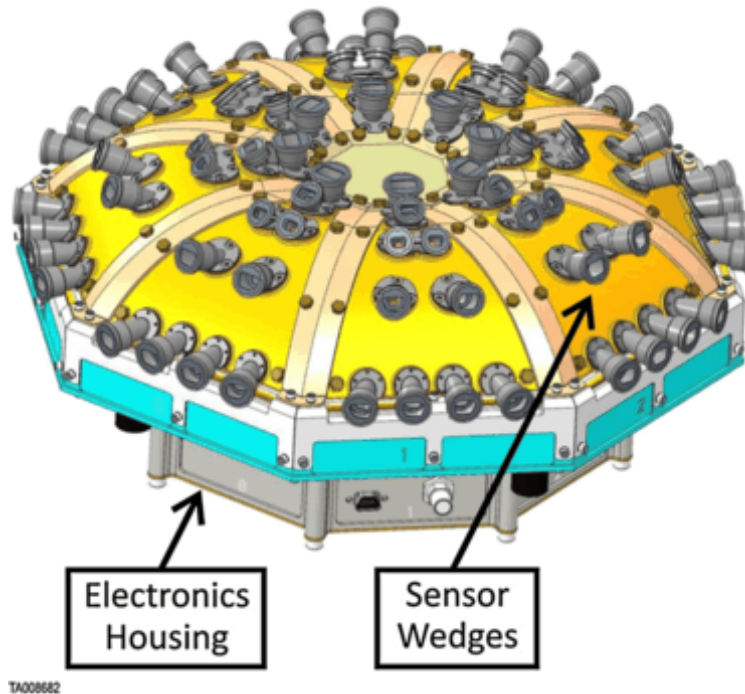


Figure 1: The EPI-Lo Instrument (see [McComas et al., 2016](#), for details).

### 2.2.1 FILE: PSP\_ISOIS-EPILO\_L2-IC

This file contains the EPI-Lo ion composition (ic) data for various particle species such as C, Fe, H,  $^3\text{He}$ ,  $^4\text{He}$ , Mg, O and Si. The variable name is structured as <species>\_<quantity>\_<channel>, where, <species> is one of the particle species; <quantity> takes ‘Counts’, ‘CountRate’ (counts/s) or ‘Flux’ ( $\text{cm}^{-2} \text{sr}^{-1} \text{sec}^{-1} \text{keV}^{-1}$ ); and <channel> takes one of the values in Column 2. The Columns ‘Look Direction’ and ‘Energy’ imply the available look directions (0 – 79) and energy ranges, respectively, in the data file. For details on look directions, see [McComas et al. \(2016\)](#).

Examples: C\_CountRate\_ChanD; H\_Flux\_ChanT.

Channels C, D, and P are triple-coincidence, or TOFxE, measurements, all measuring ions with a valid time of flight and a signal in the ion SSD. The difference is in their cadence. P is the highest cadence and used exclusively for protons. Other ions are split between C (moderate cadence) and D (slowest cadence of the three).

Channel R is a derived product from channel P. It is telemetered more frequently and constructed by joining adjacent bins from channel P. It is only of use when very high time resolution is required.

Channel T is a TOF-only channel, measuring all ions with a valid time of flight but no signal in the ion SSD. Incident energies are thus calculated in keV/nucleon and fluxes are calculated using the efficiencies and geometric factors for protons. This may be very wrong in the presence of a substantial population with  $Z>1$ . Because of the double coincidence requirement (rather than triple), counting statistics may be quite good at the price of poorer background rejection. By contrast the P channels are quite “clean”, but with lower count rates.

Species	Channel	Size	Count Rate		Counts		Flux	
			Look Direction 80	Energy (keV) (bins)	Look Direction 80	Energy (keV) (bins)	Look Direction 80	Energy (keV) (bins)
C	D	80x48	0 – 79	178 – 22872 (21)	0 – 79	178 – 22872 (21)	0 – 79	178 – 22872 (21)
Fe	C	80x48	0 – 79	431 – 24868 (41)	0 – 79	431 – 24868 (41)	0 – 79	431 – 24868 (41)
H	R	80x48	0 – 79	67 – 8736 (14)	0 – 79	67 – 8736 (14)	0 – 79	67 – 8736 (14)
	P	80x48	0 – 79	67 – 10252 (39)	0 – 79	67 – 10252 (38)	0 – 79	67 – 10252 (38)
	T	80x48	0 – 79	21 – 46367 (32)	0 – 79	21 – 46367 (32)	0 – 79	21 – 46367 (32)
He3	D	80x48	0 – 79	95 – 22536 (44)	0 – 79	95 – 22536 (44)	0 – 79	95 – 22536 (44)
He4	C	80x48	0 – 79	83 – 22540 (44)	0 – 79	83 – 22540 (44)	0 – 79	83 – 22540 (44)
Mg	D	80x48	0 – 79	218 – 23672 (22)	0 – 79	218 – 23672 (22)	0 – 79	218 – 23672 (22)
Ne	D	80x48	0 – 79	830 – 23392 (6)	0 – 79	830 – 23392 (6)	0 – 79	830 – 23392 (6)
O	C	80x48	0 – 79	205 – 23114 (43)	0 – 79	205 – 23114 (43)	0 – 79	205 – 23114 (43)
Si	D	80x48	0 – 79	327 – 23946 (20)	0 – 79	327 – 23946 (20)	0 – 79	327 – 23946 (20)

Table 2.2.1: PSP\_ISOIS-EPILO\_L2-IC: The EPI-Lo ion composition (ic) data for C, Fe, H, He3, He4, Mg, Ne, O and Si in channels D, C, R, P and T.

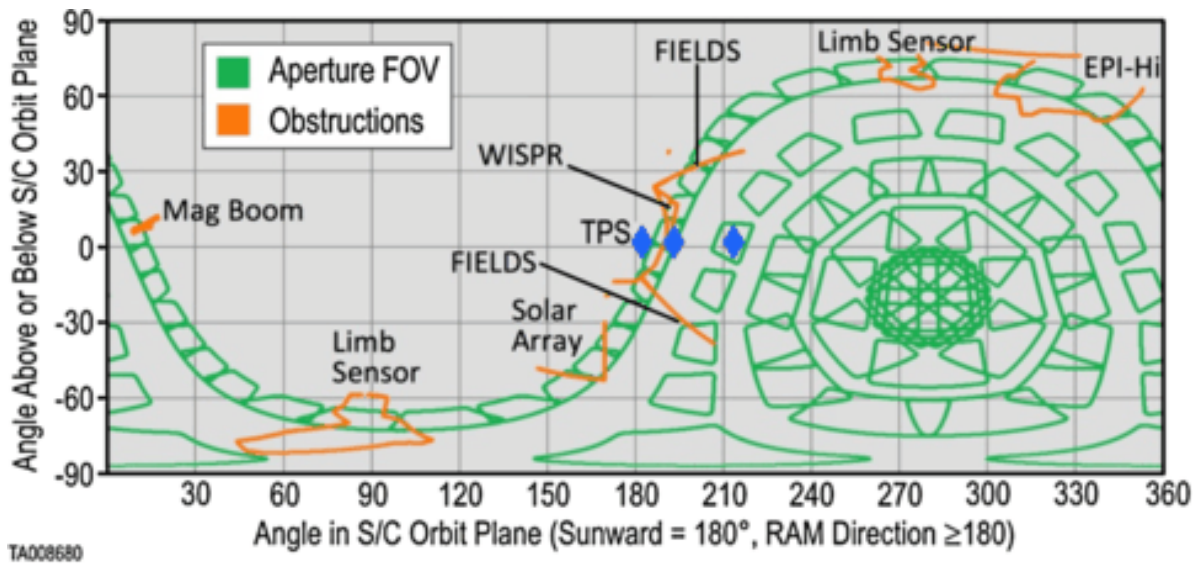


Figure 2: EPI-Lo Skymap (see [McComas et al., 2016](#), for details).

**2.2.2 FILE: PSP\_ISOIS-EPILO\_L2-PE**

EPI-Lo particle energy (pe) data for different particle species, C, electron, H, <sup>3</sup>He, He, and O. The general form of the variable name is: <species>\_<quantity>\_<channel>. Here, <species> refers to one of the particle species; <quantity> takes ‘Counts’, ‘CountRate’ (counts/s) or ‘Flux’ (cm<sup>-2</sup> sr<sup>-1</sup> sec<sup>-1</sup> keV<sup>-1</sup>); and <channel> takes to one of the values in Column 2.

Examples: C\_Flux\_ChanN; O\_Counts\_ChanX; Electron\_CountRate\_ChanE.

Channel E is the primary electron measurement, although there is substantial ion background. It does not require a valid start pulse, and thus there is limited direction information, only the knowledge that the particle was incident from one of the eight wedges. Channel F is a high-time-resolution variant of channel E; it consists of several channel E bins combined but telemetered more frequently.

Channel G contains particles with a valid SSD measurement and start pulse; as such, it has full directional information. However, incident electrons trigger a start pulse with very low efficiency, so count rates are quite low. As with channels E and F, the non-electron component is also quite high.

Species	Channel	Size	Count Rate		Counts		Flux	
			Look Direction (bins)	Energy (keV) (bins)	Look Direction (bins)	Energy (keV) (bins)	Look Direction (bins)	Energy (keV) (bins)
C	X	8 x 48	0 – 7 (8)	–	0 – 7 (8)	–	0 – 7 (8)	–
electron	E	8 x 48	0 – 7 (8)	27 – 375 (16)	0 – 7 (8)	27 – 375 (16)	0 – 7 (8)	27 – 375 (16)
	G	80 x 48	0 – 79 (80)	27 – 375 (16)	0 – 79 (80)	27 – 375 (16)	0 – 79 (80)	27 – 375 (16)
	F	8 x 48	0 – 7 (8)	33 – 375 (9)	0 – 7 (8)	33 – 375 (9)	0 – 7 (8)	33 – 375 (9)
H	E	8 x 48	0 – 7 (8)	–	0 – 7 (8)	–	0 – 7 (8)	–
	G	80 x 48	0 – 79 (80)	–	0 – 79 (80)	–	0 – 79 (80)	–
	F	8 x 48	0 – 7 (8)	–	0 – 7 (8)	–	0 – 7 (8)	–
	X	8 x 64	0 – 7 (8)	–	0 – 7 (8)	–	0 – 7 (8)	–
<sup>3</sup> He	X	8 x 48	0 – 7 (8)	–	0 – 7 (8)	–	0 – 7 (8)	–
He	X	8 x 48	0 – 7 (8)	–	0 – 7 (8)	–	0 – 7 (8)	–
O	X	8 x 48	0 – 7 (8)	–	0 – 7 (8)	–	0 – 7 (8)	–

Table 2.2.2: PSP\_ISOIS-EPILO\_L2-PE. The EPI-Lo particle energy (pe) data for electron, H, <sup>3</sup>He, He and O in channels E, G, F and X.

## 2.3 EPI-HI SCIENCE DATA

The following tables summarize the science data for the EPI-Hi Instrument. The files are named as: `<mission>_<suite-instrument>_<data level>_<file-descriptor>`. The EPI-Hi instrument consists of three telescopes HET, LET1 and LET2. The HET and LET1 telescopes have two sides (A, B) and let2 has one side (C). Sides A on LET1 and HET look sunward along the Parker Spiral and sides B on LET1 and HET look antisunward. Side C LET2 looks in the spacecraft ram direction. Full pointing information (RTN/HCI) is available in the L2 files (see [McComas et al., 2016](#), and Figure 3). The numerical values following rates in the `<file-descriptor>` represent the cadence in seconds (e.g., rates10; rates300). If no value is present, the cadence is assumed to be 1 second. Listed below are the EPI-Hi data files. The 60 s cadence products containing only the engineering singles are excluded from public release.

EPI-Hi science rates are accumulated at several cadences. The 10 s and 1 s rates are an encounter-only product. The 60 s rates are also, at a baseline, encounter-only. The 3600 s rates are the main cruise phase product. EPI-Hi produces several engineering rates that overflow their counters when accumulated for 3600 s. For those, a 1/60 sample of the 60 s rates are included in cruise data. The 60 s products are thus produced for the whole mission but those containing no science data are excluded from the public release.

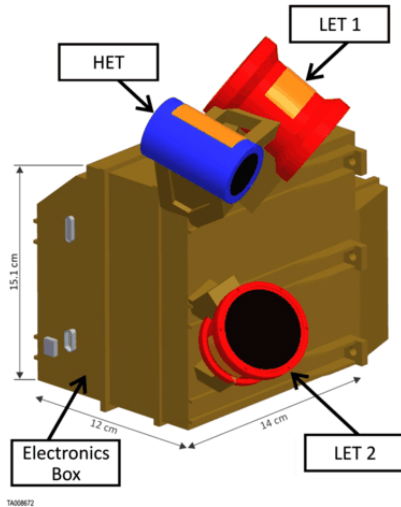
HET	LET1	LET2
psp_isois-epihi_l2-het-rates10	psp_isois-epihi_l2-let1-rates10	psp_isois-epihi_l2-let2-rates10
psp_isois-epihi_l2-het-rates300	psp_isois-epihi_l2-let1-rates300	psp_isois-epihi_l2-let2-rates300
psp_isois-epihi_l2-het-rates3600	psp_isois-epihi_l2-let1-rates3600	psp_isois-epihi_l2-let2-rates3600
psp_isois-epihi_l2-het-rates60	psp_isois-epihi_l2-let1-rates60	psp_isois-epihi_l2-let2-rates60
HET, LET1 & LET2		psp_isois-epihi_l2-second-rates

The front-end logic for each telescope is capable of accepting candidate particle detection events at a higher rate than the telescope's flight software can process. During periods of high count rates, then, some of these events are not processed and the measured count rate is depressed relative to the incident. EPI-Hi fluxes and science count rates are corrected for this effect, starting in release 9. Counts (per sample) are uncorrected.

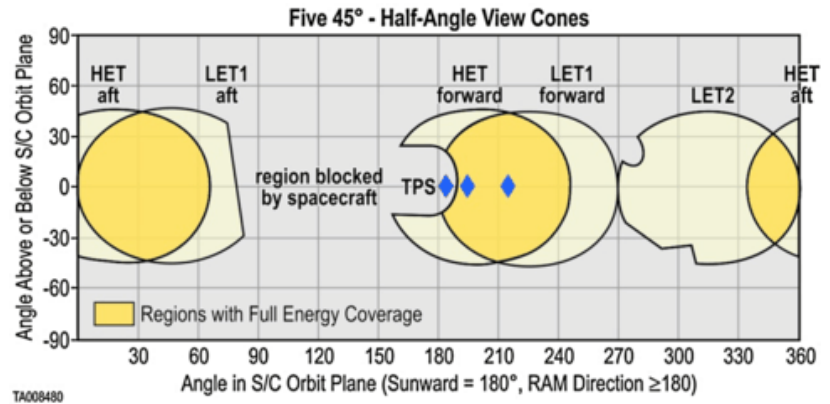
### 2.3.1 FILE: PSP\_ISOIS-EPIHI\_L2-HET-RATES10

This file contains the 10 s data of energetic particle Counts, Flux ( $\text{cm}^{-2} \text{sr}^{-1} \text{sec}^{-1} \text{MeV}^{-1}$ ) and Count Rate (counts/s) for electrons, H, He and NEUT\_DET for sides A and B, for different ranges (R1 – R7) of the High Energy Telescope (HET). The naming convention of the variables in the data files is: `<side>_<species>_<quantity>` for those quantities independent of range. Here, `<side>` stands for A or B; `<species>` stands for the particle species (electrons, H, He, etc.); and `<quantity>` represents Counts (not used in variable names, in general), Flux or Rate. For those parameters measured as a function of range, the naming convention is: `<range><side>_<species>_<quantity>`, where, `<range>` goes from R1 to R7 and `<side>` takes either A or B. Variable names without ranges (e.g., A\_Electrons\_Flux) or with double digit range (e.g., R17) have the values integrated over all





(a) EPI-Hi Instrument.



(b) EPI-Hi field of view.

Figure 3: The EPI-Hi instrument and field of view. Sides A on LET1 and HET look sunward along the Parker Spiral while sides B on LET1 and HET look antisunward. Side C on LET2 looks in the spacecraft *ram* direction. Full pointing information (RTN/HCI) is available in the L2 files (see [McComas et al., 2016](#), for details on the sides A, B and C given in the tables.)

the available ranges (R1 to R7, in general).

Examples: A\_H (measured quantity is “counts”); A\_Electrons\_Flux; R1A\_Electrons\_Rate.

Side	Range	Quantity	Electrons		H		He		NEUT_DET	
			E-bins	E-range (MeV/nuc) (bins)	E-bins	E-range (MeV/nuc) (bins)	E-bins	E-range (MeV/nuc) (bins)	E-bins	E-range (MeV/nuc) (bins)
A/B		Count	16	1 - 9 (16)	11	10 - 59 (11)	12	10 - 70 (12)	35	0 - 495 (35)
		Flux	16	1 - 9 (16)	11	10 - 59 (11)	12	10 - 70 (12)		
		Count Rate	16	1 - 9 (16)	11	10 - 59 (11)	12	10 - 70 (12)	35	0 - 495 (35)
	R1	Count	12	1 - 4 (12)	7	9 - 25 (7)	8	9 - 29 (8)		
		Flux	12	1 - 4 (12)	7	9 - 25 (7)	8	9 - 29 (8)		
		Count Rate	12	1 - 4 (12)	7	9 - 25 (7)	8	9 - 29 (8)		
	R2	Count	12	1 - 4 (12)	7	15 - 42 (7)	8	15 - 50 (8)		
		Flux	12	1 - 4 (12)	7	15 - 42 (7)	8	15 - 50 (8)		
		Count Rate	12	1 - 4 (12)	7	15 - 42 (7)	8	15 - 50 (8)		
	R3	Count	10	1 - 5 (10)	6	21 - 50 (6)	7	21 - 59 (7)		
		Flux	10	1 - 5 (10)	6	21 - 50 (6)	7	21 - 59 (7)		
		Count Rate	10	1 - 5 (10)	6	21 - 50 (6)	7	21 - 59 (7)		
	R4	Count	10	1 - 6 (10)	4	29 - 50 (4)	5	29 - 59 (5)		
		Flux	10	1 - 6 (10)	4	29 - 50 (4)	5	29 - 59 (5)		
		Count Rate	10	1 - 6 (10)	4	29 - 50 (4)	5	29 - 59 (5)		
	R5	Count	9	2 - 7 (9)	4	35 - 59 (4)	5	35 - 70 (5)		
		Flux	9	2 - 7 (9)	4	35 - 59 (4)	5	35 - 70 (5)		
		Count Rate	9	2 - 7 (9)	4	35 - 59 (4)	5	35 - 70 (5)		
	R6	Count	9	2 - 9 (9)	4	35 - 59 (4)	5	35 - 70 (5)		
		Flux	9	2 - 9 (9)	4	35 - 59 (4)	5	35 - 70 (5)		
		Count Rate	9	2 - 9 (9)	4	35 - 59 (4)	5	35 - 70 (5)		
	R7	Count	9	3 - 10 (9)	4	42 - 70 (4)	5	42 - 83 (5)		
		Flux	9	3 - 10 (9)	4	42 - 70 (4)	5	42 - 83 (5)		
		Count Rate	9	3 - 10 (9)	4	42 - 70 (4)	5	42 - 83 (5)		

Table 2.3.1: PSP\_ISOIS-EPIHI\_L2-HET-RATES10. The 10 s HET data of particle Counts, Flux and Count Rate for electrons, H, He and NEUT\_DET for sides A and B, and for ranges R1 – R7.

### 2.3.2 FILE: PSP\_ISOIS-EPIHI\_L2-HET-RATES300

This file provides the 300 s rates of energetic particle Counts, Flux ( $\text{cm}^{-2} \text{sr}^{-1} \text{sec}^{-1} \text{MeV}^{-1}$ ) and Count Rate (counts/s) for CNO, FeGroup and NetoSi ions for ranges R1 – R7 of the High Energy Telescope (HET) for sides A and B. The variables (summarized in Table 2.3.2) are named as: <side>\_<species>\_<quantity> for those quantities independent of range. Here, <side> stands for A or B; <species> stands for the particle species (CNO\_SECT, FeGroup\_SECT and NetoSi\_SECT), and <quantity> represents Counts (not used in the variable names, in general), Flux or Rate. Examples: A\_CNO\_SECT (measured quantity is “counts”); A\_FeGroup\_SECT\_Flux; A\_NetoSi\_SECT\_Rate.

Side	Quantity	CNO_SECT			FeGroup_SECT			NetoSi_SECT		
		E-bins	E-range (MeV/nuc)	Sectors (bins)	E-bins	E-range (MeV/nuc)	Sectors (bins)	E-bins	E-range (MeV/nuc)	Sectors (bins)
A/B	Count	2	36 – 68	0 – 8 (9)	1	81 – 81	0 – 8 (9)	1	57 – 57	0 – 8 (9)
	Flux	2	36 – 68	0 – 8 (9)	1 1	81 – 81	0 – 8 (9)	1 1	57 – 57	0 – 8 (9)
	Count Rate	2	36 – 68	0 – 8 (9)	1 1	81 – 81	0 – 8 (9)	1 1	57 – 57	0 – 8 (9)
ENB_SECT - measured quantity is Count; Size 1 X 25; E-bins: 1; E-range: 12 - 12; Sectors: 0 -8 (9).										

Table 2.3.2: PSP\_ISOIS-EPIHI\_L2-HET-RATES300. The 300 s cadence HET data of particle Counts, Flux and Count Rate for CNO, FeGroup and NetoSi ions for sides A and B, and integrated over ranges R1 – R7.

### 2.3.3 FILE: PSP\_ISOIS-EPIHI\_L2-HET-RATES3600

In this file, the 3600 s cadence data of particle Counts, Flux ( $\text{cm}^{-2} \text{sr}^{-1} \text{sec}^{-1} \text{MeV}^{-1}$ ) and Count Rate (counts/s) measured by High Energy Telescope (HET) are available. The names of variables (summarized in Tables 2.3.3 – 2.3.11) follow the general pattern: <side>\_<species>\_<quantity>, where, <side> stands for A or B; <species> stands for the particle species (Al, Ar, C, etc., in column 2); and <quantity> represents Counts, Flux or Count Rate. Note that “Count” is not used in the variable names, in general. Variable names without ranges (e.g., A\_C) or with double digit range (e.g., R17) have the values integrated over all the available ranges (R1 to R7, in general: e.g., B\_H\_SECT\_Flux has values averaged over R1 – R7 in Table 2.3.3). Examples: A\_C, NEUT1, NEUT2\_DET, (measured quantity is “counts”); B\_FeGroup\_SECT\_Flux; PENA\_C\_Rate; R1A\_32to50\_Flux.

Side	Species	Count			Flux			Count Rate		
		Size (bins)	Range SECT (bins)	Energy (MeV/nuc)	Size (bins)	Range SECT (bins)	Energy (MeV/nuc)	Size (bins)	Range SECT (bins)	Energy (MeV/nuc)
A/B	Al	15	–	21 – 236	15	–	21 – 236	15	–	21 – 236
	Ar	15	–	25 – 280	15	–	25 – 280	15	–	25 – 280
	C	15	–	12 – 140	15	–	12 – 140	15	–	12 – 140
	CNO_SECT	2x25 (2 bins)	R17 0 – 8 (9)	36 – 68	2x25 (1 bin)	R17 0 – 8 (9)	36 – 68	2x25 (2 bins)	R17 0 – 8 (9)	36 – 68
	Ca	15	–	25 – 280	15	–	25 – 280	15	–	25 – 280
	Cr	16	–	25 – 333	16	–	25 – 333	16	–	25 – 333
	Electrons	19	–	0 – 10	19	–	0 – 10	19	–	0 – 10
	Electron_SECT	2x25 (2 bins)	R17 0 – 8 (9)	2 – 3	2x25 (2 bins)	R17 0 – 8 (9)	3 – 3	2x25 (2 bins)	R17 0 – 8 (9)	2 – 3
	Fe	15	–	29 - 333	15	–	29 – 333	15	–	29 – 333
	FeGroup_SECT	1x25 (1 bin)	R17 0 – 8 (9)	81 – 81	1x25 (1 bin)	R17 0 – 8 (9)	81 – 81	1x25 (1 bin)	R17 0 – 8 (9)	81 – 81
	H	15	–	7 – 83	15	–	7 – 83	15	–	7 – 83
	H_SECT	2x25 (2 bins)	R17 0 – 8 (9)	18 – 34	2x25 (2 bins)	R17 0 – 8 (9)	18 – 34	2x25 (2 bins)	R17 0 – 8 (9)	18 – 34
	He	16	–	7 – 99	16	–	7 – 99	16	–	7 - 99
	He_SECT	2x25 (2 bins)	R17 0 – 8 (9)	18 – 34	2x25 (2 bins)	R17 0 – 8 (9)	18 – 34	2x25 (2 bins)	R17 0 – 8 (9)	18 – 34
	Mg	15	–	21 – 236	15	–	21 – 236	15	–	21 – 236
	N	15	–	12 – 140	15	–	12 – 140	15	–	12 – 140
	Na	15	–	18 – 198	15	–	18 – 198	15	–	18 – 198
	Ne	15	–	18 – 198	15	–	18 – 198	15	–	18 – 198
	NetoSi_SECT	1x25 (1 bin)	R17 0 – 8 (9)	57 – 57	1x25 (1 bin)	R17 0 – 8 (9)	57 – 57	1x25 (1 bin)	R17 0 – 8 (9)	57 – 57
	Ni	15	–	29 - 333	15	–	29 – 333	15	–	29 – 333
O	15	–	15 - 167	15	–	15 – 167	15	–	15 – 167	
S	16	–	21 – 280	16	–	21 – 280	16	–	21 – 280	
Si	15	–	21 – 236	15	–	21 – 236	15	–	21 – 236	
	NEUT1	35x21	–	0 – 495	–	–	–	35x21	–	0 – 495
	NEUT2_DET	35x6	–	0 – 495	–	–	–	35x6	–	0 – 495

Table 2.3.3: PSP\_ISOIS-EPIHI\_L2-HET-RATES3600. The 3600 s cadence HET data of the particle Counts, Flux and Count Rates for different particle species for sides A and B and ranges R1 – R7. R17 implies integration of the measured values over ranges R1 – R7.

Side	Species	Count		Count Rate	
		Size (bins)	Energy (MeV/nuc)	Size (bins)	Energy (MeV/nuc)
A/B	PENx_C	9	45 – 583	9	45 – 583
	PENx_Fe	9	108 – 793	9	108 – 793
	PENx_H	9	27 – 521	9	27 – 521
	PENx_He	9	27 – 521	9	27 – 521
	PENx_Mg	9	64 – 646	9	64 – 646
	PENx_N	9	45 – 583	9	45 – 583
	PENx_Ne	8	64 – 612	8	64 – 612
	PENx_O	9	54 – 612	9	54 – 612
	PENx_Si	9	76 – 687	9	76 – 687

Table 2.3.4: PSP\_ISOIS-EPIHI\_L2-HET-RATES3600 (contd.). Here, ‘x’ stands for sides A & B.

Side	Species	Count		Flux		Count Rate	
		Size (bins)	Energy (MeV/nuc)	Size (bins)	Energy (MeV/nuc)	Size (bins)	Energy (MeV/nuc)
A/B	xxx_29to32	6	14 – 538	6	14 – 538	6	14 – 538
	xxx_32to50	6	14 – 538	6	14 – 538	6	14 – 538
	xxx_Al	11	10 – 476	11	10 – 476	11	10 – 476
	xxx_Ar	11	11 – 484	11	11 – 484	11	11 – 484
	xxx_C	12	6 – 463	12	6 – 463	12	6 – 463
	xxx_Ca	11	11 – 484	11	11 – 484	11	11 – 484
	xxx_Cr	12	11 – 495	12	11 – 495	12	11 – 495
	xxx_Electrons	15	0 – 433	15	0 – 433	15	0 – 433
	xxx_Fe	11	14 – 495	11	14 – 495	11	14 – 495
	xxx_H	11	4 – 447	11	4 – 447	11	4 – 447
	xxx_He	12	4 – 450	12	4 – 450	12	4 – 450
	xxx_He_BIN	5x16 (5)	9 – 32	–	–	–	–
	xxx_He_BIN (MASS)	16 bins	–	–	–	–	–
		0 – 15 seg	–	–	–	–	–
	xxx_Mg	11	10 – 476	11	10 – 476	11	10 – 476
	xxx_N	12	6 – 463	12	6 – 463	12	6 – 463
	xxx_Na	11	8 – 469	11	8 – 469	11	8 – 469
	xxx_Ne	11	8 – 469	11	8 – 469	11	8 – 469
	xxx_Ne_BIN	4x8 (4)	23 – 65	–	–	–	–
	xxx_Ne_BIN (MASS)	8 bins	–	–	–	–	–
		0 – 7 seg	–	–	–	–	–
xxx_Ni	12	14 – 507	12	14 – 507	12	14 – 507	
xxx_O	11	7 – 463	11	7 – 463	11	7 – 463	
xxx_S	12	10 – 484	12	10 – 484	12	10 – 484	
xxx_Si	11	10 – 476	11	10 – 476	11	10 – 476	
xxx_gt50	6	14 – 538	6	14 – 538	6	14 – 538	

Table 2.3.5: PSP\_ISOIS-EPIHI\_L2-HET-RATES3600 (contd.). Here ‘xxx’ stands for R1A & R1B.

Side	Species	Count		Flux		Count Rate	
		Size (bins)	Energy (MeV/nuc)	Size (bins)	Energy (MeV/nuc)	Size (bins)	Energy (MeV/nuc)
A/B	xxx_29to32	5	23 – 538	5	23 – 538	5	23 – 538
	xxx_32to50	5	23 – 538	5	23 – 538	5	23 – 538
	xxx_Al	11	14 – 495	11	14 – 495	11	14 – 495
	xxx_Ar	11	19 – 521	11	19 – 521	11	19 – 521
	xxx_C	11	10 – 476	11	10 – 476	11	10 – 476
	xxx_Ca	11	19 – 521	11	19 – 521	11	19 – 521
	xxx_Cr	12	19 – 538	12	19 – 538	12	19 – 538
	xxx_Electrons	15	0 – 433	15	0 – 433	15	0 – 433
	xxx_Fe	11	23 – 538	11	23 – 538	11	23 – 538
	xxx_H	11	6 – 457	11	6 – 457	11	6 – 457
	xxx_He	12	6 – 463	12	6 – 463	12	6 – 463
	xxx_He_BIN xxx_He_BIN (MASS)	4x16 (4) 16 bins 0 – 15 seg	16 – 46 – –	– – –	– – –	– – –	– – –
	xxx_Mg	11	14 – 495	11	14 – 495	11	14 – 495
	xxx_N	11	10 – 476	11	10 – 476	11	10 – 476
	xxx_Na	11	14 – 495	11	14 – 495	11	14 – 495
	xxx_Ne	11	14 – 495	11	14 – 495	11	14 – 495
	xxx_Ne_BIN xxx_Ne_BIN (MASS)	4x8 (4) 8 bins 0 – 7 seg	32 – 92 – –	– – –	– – –	– – –	– – –
	xxx_Ni	11	23 – 538	11	23 – 538	11	23 – 538
	xxx_O	11	11 – 484	11	11 – 484	11	11 – 484
	xxx_S	12	16 – 521	12	16 – 521	12	16 – 521
xxx_Si	11	16 – 507	11	16 – 507	11	16 – 507	
xxx_gt50	5	23 – 538	5	23 – 538	5	23 – 538	

Table 2.3.6: PSP\_ISOIS-EPIHI\_L2-HET-RATES3600 (contd.). Here, ‘xxx’ stands for R2A and R2B.

Side	Species	Count		Flux		Count Rate	
		Size (bins)	Energy (MeV/nuc)	Size (bins)	Energy (MeV/nuc)	Size (bins)	Energy (MeV/nuc)
A/B	xxx_29to32	5	38 – 612	5	38 – 612	5	38 – 612
	xxx_32to50	5	38 – 612	5	38 – 612	5	38 – 612
	xxx_Al	9	23 – 507	9	23 – 507	9	23 – 507
	xxx_Ar	9	32 – 538	9	32 – 538	9	32 – 538
	xxx_C	9	16 – 484	9	16 – 484	9	16 – 484
	xxx_Ca	9	32 – 538	9	32 – 538	9	32 – 538
	xxx_Cr	10	32 – 559	10	32 – 559	10	32 – 559
	xxx_Electrons	13	1 – 433	13	1 – 433	13	1 – 433
	xxx_Fe	10	32 – 559	10	32 – 559	10	32 – 559
	xxx_H	10	8 – 463	10	8 – 463	10	8 – 463
	xxx_He	11	8 – 469	11	8 – 469	11	8 – 469
	xxx_He_BIN xxx_He_BIN (MASS)	4x16 (4) 16 bins 0 - 15 seg	23 – 65 – –	– – –	– – –	– – –	– – –
	xxx_Mg	9	23 – 507	9	23 – 507	9	23 – 507
	xxx_N	9	16 – 484	9	16 – 484	9	16 – 484
	xxx_Na	10	19 – 507	10	19 – 507	10	19 – 507
	xxx_Ne	10	19 – 507	10	19 – 507	10	19 – 507
	xxx_Ne_BIN xxx_Ne_BIN (MASS)	4x8 (4) 8 bins 0 - 7 seg	46 – 130 – –	– – –	– – –	– – –	– – –
	xxx_Ni	10	32 – 559	10	32 – 559	10	32 – 559
	xxx_O	9	19 – 495	9	19 – 495	9	19 – 495
	xxx_S	10	27 – 538	10	27 – 538	10	27 – 538
xxx_Si	9	27 – 521	9	27 – 521	9	27 – 521	
xxx_gt50	5	38 – 612	5	38 – 612	5	38 – 612	

Table 2.3.7: PSP\_ISOIS-EPIHI\_L2-HET-RATES3600 (contd.). Here, ‘xxx’ stands for R3A and R3B.

Side	Species	Count		Flux		Count Rate	
		Size (bins)	Energy (MeV/nuc)	Size (bins)	Energy (MeV/nuc)	Size (bins)	Energy (MeV/nuc)
A/B	xxx_29to32	5	38 – 612	5	38 – 612	5	38 – 612
	xxx_32to50	5	38 – 612	5	38 – 612	5	38 – 612
	xxx_Al	9	27 – 521	9	27 – 521	9	27 – 521
	xxx_Ar	8	38 – 538	8	38 – 538	8	38 – 538
	xxx_C	9	19 – 495	9	19 – 495	9	19 – 495
	xxx_Ca	8	38 – 538	8	38 – 538	8	38 – 538
	xxx_Cr	9	38 – 559	9	38 – 559	9	38 – 559
	xxx_Electrons	12	1 – 434	12	1 – 434	12	1 – 434
	xxx_Fe	8	45 – 559	8	45 – 559	8	45 – 559
	xxx_H	8	11 – 463	8	11 – 463	8	11 – 463
	xxx_He	9	11 – 469	9	11 – 469	9	11 – 469
	xxx_He_BIN xxx_He_BIN (MASS)	3x16 (3) 16 bins 0 - 15 seg	32 – 65 – –	– – –	– – –	– – –	– – –
	xxx_Mg	9	27 – 521	9	27 – 521	9	27 – 521
	xxx_N	9	19 – 495	9	19 – 495	9	19 – 495
	xxx_Na	8	27 – 507	8	27 – 507	8	27 – 507
	xxx_Ne	8	27 – 507	8	27 – 507	8	27 – 507
	xxx_Ne_BIN xxx_Ne_BIN (MASS)	3x8 (3) 8 bins 0 - 7 seg	65 – 130 – –	– – –	– – –	– – –	– – –
	xxx_Ni	9	45 – 583	9	45 – 583	9	45 – 583
	xxx_O	8	23 – 495	8	23 – 495	8	23 – 495
	xxx_S	9	32 – 538	9	32 – 538	9	32 – 538
xxx_Si	9	32 – 538	9	32 – 538	9	32 – 538	
xxx_gt50	5	38 – 612	5	38 – 612	5	38 – 612	

Table 2.3.8: PSP\_ISOIS-EPIHI\_L2-HET-RATES3600 (contd.). Here, ‘xxx’ stands for R4A and R4B.



Side	Species	Count		Flux		Count Rate	
		Size (bins)	Energy (MeV/nuc)	Size (bins)	Energy (MeV/nuc)	Size (bins)	Energy (MeV/nuc)
A/B	xxx_29to32	4	64 – 612	4	64 – 612	4	64 – 612
	xxx_32to50	4	64 – 612	4	64 – 612	4	64 – 612
	xxx_Al	9	32 – 538	9	32 – 538	9	32 – 538
	xxx_Ar	8	45 – 559	8	45 – 559	8	45 – 559
	xxx_C	8	23 – 495	8	23 – 495	8	23 – 495
	xxx_Ca	8	45 – 559	8	45 – 559	8	45 – 559
	xxx_Cr	9	45 – 583	9	45 – 583	9	45 – 583
	xxx_Electrons	11	1 – 435	11	1 – 435	11	1 – 435
	xxx_Fe	8	54 – 583	8	54 – 583	8	54 – 583
	xxx_H	8	14 – 469	8	14 – 469	8	14 – 469
	xxx_He	9	14 – 476	9	14 – 476	9	14 – 476
	xxx_He_BIN xxx_He_BIN (MASS)	3x16 (3) 16 bins 0 - 15 seg	32 – 65 – –	– – –	– – –	– – –	– – –
	xxx_Mg	9	32 – 538	9	32 – 538	9	32 – 538
	xxx_N	8	23 – 495	8	23 – 495	8	23 – 495
	xxx_Na	8	32 – 521	8	32 – 521	8	32 – 521
	xxx_Ne	8	32 – 521	8	32 – 521	8	32 – 521
	xxx_Ne_BIN xxx_Ne_BIN (MASS)	2x8 (2) 8 bins 0 - 7 seg	92 – 130 – –	– – –	– – –	– – –	– – –
	xxx_Ni	9	54 – 612	9	54 – 612	9	54 – 612
	xxx_O	8	27 – 507	8	27 – 507	8	27 – 507
	xxx_S	9	38 – 559	9	38 – 559	9	38 – 559
xxx_Si	8	38 – 538	8	38 – 538	8	38 – 538	
xxx_gt50	4	64 – 612	4	64 – 612	4	64 – 612	

Table 2.3.9: PSP\_ISOIS-EPIHI\_L2-HET-RATES3600 (contd.). Here, ‘xxx’ stands for R5A and R5B.

Side	Species	Count		Flux		Count Rate	
		Size (bins)	Energy (MeV/nuc)	Size (bins)	Energy (MeV/nuc)	Size (bins)	Energy (MeV/nuc)
A/B	xxx_29to32	4	64 – 612	4	64 – 612	4	64 – 612
	xxx_32to50	4	64 – 612	4	64 – 612	4	64 – 612
	xxx_Al	8	38 – 538	8	38 – 538	8	38 – 538
	xxx_Ar	9	45 – 583	9	45 – 583	9	45 – 583
	xxx_C	8	27 – 507	8	27 – 507	8	27 – 507
	xxx_Ca	9	45 – 583	9	45 – 583	9	45 – 583
	xxx_Cr	10	45 – 612	10	45 – 612	10	45 – 612
	xxx_Electrons	11	1 – 435	11	1 – 435	11	1 – 435
	xxx_Fe	9	54 – 612	9	54 – 612	9	54 – 612
	xxx_H	8	14 – 469	8	14 – 469	8	14 – 469
	xxx_He	9	14 – 476	9	14 – 476	9	14 – 476
	xxx_He_BIN xxx_He_BIN (MASS)	3x16 (3) 16 bins 0 - 15 seg	32 – 65 – –	– – –	– – –	– – –	– – –
	xxx_Mg	8	38 – 538	8	38 – 538	8	38 – 538
	xxx_N	8	27 – 507	8	27 – 507	8	27 – 507
	xxx_Na	8	38 – 538	8	38 – 538	8	38 – 538
	xxx_Ne	8	38 – 538	8	38 – 538	8	38 – 538
	xxx_Ne_BIN xxx_Ne_BIN (MASS)	3x8 (3) 8 bins 0 - 7 seg	92 – 184 – –	– – –	– – –	– – –	– – –
	xxx_Ni	9	54 – 612	9	54 – 612	9	54 – 612
	xxx_O	8	32 – 521	8	32 – 521	8	32 – 521
	xxx_S	9	45 – 583	9	45 – 583	9	45 – 583
xxx_Si	8	45 – 559	8	45 – 559	8	45 – 559	
xxx_gt50	4	64 – 612	4	64 – 612	4	64 – 612	

Table 2.3.10: PSP\_ISOIS-EPIHI\_L2-HET-RATES3600 (contd.). Here, ‘xxx’ stands for R6A and R6B.

Side	Species	Count		Flux		Count Rate	
		Size (bins)	Energy (MeV/nuc)	Size (bins)	Energy (MeV/nuc)	Size (bins)	Energy (MeV/nuc)
A/B	xxx_29to32	4	64 – 612	4	64 – 612	4	64 – 612
	xxx_32to50	4	64 – 612	4	64 – 612	4	64 – 612
	xxx_Al	8	45 – 559	8	45 – 559	8	45 – 559
	xxx_Ar	7	64 – 583	7	64 – 583	7	64 – 583
	xxx_C	7	32 – 507	7	32 – 507	7	32 – 507
	xxx_Ca	7	64 – 583	7	64 – 583	7	64 – 583
	xxx_Cr	8	64 – 612	8	64 – 612	8	64 – 612
	xxx_Electrons	11	1 – 436	11	1 – 436	11	1 – 436
	xxx_Fe	8	64 – 612	8	64 – 612	8	64 – 612
	xxx_H	8	16 – 476	8	16 – 476	8	16 – 476
	xxx_He	9	16 – 484	9	16 – 484	9	16 – 484
	xxx_He_BIN xxx_He_BIN (MASS)	2x16 (2) 16 bins 0 - 15 seg	46 – 65 – –	– – –	– – –	– – –	– – –
	xxx_Mg	8	45 – 559	8	45 – 559	8	45 – 559
	xxx_N	7	32 – 507	7	32 – 507	7	32 – 507
	xxx_Na	8	38 – 538	8	38 – 538	8	38 – 538
	xxx_Ne	8	38 – 538	8	38 – 538	8	38 – 538
	xxx_Ne_BIN xxx_Ne_BIN (MASS)	3x8 (3) 8 bins 0 - 7 seg	92 – 184 – –	– – –	– – –	– – –	– – –
	xxx_Ni	8	64 – 612	8	64 – 612	8	64 – 612
	xxx_O	7	38 – 521	7	38 – 521	7	38 – 521
	xxx_S	8	54 – 583	8	54 – 583	8	54 – 583
xxx_Si	7	54 – 559	7	54 – 559	7	54 – 559	
xxx_gt50	4	64 – 612	4	64 – 612	4	64 – 612	

Table 2.3.11: PSP\_ISOIS-EPIHI\_L2-HET-RATES3600 (contd.). Here, ‘xxx’ stands for R7A and R7B.

**2.3.4 FILE: PSP\_ISOIS-EPIHI\_L2-HET-RATES60**

This file contains the 60-second cadence data of particle Counts, Flux ( $\text{cm}^{-2} \text{sr}^{-1} \text{sec}^{-1} \text{MeV}^{-1}$ ) and Count Rate (counts/s) for Al, Ar, C, Ca, Cr, Electrons, Fe, H, He, Mg, N, Na, Ne, Ni, O, S and Si ions for ranges R1 – R7) of the High Energy Telescope (HET) for sides A and B. The measured values are summarized in Tables 2.3.12 – 2.3.20. The variable names follow the structure: <side>\_<species>\_<quantity>, where, <side> stands for A or B; <species> stands for the particle species; and <quantity> represents Counts (not used in the variable names, in general), Flux or Count Rate. Variable names without ranges (e.g., A\_C) or with double digit range (e.g., R17) have their values integrated over all the available ranges (R1 to R7, in general).

Examples: A\_Fe (measured quantity is “counts”); B\_Electron\_SECT\_Flux; PENB\_Mg\_Flux; R7A\_Ni\_Rate.

Side	Species	Count			Flux			Count Rate		
		Size (bins)	Range SECT (bins)	Energy (MeV/nuc)	Size (bins)	Range SECT (bins)	Energy (MeV/nuc)	Size (bins)	Range SECT (bins)	Energy (MeV/nuc)
A/B	Al	15	–	21 – 236	15	–	21 – 236	15	–	21 – 236
	Ar	15	–	25 – 280	15	–	25 – 280	15	–	25 – 280
	C	15	–	12 – 140	15	–	12 – 140	15	–	12 – 140
	Ca	15	–	25 – 280	15	–	25 – 280	15	–	25 – 280
	Cr	16	–	25 – 333	16	–	25 – 333	16	–	25 – 333
	Electrons	19	–	0 – 10	19	–	0 – 10	19	–	0 – 10
	Electron_SECT	2x25 (2 bins)	R17 0 – 8 (9)	2 – 3	2x25 (2 bins)	R17 0 – 8 (9)	3 – 3	2x25 (2 bins)	R17 0 – 8 (9)	2 – 3
	Fe	15	–	29 – 333	15	–	29 – 333	15	–	29 – 333
	H	15	–	7 – 83	15	–	7 – 83	15	–	7 – 83
	H_SECT	2x25 (2 bins)	R17 0 – 8 (9)	18 – 34	2x25 (2 bins)	R17 0 – 8 (9)	18 – 34	2x25 (2 bins)	R17 0 – 8 (9)	18 – 34
	He	16	–	7 – 99	16	–	7 – 99	16	–	7 – 99
	He_SECT	2x25 (2 bins)	R17 0 – 8 (9)	18 – 34	2x25 (2 bins)	R17 0 – 8 (9)	18 – 34	2x25 (2 bins)	R17 0 – 8 (9)	18 – 34
	Mg	15	–	21 – 236	15	–	21 – 236	15	–	21 – 236
	N	15	–	12 – 140	15	–	12 – 140	15	–	12 – 140
	Na	15	–	18 – 198	15	–	18 – 198	15	–	18 – 198
	Ne	15	–	18 – 198	15	–	18 – 198	15	–	18 – 198
	Ni	15	–	29 – 333	15	–	29 – 333	15	–	29 – 333
	O	15	–	15 – 167	15	–	15 – 167	15	–	15 – 167
	S	16	–	21 – 280	16	–	21 – 280	16	–	21 – 280
Si	15	–	21 – 236	15	–	21 – 236	15	–	21 – 236	

Table 2.3.12: PSP\_ISOIS-EPIHI\_HET-RATES60. The HET 60 s cadence data for various particle species. R17 implies integration of the measured values over ranges R1 – R7.

Side	Species	Count		Count Rate	
		Size (bins)	Energy (MeV/nuc)	Size (bins)	Energy (MeV/nuc)
A/B	PENx_C	9	45 – 583	9	45 – 583
	PENx_Fe	9	108 – 793	9	108 – 793
	PENx_H	9	27 – 521	9	27 – 521
	PENx_He	9	27 – 521	9	27 – 521
	PENx_Mg	9	64 – 646	9	64 – 646
	PENx_N	9	45 – 583	9	45 – 583
	PENx_Ne	8	64 – 612	8	64 – 612
	PENx_O	9	54 – 612	9	54 – 612
	PENx_Si	9	76 – 687	9	76 – 687

Table 2.3.13: PSP\_ISOIS-EPIHI\_L2-HET-RATES60 (contd.). Here, ‘x’ stands for sides A & B.

Side	Species	Count		Flux		Count Rate	
		Size (bins)	Energy (MeV/nuc)	Size (bins)	Energy (MeV/nuc)	Size (bins)	Energy (MeV/nuc)
A/B	xxx_29to32	6	14 – 538	6	14 – 538	6	14 – 538
	xxx_32to50	6	14 – 538	6	14 – 538	6	14 – 538
	xxx_Al	11	10 – 476	11	10 – 476	11	10 – 476
	xxx_Ar	11	11 – 484	11	11 – 484	11	11 – 484
	xxx_C	12	6 – 463	12	6 – 463	12	6 – 463
	xxx_Ca	11	11 – 484	11	11 – 484	11	11 – 484
	xxx_Cr	12	11 – 495	12	11 – 495	12	11 – 495
	xxx_Electrons	15	0 – 433	15	0 – 433	15	0 – 433
	xxx_Fe	11	14 – 495	11	14 – 495	11	14 – 495
	xxx_H	11	4 – 447	11	4 – 447	11	4 – 447
	xxx_He	12	4 – 450	12	4 – 450	12	4 – 450
	xxx_Mg	11	10 – 476	11	10 – 476	11	10 – 476
	xxx_N	12	6 – 463	12	6 – 463	12	6 – 463
	xxx_Na	11	8 – 469	11	8 – 469	11	8 – 469
	xxx_Ne	11	8 – 469	11	8 – 469	11	8 – 469
	xxx_Ni	12	14 – 507	12	14 – 507	12	14 – 507
	xxx_O	11	7 – 463	11	7 – 463	11	7 – 463
	xxx_S	12	10 – 484	12	10 – 484	12	10 – 484
	xxx_Si	11	10 – 476	11	10 – 476	11	10 – 476
	xxx_gt50	6	14 – 538	6	14 – 538	6	14 – 538

Table 2.3.14: PSP\_ISOIS-EPIHI\_HET-RATES60 (contd.). Here, ‘xxx’ stands for R1A and R1B.

Side	Species	Count		Flux		Count Rate	
		Size (bins)	Energy (MeV/nuc)	Size (bins)	Energy (MeV/nuc)	Size (bins)	Energy (MeV/nuc)
A/B	xxx_29to32	5	23 – 538	5	23 – 538	5	23 – 538
	xxx_32to50	5	23 – 538	5	23 – 538	5	23 – 538
	xxx_Al	11	14 – 495	11	14 – 495	11	14 – 495
	xxx_Ar	11	19 – 521	11	19 – 521	11	19 – 521
	xxx_C	11	10 – 476	11	10 – 476	11	10 – 476
	xxx_Ca	11	19 – 521	11	19 – 521	11	19 – 521
	xxx_Cr	12	19 – 538	12	19 – 538	12	19 – 538
	xxx_Electrons	15	0 – 433	15	0 – 433	15	0 – 433
	xxx_Fe	11	23 – 538	11	23 – 538	11	23 – 538
	xxx_H	11	6 – 457	11	6 – 457	11	6 – 457
	xxx_He	12	6 – 463	12	6 – 463	12	6 – 463
	xxx_He_BIN xxx_He_BIN (MASS)	4x16 (4) 16 bins 0 – 15 seg	16 – 46 – –	– – –	– – –	– – –	– – –
	xxx_Mg	11	14 – 495	11	14 – 495	11	14 – 495
	xxx_N	11	10 – 476	11	10 – 476	11	10 – 476
	xxx_Na	11	14 – 495	11	14 – 495	11	14 – 495
	xxx_Ne	11	14 – 495	11	14 – 495	11	14 – 495
	xxx_Ne_BIN xxx_Ne_BIN (MASS)	4x8 (4) 8 bins 0 – 7 seg	32 – 92 – –	– – –	– – –	– – –	– – –
	xxx_Ni	11	23 – 538	11	23 – 538	11	23 – 538
	xxx_O	11	11 – 484	11	11 – 484	11	11 – 484
	xxx_S	12	16 – 521	12	16 – 521	12	16 – 521
xxx_Si	11	16 – 507	11	16 – 507	11	16 – 507	
xxx_gt50	5	23 – 538	5	23 – 538	5	23 – 538	

Table 2.3.15: PSP\_ISOIS-EPIHI\_L2-HET-RATES60 (contd.). Here, ‘xxx’ stands for R2A and R2B.

Side	Species	Count		Flux		Count Rate	
		Size (bins)	Energy (MeV/nuc)	Size (bins)	Energy (MeV/nuc)	Size (bins)	Energy (MeV/nuc)
A/B	xxx_29to32	5	38 – 612	5	38 – 612	5	38 – 612
	xxx_32to50	5	38 – 612	5	38 – 612	5	38 – 612
	xxx_Al	9	23 – 507	9	23 – 507	9	23 – 507
	xxx_Ar	9	32 – 538	9	32 – 538	9	32 – 538
	xxx_C	9	16 – 484	9	16 – 484	9	16 – 484
	xxx_Ca	9	32 – 538	9	32 – 538	9	32 – 538
	xxx_Cr	10	32 – 559	10	32 – 559	10	32 – 559
	xxx_Electrons	13	1 – 433	13	1 – 433	13	1 – 433
	xxx_Fe	10	32 – 559	10	32 – 559	10	32 – 559
	xxx_H	10	8 – 463	10	8 – 463	10	8 – 463
	xxx_He	11	8 – 469	11	8 – 469	11	8 – 469
	xxx_He_BIN xxx_He_BIN (MASS)	4x16 (4) 16 bins 0 – 15 seg	23 – 65 – –	– – –	– – –	– – –	– – –
	xxx_Mg	9	23 – 507	9	23 – 507	9	23 – 507
	xxx_N	9	16 – 484	9	16 – 484	9	16 – 484
	xxx_Na	10	19 – 507	10	19 – 507	10	19 – 507
	xxx_Ne	10	19 – 507	10	19 – 507	10	19 – 507
	xxx_Ne_BIN xxx_Ne_BIN (MASS)	4x8 (4) 8 bins 0 – 7 seg	46 – 130 – –	– – –	– – –	– – –	– – –
	xxx_Ni	10	32 – 559	10	32 – 559	10	32 – 559
	xxx_O	9	19 – 495	9	19 – 495	9	19 – 495
	xxx_S	10	27 – 538	10	27 – 538	10	27 – 538
xxx_Si	9	27 – 521	9	27 – 521	9	27 – 521	
xxx_gt50	5	38 – 612	5	38 – 612	5	38 – 612	

Table 2.3.16: PSP\_ISOIS-EPIHI\_L2-HET-RATES60 (contd.). Here, ‘xxx’ stands for R3A and R3B.

Side	Species	Count		Flux		Count Rate	
		Size (bins)	Energy (MeV/nuc)	Size (bins)	Energy (MeV/nuc)	Size (bins)	Energy (MeV/nuc)
A/B	xxx_29to32	5	38 – 612	5	38 – 612	5	38 – 612
	xxx_32to50	5	38 – 612	5	38 – 612	5	38 – 612
	xxx_Al	9	27 – 521	9	27 – 521	9	27 – 521
	xxx_Ar	8	38 – 538	8	38 – 538	8	38 – 538
	xxx_C	9	19 – 495	9	19 – 495	9	19 – 495
	xxx_Ca	8	38 – 538	8	38 – 538	8	38 – 538
	xxx_Cr	9	38 – 559	9	38 – 559	9	38 – 559
	xxx_Electrons	12	1 – 434	12	1 – 434	12	1 – 434
	xxx_Fe	8	45 – 559	8	45 – 559	8	45 – 559
	xxx_H	8	11 – 463	8	11 – 463	8	11 – 463
	xxx_He	9	11 – 469	9	11 – 469	9	11 – 469
	xxx_He_BIN xxx_He_BIN (MASS)	3x16 (3) 16 bins 0 – 15 seg	32 – 65 – –	– – –	– – –	– – –	– – –
	xxx_Mg	9	27 – 521	9	27 – 521	9	27 – 521
	xxx_N	9	19 – 495	9	19 – 495	9	19 – 495
	xxx_Na	8	27 – 507	8	27 – 507	8	27 – 507
	xxx_Ne	8	27 – 507	8	27 – 507	8	27 – 507
	xxx_Ne_BIN xxx_Ne_BIN (MASS)	3x8 (3) 8 bins 0 – 7 seg	65 – 130 – –	– – –	– – –	– – –	– – –
	xxx_Ni	9	45 – 583	9	45 – 583	9	45 – 583
	xxx_O	8	23 – 495	8	23 – 495	8	23 – 495
	xxx_S	9	32 – 538	9	32 – 538	9	32 – 538
xxx_Si	9	32 – 538	9	32 – 538	9	32 – 538	
xxx_gt50	5	38 – 612	5	38 – 612	5	38 – 612	

Table 2.3.17: PSP\_ISOIS-EPIHI\_L2-HET-RATES60 (contd.). Here, ‘xxx’ stands for R4A and R4B.



Side	Species	Count		Flux		Count Rate	
		Size (bins)	Energy (MeV/nuc)	Size (bins)	Energy (MeV/nuc)	Size (bins)	Energy (MeV/nuc)
A/B	xxx_29to32	4	64 – 612	4	64 – 612	4	64 – 612
	xxx_32to50	4	64 – 612	4	64 – 612	4	64 – 612
	xxx_Al	9	32 – 538	9	32 – 538	9	32 – 538
	xxx_Ar	8	45 – 559	8	45 – 559	8	45 – 559
	xxx_C	8	23 – 495	8	23 – 495	8	23 – 495
	xxx_Ca	8	45 – 559	8	45 – 559	8	45 – 559
	xxx_Cr	9	45 – 583	9	45 – 583	9	45 – 583
	xxx_Electrons	11	1 – 435	11	1 – 435	11	1 – 435
	xxx_Fe	8	54 – 583	8	54 – 583	8	54 – 583
	xxx_H	8	14 – 469	8	14 – 469	8	14 – 469
	xxx_He	9	14 – 476	9	14 – 476	9	14 – 476
	xxx_He_BIN xxx_He_BIN (MASS)	3x16 (3) 16 bins 0 - 15 seg	32 – 65 – –	– – –	– – –	– – –	– – –
	xxx_Mg	9	32 – 538	9	32 – 538	9	32 – 538
	xxx_N	8	23 – 495	8	23 – 495	8	23 – 495
	xxx_Na	8	32 – 521	8	32 – 521	8	32 – 521
	xxx_Ne	8	32 – 521	8	32 – 521	8	32 – 521
	xxx_Ne_BIN xxx_Ne_BIN (MASS)	2x8 (2) 8 bins 0 - 7 seg	92 – 130 – –	– – –	– – –	– – –	– – –
	xxx_Ni	9	54 – 612	9	54 – 612	9	54 – 612
	xxx_O	8	27 – 507	8	27 – 507	8	27 – 507
	xxx_S	9	38 – 559	9	38 – 559	9	38 – 559
xxx_Si	8	38 – 538	8	38 – 538	8	38 – 538	
xxx_gt50	4	64 – 612	4	64 – 612	4	64 – 612	

Table 2.3.18: PSP\_ISOIS-EPIHI\_L2-HET-RATES60 (contd.). Here, ‘xxx’ stands for R5A and R5B.

Side	Species	Count		Flux		Count Rate	
		Size (bins)	Energy (MeV/nuc)	Size (bins)	Energy (MeV/nuc)	Size (bins)	Energy (MeV/nuc)
A/B	xxx_29to32	4	64 – 612	4	64 – 612	4	64 – 612
	xxx_32to50	4	64 – 612	4	64 – 612	4	64 – 612
	xxx_Al	8	38 – 538	8	38 – 538	8	38 – 538
	xxx_Ar	9	45 – 583	9	45 – 583	9	45 – 583
	xxx_C	8	27 – 507	8	27 – 507	8	27 – 507
	xxx_Ca	9	45 – 583	9	45 – 583	9	45 – 583
	xxx_Cr	10	45 – 612	10	45 – 612	10	45 – 612
	xxx_Electrons	11	1 – 435	11	1 – 435	11	1 – 435
	xxx_Fe	9	54 – 612	9	54 – 612	9	54 – 612
	xxx_H	8	14 – 469	8	14 – 469	8	14 – 469
	xxx_He	9	14 – 476	9	14 – 476	9	14 – 476
	xxx_He_BIN xxx_He_BIN (MASS)	3x16 (3) 16 bins 0 – 15 seg	32 – 65 – –	– – –	– – –	– – –	– – –
	xxx_Mg	8	38 – 538	8	38 – 538	8	38 – 538
	xxx_N	8	27 – 507	8	27 – 507	8	27 – 507
	xxx_Na	8	38 – 538	8	38 – 538	8	38 – 538
	xxx_Ne	8	38 – 538	8	38 – 538	8	38 – 538
	xxx_Ne_BIN xxx_Ne_BIN (MASS)	3x8 (3) 8 bins 0 – 7 seg	92 – 184 – –	– – –	– – –	– – –	– – –
	xxx_Ni	9	54 – 612	9	54 – 612	9	54 – 612
	xxx_O	8	32 – 521	8	32 – 521	8	32 – 521
	xxx_S	9	45 – 583	9	45 – 583	9	45 – 583
xxx_Si	8	45 – 559	8	45 – 559	8	45 – 559	
xxx_gt50	4	64 – 612	4	64 – 612	4	64 – 612	

Table 2.3.19: PSP\_ISOIS-EPIHI\_L2-HET-RATES60 (contd.). Here, ‘xxx’ stands for R6A and R6B.

Side	Species	Count		Flux		Count Rate	
		Size (bins)	Energy (MeV/nuc)	Size (bins)	Energy (MeV/nuc)	Size (bins)	Energy (MeV/nuc)
A/B	xxx_29to32	4	64 – 612	4	64 – 612	4	64 – 612
	xxx_32to50	4	64 – 612	4	64 – 612	4	64 – 612
	xxx_Al	8	45 – 559	8	45 – 559	8	45 – 559
	xxx_Ar	7	64 – 583	7	64 – 583	7	64 – 583
	xxx_C	7	32 – 507	7	32 – 507	7	32 – 507
	xxx_Ca	7	64 – 583	7	64 – 583	7	64 – 583
	xxx_Cr	8	64 – 612	8	64 – 612	8	64 – 612
	xxx_Electrons	11	1 – 436	11	1 – 436	11	1 – 436
	xxx_Fe	8	64 – 612	8	64 – 612	8	64 – 612
	xxx_H	8	16 – 476	8	16 – 476	8	16 – 476
	xxx_He	9	16 – 484	9	16 – 484	9	16 – 484
	xxx_He_BIN xxx_He_BIN (MASS)	2x16 (2) 16 bins 0 - 15 seg	46 – 65 – –	– – –	– – –	– – –	– – –
	xxx_Mg	8	45 – 559	8	45 – 559	8	45 – 559
	xxx_N	7	32 – 507	7	32 – 507	7	32 – 507
	xxx_Na	8	38 – 538	8	38 – 538	8	38 – 538
	xxx_Ne	8	38 – 538	8	38 – 538	8	38 – 538
	xxx_Ne_BIN xxx_Ne_BIN (MASS)	3x8 (3) 8 bins 0 - 7 seg	92 – 184 – –	– – –	– – –	– – –	– – –
	xxx_Ni	8	64 – 612	8	64 – 612	8	64 – 612
	xxx_O	7	38 – 521	7	38 – 521	7	38 – 521
	xxx_S	8	54 – 583	8	54 – 583	8	54 – 583
xxx_Si	7	54 – 559	7	54 – 559	7	54 – 559	
xxx_gt50	4	64 – 612	4	64 – 612	4	64 – 612	

Table 2.3.20: PSP\_ISOIS-EPIHI\_L2-HET-RATES60 (contd.). Here, ‘xxx’ stands for R7A and R7B.

**2.3.5 FILE: PSP\_ISOIS-EPIHI\_L2-LET1-RATES10**

This file contains the 10-second cadence data of particle Counts, Flux ( $\text{cm}^{-2} \text{sr}^{-1} \text{sec}^{-1} \text{MeV}^{-1}$ ) and Count Rate (counts/s) for Electrons, H and He ions for various ranges (R1 – R7) of the Low Energy Telescope (LET1), for sides A and B. The measured values are summarized in Table 2.3.21. The variable names follow the pattern: <side>\_<species>\_<quantity>, where, <side> stands for A or B; <species> stands for the particle species; and <quantity> represents Counts (not used in the variable names, in general), Flux or Count Rate, for variables independent of range (R1, R2, etc.). The variables for different ranges has the structure: <range><side>\_<species>\_<quantity>. For electrons, the structure is: <Electrons>\_<range><side>. Variable names without ranges (e.g., A\_C) or with double digit range (e.g., R17) have the values integrated over all the available ranges (e.g., R1 to R7, in general).

Examples: A\_Fe (measured quantity is “count”); Electrons\_R6B\_Rate; and R1A\_He\_Rate.

Side	Range	Quantity	Electrons		H		He	
			E-bins	E-range (MeV/nuc) (bins)	E-bins	E-range (MeV/nuc) (bins)	E-bins	E-range (MeV/nuc) (bins)
A/B	R1	Count			16	1 - 12 (16)	20	1 - 25 (20)
		Flux			16	1 - 12 (16)	20	1 - 25 (20)
		Count Rate			16	1 - 12 (16)	20	1 - 25 (20)
		Count			8	1 - 3 (8)	8	1 - 3 (8)
		Flux			8	1 - 3 (8)	8	1 - 3 (8)
		Count Rate			8	1 - 3 (8)	8	1 - 3 (8)
		Count			13	2 - 12 (13)	13	2 - 15 (13)
		Flux			13	2 - 12 (13)	13	2 - 15 (13)
		Count Rate			13	2 - 12 (13)	13	2 - 15 (13)
	Count	10	1 - 3 (10)					
	Flux							
	Count Rate	10	1 - 3 (10)					
	Count	10	1 - 4 (10)					
	Flux							
	Count Rate	10	1 - 4 (10)					
	Count	9	1 - 4 (9)					
	Flux							
	Count Rate	9	1 - 4 (9)					
	Count	8	2 - 5 (8)				3	21 - 29 (3)
	Flux						3	21 - 29 (3)
	Count Rate	8	2 - 5 (8)				3	21 - 29 (3)
	Count							
	Flux							
	Count Rate							

Table 2.3.21: PSP\_ISOIS-EPIHI\_L2-LET1-RATES10. The LET1 10 s data of various energetic particle species.

### 2.3.6 FILE: PSP\_ISOIS-EPIHI\_L2-LET1-RATES300

This file contains the 300 s cadence data of particle Counts, Flux ( $\text{cm}^{-2} \text{sr}^{-1} \text{sec}^{-1} \text{MeV}^{-1}$ ) and Count Rate (counts/s) for various particle species for ranges R1 & R26 (integrated over ranges R2 to R6) measured by the Low Energy Telescope (LET1), for sides A and B. The measured values are summarized in Table 2.3.22. The variable nomenclature is:  $\langle \text{range} \rangle \langle \text{side} \rangle \_ \langle \text{species} \rangle \_ \langle \text{quantity} \rangle$ , where,  $\langle \text{range} \rangle$  denotes the range (R1 to R7),  $\langle \text{side} \rangle$  stands for A or B;  $\langle \text{species} \rangle$  takes one of the particle species; and  $\langle \text{quantity} \rangle$  represents Counts (not used in variable names, in general), Flux or Count Rate. Variable names without ranges (e.g., A\_C) or with double digit range (e.g., R26) have the values integrated over all the available ranges (e.g., R2 to R6).

Examples: R1B\_NetoSi\_SECT\_Rate; R26A\_CNO\_SECT\_Flux.

Side	Range	Quantity	CNO_SECT			FeGroup_SECT			NetoSi_SECT		
			E-bins	E-range (MeV/nuc)	Sectors (bins)	E-bins	E-range (MeV/nuc)	Sectors (bins)	E-bins	E-range (MeV/nuc)	Sectors (bins)
A/B	R1	Count	1	3 - 3	0 - 8 (9)	1	3 - 3	0 - 8 (9)	1	3 - 3	0 - 8 (9)
		Flux	1	3 - 3	0 - 8 (9)	1	3 - 3	0 - 8 (9)	1	3 - 3	0 - 8 (9)
		Count Rate	1	3 - 3	0 - 8 (9)	1	3 - 3	0 - 8 (9)	1	3 - 3	0 - 8 (9)
A/B	R26	Count	3	6 - 24	0 - 24 (25)	3	6 - 24	0 - 24 (25)	3	6 - 24	0 - 24 (25)
		Flux	3	6 - 24	0 - 24 (25)	3	6 - 24	0 - 24 (25)	3	6 - 24	0 - 24 (25)
		Count Rate	3	6 - 24	0 - 24 (25)	3	6 - 24	0 - 24 (25)	3	6 - 24	0 - 24 (25)
R1 ENB_SECT - measured quantity is Counts; Size 3 x 9; E-bins: 3; E-range: 1 - 2 (MeV/nuc); Sectors: 0 - 8 (9).											
R26 ENB_SECT - measured quantity is Counts; Size 4 x 25; E-bins: 4; E-range: 2 - 12 (MeV/nuc); Sectors: 0 - 24 (25).											

Table 2.3.22: PSP\_ISOIS-EPIHI\_L2-LET1-RATES300. The LET1 300 s cadence measurements of various energetic particle species for ranges R1 and integrated over ranges R2 – R6 (R26).

### 2.3.7 FILE: PSP\_ISOIS-EPIHI\_L2-LET1-RATES3600

This file contains the 3600 s cadence measurements of particle Counts, Count Rate (counts/sec) and Flux ( $\text{cm}^{-2} \text{sr}^{-1} \text{sec}^{-1} \text{MeV}^{-1}$ ) for Al, Ar, C, Ca, Cr, Fe, H, He, Mg, N, Na, Ne, Ni, O, S and Si by the Low Energy Telescope (LET1), for sides A and B for different ranges (R1 – R6). The measured values are summarized in Tables 2.3.23 – 2.3.32 and the variables are named as:  $\langle \text{side} \rangle \_ \langle \text{species} \rangle \_ \langle \text{quantity} \rangle$ . Here,  $\langle \text{side} \rangle$  stands for A or B;  $\langle \text{species} \rangle$  stands for the particle species; and  $\langle \text{quantity} \rangle$  represents Counts (not used in variable names, in general), Flux or Rate. Variable names without ranges (e.g., A\_C) or with double digit range (e.g., R35) have their values integrated over all the available ranges (e.g., R3 to R5).

Examples: A\_C\_Flux; PENB\_C\_Rate; R1A\_32to50\_Flux; Electrons\_R5B.

Side	Species	Count		Flux		Count Rate	
		Size (bins)	Energy (MeV/nuc)	Size (bins)	Energy (MeV/nuc)	Size (bins)	Energy (MeV/nuc)
A/B	Al	28	1 – 118	28	1 – 118	28	1 – 118
	Ar	29	1 – 140	29	1 – 140	29	1 – 140
	C	27	1 – 99	27	1 – 99	27	1 – 99
	Ca	30	1 – 140	30	1 – 140	30	1 – 140
	Cr	31	1 – 140	31	1 – 140	31	1 – 140
	Fe	32	1 – 167	32	1 – 167	32	1 – 167
	H	25	1 – 42	25	1 – 42	25	1 – 42
	He	26	1 – 50	26	1 – 50	26	1 – 50
	Mg	28	1 – 118	28	1 – 118	28	1 – 118
	N	27	1 – 99	27	1 – 99	27	1 – 118
	Na	28	1 – 118	28	1 – 118	28	1 – 118
	Ne	28	1 – 118	28	1 – 118	28	1 – 118
	Ni	33	1 – 198	33	1 – 198	33	1 – 198
	O	28	1 – 118	28	1 – 118	33	1 – 118
S	29	1 – 140	29	1 – 140	29	1 – 140	
Si	29	1 – 140	29	1 – 140	29	1 – 140	

Table 2.3.23: PSP\_ISOIS-EPIHI\_L2-LET1-RATES3600. The 3600 s cadence LET1 data for various particle species for sides A and B.

Side	Species	Count		Count Rate	
		Size (bins)	Energy (MeV/nuc)	Size (bins)	Energy (MeV/nuc)
A/B	PENx_C	11	23 – 364	11	23 – 364
	PENx_Fe	11	45 – 471	11	45 – 471
	PENx_He	11	11 – 310	11	11 – 310
	PENx_Mg	10	38 – 408	10	38 – 408
	PENx_N	11	23 – 364	11	23 – 364
	PENx_Ne	11	27 – 384	11	27 – 384
	PENx_O	11	27 – 384	11	27 – 384
	PENx_Si	10	38 – 408	11	38 – 408

Table 2.3.24: PSP\_ISOIS-EPIHI\_L2-LET1-RATES3600 (contd.). Here ‘x’ denotes sides A & B.

Side	Species	Count			Flux			Count Rate		
		Size (bins)	Range SECT (bins)	Energy (MeV/nuc)	Size (bins)	Range SECT (bins)	Energy (MeV/nuc)	Size (bins)	Range SECT (bins)	Energy (MeV/nuc)
A/B	xxx_29to32	7	29 – 32	0 – 264	7	29 – 32	0 – 264	7	29 – 32	0 – 264
	xxx_32to50	7	32 – 50	0 – 264	7	32 – 50	0 – 264	7	32 – 50	0 – 264
	xxx_Al	14	–	1 – 260	14	–	1 – 260	14	–	1 – 260
	xxx_Ar	15	–	1 – 261	15	–	1 – 261	15	–	1 – 261
	xxx_C	12	–	1 – 259	12	–	1 – 259	12	–	1 – 259
	xxx_Ca	16	–	1 – 261	16	–	1 – 262	16	–	1 – 261
	xxx_CNO_SECT	1x9 (1 bin)	R1 0 – 8 (9)	3 – 3	1x9 (1 bin)	R1 0 – 8 (9)	3 – 3	1x9 (1 bin)	R1 0 – 8 (9)	3 – 3
	xxx_Cr	17	–	1 – 261	17	–	1 – 261	17	–	1 – 261
	xxx_Fe	17	–	1 – 261	17	–	1 – 261	17	–	1 – 261
	xxx_FeGroup_SECT	1x9 (1 bin)	R1 0 – 8 (9)	3 – 3	1x9 (1 bin)	R1 0 – 8 (9)	3 – 3	1x9 (1 bin)	R1 0 – 8 (9)	3 – 3
	xxx_H	12	–	0 – 258	12	–	0 – 258	12	–	0 – 258
	xxx_H_SECT	1x9 (1 bin)	R1 0 – 8 (9)	2 – 2	1x9 (1 bin)	R1 0 – 8 (9)	2 – 2	1x9 (1 bin)	R1 0 – 8 (9)	2 – 2
	xxx_He	12	–	0 – 258	12	–	0 – 258	12	–	0 – 258
	xxx_He_SECT	1x9 (1 bin)	R1 0 – 8 (9)	2 – 2	1x9 (1 bin)	R1 0 – 8 (9)	2 – 2	1x9 (1 bin)	R1 0 – 8 (9)	2 – 2
	xxx_He_BIN xxx_He_BIN (MASS)	5x16 (5) 16 bins 0 – 15 seg	– – –	1 – 3 – –	– – –	– – –	– – –	– – –	– – –	– – –
	xxx_Mg	14	–	1 – 260	14	–	1 – 260	14	–	1 – 260
	xxx_N	12	–	1 – 259	12	–	1 – 259	12	–	1 – 259
	xxx_Na	13	–	1 – 259	13	–	1 – 259	12	–	1 – 259
	xxx_Ne	13	–	1 – 259	13	–	1 – 259	13	–	1 – 259
	xxx_Ne_BIN xxx_Ne_BIN (MASS)	5x8 (5) 8 bins 0 – 7 seg	– – –	1 – 6 – –	– – –	– – –	– – –	– – –	– – –	– – –
	xxx_Ni	17	–	1 – 261	17	–	1 – 261	17	–	1 – 261
	xxx_O	13	–	1 – 259	13	–	1 – 259	13	–	1 – 259
	xxx_S	15	–	1 – 261	15	–	1 – 261	15	–	1 – 261
	xxx_Si	14	–	1 – 260	14	–	1 – 260	14	–	1 – 260
	xxx_NetoSi_SECT	1x9 (1 bin)	R1 0 – 8 (9)	3 – 3	1x9 (1 bin)	R1 0 – 8 (9)	3 – 3	1x9 (1 bin)	R1 0 – 8 (9)	3 – 3
	xxx_gt50	7	–	0 – 264	7	–	0 – 264	7	–	0 – 264

Table 2.3.25: PSP\_ISOIS-EPIHI\_L2-LET1-RATES3600 (contd.). Here, ‘xxx’ denotes R1A and R1B.

Side	Species	Count		Flux		Count Rate	
		Size (bins)	Energy (MeV/nuc)	Size (bins)	Energy (MeV/nuc)	Size (bins)	Energy (MeV/nuc)
A/B	xxx_29to32	8	1 – 320	8	1 – 320	8	1 – 320
	xxx_32to50	8	1 – 320	8	1 – 320	8	1 – 320
	xxx_Al	18	2 – 279	18	2 – 279	18	2 – 279
	xxx_Ar	20	2 – 288	20	2 – 288	20	2 – 288
	xxx_C	18	1 – 272	18	1 – 272	18	1 – 272
	xxx_Ca	20	2 – 288	20	2 – 288	20	2 – 288
	xxx_Cr	20	2 – 288	20	2 – 288	20	2 – 288
	xxx_Fe	20	2 – 288	20	2 – 288	20	2 – 288
	xxx_H	17	1 – 264	17	1 – 264	17	1 – 264
	xxx_He	17	1 – 266	17	1 – 266	17	1 – 266
	xxx_He_BIN xxx_He_BIN (MASS)	7x16 (7) 16 bins 0 – 15 seg	2 – 16 – –	– – –	– – –	– – –	– – –
	xxx_Mg	18	2 – 279	18	2 – 279	18	2 – 279
	xxx_N	18	1 – 272	18	1 – 272	18	1 – 272
	xxx_Na	18	1 – 275	18	1 – 275	18	1 – 275
	xxx_Ne	18	1 – 275	18	1 – 275	18	1 – 275
	xxx_Ne_BIN xxx_Ne_BIN (MASS)	8x8 (8) 8 bins 0 – 7 seg	3 – 32 – –	– – –	– – –	– – –	– – –
	xxx_Ni	21	2 – 294	21	2 – 294	21	2 – 294
	xxx_O	17	1 – 272	17	1 – 272	17	1 – 272
	xxx_S	20	2 – 288	20	2 – 288	20	2 – 288
	xxx_Si	18	2 – 279	18	2 – 279	18	2 – 279
xxx_gt50	8	1 – 320	8	1 – 320	8	1 – 320	

Table 2.3.26: PSP\_ISOIS-EPIHI\_L2-LET1-RATES3600 (contd.). Here, ‘xxx’ denotes R2A and R2B.



Side	Species	Count		Count Rate	
		Size (bins)	Energy (MeV/nuc)	Size (bins)	Energy (MeV/nuc)
A/B	Electrons_xxx	15	0 – 6	15	0 – 6
	xxx_He_BIN	5x16 (5)	8 – 32	–	–
	xxx_He_BIN (MASS)	16 bins 0 - 15 seg	–	–	–
	xxx_Ne_BIN	6x8 (4)	16 – 92	–	–
	xxx_Ne_BIN (MASS)	8 bins 0 - 7 seg	–	–	–

Table 2.3.27: PSP\_ISOIS-EPIHI\_L2-LET1-RATES3600 (contd.). Here, ‘xxx’ stands for R3A and R3B.

Side	Species	Count		Flux		Count Rate	
		Size (bins)	Energy (MeV/nuc)	Size (bins)	Energy (MeV/nuc)	Size (bins)	Energy (MeV/nuc)
A/B	xxxx_29to32	6	8 – 384	6	8 – 384	6	8 – 384
	xxxx_32to50	6	8 – 384	6	8 – 384	6	8 – 384
	xxxx_Al	13	8 – 310	13	8 – 310	13	8 – 310
	xxxx_Ar	13	10 – 320	13	10 – 320	13	10 – 320
	xxxx_C	14	5 – 294	14	5 – 294	14	5 – 294
	xxxx_Ca	14	10 – 332	14	10 – 332	14	10 – 332
	xxxx_Cr	14	10 – 332	14	10 – 332	14	10 – 332
	xxxx_Fe	14	10 – 332	14	10 – 332	14	10 – 332
	xxxx_H	13	3 – 275	13	3 – 275	13	3 – 275
	xxxx_He	14	3 – 279	14	3 – 279	14	3 – 279
	xxxx_Mg	13	8 – 310	13	8 – 310	13	8 – 310
	xxxx_N	14	5 – 294	14	5 – 294	14	5 – 294
	xxxx_Na	14	7 – 310	14	7 – 310	14	7 – 310
	xxxx_Ne	14	7 – 310	14	7 – 310	14	7 – 310
	xxxx_Ni	15	10 – 347	15	10 – 347	15	10 – 347
	xxxx_O	14	6 – 301	14	6 – 301	14	6 – 301
	xxxx_S	13	10 – 320	13	10 – 320	13	10 – 320
	xxxx_Si	14	8 – 320	14	8 – 320	14	8 – 320
xxxx_gt50	6	8 – 384	6	8 – 384	6	8 – 384	

Table 2.3.28: PSP\_ISOIS-EPIHI\_L2-LET1-RATES3600 (contd.). Here, ‘xxxx’ stands for R35A and R35B which implies the values are integratd over ranges R3 – R5 for sides A and B.

Side	Species	Count		Count Rate	
		Size (bins)	Energy (MeV/nuc)	Size (bins)	Energy (MeV/nuc)
A/B	Electrons_xxx	16	0 – 7	16	0 – 7

Table 2.3.29: PSP\_ISOIS-EPIHI\_L2-LET1-RATES3600 (contd.). Here, ‘xxx’ stands for R4A and R4B.

Side	Species	Count		Count Rate	
		Size (bins)	Energy (MeV/nuc)	Size (bins)	Energy (MeV/nuc)
A/B	Electrons_xxx	15	1 – 7	15	1 – 7

Table 2.3.30: PSP\_ISOIS-EPIHI\_L2-LET1-RATES3600 (contd.). Here, ‘xxx’ stands for R5A and R5B.

Side	Species	Count	
		Size (bins)	Energy (MeV/nuc)
A/B	xxxx_He_BIN xxxx_He_BIN (MASS)	5x16 (5) 16 bins 0 - 15 seg	16 – 92
	xxxx_Ne_BIN xxxx_Ne_BIN (MASS)	6x8 (6) 8 bins 0 - 7 seg	16 – 92

Table 2.3.31: PSP\_ISOIS-EPIHI\_L2-LET1-RATES3600 (contd.). Here, ‘xxxx’ stands for R45A and R45B and the values are integrated over ranges R4 – R5.

Side	Species	Count		Flux		Count Rate	
		Size (bins)	Energy (MeV/nuc)	Size (bins)	Energy (MeV/nuc)	Size (bins)	Energy (MeV/nuc)
A/B	xxx_29to32	4	32 – 384	4	32 – 384	4	32 – 384
	xxx_32to50	4	32 – 384	4	32 – 384	4	32 – 384
	xxx_Al	8	23 – 320	8	23 – 320	8	23 – 320
	xxx_Ar	7	32 – 332	7	32 – 332	7	32 – 332
	xxx_C	9	16 – 310	9	16 – 310	9	16 – 310
	xxx_Ca	7	32 – 332	7	32 – 332	7	32 – 332
	xxx_Cr	7	32 – 332	7	32 – 332	7	32 – 332
	Electrons_xxx	13	1 – 7	–	–	13	1 – 7
	xxx_Fe	7	38 – 347	7	38 – 347	7	38 – 347
	xxx_H	8	8 – 279	8	8 – 279	8	8 – 279
	xxx_He	9	8 – 283	9	8 – 283	9	8 – 283
	xxx_He_BIN	3x16 (3)	23 – 46	–	–	–	–
	xxx_He_BIN (MASS)	16 bins	–	–	–	–	–
		0 - 15 seg	–	–	–	–	–
	xxx_Mg	8	23 – 320	8	23 – 320	8	23 – 320
	xxx_N	9	16 – 310	9	16 – 310	9	16 – 310
	xxx_Na	9	19 – 320	9	19 – 320	9	19 – 320
	xxx_Ne	9	19 – 320	9	19 – 320	9	19 – 320
	xxx_Ne_BIN	3x8 (3)	46 – 92	–	–	–	–
	xxx_Ne_BIN (MASS)	8 bins	–	–	–	–	–
	0 - 7 seg	–	–	–	–	–	
xxx_Ni	8	38 – 364	8	38 – 364	8	38 – 364	
xxx_O	9	19 – 320	9	19 – 320	9	19 – 320	
xxx_S	7	32 – 332	7	32 – 332	7	32 – 332	
xxx_Si	8	27 – 332	8	27 – 332	8	27 – 332	
xxx_gt50	4	32 – 384	4	32 – 384	4	32 – 384	

Table 2.3.32: PSP\_ISOIS-EPIHI\_L2-LET1-RATES3600 (contd.). Here, ‘xxx’ stands for R6A and R6B.

### 2.3.8 FILE: PSP\_ISOIS-EPIHI\_L2-LET1-RATES60

This file contains the LET1 (Low Energy Telescope) 60 s cadence measurements of particle Counts, Flux ( $\text{cm}^{-2} \text{sr}^{-1} \text{sec}^{-1} \text{MeV}^{-1}$ ) and Count Rate (counts/s) of Al, Ar, C, Ca, Cr, Fe, H, He, Mg, N, Na, Ne, Ni, O, S and Si for sides A and B. The values of these variables are summarized in Tables 2.3.33 – 2.3.29. The variables are named as: <side>\_<species>\_<quantity>, where, <side> stands for A or B; <species> stands for the particle species; and <quantity> represents Count, Flux or Rate (“Count” is not used in the variable names, in general). Variable names without ranges (e.g. A\_C) or with double digit range (e.g. R35) have the values integrated over all the available ranges (e.g. R3 to R5).

Examples: A\_C\_Flux, PENB\_C\_Rate, R1A\_32to50\_Flux.

Side	Species	Counts		Flux		Count Rate	
		Size (bins)	Energy (MeV/nuc)	Size (bins)	Energy (MeV/nuc)	Size (bins)	Energy (MeV/nuc)
A/B	Al	28	1 – 118	28	1 – 118	28	1 – 118
	Ar	29	1 – 140	29	1 – 140	29	1 – 140
	C	27	1 – 99	27	1 – 99	27	1 – 99
	Ca	30	1 – 140	30	1 – 140	30	1 – 140
	Cr	31	1 – 140	31	1 – 140	31	1 – 140
	Fe	32	1 – 167	32	1 – 167	32	1 – 167
	H	25	1 – 42	25	1 – 42	25	1 – 42
	He	26	1 – 50	26	1 – 50	26	1 – 50
	Mg	28	1 – 118	28	1 – 118	28	1 – 118
	N	27	1 – 99	27	1 – 99	27	1 – 99
	Na	28	1 – 118	28	1 – 118	28	1 – 118
	Ne	28	1 – 118	28	1 – 118	28	1 – 118
	Ni	33	1 – 198	33	1 – 198	33	1 – 198
	O	28	1 – 118	28	2 – 118	28	1 – 118
	S	29	1 – 140	29	1 – 140	29	1 – 140
Si	29	1 – 140	29	1 – 140	29	1 – 140	

Table 2.3.33: PSP\_ISOIS-EPIHI\_L2-LET1-RATES60. The LET1 measurements of different particle species at a cadence of 60 s for sides A and B.

Side	Species	Count		Count Rate	
		Size (bins)	Energy (MeV/nuc)	Size (bins)	Energy (MeV/nuc)
A/B	PENx_C	9	45 – 583	9	45 – 583
	PENx_Fe	9	108 – 793	9	108 – 793
	PENx_H	9	27 – 521	9	27 – 521
	PENx_He	9	27 – 521	9	27 – 521
	PENx_Mg	9	64 – 646	9	64 – 646
	PENx_N	9	45 – 583	9	45 – 583
	PENx_Ne	8	64 – 612	8	64 – 612
	PENx_O	9	54 – 612	9	54 – 612
	PENx_Si	9	76 – 687	9	76 – 687

Table 2.3.34: PSP\_ISOIS-EPIHI\_L2-LET1-RATES60 (contd.). Here, ‘x’ stands for sides A & B.

Side	Species	Count			Flux			Count Rate		
		Size (bins)	Range SECT (bins)	Energy (MeV/nuc)	Size (bins)	Range SECT (bins)	Energy (MeV/nuc)	Size (bins)	Range SECT (bins)	Energy (MeV/nuc)
A/B	xxx_29to32	7	–	0 – 264	7	–	0 – 264	7	–	0 – 264
	xxx_32to50	7	–	0 – 264	7	–	0 – 264	7	–	0 – 264
	xxx_Al	14	–	1 – 260	14	–	1 – 260	14	–	1 – 260
	xxx_Ar	15	–	1 – 261	15	–	1 – 261	15	–	1 – 261
	xxx_C	12	–	1 – 259	12	–	1 – 259	12	–	1 – 259
	xxx_Ca	16	–	1 – 261	16	–	1 – 261	16	–	1 – 261
	xxx_Cr	17	–	1 – 261	17	–	1 – 261	17	–	1 – 261
	xxx_Fe	17	–	1 – 261	17	–	1 – 261	17	–	1 – 261
	xxx_H	12	–	0 – 258	12	–	0 – 258	12	–	0 – 258
	xxx_H_SECT	1x9 (1 bin)	R1 0 – 8 (9)	2 – 2	1x9 (1 bin)	R1 0 – 8 (9)	2 – 2	1x9 (1 bin)	R1 0 – 8 (9)	2 – 2
	xxx_He	12	–	0 – 258	12	–	0 – 258	12	–	0 – 258
	xxx_He_SECT	1x9 (1 bin)	R1 0 – 8 (9)	2 – 2	1x9 (1 bin)	R1 0 – 8 (9)	2 – 2	1x9 (1 bin)	R1 0 – 8 (9)	2 – 2
	xxx_Mg	14	–	1 – 260	14	–	1 – 260	14	–	1 – 260
	xxx_N	12	–	1 – 259	12	–	1 – 259	12	–	1 – 259
	xxx_Na	13	–	1 – 259	13	–	1 – 259	13	–	1 – 259
	xxx_Ne	13	–	1 – 259	13	–	1 – 259	13	–	1 – 259
	xxx_Ni	17	–	1 – 261	17	–	1 – 261	17	–	1 – 261
	xxx_O	13	–	1 – 259	13	–	1 – 259	13	–	1 – 259
	xxx_S	15	–	1 – 259	15	–	1 – 259	15	–	1 – 259
	xxx_Si	14	–	1 – 260	14	–	1 – 260	14	–	1 – 260
xxx_gt50	7	–	0 – 264	7	–	0 – 264	7	–	0 – 264	

Table 2.3.35: PSP\_ISOIS-EPIHI\_L2-LET1-RATES60 (contd.). Here, ‘xxx’ stands for R1A and R1B.

Side	Species	Count			Flux (1/cm <sup>2</sup> sr sec MeV)			Count Rate		
		Size (bins)	Range SECT (bins)	Energy (MeV/nuc)	Size (bins)	Range SECT (bins)	Energy (MeV/nuc)	Size (bins)	Range SECT (bins)	Energy (MeV/nuc)
	xxxx_H_SECT	3x25 (3 bins)	R26 0 – 24 (25)	3 – 12	3x25 (3 bins)	R26 0 – 24	3 – 12	3x25 (3 bins)	R26 0 – 24 (25)	3 – 12
A/B	xxxx_He_SECT	3x25 (3 bins)	R26 0 – 24 (25)	3 – 12	3x25 (3 bins)	R26 0 – 24 (25)	3 – 12	3x25 (3 bins)	R26 0 – 24 (25)	3 – 12
	xxxx_ENA_SECT	8 x 25 (8 bins)	R26 0 – 24 (25)	3 – 12 – –	– – –	– – –	– – –	– – –	– – –	– – –

Table 2.3.36: PSP\_ISOIS-EPIHI\_L2-LET1-RATES60 (contd.). Here, ‘xxxx’ stands for R26A and R26B. The variables have values integrated over ranges R2 – R6.

Side	Species	Count		Flux		Count Rate	
		Size (bins)	Energy (MeV/nuc)	Size (bins)	Energy (MeV/nuc)	Size (bins)	Energy (MeV/nuc)
A/B	xxx_29to32	8	1 – 320	8	1 – 320	8	1 – 320
	xxx_32to50	8	1 – 320	8	1 – 320	8	1 – 320
	xxx_Al	18	2 – 279	18	2 – 279	18	2 – 279
	xxx_Ar	20	2 – 288	20	2 – 288	20	2 – 288
	xxx_C	18	1 – 272	18	1 – 272	18	1 – 272
	xxx_Ca	20	2 – 288	20	2 – 288	20	2 – 288
	xxx_Cr	20	2 – 288	20	2 – 288	20	2 – 288
	xxx_Fe	20	2 – 288	20	2 – 288	20	2 – 288
	xxx_H	17	1 – 264	17	1 – 264	17	1 – 264
	xxx_He	17	1 – 266	17	1 – 266	17	1 – 266
	xxx_Mg	18	2 – 279	18	2 – 279	18	2 – 279
	xxx_N	18	1 – 272	18	2 – 272	18	2 – 272
	xxx_Na	18	1 – 275	18	1 – 275	18	1 – 275
	xxx_Ne	18	1 – 275	18	1 – 275	18	1 – 275
	xxx_Ni	21	2 – 294	21	2 – 294	21	2 – 294
	xxx_O	17	1 – 272	17	1 – 272	17	1 – 272
	xxx_S	20	2 – 288	20	2 – 288	20	2 – 288
	xxx_Si	18	2 – 279	18	2 – 279	18	2 – 279
xxx_gt50	8	1 – 320	8	1 – 320	8	1 – 320	

Table 2.3.37: PSP\_ISOIS-EPIHI\_L2-LET1-RATES60 (contd.). Here, ‘xxx’ stands for R2A and R2B.

Side	Species	Count		Flux		Count Rate	
		Size (bins)	Energy (MeV/nuc)	Size (bins)	Energy (MeV/nuc)	Size (bins)	Energy (MeV/nuc)
A/B	xxxx_29to32	6	8 – 384	6	8 – 384	6	8 – 384
	xxxx_32to50	6	8 – 384	6	8 – 384	6	8 – 384
	xxxx_Al	13	8 – 310	13	8 – 310	13	8 – 310
	xxxx_Ar	13	10 – 320	13	10 – 320	13	10 – 320
	xxxx_C	14	5 – 294	14	5 – 294	14	5 – 294
	xxxx_Ca	14	10 – 332	14	10 – 332	14	10 – 332
	xxxx_Cr	14	10 – 332	14	10 – 332	14	10 – 332
	xxxx_Fe	14	10 – 332	14	10 – 332	14	10 – 332
	xxxx_H	13	3 – 275	13	3 – 275	13	3 – 275
	xxxx_He	14	3 – 279	14	3 – 279	14	3 – 279
	xxxx_Mg	13	8 – 310	13	8 – 310	13	8 – 310
	xxxx_N	14	5 – 294	14	5 – 294	14	5 – 294
	xxxx_Na	14	7 – 310	14	7 – 310	14	7 – 310
	xxxx_Ne	14	7 – 310	14	7 – 310	14	7 – 310
	xxxx_Ni	15	10 – 347	15	10 – 347	15	10 – 347
	xxxx_O	14	6 – 301	14	6 – 301	14	6 – 301
	xxxx_S	13	10 – 320	13	10 – 320	13	10 – 320
	xxxx_Si	14	8 – 320	14	8 – 320	14	8 – 320
xxxx_gt50	6	8 – 384	6	8 – 384	6	8 – 384	

Table 2.3.38: PSP\_ISOIS-EPIHI\_L2-LET1-RATES60 (contd.). Here, ‘xxxx’ stands for R35A and R35B. The values are integrated over ranges R3 – R5.

Side	Species	Count		Flux		Count Rate	
		Size (bins)	Energy (MeV/nuc)	Size (bins)	Energy (MeV/nuc)	Size (bins)	Energy (MeV/nuc)
A/B	xxx_29to32	4	32 – 384	4	32 – 384	4	32 – 384
	xxx_32to50	4	32 – 384	4	32 – 384	4	32 – 384
	xxx_Al	8	23 – 320	8	23 – 320	8	23 – 320
	xxx_Ar	7	32 – 332	7	32 – 332	7	32 – 332
	xxx_C	9	16 – 310	9	16 – 310	9	16 – 310
	xxx_Ca	7	32 – 332	7	32 – 332	7	32 – 332
	xxx_Cr	7	32 – 332	7	32 – 332	7	32 – 332
	Electrons_xxx	13	1 – 7	–	–	13	1 – 7
	xxx_Fe	7	38 – 347	7	38 – 347	7	38 – 347
	xxx_H	8	8 – 279	8	8 – 279	8	8 – 279
	xxx_He	9	8 – 283	9	8 – 283	9	8 – 283
	xxx_He_BIN xxx_He_BIN (MASS)	3x16 (3) 16 bins 0 – 15 seg	23 – 46 – –	– – –	– – –	– – –	– – –
	xxx_Mg	8	23 – 320	8	23 – 320	8	23 – 320
	xxx_N	9	16 – 310	9	16 – 310	9	16 – 310
	xxx_Na	9	19 – 320	9	19 – 320	9	19 – 320
	xxx_Ne	9	19 – 320	9	19 – 320	9	19 – 320
	xxx_Ne_BIN xxx_Ne_BIN (MASS)	3x8 (3) 8 bins 0 – 7 seg	46 – 92 – –	– – –	– – –	– – –	– – –
	xxx_Ni	8	38 – 364	8	38 – 364	8	38 – 364
	xxx_O	9	19 – 320	9	19 – 320	9	19 – 320
	xxx_S	7	32 – 332	7	32 – 332	7	32 – 332
xxx_Si	8	27 – 332	8	27 – 332	8	27 – 332	
xxx_gt50	4	32 – 384	4	32 – 384	4	32 – 384	

Table 2.3.39: PSP\_ISOIS-EPIHI\_L2-LET1-RATES60 (contd.). Here, ‘xxx’ stands for R6A and R6B.



**2.3.9 FILE: PSP\_ISOIS-EPIHI\_L2-LET2-RATES10**

This file contains the 10-second cadence data of particle Counts, Flux ( $\text{cm}^{-2} \text{sr}^{-1} \text{sec}^{-1} \text{MeV}^{-1}$ ) and Count Rate (counts/s) for Electrons, H and He ions for various ranges (R1 – R7) of the single-sided (depicted as C) Low Energy Telescope (LET2). Table 2.3.40 summarizes the measured values. The variable names follow the structure: <side>\_<species>\_<quantity>, where, <side> stands for C; <species> stands for the particle species, and <quantity> represents Counts (not used in the variable names, in general), Flux or Rate for those variables independent of range. The variable names for different ranges (R1 – R5) are of the form: <range><side>\_<species>\_<quantity>. For electrons, the structure is: <Electrons>\_<range><side>. Variable names without ranges (e.g., A\_C) or with double digit range (e.g., R17) have the values integrated over all the available ranges (e.g., R1 to R7).

Examples: C\_He (measured quantity is “count”); Electrons\_R3C\_Rate; R1C\_He\_Rate.

Side	Range	Quantity	Electrons		H		He	
			E-bins	E-range (MeV/nuc) (bins)	E-bins	E-range (MeV/nuc) (bins)	E-bins	E-range (MeV/nuc) (bins)
C		Count			16	1 - 12 (16)	20	1 - 25 (20)
		Flux			16	1 - 12 (16)	20	1 - 25 (20)
		Count Rate			16	1 - 12 (16)	20	1 - 25 (20)
	R1	Count			8	1 - 3 (8)	8	1 - 3 (8)
		Flux			8	1 - 3 (8)	8	1 - 3 (8)
		Count Rate			8	1 - 3 (8)	8	1 - 3 (8)
	R2	Count			13	2 - 12 (13)	13	2 - 15 (13)
		Flux			13	2 - 12 (13)	13	2 - 15 (13)
		Count Rate			13	2 - 12 (13)	13	2 - 15 (13)
	R35	Count			5	7 - 15 (5)	9	7 - 29 (9)
		Flux			5	7 - 15 (5)	9	7 - 29 (9)
		Count Rate			5	7 - 15 (5)	9	7 - 29 (9)
	R3	Count	10	1 - 3 (10)				
		Flux						
		Count Rate	10	1 - 3 (10)				
	R4	Count	10	1 - 4 (10)				
		Flux						
		Count Rate	10	1 - 4 (10)				
	R5	Count	9	1 - 4 (9)				
		Flux						
		Count Rate	9	1 - 4 (9)				

Table 2.3.40: PSP\_ISOIS-EPIHI\_L2-LET2-RATES10. The 10 s cadence data of LET2 for various energetic particle species.

**2.3.10 FILE: PSP\_ISOIS-EPIHI\_L2-LET2-RATES300**

This file contains the 300 s cadence data of particle Counts, Flux ( $\text{cm}^{-2} \text{sr}^{-1} \text{sec}^{-1} \text{MeV}^{-1}$ ) and Count Rate (counts/s) for various particle species for ranges R1 & R26 (integrated over Ranges 2 – 6) measured by the single-sided (named C) Low Energy Telescope (LET2). The measured values are summarized in Table 2.3.41. The variable naming is: <range><side>\_<species>\_<quantity>, where, <range> denotes the range (R1 and R26), <side> stands for C; <species> takes one of the particle species; and <quantity> represents Counts (not used in variable names, in general), Flux or Rate. Variable names without ranges (e.g., A\_C) or with double digit range (e.g., R25) have the values integrated over all the available ranges (e.g., R2 to R5).

Examples: R1C\_NetoSi\_SECT\_Rate; R25C\_CNO\_SECT\_Flux.

Side	Range	Quantity	CNO_SECT			FeGroup_SECT			NetoSi_SECT		
			E-bins	E-range (MeV/nuc)	Sectors (bins)	E-bins	E-range (MeV/nuc)	Sectors (bins)	E-bins	E-range (MeV/nuc)	Sectors (bins)
C	R1	Count	1	3 - 3	0 - 8 (9)	1	3 - 3	0 - 8 (9)	1	3 - 3	0 - 8 (9)
		Flux	1	3 - 3	0 - 8 (9)	1	3 - 3	0 - 8 (9)	1	3 - 3	0 - 8 (9)
		Count Rate	1	3 - 3	0 - 8 (9)	1	3 - 3	0 - 8 (9)	1	3 - 3	0 - 8 (9)
C	R26	Count	3	6 - 24	0 - 24 (25)	3	6 - 24	0 - 24 (25)	3	6 - 24	0 - 24 (25)
		Flux	3	6 - 24	0 - 24 (25)	3	6 - 24	0 - 24 (25)	3	6 - 24	0 - 24 (25)
		Count Rate	3	6 - 24	0 - 24 (25)	3	6 - 24	0 - 24 (25)	3	6 - 24	0 - 24 (25)
R1 ENB_SECT – measured quantity is Counts; Size 3 x 9; E-bins: 3; E-range: 1 - 2 (MeV/nuc); Sectors: 0 - 8 (9).											
R26 ENB_SECT – measured quantity is Counts; Size 4 x 25; E-bins: 4; E-range: 2 - 12 (MeV/nuc); Sectors: 0 - 24 (25).											

Table 2.3.41: PSP\_ISOIS-EPIHI\_L2-LET2-RATES300. The LET2 300 s cadence measurements of various energetic particle species for ranges R1 and integrated over ranges R2 – R6 (R26).

**2.3.11 FILE: PSP\_ISOIS-EPIHI\_L2-LET2-RATES3600**

This file contains the 3600 s cadence data of particle Counts, Flux ( $\text{cm}^{-2} \text{sr}^{-1} \text{sec}^{-1} \text{MeV}^{-1}$ ) and Count Rate (counts/s) for Al, Ar, C, Ca, Cr, Fe, H, He, Mg, N, Na, Ne, Ni, O, S and Si by the single sided (depicted as C) Low Energy Telescope (LET2). The measured values of these variables are summarized in Tables 2.3.42 – 2.3.49. The variables are named as: <side>\_<species>\_<quantity>, where, <side> stands for C; <species> represents the particle species; and <quantity> denotes Counts (not used in the variable names, in general), Flux or Rate. Variable names without ranges (e.g. C\_Al) or with double digit range (e.g. R25) have the values integrated over all the available ranges (e.g. R2 to R5).

Examples: C\_Si\_Flux; PENB\_C\_Rate; R1C\_32to50\_Flux; Electrons\_R5C.

Side	Species	Count		Flux		Count Rate	
		Size (bins)	Energy (MeV/nuc)	Size (bins)	Energy (MeV/nuc)	Size (bins)	Energy (MeV/nuc)
C	Al	27	1 – 99	27	1 – 99	27	1 – 99
	Ar	29	1 – 118	28	1 – 118	28	1 – 118
	C	25	1 – 70	25	1 – 70	25	1 – 70
	Ca	30	1 – 140	30	1 – 140	30	1 – 140
	Cr	31	1 – 140	31	1 – 140	31	1 – 140
	Fe	31	1 – 140	31	1 – 140	31	1 – 140
	H	24	1 – 35	24	1 – 35	24	1 – 35
	He	25	1 – 42	25	1 – 42	25	1 – 42
	Mg	27	1 – 99	27	1 – 99	27	1 – 99
	N	25	1 – 70	25	1 – 70	25	1 – 70
	Na	27	1 – 99	27	1 – 99	27	1 – 99
	Ne	27	1 – 99	27	1 – 99	27	1 – 99
	Ni	32	1 – 167	32	1 – 167	32	1 – 167
	O	26	1 – 83	26	1 – 83	26	1 – 83
	S	28	1 – 118	28	1 – 118	28	1 – 118
Si	28	1 – 117	28	1 – 118	28	1 – 118	

Table 2.3.42: PSP\_ISOIS-EPIHI\_L2-LET2-RATES3600. The 3600 s cadence data for various particle species for the single-sided (side C) telescope LET2.

Side	Species	Count		Count Rate	
		Size (bins)	Energy (MeV/nuc)	Size (bins)	Energy (MeV/nuc)
C	PENx_C	11	23 – 364	11	23 – 364
	PENx_Fe	11	45 – 471	11	45 – 471
	PENx_He	11	11 – 310	11	11 – 310
	PENx_Mg	10	38 – 408	10	38 – 408
	PENx_N	11	23 – 364	11	23 – 364
	PENx_Ne	11	27 – 384	11	27 – 384
	PENx_O	11	27 – 384	11	27 – 384
	PENx_Si	10	38 – 408	11	38 – 408

Table 2.3.43: PSP\_ISOIS-EPIHI\_L2-LET2-RATES3600 (contd.). Here, ‘x’ stands for side C.

Side	Species	Count			Flux			Count Rate		
		Size (bins)	Range SECT (bins)	Energy (MeV/nuc)	Size (bins)	Range SECT (bins)	Energy (MeV/nuc)	Size (bins)	Range SECT (bins)	Energy (MeV/nuc)
C	xxx_29to32	7	29 – 32	0 – 264	7	29 – 32	0 – 264	7	29 – 32	0 – 264
	xxx_32to50	7	32 – 50	0 – 264	7	32 – 50	0 – 264	7	32 – 50	0 – 264
	xxx_Al	14	–	1 – 260	14	–	1 – 260	14	–	1 – 260
	xxx_Ar	15	–	1 – 261	15	–	1 – 261	15	–	1 – 261
	xxx_C	12	–	1 – 259	12	–	1 – 259	12	–	1 – 259
	xxx_Ca	16	–	1 – 261	16	–	1 – 262	16	–	1 – 261
	xxx_CNO_SECT	1x9 (1 bin)	R1 0 – 8 (9)	3 – 3	1x9 (1 bin)	R1 0 – 8 (9)	3 – 3	1x9 (1 bin)	R1 0 – 8 (9)	3 – 3
	xxx_Cr	17	–	1 – 261	17	–	1 – 261	17	–	1 – 261
	xxx_Fe	17	–	1 – 261	17	–	1 – 261	17	–	1 – 261
	xxx_FeGroup_SECT	1x9 (1 bin)	R1 0 – 8 (9)	3 – 3	1x9 (1 bin)	R1 0 – 8 (9)	3 – 3	1x9 (1 bin)	R1 0 – 8 (9)	3 – 3
	xxx_H	12	–	0 – 258	12	–	0 – 258	12	–	0 – 258
	xxx_H_SECT	1x9 (1 bin)	R1 0 – 8 (9)	2 – 2	1x9 (1 bin)	R1 0 – 8 (9)	2 – 2	1x9 (1 bin)	R1 0 – 8 (9)	2 – 2
	xxx_He	12	–	0 – 258	12	–	0 – 258	12	–	0 – 258
	xxx_He_SECT	1x9 (1 bin)	R1 0 – 8 (9)	2 – 2	1x9 (1 bin)	R1 0 – 8 (9)	2 – 2	1x9 (1 bin)	R1 0 – 8 (9)	2 – 2
	xxx_He_BIN xxx_He_BIN (MASS)	5x16 (5) 16 bins 0 – 15 seg	– – –	1 – 3 – –	– – –	– – –	– – –	– – –	– – –	– – –
	xxx_Mg	14	–	1 – 260	14	–	1 – 260	14	–	1 – 260
	xxx_N	12	–	1 – 259	12	–	1 – 259	12	–	1 – 259
	xxx_Na	13	–	1 – 259	13	–	1 – 259	12	–	1 – 259
	xxx_Ne	13	–	1 – 259	13	–	1 – 259	13	–	1 – 259
	xxx_Ne_BIN xxx_Ne_BIN (MASS)	5x8 (5) 8 bins 0 – 7 seg	– – –	1 – 6 – –	– – –	– – –	– – –	– – –	– – –	– – –
	xxx_Ni	17	–	1 – 261	17	–	1 – 261	17	–	1 – 261
	xxx_O	13	–	1 – 259	13	–	1 – 259	13	–	1 – 259
	xxx_S	15	–	1 – 261	15	–	1 – 261	15	–	1 – 261
	xxx_Si	14	–	1 – 260	14	–	1 – 260	14	–	1 – 260
xxx_NetoSi_SECT	1x9 (1 bin)	R1 0 – 8 (9)	3 – 3	1x9 (1 bin)	R1 0 – 8 (9)	3 – 3	1x9 (1 bin)	R1 0 – 8 (9)	3 – 3	
xxx_gt50	7	–	0 – 264	7	–	0 – 264	7	–	0 – 264	

Table 2.3.44: PSP\_ISOIS-EPIHI\_L2-LET2-RATES3600 (contd.). Here, ‘xxx’ stands for R1C.

Side	Species	Count			Flux			Count Rate		
		Size (bins)	Range SECT (bins)	Energy (MeV/nuc)	Size (bins)	Range SECT (bins)	Energy (MeV/nuc)	Size (bins)	Range SECT (bins)	Energy (MeV/nuc)
C	xxxx_CNO_SECT	3x25 (3 bins)	R25 0 – 24 (25)	6 – 24	3x25 (3 bins)	R25 0 – 24 (25)	6 – 24	3x25 (3 bins)	R25 0 – 24 (25)	6 – 24
	xxxx_FeGroup_SECT	3x25 (3 bins)	R25 0 – 24 (25)	6 – 24	3x25 (3 bins)	R25 0 – 24 (25)	6 – 24	3x25 (3 bins)	R25 0 – 24 (25)	6 – 24
	xxxx_H_SECT	3x25 (3 bins)	R25 0 – 24 (25)	3 – 12	3x25 (3 bins)	R25 0 – 24 (25)	3 – 12	3x25 (3 bins)	R25 0 – 24 (25)	3 – 12
	xxxx_He_SECT	3x25 (3 bins)	R25 0 – 24 (25)	3 – 12	3x25 (3 bins)	R25 0 – 24 (25)	3 – 12	3x25 (3 bins)	R25 0 – 24 (25)	3 – 12
	xxxx_NetoSi_SECT	3x25 (3 bins)	R25 0 – 24 (25)	6 – 24	3x25 (3 bins)	R25 0 – 24 (25)	6 – 24	3x25 (3 bins)	R25 0 – 24 (25)	6 – 24

Table 2.3.45: PSP\_ISOIS-EPIHI\_L2-LET2-RATES3600 (contd.). Here, ‘xxxx’ stands for R25C and the values are integrated over ranges R2 – R5.

Side	Species	Count		Flux		Count Rate	
		Size (bins)	Energy (MeV/nuc)	Size (bins)	Energy (MeV/nuc)	Size (bins)	Energy (MeV/nuc)
C	xxx_29to32	8	1 – 320	8	1 – 320	8	1 – 320
	xxx_32to50	8	1 – 320	8	1 – 320	8	1 – 320
	xxx_Al	18	2 – 279	18	2 – 279	18	2 – 279
	xxx_Ar	20	2 – 288	20	2 – 288	20	2 – 288
	xxx_C	18	1 – 272	18	1 – 272	18	1 – 272
	xxx_Ca	20	2 – 288	20	2 – 288	20	2 – 288
	xxx_Cr	20	2 – 288	20	2 – 288	20	2 – 288
	xxx_Fe	20	2 – 288	20	2 – 288	20	2 – 288
	xxx_H	17	1 – 264	17	1 – 264	17	1 – 264
	xxx_He	17	1 – 266	17	1 – 266	17	1 – 266
	xxx_He_BIN	7x16 (7)	2 – 16	–	–	–	–
	xxx_He_BIN (MASS)	16 bins	–	–	–	–	–
		0 – 15 seg	–	–	–	–	–
	xxx_Mg	18	2 – 279	18	2 – 279	18	2 – 279
	xxx_N	18	1 – 272	18	1 – 272	18	1 – 272
	xxx_Na	18	1 – 275	18	1 – 275	18	1 – 275
	xxx_Ne	18	1 – 275	18	1 – 275	18	1 – 275
	xxx_Ne_BIN	8x8 (8)	3 – 32	–	–	–	–
	xxx_Ne_BIN (MASS)	8 bins	–	–	–	–	–
		0 – 7 seg	–	–	–	–	–
xxx_Ni	21	2 – 294	21	2 – 294	21	2 – 294	
xxx_O	17	1 – 272	17	1 – 272	17	1 – 272	
xxx_S	20	2 – 288	20	2 – 288	20	2 – 288	
xxx_Si	18	2 – 279	18	2 – 279	18	2 – 279	
xxx_gt50	8	1 – 320	8	1 – 320	8	1 – 320	

Table 2.3.46: PSP\_ISOIS-EPIHI\_L2-LET2-RATES3600 (contd.). Here, ‘xxx’ stands for R2C.

Side	Species	Count		Count Rate	
		Size (bins)	Energy (MeV/nuc)	Size (bins)	Energy (MeV/nuc)
C	Electrons_R3C	15	0 – 6	15	0 – 6
	R3C_He_BIN	5x16 (5)	8 – 32	–	–
	R3C_He_BIN (MASS)	16 bins	–	–	–
		0 – 15 seg	–	–	–
	R3C_Ne_BIN	6x8 (6)	16 – 92	–	–
	R3C_Ne_BIN (MASS)	8 bins	–	–	–
		0 – 7 seg	–	–	–
	Electrons_R4C	16	0 – 7	16	0 – 7
	Electrons_R5C	15	1 – 7	15	1 – 7

Table 2.3.47: PSP\_ISOIS-EPIHI\_L2-LET2-RATES3600 (contd.). LET2 electron measurements for ranges R3, R4 and R5.

Side	Species	Count		Flux		Count Rate	
		Size (bins)	Energy (MeV/nuc)	Size (bins)	Energy (MeV/nuc)	Size (bins)	Energy (MeV/nuc)
C	xxxx_29to32	6	8 – 384	6	8 – 384	6	8 – 384
	xxxx_32to50	6	8 – 384	6	8 – 384	6	8 – 384
	xxxx_Al	13	8 – 310	13	8 – 310	13	8 – 310
	xxxx_Ar	13	10 – 320	13	10 – 320	13	10 – 320
	xxxx_C	14	5 – 294	14	5 – 294	14	5 – 294
	xxxx_Ca	14	10 – 332	14	10 – 332	14	10 – 332
	xxxx_Cr	14	10 – 332	14	10 – 332	14	10 – 332
	xxxx_Fe	14	10 – 332	14	10 – 332	14	10 – 332
	xxxx_H	13	3 – 275	13	3 – 275	13	3 – 275
	xxxx_He	14	3 – 279	14	3 – 279	14	3 – 279
	xxxx_Mg	13	8 – 310	13	8 – 310	13	8 – 310
	xxxx_N	14	5 – 294	14	5 – 294	14	5 – 294
	xxxx_Na	14	7 – 310	14	7 – 310	14	7 – 310
	xxxx_Ne	14	7 – 310	14	7 – 310	14	7 – 310
	xxxx_Ni	15	10 – 347	15	10 – 347	15	10 – 347
	xxxx_O	14	6 – 301	14	6 – 301	14	6 – 301
	xxxx_S	13	10 – 320	13	10 – 320	13	10 – 320
	xxxx_Si	14	8 – 320	14	8 – 320	14	8 – 320
xxxx_gt50	6	8 – 384	6	8 – 384	6	8 – 384	

Table 2.3.48: PSP\_ISOIS-EPIHI\_L2-LET2-RATES3600 (contd.). Here, ‘xxxx’ stands for R35C which implies that the values are integrated over ranges R3 – R5.

Side	Species	Count	
		Size (bins)	Energy (MeV/nuc)
C	xxxx_He_BIN xxxx_He_BIN (MASS)	5x16 (5) 16 bins 0 - 15 seg	8 - 32
	xxxx_Ne_BIN xxxx_Ne_BIN (MASS)	6x8 (6) 6 bins 0 - 7 seg	16 - 92

Table 2.3.49: PSP\_ISOIS-EPIHI\_L2-LET2-RATES3600 (contd.). Here, 'xxxx' stands for R45C and the values presented here are integrated over ranges R4 – R5.

**2.3.12 FILE: PSP\_ISOIS-EPIHI\_L2-LET2-RATES60**

This file contains the 60 s cadence measurements of particle Counts, Flux ( $\text{cm}^{-2} \text{sr}^{-1} \text{sec}^{-1} \text{MeV}^{-1}$ ) and Count Rate (counts/s) of Al, Ar, C, Ca, Cr, Fe, H, He, Mg, N, Na, Ne, Ni, O, S and Si coming from sides A and B made by the Low Energy Telescope (LET1). The values of these variables are summarized in Tables 2.3.33 – 2.3.29. The variables are named as: <side>\_<species>\_<quantity>, where, <side> stands for A or B; <species> stands for the particle species; and <quantity> represents Counts (not used in the variable names, in general), Flux or Rate. Variable names without ranges (e.g. A\_C) or with double digit range (e.g. R25) have the values integrated over all the available ranges (e.g. R2 to R5).  
Examples: A\_C\_Flux; PENB\_C\_Rate; R1A\_32to50\_Flux.

Side	Species	Counts		Flux		Count Rate	
		Size (bins)	Energy (MeV/nuc)	Size (bins)	Energy (MeV/nuc)	Size (bins)	Energy (MeV/nuc)
C	Al	27	1 - 99	27	1 - 99	27	1 - 99
	Ar	28	1 - 118	28	1 - 118	28	1 - 118
	C	25	1 - 70	25	1 - 70	25	1 - 70
	Ca	30	1 - 140	30	1 - 140	30	1 - 140
	Cr	31	1 - 140	31	1 - 140	31	1 - 140
	Fe	31	1 - 140	31	1 - 140	31	1 - 140
	H	24	1 - 35	24	1 - 35	24	1 - 35
	He	25	1 - 42	25	1 - 42	25	1 - 42
	Mg	27	1 - 99	27	1 - 99	27	1 - 99
	N	25	1 - 70	25	1 - 70	25	1 - 70
	Na	27	1 - 99	27	1 - 99	27	1 - 99
	Ne	27	1 - 99	27	1 - 99	27	1 - 99
	Ni	32	1 - 167	32	1 - 167	32	1 - 167
	O	26	1 - 83	26	2 - 83	26	1 - 83
	S	28	1 - 118	28	1 - 118	28	1 - 118
	Si	28	1 - 118	28	1 - 118	28	1 - 118

Table 2.3.50: PSP\_ISOIS-EPIHI\_L2-LET2-RATES60. The 60 s cadence measurements of the single-sided (side C) telescope LET2 for different particle species.

Side	Species	Counts		Count Rate	
		Size (bins)	Energy (MeV/nuc)	Size (bins)	Energy (MeV/nuc)
C	PENx_C	11	23 – 364	11	23 – 364
	PENx_Fe	11	45 – 471	11	45 – 471
	PENx_He	11	11 – 310	11	11 – 310
	PENx_Mg	10	38 – 408	10	38 – 408
	PENx_N	11	23 – 364	11	23 – 364
	PENx_Ne	11	27 – 384	11	27 – 384
	PENx_O	11	27 – 384	11	27 – 384
	PENx_Si	10	38 – 408	11	38 – 408

Table 2.3.51: PSP\_ISOIS-EPIHI\_L2-LET2-RATES60 (contd.). Here ‘x’ stands for side C.

Side	Species	Count			Flux			Count Rate		
		Size (bins)	Range SECT (bins)	Energy (MeV/nuc)	Size (bins)	Range SECT (bins)	Energy (MeV/nuc)	Size (bins)	Range SECT (bins)	Energy (MeV/nuc)
C	xxx_29to32	7	29 – 32	0 – 264	7	29 – 32	0 – 264	7	29 – 32	0 – 264
	xxx_32to50	7	32 – 50	0 – 264	7	32 – 50	0 – 264	7	32 – 50	0 – 264
	xxx_Al	14	–	1 – 260	14	–	1 – 260	14	–	1 – 260
	xxx_Ar	15	–	1 – 261	15	–	1 – 261	15	–	1 – 261
	xxx_C	12	–	1 – 259	12	–	1 – 259	12	–	1 – 259
	xxx_Ca	16	–	1 – 261	16	–	1 – 262	16	–	1 – 261
	xxx_Cr	17	–	1 – 261	17	–	1 – 261	17	–	1 – 261
	xxx_Fe	17	–	1 – 261	17	–	1 – 261	17	–	1 – 261
	xxx_H	12	–	0 – 258	12	–	0 – 258	12	–	0 – 258
	xxx_H_SECT	1x9 (1 bin)	R1 0 – 8 (9)	2 – 2	1x9 (1 bin)	R1 0 – 8 (9)	2 – 2	1x9 (1 bin)	R1 0 – 8 (9)	2 – 2
	xxx_He	12	–	0 – 258	12	–	0 – 258	12	–	0 – 258
	xxx_He_SECT	1x9 (1 bin)	R1 0 – 8 (9)	2 – 2	1x9 (1 bin)	R1 0 – 8 (9)	2 – 2	1x9 (1 bin)	R1 0 – 8 (9)	2 – 2
	xxx_Mg	14	–	1 – 260	14	–	1 – 260	14	–	1 – 260
	xxx_N	12	–	1 – 259	12	–	1 – 259	12	–	1 – 259
	xxx_Na	13	–	1 – 259	13	–	1 – 259	12	–	1 – 259
	xxx_Ne	13	–	1 – 259	13	–	1 – 259	13	–	1 – 259
	xxx_Ni	17	–	1 – 261	17	–	1 – 261	17	–	1 – 261
	xxx_O	13	–	1 – 259	13	–	1 – 259	13	–	1 – 259
	xxx_S	15	–	1 – 261	15	–	1 – 261	15	–	1 – 261
	xxx_Si	14	–	1 – 260	14	–	1 – 260	14	–	1 – 260
	xxx_gt50	7	–	0 – 264	7	–	0 – 264	7	–	0 – 264
R1 ENA_SECT - measured quantity is Counts; Size 8 x 9; E-bins: 8; E-range: 1 - 3 (MeV/nuc); Sectors: 0 - 8 (9).										

Table 2.3.52: PSP\_ISOIS-EPIHI\_L2-LET2-RATES60 (contd.). Here, ‘xxx’ stands for R1C.



Side	Species	Count			Flux			Count Rate		
		Size (bins)	Range SECT (bins)	Energy (MeV/nuc)	Size (bins)	Range SECT (bins)	Energy (MeV/nuc)	Size (bins)	Range SECT (bins)	Energy (MeV/nuc)
C	xxxx_H_SECT	3x25 (3 bins)	R26 0 – 24 (25)	3 – 12	3x25 (3 bins)	R26 0 – 24 (25)	3 – 12	3x25 (3 bins)	R26 0 – 24 (25)	3 – 12
	xxxx_He_SECT	3x25 (3 bins)	R26 0 – 24 (25)	3 – 12	3x25 (3 bins)	R26 0 – 24 (25)	3 – 12	3x25 (3 bins)	R26 0 – 24 (25)	3 – 12
	xxxx_ENA_SECT	8x25 (8 bins)	R26 0 – 24 (25)	2 – 12	–	–	–	–	–	–

Table 2.3.53: PSP\_ISOIS-EPIHI\_L2-LET2-RATES60 (contd.). Here, ‘xxxx’ stands for R25C which implies that the values are integrated over ranges R2 – R5.

Side	Species	Count		Flux		Count Rate	
		Size (bins)	Energy (MeV/nuc)	Size (bins)	Energy (MeV/nuc)	Size (bins)	Energy (MeV/nuc)
A/B	xxx_29to32	8	1 – 320	8	1 – 320	8	1 – 320
	xxx_32to50	8	1 – 320	8	1 – 320	8	1 – 320
	xxx_Al	18	2 – 279	18	2 – 279	18	2 – 279
	xxx_Ar	20	2 – 288	20	2 – 288	20	2 – 288
	xxx_C	18	1 – 272	18	1 – 272	18	1 – 272
	xxx_Ca	20	2 – 288	20	2 – 288	20	2 – 288
	xxx_Cr	20	2 – 288	20	2 – 288	20	2 – 288
	xxx_Fe	20	2 – 288	20	2 – 288	20	2 – 288
	xxx_H	17	1 – 264	17	1 – 264	17	1 – 264
	xxx_He	17	1 – 266	17	1 – 266	17	1 – 266
	xxx_Mg	18	2 – 279	18	2 – 279	18	2 – 279
	xxx_N	18	1 – 272	18	1 – 272	18	1 – 272
	xxx_Na	18	1 – 275	18	1 – 275	18	1 – 275
	xxx_Ne	18	1 – 275	18	1 – 275	18	1 – 275
	xxx_Ni	21	2 – 294	21	2 – 294	21	2 – 294
	xxx_O	17	1 – 272	17	1 – 272	17	1 – 272
	xxx_S	20	2 – 288	20	2 – 288	20	2 – 288
xxx_Si	18	2 – 279	18	2 – 279	18	2 – 279	
xxx_gt50	8	1 – 320	8	1 – 320	8	1 – 320	

Table 2.3.54: PSP\_ISOIS-EPIHI\_L2-LET2-RATES60 (contd.). Here, ‘xxx’ stands for R2C.

Side	Species	Count		Count Rate	
		Size (bins)	Energy (MeV/nuc)	Size (bins)	Energy (MeV/nuc)
C	Electrons_R3C	15	0 – 6	15	0 – 6
	R3C_He_BIN	5x16 (5)	8 – 32	–	–
	R3C_He_BIN (MASS)	16 bins	–	–	–
		0 – 15 seg	–	–	–
	R3C_Ne_BIN	6x8 (6)	16 – 92	–	–
	R3C_Ne_BIN (MASS)	8 bins	–	–	–
		0 – 7 seg	–	–	–
	Electrons_R4C	16	0 – 7	16	0 – 7
	Electrons_R5C	15	1 – 7	15	1 – 7

Table 2.3.55: PSP\_ISOIS-EPIHI\_L2-LET2-RATES60 (contd.). LET2 electron measurements for ranges R3, R4 and R5.

Side	Species	Count		Flux		Count Rate	
		Size (bins)	Energy (MeV/nuc)	Size (bins)	Energy (MeV/nuc)	Size (bins)	Energy (MeV/nuc)
C	xxxx_29to32	6	8 – 384	6	8 – 384	6	8 – 384
	xxxx_32to50	6	8 – 384	6	8 – 384	6	8 – 384
	xxxx_Al	13	8 – 310	13	8 – 310	13	8 – 310
	xxxx_Ar	13	10 – 320	13	10 – 320	13	10 – 320
	xxxx_C	14	5 – 294	14	5 – 294	14	5 – 294
	xxxx_Ca	14	10 – 332	14	10 – 332	14	10 – 332
	xxxx_Cr	14	10 – 332	14	10 – 332	14	10 – 332
	xxxx_Fe	14	10 – 332	14	10 – 332	14	10 – 332
	xxxx_H	13	3 – 275	13	3 – 275	13	3 – 275
	xxxx_He	14	3 – 279	14	3 – 279	14	3 – 279
	xxxx_Mg	13	8 – 310	13	8 – 310	13	8 – 310
	xxxx_N	14	5 – 294	14	5 – 294	14	5 – 294
	xxxx_Na	14	7 – 310	14	7 – 310	14	7 – 310
	xxxx_Ne	14	7 – 310	14	7 – 310	14	7 – 310
	xxxx_Ni	15	10 – 347	15	10 – 347	15	10 – 347
	xxxx_O	14	6 – 301	14	6 – 301	14	6 – 301
	xxxx_S	13	10 – 320	13	10 – 320	13	10 – 320
	xxxx_Si	14	8 – 320	14	8 – 320	14	8 – 320
	xxxx_gt50	6	8 – 384	6	8 – 384	6	8 – 384

Table 2.3.56: PSP\_ISOIS-EPIHI\_L2-LET2-RATES60 (contd.). Here, ‘xxxx’ stands for R35C which implies that the values are integrated over ranges R3 – R5.

**2.3.13 FILE: PSP\_ISOIS-EPIHI\_L2-SECOND-RATES**

This file contains the 1 s cadence measurements of particle Counts, Flux ( $\text{cm}^{-2} \text{sr}^{-1} \text{sec}^{-1} \text{MeV}^{-1}$ ) and Count Rate (counts/s) of Electrons and H for sides A and B for the double-sided High Energy Telescope (HET) and the Low Energy Telescopes (LET1), and the single-sided Low Energy Telescope (LET2). The values of these variables are summarized in Table 2.3.57. The variables are named as: <tel>\_<side>\_<species>\_<quantity>, where, <tel> stands for HET, LET1 or LET2; <side> stands for A, B or C; <species> stands for the particle species; and <quantity> represents Counts (not used in variable names, in general), Flux or Rate.

Examples: HET\_A\_Electrons\_Flux; LET1\_B\_H\_Rate; LET2\_C\_H.

Side	Range	Quantity	Electrons		H	
			E-bins	E-range (MeV/nuc) (bins)	E-bins	E-range (MeV/nuc) (bins)
C	HET_A	Count	3	1 – 3	2	13 – 24
		Flux	3	1 – 3	2	13 – 24
		Count Rate	3	1 – 3	2	13 – 24
	HET_B	Count	3	1 – 3	2	13 – 24
		Flux	3	1 – 3	2	13 – 24
		Count Rate	3	1 – 3	2	13 – 24
	LET1_A	Count	2	1 – 2	3	2 – 11
		Flux	2	1 – 2	3	2 – 11
		Count Rate	2	1 – 2	3	2 – 11
	LET1_B	Count	2	1 – 2	3	2 – 11
		Flux	2	1 – 2	3	2 – 11
		Count Rate	2	1 – 2	3	2 – 11
	LET2_C	Count	2	1 – 2	3	2 – 11
		Flux	2	1 – 2	3	2 – 11
		Count Rate	2	1 – 2	3	2 – 11

Table 2.3.57: PSP\_ISOIS-EPIHI\_L2-SECOND-RATES. The EPI-Hi 1 s data of Electrons and H for HET, LET1 and LET2.

## **2.4 IS⊙IS SCIENCE DATA**

### **2.4.1 FILE: PSP\_ISOIS-EPIHI\_L2-SECOND-RATES**

This file contains a selection of EPI-Lo and EPI-Hi level 2 data, with some averaging over direction for EPI-Lo. It is intended as a small file “quicklook” to help identify periods of interest and should not be used for quantitative analysis.

## 3 DATA QUALITY FLAGS AND FILL

### 3.1 MOTIVATION

Any data product may be affected by one or more factors that reduce the quality, and thereby compromise the interpretation, of the data. These factors fall into four broad types, listed here in order of increasing severity:

- factors that warrant an advisory or further information.
- factors that warrant using caution when deriving results.
- factors that make certain data not scientifically useful but may still be useful for analyzing instrument response. These data, including count rates, are replaced with fill values in the public release.
- factors that make certain processed data meaningless, e.g. fluxes. In these cases the relevant data will not be produced at all.

Any of these factors that impact the data product will be noted with a data-quality variable, or “quality flag”. EPI-Hi level-2 data have a single quality flag variable while EPI-Lo level-2 data have one quality flag per channel (i.e., one per timebase/Epoch variable).

Flags in EPI-Hi files are named `Quality_Flag`; in EPI-Lo files, like `Quality_Flag_ChanT` (for channel T timebase).

### 3.2 QUALITY FLAG STRUCTURE

The quality-flag variable is an array, indexed by category. Each timestamp and category has a value from 0-127. A quality flag of 0 indicates no known factors of that category that reduce quality in the associated data at the corresponding timestamp. Nonzero quality flags indicate a known factor in the data with higher values representing increased severity. Each index in the quality flag array represents a different category which may affect different variables and products within the data, so a full understanding of a factor affecting the data requires knowledge of both the category and severity.

Unused categories are populated with zero (“perfect” data) and should be ignored.

If the severity is high enough some parts of the data may be omitted as noted below:

**Low (1 – 31)** there are informational warnings and caveats that are unlikely to affect the scientific validity of the data

**Medium (32 – 63)** users should take caution when deriving results and contact the instrument team for details, as the data may not be scientifically useful in some cases.

**High (64 – 95)** affected data are not scientifically useful and are removed from public release

**Severe (96 – 127)** data are completely invalid, affected fluxes are not calculated

The SOC aims to ensure that the interpretation of a quality-flag value within a category that applies to multiple data products does not vary drastically among those data products.

### 3.3 EXISTING CATEGORIES

#### 3.3.1 WARM UP

Used for potential issues with data just after instrument turn-on. Index 0 in the quality flags variable.

**EPI-Lo high-voltage ramp-up** 110 (Severe): during periods flagged with this value, the EPI-Lo high voltage and/or bias voltage are still ramping up, so the instrument may not be sensitive to incident particles. Affects counts and counts rates, making fluxes meaningless. Affects all EPI-Lo level 2 science files (`psp_isois-epilo_12-xx`), all counts, count rate, and flux variables.

#### 3.3.2 LIVETIME

Used for potential issues in calculating instrument livetime. Index 1 in the quality flags variable.

**Partial processing** 45 (Medium): EPI-Hi count rates (and fluxes) are ordinarily corrected for the fraction of valid events which are not processed by the flight software. This value indicates this fraction is only available for a portion of the integration period and fluxes may be inaccurate, particularly during periods of high and rapidly-varying count rates. Affects all EPI-Hi level 2 rates (`psp_isois-hi_let1-rates3600`, etc.), count rate and flux variables.

**Not calculated** 55 (Medium): The fraction of events processed is completely unknown and all events are assumed to be processed. Count rates and fluxes may be inaccurate during periods of high count rates. Affects all EPI-Hi level 2 rates (`psp_isois-hi_let1-rates3600`, etc.), count rate and flux variables.

#### 3.3.3 PITCH ANGLE CALCULATIONS

Used for potential issues with the pitch angle calculation based on magnetic field data from FIELDS. Index 2 in the quality flags variable.

**Preliminary pitch angles** 80 (High): Magnetic field data from FIELDS is preliminary and not suitable for pitch angle calculations. As such, pitch angles are not included in public release. Affects all level 2 files, EPI-Hi and EPI-Lo, pitch angle variables.

### 3.4 FILL VALUES

IS $\odot$ IS data files use fill values to indicate invalid or missing data. The valid range and the fill value used are provided for each variable in the CDF files according to ISTP/SPDF metadata standards. Values outside the valid range, in particular fill values, should not be interpreted as meaningful data.

Fill usually indicates data are not recoverable and not scientifically meaningful. Do not use count rates as a substitute for filled flux values. If the instrument team and SOC are able to recover meaningful data, those will be added to a future release.

Certain well-defined quality issues, described above, will result in fill values. Other sources of fill include:

- Uncalibrated data products
- Data products with known routinely high levels of background where the background subtraction has not been completed
- Time periods known to be related to instrument testing or other nonphysical sources of apparent counts
- Times where a portion of the data has been lost or corrupted but the rest is recoverable; the known lost data is replaced with fill

Fill values are not generated during periods when the instrument is off or in a mode that does not produce a particular product (for example, encounter-only data products during the cruise phase of the orbit). Do not assume a regular cadence of timestamps; the cadence may change, samples may be cut short, and samples may be missing. Use the time variables specified according to the ISTP/SPDF metadata standard to interpret time of data collection.

## 4 EPI-LO DECODER RING

We have produced a summary of the EPI-Lo data called the EPI-Lo Channel Definition “crib sheet”. The intent is to guide the user from a description of physical measurements to specific data products. Note that this relationship is time dependent and Figure 4 only applies during the first eight orbits (launch until 14 June 2021, LUT Regime Index = 6). The time dependence is due to instrument configuration changes (e.g., changing definitions of species and energy bins due to adjustment to lookup tables or LUTs) and unplanned changes (e.g., sensitivity variations or background increase due to dust impacts admitting more light).

The lookup tables were adjusted on 14 June 2021 and were updated to adjust box locations for species and Figure 5 reflects the updates.

The upper table in Figure 4 references only data products that include time-of-flight TOF measurements and the lower table references only measurements that employ the energy/solid state detector (SSD) system. Both have the same columns. The Mode identifies one of four instrument modes: Ion Composition (IC), Particle Composition (PC), Ion Energy (IE) or Particle Energy (PE), (PC and IE are not included in Release 1) which relate to the types of measurements made. The instrument can cycle through up to eight different mode intervals (slots) per second. Typically the slot pattern covers all four modes in an alternating pattern (e.g., IC,PE,IC,IE,IC,PE,IC,PC). The next column is the channel/rate name and the associated mnemonic. Different channels can measure multiple types of particles, so it is useful to provide a non-descriptive, but memorable, name for the different data products to help avoid confusion like “During this period the Electron data are mostly protons” in favor of ‘During this period the [E] rates are mostly protons. The mnemonic and associated system is based largely on what we expect to see in each the given channel (e.g., [E] for electrons). The next column provides the official, descriptive label for each data type. The Channel ID provides the useful range and naming of individual channels associated with each data type or sub group thereof. Species mass provides the species or type (or alternate information). The energy range associated with the channel ID list is given in keV and MeV/nuc (where applicable). The CDF data file needed to study the particles described on a given row are in the Logical Source. Within each file the variable name is given for physical units and counting rate. Finally, there are miscellaneous notes on each row in the last column. See Release Notes on details for variables and calibrated data products.



PSP / ISOIS / EPI-Lo Rate Channel Definitions			LUT Regime Index 0 to 5			Orbits 1 - 8			TRIPLES (except T = DOUBLES)			
Mode	Channel / rate	Label	ChanID		species mass	E (keV)		E (MeV/nuc)		Logical	Variable	comments
	mnemonic		low	high	amu	low	high	low	high	Source	Name	
IC IC	[P] Protons	High Res. Protons High Res. Protons	P000 P041	P040 P047	H	1	60 8,990	0.060	8.990	psp_isois-epilo_l2-ic	H_Flux_ChanP	box not defined
IC IC IC IC IC IC IC	[C] Composition	Ions Group 1 Ions Group 1 Ions Group 1 Ions Group 1 Ions Group 1 Ions Group 1 Ions Group 1	C048 C094 C141 C146 C187 C193 C198	C093 C140 C145 C186 C192 C197 C238	He-3 He-4 O Fe Fe	3 4 16 Null 56	84 20,000 72 20,000 227 20,600 Null 453 22,300	0.028 0.018 0.014 0.008	6.667 5.000 1.288 0.398	psp_isois-epilo_l2-ic psp_isois-epilo_l2-ic psp_isois-epilo_l2-ic psp_isois-epilo_l2-ic	He3_CountRate_ChanC He4_Flux_ChanC O_CountRate_ChanC Fe_CountRate_ChanC	box not defined box not defined non-standard boxes box not defined
IC IC IC IC	[D] D = Comp. + 1	Ions Group 2 Ions Group 2 Ions Group 2 Ions Group 2	D240 D261 D352 D367	D260 D351 D366 D431	C Si	12 28	197 20,400 529 21,400	0.016 0.019	1.700 0.764	psp_isois-epilo_l2-ic psp_isois-epilo_l2-ic	C_CountRate_ChanD Si_CountRate_ChanD	box not defined box not defined
IC	[T] TOF Only	Ion TOF	T000	T031	Ions	1	44,900 30	44.900	0.030	psp_isois-epilo_l2-ic	H_Flux_ChanT	no composition
IC IC	[R] R = Proton + 1 [R] skip Q = Quadrant	Hi Time Res Protons Hi Time Res Protons	R000 R015	R014 R015	H H	1	60 8,320 Null	0.060	8.320	psp_isois-epilo_l2-ic	H_Flux_ChanR	non-standard boxes

PSP / ISOIS / EPI-Lo Rate Channel Definitions			LUT Regime Index 0 to 5			Orbits 1 - 8			SINGLES			
Mode	Channel / rate	Label	ChanID		species mass	E (keV)		E (MeV/nuc)		Logical	Variable	comments
	mnemonic		low	high	amu	low	high	low	high	Source	Name	
PE PE	[E] Electron	High Res Electrons High Res Electrons	E000 E001	E000 E047	deposited deposited	null	15 250,000	0.015	250			hi/lo gain, no comp. hi/lo gain, no comp.
PE PE	[E]	High Res Electrons High Res Electrons	E000 E002	E016 E031	e- cal H cal	1	26 388 399 10,200	0.026 0.399	0.388 10.2	psp_isois-epilo_l2-pe psp_isois-epilo_l2-pe	Electron_CountRate_ChanE H_CountRate_ChanE	hi/lo gain, no comp. hi/lo gain, no comp.
PE PE PE	[F] F = Elect. + 1	High Time Res. Electrons High Time Res. Electrons High Time Res. Electrons	F000 F001 F000	F000 F015 F011	deposited deposited H cal	1	35 250,000 399 10,200	0.035 0.399	250 10.2	psp_isois-epilo_l2-pe psp_isois-epilo_l2-pe	Electron_CountRate_ChanF H_CountRate_ChanF	hi/lo gain, no comp. hi/lo gain, no comp. hi/lo gain, no comp.
PE PE	[G] G = Elect + 2	High Look Res Electrons High Look Res Electrons	E000 E001	G000 G047	deposited deposited	null	15 250,000	0.015	250	psp_isois-epilo_l2-pe	Electron_CountRate_ChanG	hi/lo gain, no comp. hi/lo gain, no comp.

PSP / ISOIS / EPI-Lo Rate Channel Definitions			LUT Regime Index 6 to TBD		Orbits 8 - TBD		TRIPLES (except T = DOUBLES)						
Mode	Channel / rate	Label	ChanID		species mass	E (keV)		E (MeV/nuc)		Logical	Variable	comments	
	mnemonic		low	high	amu	low	high	low	high	Source	Name		
IC	[P] Protons	High Res. Protons	P000	P038	H	1	67.0	10,252	0.067	10.25	psp_isois-epilo_I2-ic	H_Flux_ChanP	
IC	[P]	High Res. Protons	P039	P039	H	1			0.000	0.00			box not defined
IC	[P]	High Res. Protons	P040	P041									background box
IC	[P]	High Res. Protons	P042	P047									background box
IC	[C] Composition	Ions Group 1	C050	C093	He-3	3	94.8	22,536	0.032	7.51	psp_isois-epilo_I2-ic	He3_CountRate_ChanC	
IC	[C]	Ions Group 1	C094	C095	He-3 Bkg								background boxes
IC	[C]	Ions Group 1	C100	C143	He-4	4	82.8	22,540	0.021	5.64	psp_isois-epilo_I2-ic	He4_Flux_ChanC	
IC	[C]	Ions Group 1	C144	C144	He-4 Bkg								background boxes
IC	[C]	Ions Group 1	C150	C150	O	16							box not defined
IC	[C]	Ions Group 1	C151	C193	O	16	204.8	23,114	0.013	1.44	psp_isois-epilo_I2-ic	O_CountRate_ChanC	
IC	[C]	Ions Group 1	C194	C194	O Bkg								background boxes
IC	[C]	Ions Group 1	C195	C196	Fe	56							box not defined
IC	[C]	Ions Group 1	C197	C238	Fe	56	431.2	24,868	0.008	0.44	psp_isois-epilo_I2-ic	Fe_CountRate_ChanC	
IC	[C]	Ions Group 1	C239	C239	Fe Bkg								background boxes
IC	[D] D = Comp. + "1"	Ions Group 2	D250	D271	C	12	177.8	22,872	0.015	1.91	psp_isois-epilo_I2-ic	C_CountRate_ChanD	
IC	[D]	Ions Group 2	D272	D272	C Bkg								background box
IC	[D]	Ions Group 2	D300	D321	Mg	24	218.3	23,672	0.009	0.99	psp_isois-epilo_I2-ic	Mg_CountRate_ChanD	
IC	[D]	Ions Group 2	D322	D322	Mg Bkg								background box
IC	[D]	Ions Group 2	D330	D334	Ne								box not defined
IC	[D]	Ions Group 2	D335	D340	Ne	20	830.0	23,392	0.042	1.17	psp_isois-epilo_I2-ic	Ne_CountRate_ChanD	
IC	[D]	Ions Group 2	D341	D341	Ne Bkg								background box
IC	[D]	Ions Group 2	D352	D371	Si	28	326.8	23,946	0.012	0.86	psp_isois-epilo_I2-ic	Si_CountRate_ChanD	
IC	[D]	Ions Group 2	D372	D372	Si Bkg								background box
IC	[T] TOF Only	Ion TOF	T000	T031	Ions	1	46,367.0	21	46.367	0.02	psp_isois-epilo_I2-ic	H_Flux_ChanT	no composition
IC	[R] R = Proton + "1"	Hi Time Res Protons	R000	R013	H	1	67	8,736	0.067	8.74	psp_isois-epilo_I2-ic	H_Flux_ChanR	
IC	[R]	Hi Time Res Protons	R014	R014	H	1	Null						non-standard boxes
IC	[R] skip Q = Quadrant	Hi Time Res Protons	R015	R015	H	1	Null						non-standard boxes

PSP / ISOIS / EPI-Lo Rate Channel Definitions			LUT Regime Index 6 to TBD		Orbits 8 - TBD		SINGLES						
Mode	Channel / rate	Label	ChanID		species mass	E (keV)		E (MeV/nuc)		Logical	Variable	comments	
	mnemonic		low	high	amu	low	high	low	high	Source	Name		
PE	[E] Electron	High Res Electrons	E000	E000	deposited	null						hi/lo gain, no comp.	
PE	[E]	High Res Electrons	E001	E047	deposited		15	250,000	0.015	250		hi/lo gain, no comp.	
PE	[E]	High Res Electrons	E000	E016	e- cal		26	388	0.026	0.388	psp_isois-epilo_I2-pe	Electron_CountRate_ChanE	hi/lo gain, no comp.
PE	[E]	High Res Electrons	E002	E031	H cal	1	399	10,200	0.399	10.2	psp_isois-epilo_I2-pe	H_CountRate_ChanE	hi/lo gain, no comp.
PE	[F] F = Elect. + 1	High Time Res. Electrons	F000	F000	deposited	null						hi/lo gain, no comp.	
PE	[F]	High Time Res. Electrons	F001	F015	deposited		35	250,000	0.035	250	psp_isois-epilo_I2-pe	Electron_CountRate_ChanF	hi/lo gain, no comp.
PE	[F]	High Time Res. Electrons	F000	F011	H cal	1	399	10,200	0.399	10.2	psp_isois-epilo_I2-pe	H_CountRate_ChanF	hi/lo gain, no comp.
PE	[G] G = Elect + 2	High Look Res Electrons	E000	G000	deposited	null						hi/lo gain, no comp.	
PE	[G]	High Look Res Electrons	E001	G047	deposited		15	250,000	0.015	250	psp_isois-epilo_I2-pe	Electron_CountRate_ChanG	hi/lo gain, no comp.

## 5 GENERAL LIST OF VARIABLES

### 5.1 PSP\_ISOIS-EPIHI\_L2-HET-RATES10

A\_Electrons  
A\_Electrons\_Rate  
A\_H  
A\_H\_Flux  
A\_H\_Rate  
A\_He  
A\_He\_Flux  
A\_He\_Rate  
B\_Electrons  
B\_Electrons\_Rate  
B\_H  
B\_H\_Flux  
B\_H\_Rate  
B\_He  
B\_He\_Flux  
B\_He\_Rate  
HCI\_Lat  
HCI\_Lon  
HCI\_R  
HET\_A\_HCI  
HET\_A\_PA  
HET\_A\_RTN  
HET\_A\_SA  
HET\_B\_HCI  
HET\_B\_PA  
HET\_B\_RTN  
HET\_B\_SA  
HGC\_Lat  
HGC\_Lon  
HGC\_R  
Quality\_Flag

### 5.2 PSP\_ISOIS-EPIHI\_L2-HET-RATES300

A\_CNO\_SECT\_Rate  
A\_FeGroup\_SECT\_Rate  
A\_NetoSi\_SECT\_Rate  
B\_CNO\_SECT\_Rate  
B\_FeGroup\_SECT\_Rate  
B\_NetoSi\_SECT\_Rate

HCI\_Lat  
HCI\_Lon  
HCI\_R  
HET\_A\_HCI  
HET\_A\_PA  
HET\_A\_R17\_SECT\_HCI  
HET\_A\_R17\_SECT\_PA  
HET\_A\_R17\_SECT\_RTN  
HET\_A\_R17\_SECT\_SA  
HET\_A\_RTN  
HET\_A\_SA  
HET\_B\_HCI  
HET\_B\_PA  
HET\_B\_R17\_SECT\_HCI  
HET\_B\_R17\_SECT\_PA  
HET\_B\_R17\_SECT\_RTN  
HET\_B\_R17\_SECT\_SA  
HET\_B\_RTN  
HET\_B\_SA  
HGC\_Lat  
HGC\_Lon  
HGC\_R  
Quality\_Flag

### **5.3 PSP\_ISOIS-EPIHI\_L2-HET-RATES3600**

A\_Al  
A\_Al\_Rate  
A\_Ar  
A\_Ar\_Rate  
A\_C  
A\_CNO\_SECT\_Rate  
A\_C\_Rate  
A\_Ca  
A\_Ca\_Rate  
A\_Cr  
A\_Cr\_Rate  
A\_Electrons  
A\_Electrons\_Rate  
A\_Electrons\_SECT\_Rate  
A\_Fe  
A\_FeGroup\_SECT\_Rate  
A\_Fe\_Rate  
A\_H

A\_H\_Flux  
A\_H\_Rate  
A\_H\_SECT\_Flux  
A\_H\_SECT\_Rate  
A\_He  
A\_He\_Flux  
A\_He\_Rate  
A\_He\_SECT\_Flux  
A\_He\_SECT\_Rate  
A\_Mg  
A\_Mg\_Rate  
A\_N  
A\_N\_Rate  
A\_Na  
A\_Na\_Rate  
A\_Ne  
A\_Ne\_Rate  
A\_NetoSi\_SECT\_Rate  
A\_Ni  
A\_Ni\_Rate  
A\_O  
A\_O\_Rate  
A\_S  
A\_S\_Rate  
A\_Si  
A\_Si\_Rate  
B\_Al  
B\_Al\_Rate  
B\_Ar  
B\_Ar\_Rate  
B\_C  
B\_CNO\_SECT\_Rate  
B\_C\_Rate  
B\_Ca  
B\_Ca\_Rate  
B\_Cr  
B\_Cr\_Rate  
B\_Electrons  
B\_Electrons\_Rate  
B\_Electrons\_SECT\_Rate  
B\_Fe  
B\_FeGroup\_SECT\_Rate  
B\_Fe\_Rate  
B\_H  
B\_H\_Flux

B\_H\_Rate  
B\_H\_SECT\_Flux  
B\_H\_SECT\_Rate  
B\_He  
B\_He\_Flux  
B\_He\_Rate  
B\_He\_SECT\_Flux  
B\_He\_SECT\_Rate  
B\_Mg  
B\_Mg\_Rate  
B\_N  
B\_N\_Rate  
B\_Na  
B\_Na\_Rate  
B\_Ne  
B\_Ne\_Rate  
B\_NetoSi\_SECT\_Rate  
B\_Ni  
B\_Ni\_Rate  
B\_O  
B\_O\_Rate  
B\_S  
B\_S\_Rate  
B\_Si  
B\_Si\_Rate  
HCI\_Lat  
HCI\_Lon  
HCI\_R  
HET\_A\_HCI  
HET\_A\_PA  
HET\_A\_R17\_SECT\_HCI  
HET\_A\_R17\_SECT\_PA  
HET\_A\_R17\_SECT\_RTN  
HET\_A\_R17\_SECT\_SA  
HET\_A\_RTN  
HET\_A\_SA  
HET\_B\_HCI  
HET\_B\_PA  
HET\_B\_R17\_SECT\_HCI  
HET\_B\_R17\_SECT\_PA  
HET\_B\_R17\_SECT\_RTN  
HET\_B\_R17\_SECT\_SA  
HET\_B\_RTN  
HET\_B\_SA  
HGC\_Lat

HGC\_Lon  
HGC\_R  
Quality\_Flag  
R1A\_He\_BIN  
R1A\_Ne\_BIN  
R1B\_He\_BIN  
R1B\_Ne\_BIN  
R2A\_He\_BIN  
R2A\_Ne\_BIN  
R2B\_He\_BIN  
R2B\_Ne\_BIN  
R3A\_He\_BIN  
R3A\_Ne\_BIN  
R3B\_He\_BIN  
R3B\_Ne\_BIN  
R4A\_He\_BIN  
R4A\_Ne\_BIN  
R4B\_He\_BIN  
R4B\_Ne\_BIN  
R5A\_He\_BIN  
R5A\_Ne\_BIN  
R5B\_He\_BIN  
R5B\_Ne\_BIN  
R6A\_He\_BIN  
R6A\_Ne\_BIN  
R6B\_He\_BIN  
R6B\_Ne\_BIN  
R7A\_He\_BIN  
R7A\_Ne\_BIN  
R7B\_He\_BIN  
R7B\_Ne\_BIN

#### **5.4 PSP\_ISOIS-EPIHI\_L2-HET-RATES60**

A\_Al  
A\_Al\_Rate  
A\_Ar  
A\_Ar\_Rate  
A\_C  
A\_C\_Rate  
A\_Ca  
A\_Ca\_Rate  
A\_Cr  
A\_Cr\_Rate

A\_Electrons  
A\_Electrons\_Rate  
A\_Electrons\_SECT\_Rate  
A\_Fe  
A\_Fe\_Rate  
A\_H  
A\_H\_Flux  
A\_H\_Rate  
A\_H\_SECT\_Flux  
A\_H\_SECT\_Rate  
A\_He  
A\_He\_Flux  
A\_He\_Rate  
A\_He\_SECT\_Flux  
A\_He\_SECT\_Rate  
A\_Mg  
A\_Mg\_Rate  
A\_N  
A\_N\_Rate  
A\_Na  
A\_Na\_Rate  
A\_Ne  
A\_Ne\_Rate  
A\_Ni  
A\_Ni\_Rate  
A\_O  
A\_O\_Rate  
A\_S  
A\_S\_Rate  
A\_Si  
A\_Si\_Rate  
B\_Al  
B\_Al\_Rate  
B\_Ar  
B\_Ar\_Rate  
B\_C  
B\_C\_Rate  
B\_Ca  
B\_Ca\_Rate  
B\_Cr  
B\_Cr\_Rate  
B\_Electrons  
B\_Electrons\_Rate  
B\_Electrons\_SECT\_Rate  
B\_Fe



B\_Fe\_Rate  
B\_H  
B\_H\_Flux  
B\_H\_Rate  
B\_H\_SECT\_Flux  
B\_H\_SECT\_Rate  
B\_He  
B\_He\_Flux  
B\_He\_Rate  
B\_He\_SECT\_Flux  
B\_He\_SECT\_Rate  
B\_Mg  
B\_Mg\_Rate  
B\_N  
B\_N\_Rate  
B\_Na  
B\_Na\_Rate  
B\_Ne  
B\_Ne\_Rate  
B\_Ni  
B\_Ni\_Rate  
B\_O  
B\_O\_Rate  
B\_S  
B\_S\_Rate  
B\_Si  
B\_Si\_Rate  
HCI\_Lat  
HCI\_Lon  
HCI\_R  
HET\_A\_HCI  
HET\_A\_PA  
HET\_A\_R17\_SECT\_HCI  
HET\_A\_R17\_SECT\_PA  
HET\_A\_R17\_SECT\_RTN  
HET\_A\_R17\_SECT\_SA  
HET\_A\_RTN  
HET\_A\_SA  
HET\_B\_HCI  
HET\_B\_PA  
HET\_B\_R17\_SECT\_HCI  
HET\_B\_R17\_SECT\_PA  
HET\_B\_R17\_SECT\_RTN  
HET\_B\_R17\_SECT\_SA  
HET\_B\_RTN

HET\_B\_SA  
HGC\_Lat  
HGC\_Lon  
HGC\_R  
Quality\_Flag

## 5.5 PSP\_ISOIS-EPIHI\_L2-LET1-RATES10

A\_Electrons  
A\_Electrons\_Rate  
A\_H  
A\_H\_Flux  
A\_H\_Rate  
A\_He  
A\_He\_Flux  
A\_He\_Rate  
B\_Electrons  
B\_Electrons\_Rate  
B\_H  
B\_H\_Flux  
B\_H\_Rate  
B\_He  
B\_He\_Flux  
B\_He\_Rate  
HCI\_Lat  
HCI\_Lon  
HCI\_R  
HGC\_Lat  
HGC\_Lon  
HGC\_R  
LET1\_A\_HCI  
LET1\_A\_PA  
LET1\_A\_RTN  
LET1\_A\_SA  
LET1\_B\_HCI  
LET1\_B\_PA  
LET1\_B\_RTN  
LET1\_B\_SA  
Quality\_Flag

## 5.6 PSP\_ISOIS-EPIHI\_L2-LET1-RATES300

HCI\_Lat  
HCI\_Lon  
HCI\_R  
HGC\_Lat  
HGC\_Lon  
HGC\_R  
LET1\_A\_HCI  
LET1\_A\_PA  
LET1\_A\_R1\_SECT\_HCI  
LET1\_A\_R1\_SECT\_PA  
LET1\_A\_R1\_SECT\_RTN  
LET1\_A\_R1\_SECT\_SA  
LET1\_A\_R26\_SECT\_HCI  
LET1\_A\_R26\_SECT\_PA  
LET1\_A\_R26\_SECT\_RTN  
LET1\_A\_R26\_SECT\_SA  
LET1\_A\_RTN  
LET1\_A\_SA  
LET1\_B\_HCI  
LET1\_B\_PA  
LET1\_B\_R1\_SECT\_HCI  
LET1\_B\_R1\_SECT\_PA  
LET1\_B\_R1\_SECT\_RTN  
LET1\_B\_R1\_SECT\_SA  
LET1\_B\_R26\_SECT\_HCI  
LET1\_B\_R26\_SECT\_PA  
LET1\_B\_R26\_SECT\_RTN  
LET1\_B\_R26\_SECT\_SA  
LET1\_B\_RTN  
LET1\_B\_SA  
Quality\_Flag  
R1A\_CNO\_SECT\_Rate  
R1A\_FeGroup\_SECT\_Rate  
R1A\_NetoSi\_SECT\_Rate  
R1B\_CNO\_SECT\_Rate  
R1B\_FeGroup\_SECT\_Rate  
R1B\_NetoSi\_SECT\_Rate  
R26A\_CNO\_SECT\_Rate  
R26A\_FeGroup\_SECT\_Rate  
R26A\_NetoSi\_SECT\_Rate  
R26B\_CNO\_SECT\_Rate  
R26B\_FeGroup\_SECT\_Rate  
R26B\_NetoSi\_SECT\_Rate

## 5.7 PSP\_ISOIS-EPIHI\_L2-LET1-RATES3600

A\_Al  
A\_Al\_Rate  
A\_Ar  
A\_Ar\_Rate  
A\_C  
A\_C\_Rate  
A\_Ca  
A\_Ca\_Rate  
A\_Cr  
A\_Cr\_Rate  
A\_Electrons  
A\_Electrons\_Rate  
A\_Fe  
A\_Fe\_Rate  
A\_H  
A\_H\_Flux  
A\_H\_Rate  
A\_He  
A\_He\_Flux  
A\_He\_Rate  
A\_Mg  
A\_Mg\_Rate  
A\_N  
A\_N\_Rate  
A\_Na  
A\_Na\_Rate  
A\_Ne  
A\_Ne\_Rate  
A\_Ni  
A\_Ni\_Rate  
A\_O  
A\_O\_Rate  
A\_S  
A\_S\_Rate  
A\_Si  
A\_Si\_Rate  
B\_Al  
B\_Al\_Rate  
B\_Ar  
B\_Ar\_Rate  
B\_C

B\_C\_Rate  
B\_Ca  
B\_Ca\_Rate  
B\_Cr  
B\_Cr\_Rate  
B\_Electrons  
B\_Electrons\_Rate  
B\_Fe  
B\_Fe\_Rate  
B\_H  
B\_H\_Flux  
B\_H\_Rate  
B\_He  
B\_He\_Flux  
B\_He\_Rate  
B\_Mg  
B\_Mg\_Rate  
B\_N  
B\_N\_Rate  
B\_Na  
B\_Na\_Rate  
B\_Ne  
B\_Ne\_Rate  
B\_Ni  
B\_Ni\_Rate  
B\_O  
B\_O\_Rate  
B\_S  
B\_S\_Rate  
B\_Si  
B\_Si\_Rate  
HCI\_Lat  
HCI\_Lon  
HCI\_R  
HGC\_Lat  
HGC\_Lon  
HGC\_R  
LET1\_A\_HCI  
LET1\_A\_PA  
LET1\_A\_R1\_SECT\_HCI  
LET1\_A\_R1\_SECT\_PA  
LET1\_A\_R1\_SECT\_RTN  
LET1\_A\_R1\_SECT\_SA  
LET1\_A\_R26\_SECT\_HCI  
LET1\_A\_R26\_SECT\_PA

LET1\_A\_R26\_SECT\_RTN  
LET1\_A\_R26\_SECT\_SA  
LET1\_A\_RTN  
LET1\_A\_SA  
LET1\_B\_HCI  
LET1\_B\_PA  
LET1\_B\_R1\_SECT\_HCI  
LET1\_B\_R1\_SECT\_PA  
LET1\_B\_R1\_SECT\_RTN  
LET1\_B\_R1\_SECT\_SA  
LET1\_B\_R26\_SECT\_HCI  
LET1\_B\_R26\_SECT\_PA  
LET1\_B\_R26\_SECT\_RTN  
LET1\_B\_R26\_SECT\_SA  
LET1\_B\_RTN  
LET1\_B\_SA  
Quality\_Flag  
R1A\_CNO\_SECT\_Rate  
R1A\_FeGroup\_SECT\_Rate  
R1A\_H\_SECT\_Flux  
R1A\_H\_SECT\_Rate  
R1A\_He\_BIN  
R1A\_He\_SECT\_Flux  
R1A\_He\_SECT\_Rate  
R1A\_Ne\_BIN  
R1A\_NetoSi\_SECT\_Rate  
R1B\_CNO\_SECT\_Rate  
R1B\_FeGroup\_SECT\_Rate  
R1B\_H\_SECT\_Flux  
R1B\_H\_SECT\_Rate  
R1B\_He\_BIN  
R1B\_He\_SECT\_Flux  
R1B\_He\_SECT\_Rate  
R1B\_Ne\_BIN  
R1B\_NetoSi\_SECT\_Rate  
R26A\_CNO\_SECT\_Rate  
R26A\_FeGroup\_SECT\_Rate  
R26A\_H\_SECT\_Flux  
R26A\_H\_SECT\_Rate  
R26A\_He\_SECT\_Flux  
R26A\_He\_SECT\_Rate  
R26A\_NetoSi\_SECT\_Rate  
R26B\_CNO\_SECT\_Rate  
R26B\_FeGroup\_SECT\_Rate  
R26B\_H\_SECT\_Flux

R26B\_H\_SECT\_Rate  
R26B\_He\_SECT\_Flux  
R26B\_He\_SECT\_Rate  
R26B\_NetoSi\_SECT\_Rate  
R2A\_He\_BIN  
R2A\_Ne\_BIN  
R2B\_He\_BIN  
R2B\_Ne\_BIN  
R3A\_He\_BIN  
R3A\_Ne\_BIN  
R3B\_He\_BIN  
R3B\_Ne\_BIN  
R45A\_He\_BIN  
R45A\_Ne\_BIN  
R45B\_He\_BIN  
R45B\_Ne\_BIN  
R6A\_He\_BIN  
R6A\_Ne\_BIN  
R6B\_He\_BIN  
R6B\_Ne\_BIN

## 5.8 PSP\_ISOIS-EPIHI\_L2-LET1-RATES60

A\_Al  
A\_Al\_Rate  
A\_Ar  
A\_Ar\_Rate  
A\_C  
A\_C\_Rate  
A\_Ca  
A\_Ca\_Rate  
A\_Cr  
A\_Cr\_Rate  
A\_Electrons  
A\_Electrons\_Rate  
A\_Fe  
A\_Fe\_Rate  
A\_H  
A\_H\_Flux  
A\_H\_Rate  
A\_He  
A\_He\_Flux  
A\_He\_Rate  
A\_Mg

A\_Mg\_Rate  
A\_N  
A\_N\_Rate  
A\_Na  
A\_Na\_Rate  
A\_Ne  
A\_Ne\_Rate  
A\_Ni  
A\_Ni\_Rate  
A\_O  
A\_O\_Rate  
A\_S  
A\_S\_Rate  
A\_Si  
A\_Si\_Rate  
B\_Al  
B\_Al\_Rate  
B\_Ar  
B\_Ar\_Rate  
B\_C  
B\_C\_Rate  
B\_Ca  
B\_Ca\_Rate  
B\_Cr  
B\_Cr\_Rate  
B\_Electrons  
B\_Electrons\_Rate  
B\_Fe  
B\_Fe\_Rate  
B\_H  
B\_H\_Flux  
B\_H\_Rate  
B\_He  
B\_He\_Flux  
B\_He\_Rate  
B\_Mg  
B\_Mg\_Rate  
B\_N  
B\_N\_Rate  
B\_Na  
B\_Na\_Rate  
B\_Ne  
B\_Ne\_Rate  
B\_Ni  
B\_Ni\_Rate



B\_O  
B\_O\_Rate  
B\_S  
B\_S\_Rate  
B\_Si  
B\_Si\_Rate  
HCI\_Lat  
HCI\_Lon  
HCI\_R  
HGC\_Lat  
HGC\_Lon  
HGC\_R  
LET1\_A\_HCI  
LET1\_A\_PA  
LET1\_A\_R1\_SECT\_HCI  
LET1\_A\_R1\_SECT\_PA  
LET1\_A\_R1\_SECT\_RTN  
LET1\_A\_R1\_SECT\_SA  
LET1\_A\_R26\_SECT\_HCI  
LET1\_A\_R26\_SECT\_PA  
LET1\_A\_R26\_SECT\_RTN  
LET1\_A\_R26\_SECT\_SA  
LET1\_A\_RTN  
LET1\_A\_SA  
LET1\_B\_HCI  
LET1\_B\_PA  
LET1\_B\_R1\_SECT\_HCI  
LET1\_B\_R1\_SECT\_PA  
LET1\_B\_R1\_SECT\_RTN  
LET1\_B\_R1\_SECT\_SA  
LET1\_B\_R26\_SECT\_HCI  
LET1\_B\_R26\_SECT\_PA  
LET1\_B\_R26\_SECT\_RTN  
LET1\_B\_R26\_SECT\_SA  
LET1\_B\_RTN  
LET1\_B\_SA  
Quality\_Flag  
R1A\_H\_SECT\_Flux  
R1A\_H\_SECT\_Rate  
R1A\_He\_SECT\_Flux  
R1A\_He\_SECT\_Rate  
R1B\_H\_SECT\_Flux  
R1B\_H\_SECT\_Rate  
R1B\_He\_SECT\_Flux  
R1B\_He\_SECT\_Rate

R26A\_H\_SECT\_Flux  
R26A\_H\_SECT\_Rate  
R26A\_He\_SECT\_Flux  
R26A\_He\_SECT\_Rate  
R26B\_H\_SECT\_Flux  
R26B\_H\_SECT\_Rate  
R26B\_He\_SECT\_Flux  
R26B\_He\_SECT\_Rate

## 5.9 PSP\_ISOIS-EPIHI\_L2-LET2-RATES10

C\_Electrons  
C\_Electrons\_Rate  
C\_H  
C\_H\_Flux  
C\_H\_Rate  
C\_He  
C\_He\_Flux  
C\_He\_Rate  
HCI\_Lat  
HCI\_Lon  
HCI\_R  
HGC\_Lat  
HGC\_Lon  
HGC\_R  
LET2\_C\_HCI  
LET2\_C\_PA  
LET2\_C\_RTN  
LET2\_C\_SA  
Quality\_Flag

## 5.10 PSP\_ISOIS-EPIHI\_L2-LET2-RATES300

HCI\_Lat  
HCI\_Lon  
HCI\_R  
HGC\_Lat  
HGC\_Lon  
HGC\_R  
LET2\_C\_HCI  
LET2\_C\_PA  
LET2\_C\_R1\_SECT\_HCI  
LET2\_C\_R1\_SECT\_PA

LET2\_C\_R1\_SECT\_RTN  
LET2\_C\_R1\_SECT\_SA  
LET2\_C\_R25\_SECT\_HCI  
LET2\_C\_R25\_SECT\_PA  
LET2\_C\_R25\_SECT\_RTN  
LET2\_C\_R25\_SECT\_SA  
LET2\_C\_RTN  
LET2\_C\_SA  
Quality\_Flag  
R1C\_CNO\_SECT\_Rate  
R1C\_FeGroup\_SECT\_Rate  
R1C\_NetoSi\_SECT\_Rate  
R25C\_CNO\_SECT\_Rate  
R25C\_FeGroup\_SECT\_Rate  
R25C\_NetoSi\_SECT\_Rate

## 5.11 PSP\_ISOIS-EPIHI\_L2-LET2-RATES3600

C\_Al  
C\_Al\_Rate  
C\_Ar  
C\_Ar\_Rate  
C\_C  
C\_C\_Rate  
C\_Ca  
C\_Ca\_Rate  
C\_Cr  
C\_Cr\_Rate  
C\_Electrons  
C\_Electrons\_Rate  
C\_Fe  
C\_Fe\_Rate  
C\_H  
C\_H\_Flux  
C\_H\_Rate  
C\_He  
C\_He\_Flux  
C\_He\_Rate  
C\_Mg  
C\_Mg\_Rate  
C\_N  
C\_N\_Rate  
C\_Na  
C\_Na\_Rate

C\_Ne  
C\_Ne\_Rate  
C\_Ni  
C\_Ni\_Rate  
C\_O  
C\_O\_Rate  
C\_S  
C\_S\_Rate  
C\_Si  
C\_Si\_Rate  
HCI\_Lat  
HCI\_Lon  
HCI\_R  
HGC\_Lat  
HGC\_Lon  
HGC\_R  
LET2\_C\_HCI  
LET2\_C\_PA  
LET2\_C\_R1\_SECT\_HCI  
LET2\_C\_R1\_SECT\_PA  
LET2\_C\_R1\_SECT\_RTN  
LET2\_C\_R1\_SECT\_SA  
LET2\_C\_R25\_SECT\_HCI  
LET2\_C\_R25\_SECT\_PA  
LET2\_C\_R25\_SECT\_RTN  
LET2\_C\_R25\_SECT\_SA  
LET2\_C\_RTN  
LET2\_C\_SA  
Quality\_Flag  
R1C\_CNO\_SECT\_Rate  
R1C\_FeGroup\_SECT\_Rate  
R1C\_H\_SECT\_Flux  
R1C\_H\_SECT\_Rate  
R1C\_He\_BIN  
R1C\_He\_SECT\_Flux  
R1C\_He\_SECT\_Rate  
R1C\_Ne\_BIN  
R1C\_NetoSi\_SECT\_Rate  
R25C\_CNO\_SECT\_Rate  
R25C\_FeGroup\_SECT\_Rate  
R25C\_H\_SECT\_Flux  
R25C\_H\_SECT\_Rate  
R25C\_He\_SECT\_Flux  
R25C\_He\_SECT\_Rate  
R25C\_NetoSi\_SECT\_Rate

R2C\_He\_BIN  
R2C\_Ne\_BIN  
R3C\_He\_BIN  
R3C\_Ne\_BIN  
R45C\_He\_BIN  
R45C\_Ne\_BIN

## 5.12 PSP\_ISOIS-EPIHI\_L2-LET2-RATES60

C\_Al  
C\_Al\_Rate  
C\_Ar  
C\_Ar\_Rate  
C\_C  
C\_C\_Rate  
C\_Ca  
C\_Ca\_Rate  
C\_Cr  
C\_Cr\_Rate  
C\_Electrons  
C\_Electrons\_Rate  
C\_Fe  
C\_Fe\_Rate  
C\_H  
C\_H\_Flux  
C\_H\_Rate  
C\_He  
C\_He\_Flux  
C\_He\_Rate  
C\_Mg  
C\_Mg\_Rate  
C\_N  
C\_N\_Rate  
C\_Na  
C\_Na\_Rate  
C\_Ne  
C\_Ne\_Rate  
C\_Ni  
C\_Ni\_Rate  
C\_O  
C\_O\_Rate  
C\_S  
C\_S\_Rate  
C\_Si

C\_Si\_Rate  
HCI\_Lat  
HCI\_Lon  
HCI\_R  
HGC\_Lat  
HGC\_Lon  
HGC\_R  
LET2\_C\_HCI  
LET2\_C\_PA  
LET2\_C\_R1\_SECT\_HCI  
LET2\_C\_R1\_SECT\_PA  
LET2\_C\_R1\_SECT\_RTN  
LET2\_C\_R1\_SECT\_SA  
LET2\_C\_R25\_SECT\_HCI  
LET2\_C\_R25\_SECT\_PA  
LET2\_C\_R25\_SECT\_RTN  
LET2\_C\_R25\_SECT\_SA  
LET2\_C\_RTN  
LET2\_C\_SA  
Quality\_Flag  
R1C\_H\_SECT\_Flux  
R1C\_H\_SECT\_Rate  
R1C\_He\_SECT\_Flux  
R1C\_He\_SECT\_Rate  
R25C\_H\_SECT\_Flux  
R25C\_H\_SECT\_Rate  
R25C\_He\_SECT\_Flux  
R25C\_He\_SECT\_Rate

### **5.13 PSP\_ISOIS-EPIHI\_L2-SECOND-RATES**

HCI\_Lat  
HCI\_Lon  
HCI\_R  
HET\_A\_Electrons  
HET\_A\_Electrons\_Rate  
HET\_A\_H  
HET\_A\_HCI  
HET\_A\_H\_Rate  
HET\_A\_PA  
HET\_A\_RTN  
HET\_A\_SA  
HET\_B\_Electrons  
HET\_B\_Electrons\_Rate

HET\_B\_H  
HET\_B\_HCI  
HET\_B\_H\_Rate  
HET\_B\_PA  
HET\_B\_RTN  
HET\_B\_SA  
HGC\_Lat  
HGC\_Lon  
HGC\_R  
LET1\_A\_Electrons  
LET1\_A\_Electrons\_Rate  
LET1\_A\_H  
LET1\_A\_HCI  
LET1\_A\_H\_Rate  
LET1\_A\_PA  
LET1\_A\_RTN  
LET1\_A\_SA  
LET1\_B\_Electrons  
LET1\_B\_Electrons\_Rate  
LET1\_B\_H  
LET1\_B\_HCI  
LET1\_B\_H\_Rate  
LET1\_B\_PA  
LET1\_B\_RTN  
LET1\_B\_SA  
LET2\_C\_Electrons  
LET2\_C\_Electrons\_Rate  
LET2\_C\_H  
LET2\_C\_HCI  
LET2\_C\_H\_Rate  
LET2\_C\_PA  
LET2\_C\_RTN  
LET2\_C\_SA  
Quality\_Flag

## 5.14 PSP\_ISOIS-EPILO\_L2-IC

C\_CountRate\_ChanD  
C\_Counts\_ChanD  
Fe\_CountRate\_ChanC  
Fe\_Counts\_ChanC  
HCI\_ChanC  
HCI\_ChanD  
HCI\_ChanP

HCI\_ChanR  
HCI\_ChanT  
HCI\_Lat\_ChanC  
HCI\_Lat\_ChanD  
HCI\_Lat\_ChanP  
HCI\_Lat\_ChanR  
HCI\_Lat\_ChanT  
HCI\_Lon\_ChanC  
HCI\_Lon\_ChanD  
HCI\_Lon\_ChanP  
HCI\_Lon\_ChanR  
HCI\_Lon\_ChanT  
HCI\_R\_ChanC  
HCI\_R\_ChanD  
HCI\_R\_ChanP  
HCI\_R\_ChanR  
HCI\_R\_ChanT  
HGC\_Lat\_ChanC  
HGC\_Lat\_ChanD  
HGC\_Lat\_ChanP  
HGC\_Lat\_ChanR  
HGC\_Lat\_ChanT  
HGC\_Lon\_ChanC  
HGC\_Lon\_ChanD  
HGC\_Lon\_ChanP  
HGC\_Lon\_ChanR  
HGC\_Lon\_ChanT  
HGC\_R\_ChanC  
HGC\_R\_ChanD  
HGC\_R\_ChanP  
HGC\_R\_ChanR  
HGC\_R\_ChanT  
H\_CountRate\_ChanP  
H\_CountRate\_ChanR  
H\_CountRate\_ChanT  
H\_Counts\_ChanP  
H\_Counts\_ChanR  
H\_Counts\_ChanT  
H\_Flux\_ChanP  
H\_Flux\_ChanR  
H\_Flux\_ChanT  
He3\_CountRate\_ChanC  
He3\_Counts\_ChanC  
He4\_CountRate\_ChanC  
He4\_Counts\_ChanC



He4\_Flux\_ChanC  
Look\_Direction\_80\_DELTAMINUS  
Look\_Direction\_80\_DELTAPLUS  
Mg\_CountRate\_ChanD  
Mg\_Counts\_ChanD  
N\_CountRate\_ChanD  
N\_Counts\_ChanD  
Ne\_CountRate\_ChanD  
Ne\_Counts\_ChanD  
O\_CountRate\_ChanC  
O\_Counts\_ChanC  
PA\_ChanC  
PA\_ChanD  
PA\_ChanP  
PA\_ChanR  
PA\_ChanT  
Quality\_Flag\_ChanC  
Quality\_Flag\_ChanD  
Quality\_Flag\_ChanP  
Quality\_Flag\_ChanR  
Quality\_Flag\_ChanT  
RTN\_ChanC  
RTN\_ChanD  
RTN\_ChanP  
RTN\_ChanR  
RTN\_ChanT  
SA\_ChanC  
SA\_ChanD  
SA\_ChanP  
SA\_ChanR  
SA\_ChanT  
Si\_CountRate\_ChanD  
Si\_Counts\_ChanD

## **5.15 PSP\_ISOIS-EPILO\_L2-PE**

Electron\_CountRate\_ChanE  
Electron\_CountRate\_ChanF  
Electron\_CountRate\_ChanG  
Electron\_Counts\_ChanE  
Electron\_Counts\_ChanF  
Electron\_Counts\_ChanG  
HCI\_ChanE  
HCI\_ChanF

HCI\_ChanG  
HCI\_Lat\_ChanE  
HCI\_Lat\_ChanF  
HCI\_Lat\_ChanG  
HCI\_Lon\_ChanE  
HCI\_Lon\_ChanF  
HCI\_Lon\_ChanG  
HCI\_R\_ChanE  
HCI\_R\_ChanF  
HCI\_R\_ChanG  
HGC\_Lat\_ChanE  
HGC\_Lat\_ChanF  
HGC\_Lat\_ChanG  
HGC\_Lon\_ChanE  
HGC\_Lon\_ChanF  
HGC\_Lon\_ChanG  
HGC\_R\_ChanE  
HGC\_R\_ChanF  
HGC\_R\_ChanG  
H\_CountRate\_ChanE  
H\_CountRate\_ChanF  
H\_CountRate\_ChanG  
H\_Counts\_ChanE  
H\_Counts\_ChanF  
H\_Counts\_ChanG  
Look\_Direction\_08\_DELTAMINUS  
Look\_Direction\_08\_DELTAPLUS  
Look\_Direction\_80\_DELTAMINUS  
Look\_Direction\_80\_DELTAPLUS  
PA\_ChanE  
PA\_ChanF  
PA\_ChanG  
Quality\_Flag\_ChanE  
Quality\_Flag\_ChanF  
Quality\_Flag\_ChanG  
RTN\_ChanE  
RTN\_ChanF  
RTN\_ChanG  
SA\_ChanE  
SA\_ChanF  
SA\_ChanG

## 5.16 PSP\_ISOIS\_L2-EPHEM

Clock\_Angle  
HCI\_Lat  
HCI\_Lon  
HCI\_R  
HGC\_Lat  
HGC\_Lon  
HGC\_R  
Ram\_Pointing  
Roll\_Angle  
Spiral\_HETA  
Spiral\_LET1A  
Spiral\_LET2C  
Spiral\_Lo  
Sun\_Angle  
Umbra\_Pointing

## 5.17 PSP\_ISOIS\_L2-SUMMARY

A\_H\_Rate\_TS  
A\_Heavy\_Rate\_TS  
Electron\_CountRate\_ChanE  
HET\_A\_Electrons\_Rate\_TS  
HET\_A\_H\_Rate\_TS  
H\_CountRate\_ChanP\_SP

## 6 CDF CONTENTS

### 6.1 PSP\_ISOIS-EPILO\_L2-IC

ISOIS-EPILO>Integrated Science Investigation of the Sun, Energetic Particle Instrument Lo  
L2-ic>Level 2 ic

EPI-Lo, Ion Composition mode.

Instrument paper: Integrated Science Investigation of the Sun (ISIS): Design of the Energetic Particle Investigation. McComas, D. J. et al (2016). Space Sci. Rev., doi:10.1007/s11214-014-0059-1

1 minute to 1 hour

Cite McComas et al (2016), doi:10.1007/s11214-014-0059-1

#### 6.1.1 PRIMARY VARIABLES

**6.1.1.1 H\_Flux\_ChanP** H flux channel P (HiResProtons) ( $\text{cm}^{-2}\text{sr}^{-1}\text{sec}^{-1}\text{keV}^{-1}$ )

Size:  $80 \times 48$  time-varying

particle\_flux>differential\_directional\_number

Ion Composition mode.

Look\_Direction\_80 0 – 79 (80 bins)

H\_ChanP\_Energy 70 – 9464 keV (39 bins)

**6.1.1.2 H\_Flux\_ChanR** H flux channel R (HiTimeResProtons) ( $\text{cm}^{-2}\text{sr}^{-1}\text{sec}^{-1}\text{keV}^{-1}$ )

Size:  $80 \times 48$  time-varying

particle\_flux>differential\_directional\_number

Ion Composition mode.

Look\_Direction\_80 0 – 79 (80 bins)

H\_ChanR\_Energy 80 – 7441 keV (14 bins)

**6.1.1.3 H\_Flux\_ChanT** H flux channel T (IonTOF) ( $\text{cm}^{-2}\text{sr}^{-1}\text{sec}^{-1}(\text{keV}/\text{nuc})^{-1}$ )

Size:  $80 \times 47$  time-varying

particle\_flux>differential\_directional\_number

Ion Composition mode. May contain significant photon counts, particularly directions L31, L34, L35. See Hill, M.E. et al., 2020, ApJS, doi:10.3847/1538-4365/ab643d .

Look\_Direction\_80 0 – 79 (80 bins)

H\_ChanT\_Energy 20 – 34454 keV/nuc (31 bins)

**6.1.1.4 He4\_Flux\_ChanC** He4 flux channel C (Ions1) ( $\text{cm}^{-2}\text{sr}^{-1}\text{sec}^{-1}\text{keV}^{-1}$ )

Size:  $80 \times 48$  time-varying

particle\_flux>differential\_directional\_number

Ion Composition mode.

Look\_Direction\_80 0 – 79 (80 bins)

He4\_ChanC\_Energy 85 – 20909 keV (44 bins)

## 6.1.2 OTHER DATA

### 6.1.2.1 C\_CountRate\_ChanD C count rate channel D (Ions2) (counts/sec)

Size: 80 × 48 time-varying

particle\_flux>differential\_directional\_number\_rate

Ion Composition mode. Corrected for deadtime.

Look\_Direction\_80 0 – 79 (80 bins)

C\_ChanD\_Energy 182 – 19902 keV (22 bins)

### 6.1.2.2 C\_Counts\_ChanD C counts channel D (Ions2) (counts)

Size: 80 × 48 time-varying

particle\_flux>differential\_directional\_number\_rate

Ion Composition mode. Raw counts per integration.

Look\_Direction\_80 0 – 79 (80 bins)

C\_ChanD\_Energy 182 – 19902 keV (22 bins)

### 6.1.2.3 Fe\_CountRate\_ChanC Fe count rate channel C (Ions1) (counts/sec)

Size: 80 × 48 time-varying

particle\_flux>differential\_directional\_number\_rate

Ion Composition mode. Corrected for deadtime.

Look\_Direction\_80 0 – 79 (80 bins)

Fe\_ChanC\_Energy 444 – 23773 keV (42 bins)

### 6.1.2.4 Fe\_Counts\_ChanC Fe counts channel C (Ions1) (counts)

Size: 80 × 48 time-varying

particle\_flux>differential\_directional\_number\_rate

Ion Composition mode. Raw counts per integration.

Look\_Direction\_80 0 – 79 (80 bins)

Fe\_ChanC\_Energy 444 – 23773 keV (42 bins)

### 6.1.2.5 HCI\_ChanC HCI flow direction ChanC

Size: 80 × 3 time-varying

position>direction

Unit vector, after Fraenz and Harper, PSS, 2002. ChanC timebase.

Look\_Direction\_80 0 – 79 (80 bins)

**6.1.2.6 HCI\_ChanD** HCI flow direction ChanD

Size:  $80 \times 3$  time-varying

position>direction

Unit vector, after Fraenz and Harper, PSS, 2002. ChanD timebase.

Look\_Direction\_80 0 – 79 (80 bins)

**6.1.2.7 HCI\_ChanP** HCI flow direction ChanP

Size:  $80 \times 3$  time-varying

position>direction

Unit vector, after Fraenz and Harper, PSS, 2002. ChanP timebase.

Look\_Direction\_80 0 – 79 (80 bins)

**6.1.2.8 HCI\_ChanR** HCI flow direction ChanR

Size:  $80 \times 3$  time-varying

position>direction

Unit vector, after Fraenz and Harper, PSS, 2002. ChanR timebase.

Look\_Direction\_80 0 – 79 (80 bins)

**6.1.2.9 HCI\_ChanT** HCI flow direction ChanT

Size:  $80 \times 3$  time-varying

position>direction

Unit vector, after Fraenz and Harper, PSS, 2002. ChanT timebase.

Look\_Direction\_80 0 – 79 (80 bins)

**6.1.2.10 HCI\_Lat\_ChanC** HCI latitude ChanC (degrees)

time-varying

position>latitude

At timestamp. After Fraenz and Harper, PSS, 2002. ChanC timebase.

**6.1.2.11 HCI\_Lat\_ChanD** HCI latitude ChanD (degrees)

time-varying

position>latitude

At timestamp. After Fraenz and Harper, PSS, 2002. ChanD timebase.

**6.1.2.12 HCI\_Lat\_ChanP** HCI latitude ChanP (degrees)  
time-varying  
position>latitude  
At timestamp. After Fraenz and Harper, PSS, 2002. ChanP timebase.

**6.1.2.13 HCI\_Lat\_ChanR** HCI latitude ChanR (degrees)  
time-varying  
position>latitude  
At timestamp. After Fraenz and Harper, PSS, 2002. ChanR timebase.

**6.1.2.14 HCI\_Lat\_ChanT** HCI latitude ChanT (degrees)  
time-varying  
position>latitude  
At timestamp. After Fraenz and Harper, PSS, 2002. ChanT timebase.

**6.1.2.15 HCI\_Lon\_ChanC** HCI longitude ChanC (degrees)  
time-varying  
position>longitude  
At timestamp. After Fraenz and Harper, PSS, 2002. ChanC timebase.

**6.1.2.16 HCI\_Lon\_ChanD** HCI longitude ChanD (degrees)  
time-varying  
position>longitude  
At timestamp. After Fraenz and Harper, PSS, 2002. ChanD timebase.

**6.1.2.17 HCI\_Lon\_ChanP** HCI longitude ChanP (degrees)  
time-varying  
position>longitude  
At timestamp. After Fraenz and Harper, PSS, 2002. ChanP timebase.

**6.1.2.18 HCI\_Lon\_ChanR** HCI longitude ChanR (degrees)  
time-varying  
position>longitude  
At timestamp. After Fraenz and Harper, PSS, 2002. ChanR timebase.

**6.1.2.19 HCI\_Lon\_ChanT** HCI longitude ChanT (degrees)  
time-varying  
position>longitude  
At timestamp. After Fraenz and Harper, PSS, 2002. ChanT timebase.

**6.1.2.20 HCI\_R\_ChanC** Heliocentric distance ChanC (AU)  
time-varying  
position>radial  
At timestamp. After Fraenz and Harper, PSS, 2002. ChanC timebase.

**6.1.2.21 HCI\_R\_ChanD** Heliocentric distance ChanD (AU)  
time-varying  
position>radial  
At timestamp. After Fraenz and Harper, PSS, 2002. ChanD timebase.

**6.1.2.22 HCI\_R\_ChanP** Heliocentric distance ChanP (AU)  
time-varying  
position>radial  
At timestamp. After Fraenz and Harper, PSS, 2002. ChanP timebase.

**6.1.2.23 HCI\_R\_ChanR** Heliocentric distance ChanR (AU)  
time-varying  
position>radial  
At timestamp. After Fraenz and Harper, PSS, 2002. ChanR timebase.

**6.1.2.24 HCI\_R\_ChanT** Heliocentric distance ChanT (AU)  
time-varying  
position>radial  
At timestamp. After Fraenz and Harper, PSS, 2002. ChanT timebase.

**6.1.2.25 HGC\_Lat\_ChanC** HGC latitude ChanC (degrees)  
time-varying  
position>latitude  
At timestamp. After Fraenz and Harper, PSS, 2002. ChanC timebase.



**6.1.2.26 HGC\_Lat\_ChanD** HGC latitude ChanD (degrees)  
time-varying  
position>latitude  
At timestamp. After Fraenz and Harper, PSS, 2002. ChanD timebase.

**6.1.2.27 HGC\_Lat\_ChanP** HGC latitude ChanP (degrees)  
time-varying  
position>latitude  
At timestamp. After Fraenz and Harper, PSS, 2002. ChanP timebase.

**6.1.2.28 HGC\_Lat\_ChanR** HGC latitude ChanR (degrees)  
time-varying  
position>latitude  
At timestamp. After Fraenz and Harper, PSS, 2002. ChanR timebase.

**6.1.2.29 HGC\_Lat\_ChanT** HGC latitude ChanT (degrees)  
time-varying  
position>latitude  
At timestamp. After Fraenz and Harper, PSS, 2002. ChanT timebase.

**6.1.2.30 HGC\_Lon\_ChanC** HGC longitude ChanC (degrees)  
time-varying  
position>longitude  
At timestamp. After Fraenz and Harper, PSS, 2002. ChanC timebase.

**6.1.2.31 HGC\_Lon\_ChanD** HGC longitude ChanD (degrees)  
time-varying  
position>longitude  
At timestamp. After Fraenz and Harper, PSS, 2002. ChanD timebase.

**6.1.2.32 HGC\_Lon\_ChanP** HGC longitude ChanP (degrees)  
time-varying  
position>longitude  
At timestamp. After Fraenz and Harper, PSS, 2002. ChanP timebase.

**6.1.2.33 HGC\_Lon\_ChanR** HGC longitude ChanR (degrees)  
time-varying  
position>longitude  
At timestamp. After Fraenz and Harper, PSS, 2002. ChanR timebase.

**6.1.2.34 HGC\_Lon\_ChanT** HGC longitude ChanT (degrees)  
time-varying  
position>longitude  
At timestamp. After Fraenz and Harper, PSS, 2002. ChanT timebase.

**6.1.2.35 HGC\_R\_ChanC** Heliocentric distance ChanC (AU)  
time-varying  
position>radial  
At timestamp. After Fraenz and Harper, PSS, 2002. ChanC timebase.

**6.1.2.36 HGC\_R\_ChanD** Heliocentric distance ChanD (AU)  
time-varying  
position>radial  
At timestamp. After Fraenz and Harper, PSS, 2002. ChanD timebase.

**6.1.2.37 HGC\_R\_ChanP** Heliocentric distance ChanP (AU)  
time-varying  
position>radial  
At timestamp. After Fraenz and Harper, PSS, 2002. ChanP timebase.

**6.1.2.38 HGC\_R\_ChanR** Heliocentric distance ChanR (AU)  
time-varying  
position>radial  
At timestamp. After Fraenz and Harper, PSS, 2002. ChanR timebase.

**6.1.2.39 HGC\_R\_ChanT** Heliocentric distance ChanT (AU)  
time-varying  
position>radial  
At timestamp. After Fraenz and Harper, PSS, 2002. ChanT timebase.

**6.1.2.40 H\_CountRate\_ChanP** H count rate channel P (HiResProtons) (counts/sec)

Size: 80  $\times$  48 time-varying

particle\_flux>differential\_directional\_number\_rate

Ion Composition mode. Corrected for deadtime.

Look\_Direction\_80 0 – 79 (80 bins)

H\_ChanP\_Energy 70 – 9464 keV (39 bins)

**6.1.2.41 H\_CountRate\_ChanR** H count rate channel R (HiTimeResProtons) (counts/sec)

Size: 80  $\times$  48 time-varying

particle\_flux>differential\_directional\_number\_rate

Ion Composition mode. Corrected for deadtime.

Look\_Direction\_80 0 – 79 (80 bins)

H\_ChanR\_Energy 80 – 7441 keV (14 bins)

**6.1.2.42 H\_CountRate\_ChanT** H count rate channel T (IonTOF) (counts/sec)

Size: 80  $\times$  47 time-varying

particle\_flux>differential\_directional\_number\_rate

Ion Composition mode. Corrected for deadtime. May contain significant photon counts, particularly directions L31, L34, L35. See Hill, M.E. et al., 2020, ApJS, doi:10.3847/1538-4365/ab643d .

Look\_Direction\_80 0 – 79 (80 bins)

H\_ChanT\_Energy 20 – 34454 keV/nuc (31 bins)

**6.1.2.43 H\_Counts\_ChanP** H counts channel P (HiResProtons) (counts)

Size: 80  $\times$  48 time-varying

particle\_flux>differential\_directional\_number\_rate

Ion Composition mode. Raw counts per integration.

Look\_Direction\_80 0 – 79 (80 bins)

H\_ChanP\_Energy 70 – 9464 keV (39 bins)

**6.1.2.44 H\_Counts\_ChanR** H counts channel R (HiTimeResProtons) (counts)

Size: 80  $\times$  48 time-varying

particle\_flux>differential\_directional\_number\_rate

Ion Composition mode. Raw counts per integration.

Look\_Direction\_80 0 – 79 (80 bins)

H\_ChanR\_Energy 80 – 7441 keV (14 bins)

**6.1.2.45 H\_Counts\_ChanT** H counts channel T (IonTOF) (counts)

Size:  $80 \times 47$  time-varying

particle\_flux>differential\_directional\_number\_rate

Ion Composition mode. Raw counts per integration. May contain significant photon counts, particularly directions L31, L34, L35. See Hill, M.E. et al., 2020, ApJS, doi:10.3847/1538-4365/ab643d .

Look\_Direction\_80 0 – 79 (80 bins)

H\_ChanT\_Energy 20 – 34454 keV/nuc (31 bins)

**6.1.2.46 He3\_CountRate\_ChanC** He3 count rate channel C (Ions1) (counts/sec)

Size:  $80 \times 48$  time-varying

particle\_flux>differential\_directional\_number\_rate

Ion Composition mode. Corrected for deadtime.

Look\_Direction\_80 0 – 79 (80 bins)

He3\_ChanC\_Energy 98 – 20905 keV (44 bins)

**6.1.2.47 He3\_Counts\_ChanC** He3 counts channel C (Ions1) (counts)

Size:  $80 \times 48$  time-varying

particle\_flux>differential\_directional\_number\_rate

Ion Composition mode. Raw counts per integration.

Look\_Direction\_80 0 – 79 (80 bins)

He3\_ChanC\_Energy 98 – 20905 keV (44 bins)

**6.1.2.48 He4\_CountRate\_ChanC** He4 count rate channel C (Ions1) (counts/sec)

Size:  $80 \times 48$  time-varying

particle\_flux>differential\_directional\_number\_rate

Ion Composition mode. Corrected for deadtime.

Look\_Direction\_80 0 – 79 (80 bins)

He4\_ChanC\_Energy 85 – 20909 keV (44 bins)

**6.1.2.49 He4\_Counts\_ChanC** He4 counts channel C (Ions1) (counts)

Size:  $80 \times 48$  time-varying

particle\_flux>differential\_directional\_number\_rate

Ion Composition mode. Raw counts per integration.

Look\_Direction\_80 0 – 79 (80 bins)

He4\_ChanC\_Energy 85 – 20909 keV (44 bins)

**6.1.2.50 Mg\_CountRate\_ChanD** Mg count rate channel D (Ions2) (counts/sec)

Size: 80  $\times$  48 time-varying

particle\_flux>differential\_directional\_number\_rate

Ion Composition mode. Corrected for deadtime.

Look\_Direction\_80 0 – 79 (80 bins)

Mg\_ChanD\_Energy 231 – 20942 keV (22 bins)

**6.1.2.51 Mg\_Counts\_ChanD** Mg counts channel D (Ions2) (counts)

Size: 80  $\times$  48 time-varying

particle\_flux>differential\_directional\_number\_rate

Ion Composition mode. Raw counts per integration.

Look\_Direction\_80 0 – 79 (80 bins)

Mg\_ChanD\_Energy 231 – 20942 keV (22 bins)

**6.1.2.52 N\_CountRate\_ChanD** N count rate channel D (Ions2) (counts/sec)

Size: 80  $\times$  48 time-varying

particle\_flux>differential\_directional\_number\_rate

Ion Composition mode. Corrected for deadtime.

Look\_Direction\_80 0 – 79 (80 bins)

N\_ChanD\_Energy

**6.1.2.53 N\_Counts\_ChanD** N counts channel D (Ions2) (counts)

Size: 80  $\times$  48 time-varying

particle\_flux>differential\_directional\_number\_rate

Ion Composition mode. Raw counts per integration.

Look\_Direction\_80 0 – 79 (80 bins)

N\_ChanD\_Energy

**6.1.2.54 Ne\_CountRate\_ChanD** Ne count rate channel D (Ions2) (counts/sec)

Size: 80  $\times$  48 time-varying

particle\_flux>differential\_directional\_number\_rate

Ion Composition mode. Corrected for deadtime.

Look\_Direction\_80 0 – 79 (80 bins)

Ne\_ChanD\_Energy 652 – 17605 keV (7 bins)

**6.1.2.55 Ne\_Counts\_ChanD** Ne counts channel D (Ions2) (counts)

Size: 80  $\times$  48 time-varying

particle\_flux>differential\_directional\_number\_rate

Ion Composition mode. Raw counts per integration.

Look\_Direction\_80 0 – 79 (80 bins)

Ne\_ChanD\_Energy 652 – 17605 keV (7 bins)

**6.1.2.56 O\_CountRate\_ChanC** O count rate channel C (Ions1) (counts/sec)

Size: 80 × 48 time-varying

particle\_flux>differential\_directional\_number\_rate

Ion Composition mode. Corrected for deadtime.

Look\_Direction\_80 0 – 79 (80 bins)

O\_ChanC\_Energy 210 – 21397 keV (43 bins)

**6.1.2.57 O\_Counts\_ChanC** O counts channel C (Ions1) (counts)

Size: 80 × 48 time-varying

particle\_flux>differential\_directional\_number\_rate

Ion Composition mode. Raw counts per integration.

Look\_Direction\_80 0 – 79 (80 bins)

O\_ChanC\_Energy 210 – 21397 keV (43 bins)

**6.1.2.58 PA\_ChanC** Pitch angle ChanC (degree)

Size: 80 time-varying

position>angle

Look\_Direction\_80 0 – 79 (80 bins)

**6.1.2.59 PA\_ChanD** Pitch angle ChanD (degree)

Size: 80 time-varying

position>angle

Look\_Direction\_80 0 – 79 (80 bins)

**6.1.2.60 PA\_ChanP** Pitch angle ChanP (degree)

Size: 80 time-varying

position>angle

Look\_Direction\_80 0 – 79 (80 bins)

**6.1.2.61 PA\_ChanR** Pitch angle ChanR (degree)

Size: 80 time-varying

position>angle  
Look\_Direction\_80 0 – 79 (80 bins)

**6.1.2.62 PA\_ChanT** Pitch angle ChanT (degree)

Size: 80 time-varying  
position>angle  
Look\_Direction\_80 0 – 79 (80 bins)

**6.1.2.63 RTN\_ChanC** RTN flow direction ChanC

Size:  $80 \times 3$  time-varying  
position>direction  
Unit vector, after Fraenz and Harper, PSS, 2002. ChanC timebase.  
Look\_Direction\_80 0 – 79 (80 bins)

**6.1.2.64 RTN\_ChanD** RTN flow direction ChanD

Size:  $80 \times 3$  time-varying  
position>direction  
Unit vector, after Fraenz and Harper, PSS, 2002. ChanD timebase.  
Look\_Direction\_80 0 – 79 (80 bins)

**6.1.2.65 RTN\_ChanP** RTN flow direction ChanP

Size:  $80 \times 3$  time-varying  
position>direction  
Unit vector, after Fraenz and Harper, PSS, 2002. ChanP timebase.  
Look\_Direction\_80 0 – 79 (80 bins)

**6.1.2.66 RTN\_ChanR** RTN flow direction ChanR

Size:  $80 \times 3$  time-varying  
position>direction  
Unit vector, after Fraenz and Harper, PSS, 2002. ChanR timebase.  
Look\_Direction\_80 0 – 79 (80 bins)

**6.1.2.67 RTN\_ChanT** RTN flow direction ChanT

Size:  $80 \times 3$  time-varying  
position>direction  
Unit vector, after Fraenz and Harper, PSS, 2002. ChanT timebase.

Look\_Direction\_80 0 – 79 (80 bins)

**6.1.2.68 SA\_ChanC** Nominal Parker Spiral angle ChanC (degree)

Size: 80 time-varying

position>angle

Angle between particle direction and nominal outward Parker Spiral, based on 400km/s solar wind and corotation breakdown at 10Rs.

Look\_Direction\_80 0 – 79 (80 bins)

**6.1.2.69 SA\_ChanD** Nominal Parker Spiral angle ChanD (degree)

Size: 80 time-varying

position>angle

Angle between particle direction and nominal outward Parker Spiral, based on 400km/s solar wind and corotation breakdown at 10Rs.

Look\_Direction\_80 0 – 79 (80 bins)

**6.1.2.70 SA\_ChanP** Nominal Parker Spiral angle ChanP (degree)

Size: 80 time-varying

position>angle

Angle between particle direction and nominal outward Parker Spiral, based on 400km/s solar wind and corotation breakdown at 10Rs.

Look\_Direction\_80 0 – 79 (80 bins)

**6.1.2.71 SA\_ChanR** Nominal Parker Spiral angle ChanR (degree)

Size: 80 time-varying

position>angle

Angle between particle direction and nominal outward Parker Spiral, based on 400km/s solar wind and corotation breakdown at 10Rs.

Look\_Direction\_80 0 – 79 (80 bins)

**6.1.2.72 SA\_ChanT** Nominal Parker Spiral angle ChanT (degree)

Size: 80 time-varying

position>angle

Angle between particle direction and nominal outward Parker Spiral, based on 400km/s solar wind and corotation breakdown at 10Rs.

Look\_Direction\_80 0 – 79 (80 bins)



**6.1.2.73 Si\_CountRate\_ChanD** Si count rate channel D (Ions2) (counts/sec)

Size: 80  $\times$  48 time-varying

particle\_flux>differential\_directional\_number\_rate

Ion Composition mode. Corrected for deadtime.

Look\_Direction\_80 0 – 79 (80 bins)

Si\_ChanD\_Energy 321 – 21454 keV (21 bins)

**6.1.2.74 Si\_Counts\_ChanD** Si counts channel D (Ions2) (counts)

Size: 80  $\times$  48 time-varying

particle\_flux>differential\_directional\_number\_rate

Ion Composition mode. Raw counts per integration.

Look\_Direction\_80 0 – 79 (80 bins)

Si\_ChanD\_Energy 321 – 21454 keV (21 bins)

**6.1.3 OTHER SUPPORT**

**6.1.3.1 Look\_Direction\_80\_DELTAMINUS** Size: 80 constant number

**6.1.3.2 Look\_Direction\_80\_DELTAPLUS** Size: 80 constant number

**6.1.3.3 Quality\_Flag\_ChanC** Data-quality flag for channel C (Ions1)

Size: 10 time-varying

flag>status

Quality flag number ChanICB 0 – 9 (10 bins)

**6.1.3.4 Quality\_Flag\_ChanD** Data-quality flag for channel D (Ions2)

Size: 10 time-varying

flag>status

Quality flag number ChanICB 0 – 9 (10 bins)

**6.1.3.5 Quality\_Flag\_ChanP** Data-quality flag for channel P (HiResProtons)

Size: 10 time-varying

flag>status

Quality flag number ChanICB 0 – 9 (10 bins)

**6.1.3.6 Quality\_Flag\_ChanR** Data-quality flag for channel R (HiTimeResProtons)

Size: 10 time-varying

flag>status

Quality flag number ChanICB 0 – 9 (10 bins)

**6.1.3.7 Quality\_Flag\_ChanT** Data-quality flag for channel T (IonTOF)

Size: 10 time-varying

flag>status

Quality flag number ChanICB 0 – 9 (10 bins)

## 6.2 PSP\_ISOIS-EPILO\_L2-PE

ISOIS-EPILO>Integrated Science Investigation of the Sun, Energetic Particle Instrument Lo

L2-pe>Level 2 pe

EPI-Lo, Particle Energy mode.

Instrument paper: Integrated Science Investigation of the Sun (ISIS): Design of the Energetic Particle Investigation. McComas, D. J. et al (2016). Space Sci. Rev., doi:10.1007/s11214-014-0059-1

1 minute to 1 hour

Cite McComas et al (2016), doi:10.1007/s11214-014-0059-1

### 6.2.1 PRIMARY VARIABLES

#### 6.2.2 OTHER DATA

**6.2.2.1 Electron\_CountRate\_ChanE** Electron count rate channel E (HiResElectrons)  
(counts/sec)

Size:  $8 \times 48$  time-varying

particle\_flux>differential\_directional\_number\_rate

Particle Energy mode. Corrected for deadtime.

Look\_Direction\_08 0 – 7 (8 bins)

Electron\_ChanE\_Energy 12 – 9065 keV (32 bins)

**6.2.2.2 Electron\_CountRate\_ChanF** Electron count rate channel F (HiTimeResElectrons)  
(counts/sec)

Size:  $8 \times 48$  time-varying

particle\_flux>differential\_directional\_number\_rate

Particle Energy mode. Corrected for deadtime.

Look\_Direction\_08 0 – 7 (8 bins)

Electron\_ChanF\_Energy 19 – 6607 keV (12 bins)

**6.2.2.3 Electron\_CountRate\_ChanG** Electron count rate channel G (HiLookResElectrons) (counts/sec)

Size:  $80 \times 48$  time-varying

particle\_flux>differential\_directional\_number\_rate

Particle Energy mode. Corrected for deadtime.

Look\_Direction\_80 0 – 79 (80 bins)

Electron\_ChanG\_Energy 12 – 9065 keV (32 bins)

**6.2.2.4 Electron\_Counts\_ChanE** Electron counts channel E (HiResElectrons) (counts)

Size:  $8 \times 48$  time-varying

particle\_flux>differential\_directional\_number\_rate

Particle Energy mode. Raw counts per integration.

Look\_Direction\_08 0 – 7 (8 bins)

Electron\_ChanE\_Energy 12 – 9065 keV (32 bins)

**6.2.2.5 Electron\_Counts\_ChanF** Electron counts channel F (HiTimeResElectrons) (counts)

Size:  $8 \times 48$  time-varying

particle\_flux>differential\_directional\_number\_rate

Particle Energy mode. Raw counts per integration.

Look\_Direction\_08 0 – 7 (8 bins)

Electron\_ChanF\_Energy 19 – 6607 keV (12 bins)

**6.2.2.6 Electron\_Counts\_ChanG** Electron counts channel G (HiLookResElectrons) (counts)

Size:  $80 \times 48$  time-varying

particle\_flux>differential\_directional\_number\_rate

Particle Energy mode. Raw counts per integration.

Look\_Direction\_80 0 – 79 (80 bins)

Electron\_ChanG\_Energy 12 – 9065 keV (32 bins)

**6.2.2.7 HCI\_ChanE** HCI flow direction ChanE

Size:  $8 \times 3$  time-varying

position>direction

Unit vector, after Fraenz and Harper, PSS, 2002. ChanE timebase.

Look\_Direction\_08 0 – 7 (8 bins)

**6.2.2.8 HCI\_ChanF** HCI flow direction ChanF

Size:  $8 \times 3$  time-varying

position>direction

Unit vector, after Fraenz and Harper, PSS, 2002. ChanF timebase.

Look\_Direction\_08 0 – 7 (8 bins)

#### **6.2.2.9 HCI\_ChanG** HCI flow direction ChanG

Size:  $80 \times 3$  time-varying

position>direction

Unit vector, after Fraenz and Harper, PSS, 2002. ChanG timebase.

Look\_Direction\_80 0 – 79 (80 bins)

#### **6.2.2.10 HCI\_Lat\_ChanE** HCI latitude ChanE (degrees)

time-varying

position>latitude

At timestamp. After Fraenz and Harper, PSS, 2002. ChanE timebase.

#### **6.2.2.11 HCI\_Lat\_ChanF** HCI latitude ChanF (degrees)

time-varying

position>latitude

At timestamp. After Fraenz and Harper, PSS, 2002. ChanF timebase.

#### **6.2.2.12 HCI\_Lat\_ChanG** HCI latitude ChanG (degrees)

time-varying

position>latitude

At timestamp. After Fraenz and Harper, PSS, 2002. ChanG timebase.

#### **6.2.2.13 HCI\_Lon\_ChanE** HCI longitude ChanE (degrees)

time-varying

position>longitude

At timestamp. After Fraenz and Harper, PSS, 2002. ChanE timebase.

#### **6.2.2.14 HCI\_Lon\_ChanF** HCI longitude ChanF (degrees)

time-varying

position>longitude

At timestamp. After Fraenz and Harper, PSS, 2002. ChanF timebase.

**6.2.2.15 HCI\_Lon\_ChanG** HCI longitude ChanG (degrees)  
time-varying  
position>longitude  
At timestamp. After Fraenz and Harper, PSS, 2002. ChanG timebase.

**6.2.2.16 HCI\_R\_ChanE** Heliocentric distance ChanE (AU)  
time-varying  
position>radial  
At timestamp. After Fraenz and Harper, PSS, 2002. ChanE timebase.

**6.2.2.17 HCI\_R\_ChanF** Heliocentric distance ChanF (AU)  
time-varying  
position>radial  
At timestamp. After Fraenz and Harper, PSS, 2002. ChanF timebase.

**6.2.2.18 HCI\_R\_ChanG** Heliocentric distance ChanG (AU)  
time-varying  
position>radial  
At timestamp. After Fraenz and Harper, PSS, 2002. ChanG timebase.

**6.2.2.19 HGC\_Lat\_ChanE** HGC latitude ChanE (degrees)  
time-varying  
position>latitude  
At timestamp. After Fraenz and Harper, PSS, 2002. ChanE timebase.

**6.2.2.20 HGC\_Lat\_ChanF** HGC latitude ChanF (degrees)  
time-varying  
position>latitude  
At timestamp. After Fraenz and Harper, PSS, 2002. ChanF timebase.

**6.2.2.21 HGC\_Lat\_ChanG** HGC latitude ChanG (degrees)  
time-varying  
position>latitude  
At timestamp. After Fraenz and Harper, PSS, 2002. ChanG timebase.

**6.2.2.22 HGC\_Lon\_ChanE** HGC longitude ChanE (degrees)  
time-varying  
position>longitude  
At timestamp. After Fraenz and Harper, PSS, 2002. ChanE timebase.

**6.2.2.23 HGC\_Lon\_ChanF** HGC longitude ChanF (degrees)  
time-varying  
position>longitude  
At timestamp. After Fraenz and Harper, PSS, 2002. ChanF timebase.

**6.2.2.24 HGC\_Lon\_ChanG** HGC longitude ChanG (degrees)  
time-varying  
position>longitude  
At timestamp. After Fraenz and Harper, PSS, 2002. ChanG timebase.

**6.2.2.25 HGC\_R\_ChanE** Heliocentric distance ChanE (AU)  
time-varying  
position>radial  
At timestamp. After Fraenz and Harper, PSS, 2002. ChanE timebase.

**6.2.2.26 HGC\_R\_ChanF** Heliocentric distance ChanF (AU)  
time-varying  
position>radial  
At timestamp. After Fraenz and Harper, PSS, 2002. ChanF timebase.

**6.2.2.27 HGC\_R\_ChanG** Heliocentric distance ChanG (AU)  
time-varying  
position>radial  
At timestamp. After Fraenz and Harper, PSS, 2002. ChanG timebase.

**6.2.2.28 H\_CountRate\_ChanE** H count rate channel E (HiResElectrons) (counts/sec)  
Size:  $8 \times 48$  time-varying  
particle\_flux>differential\_directional\_number\_rate  
Particle Energy mode. Corrected for deadtime.  
Look\_Direction\_08 0 – 7 (8 bins)

H\_ChanE\_Energy

**6.2.2.29 H\_CountRate\_ChanF** H count rate channel F (HiTimeResElectrons) (counts/sec)

Size:  $8 \times 48$  time-varying

particle\_flux>differential\_directional\_number\_rate

Particle Energy mode. Corrected for deadtime.

Look\_Direction\_08 0 – 7 (8 bins)

H\_ChanF\_Energy

**6.2.2.30 H\_CountRate\_ChanG** H count rate channel G (HiLookResElectrons) (counts/sec)

Size:  $80 \times 48$  time-varying

particle\_flux>differential\_directional\_number\_rate

Particle Energy mode. Corrected for deadtime.

Look\_Direction\_80 0 – 79 (80 bins)

H\_ChanG\_Energy

**6.2.2.31 H\_Counts\_ChanE** H counts channel E (HiResElectrons) (counts)

Size:  $8 \times 48$  time-varying

particle\_flux>differential\_directional\_number\_rate

Particle Energy mode. Raw counts per integration.

Look\_Direction\_08 0 – 7 (8 bins)

H\_ChanE\_Energy

**6.2.2.32 H\_Counts\_ChanF** H counts channel F (HiTimeResElectrons) (counts)

Size:  $8 \times 48$  time-varying

particle\_flux>differential\_directional\_number\_rate

Particle Energy mode. Raw counts per integration.

Look\_Direction\_08 0 – 7 (8 bins)

H\_ChanF\_Energy

**6.2.2.33 H\_Counts\_ChanG** H counts channel G (HiLookResElectrons) (counts)

Size:  $80 \times 48$  time-varying

particle\_flux>differential\_directional\_number\_rate

Particle Energy mode. Raw counts per integration.

Look\_Direction\_80 0 – 79 (80 bins)

H\_ChanG\_Energy

**6.2.2.34 PA\_ChanE** Pitch angle ChanE (degree)

Size: 8 time-varying

position>angle

Look\_Direction\_08 0 – 7 (8 bins)

**6.2.2.35 PA\_ChanF** Pitch angle ChanF (degree)

Size: 8 time-varying

position>angle

Look\_Direction\_08 0 – 7 (8 bins)

**6.2.2.36 PA\_ChanG** Pitch angle ChanG (degree)

Size: 80 time-varying

position>angle

Look\_Direction\_80 0 – 79 (80 bins)

**6.2.2.37 RTN\_ChanE** RTN flow direction ChanE

Size:  $8 \times 3$  time-varying

position>direction

Unit vector, after Fraenz and Harper, PSS, 2002. ChanE timebase.

Look\_Direction\_08 0 – 7 (8 bins)

**6.2.2.38 RTN\_ChanF** RTN flow direction ChanF

Size:  $8 \times 3$  time-varying

position>direction

Unit vector, after Fraenz and Harper, PSS, 2002. ChanF timebase.

Look\_Direction\_08 0 – 7 (8 bins)

**6.2.2.39 RTN\_ChanG** RTN flow direction ChanG

Size:  $80 \times 3$  time-varying

position>direction

Unit vector, after Fraenz and Harper, PSS, 2002. ChanG timebase.

Look\_Direction\_80 0 – 79 (80 bins)

**6.2.2.40 SA\_ChanE** Nominal Parker Spiral angle ChanE (degree)

Size: 8 time-varying

position>angle



Angle between particle direction and nominal outward Parker Spiral, based on 400km/s solar wind and corotation breakdown at 10Rs.

Look\_Direction\_08 0 – 7 (8 bins)

**6.2.2.41 SA\_ChanF** Nominal Parker Spiral angle ChanF (degree)

Size: 8 time-varying

position>angle

Angle between particle direction and nominal outward Parker Spiral, based on 400km/s solar wind and corotation breakdown at 10Rs.

Look\_Direction\_08 0 – 7 (8 bins)

**6.2.2.42 SA\_ChanG** Nominal Parker Spiral angle ChanG (degree)

Size: 80 time-varying

position>angle

Angle between particle direction and nominal outward Parker Spiral, based on 400km/s solar wind and corotation breakdown at 10Rs.

Look\_Direction\_80 0 – 79 (80 bins)

**6.2.3 OTHER SUPPORT**

**6.2.3.1 Look\_Direction\_08\_DELTAMINUS** Size: 8 constant number

**6.2.3.2 Look\_Direction\_08\_DELTAPLUS** Size: 8 constant number

**6.2.3.3 Look\_Direction\_80\_DELTAMINUS** Size: 80 constant number

**6.2.3.4 Look\_Direction\_80\_DELTAPLUS** Size: 80 constant number

**6.2.3.5 Quality\_Flag\_ChanE** Data-quality flag for channel E (HiResElectrons)

Size: 10 time-varying

flag>status

Quality flag number ChanPEB 0 – 9 (10 bins)

**6.2.3.6 Quality\_Flag\_ChanF** Data-quality flag for channel F (HiTimeResElectrons)

Size: 10 time-varying

flag>status

Quality flag number ChanPEB 0 – 9 (10 bins)

**6.2.3.7 Quality\_Flag\_ChanG** Data-quality flag for channel G (HiLookResElectrons)

Size: 10 time-varying

flag>status

Quality flag number ChanPEB 0 – 9 (10 bins)

## 6.3 PSP\_ISOIS-EPIHI\_L2-HET-RATES10

ISOIS-EPIHI>Integrated Science Investigation of the Sun, Energetic Particle Instrument Hi

L2-HET-rates10>Level 2 HET 10-second rates

EPI-Hi 10 second rates cdf. Time tags indicate midpoint of integration.

Instrument paper: Integrated Science Investigation of the Sun (ISIS): Design of the Energetic Particle Investigation. McComas, D. J. et al (2016). Space Sci. Rev., doi:10.1007/s11214-014-0059-1

1 minute to 1 hour

Cite McComas et al (2016), doi:10.1007/s11214-014-0059-1

### 6.3.1 PRIMARY VARIABLES

**6.3.1.1 A\_H\_Flux** H flux side A ( $\text{cm}^{-2}\text{sr}^{-1}\text{sec}^{-1}\text{MeV}^{-1}$ )

Size: 13 time-varying

particle\_flux>differential\_directional\_number

Energy Bins for H 9 – 70 MeV (13 bins)

**6.3.1.2 A\_He\_Flux** He flux side A ( $\text{cm}^{-2}\text{sr}^{-1}\text{sec}^{-1}(\text{MeV}/\text{nuc})^{-1}$ )

Size: 14 time-varying

particle\_flux>differential\_directional\_number

Energy Bins for He 9 – 83 MeV/nuc (14 bins)

**6.3.1.3 B\_H\_Flux** H flux side B ( $\text{cm}^{-2}\text{sr}^{-1}\text{sec}^{-1}\text{MeV}^{-1}$ )

Size: 13 time-varying

particle\_flux>differential\_directional\_number

Energy Bins for H 9 – 70 MeV (13 bins)

**6.3.1.4 B\_He\_Flux** He flux side B ( $\text{cm}^{-2}\text{sr}^{-1}\text{sec}^{-1}(\text{MeV}/\text{nuc})^{-1}$ )

Size: 14 time-varying

particle\_flux>differential\_directional\_number

Energy Bins for He 9 – 83 MeV/nuc (14 bins)

## 6.3.2 OTHER DATA

**6.3.2.1 A\_Electrons** Electrons counts side A (counts)

Size: 18 time-varying

particle\_flux>differential\_directional\_number\_rate

Energy Bins for Electrons 1 – 10 MeV (18 bins)

**6.3.2.2 A\_Electrons\_Rate** Electrons count rate side A ( $\text{counts s}^{-1}$ )

Size: 18 time-varying

particle\_flux>differential\_directional\_number\_rate

Energy Bins for Electrons 1 – 10 MeV (18 bins)

**6.3.2.3 A\_H** H counts side A (counts)

Size: 13 time-varying

particle\_flux>differential\_directional\_number\_rate

Energy Bins for H 9 – 70 MeV (13 bins)

**6.3.2.4 A\_H\_Rate** H count rate side A ( $\text{counts s}^{-1}$ )

Size: 13 time-varying

particle\_flux>differential\_directional\_number\_rate

Energy Bins for H 9 – 70 MeV (13 bins)

**6.3.2.5 A\_He** He counts side A (counts)

Size: 14 time-varying

particle\_flux>differential\_directional\_number\_rate

Energy Bins for He 9 – 83 MeV/nuc (14 bins)

**6.3.2.6 A\_He\_Rate** He count rate side A ( $\text{counts s}^{-1}$ )

Size: 14 time-varying

particle\_flux>differential\_directional\_number\_rate  
Energy Bins for He 9 – 83 MeV/nuc (14 bins)

**6.3.2.7 B\_Electrons** Electrons counts side B (counts)

Size: 18 time-varying

particle\_flux>differential\_directional\_number\_rate  
Energy Bins for Electrons 1 – 10 MeV (18 bins)

**6.3.2.8 B\_Electrons\_Rate** Electrons count rate side B (counts s<sup>-1</sup>)

Size: 18 time-varying

particle\_flux>differential\_directional\_number\_rate  
Energy Bins for Electrons 1 – 10 MeV (18 bins)

**6.3.2.9 B\_H** H counts side B (counts)

Size: 13 time-varying

particle\_flux>differential\_directional\_number\_rate  
Energy Bins for H 9 – 70 MeV (13 bins)

**6.3.2.10 B\_H\_Rate** H count rate side B (counts s<sup>-1</sup>)

Size: 13 time-varying

particle\_flux>differential\_directional\_number\_rate  
Energy Bins for H 9 – 70 MeV (13 bins)

**6.3.2.11 B\_He** He counts side B (counts)

Size: 14 time-varying

particle\_flux>differential\_directional\_number\_rate  
Energy Bins for He 9 – 83 MeV/nuc (14 bins)

**6.3.2.12 B\_He\_Rate** He count rate side B (counts s<sup>-1</sup>)

Size: 14 time-varying

particle\_flux>differential\_directional\_number\_rate  
Energy Bins for He 9 – 83 MeV/nuc (14 bins)

**6.3.2.13 HCI\_Lat** HCI latitude (degrees)

time-varying

position>latitude

At timestamp. After Fraenz and Harper, PSS, 2002.

**6.3.2.14 HCI\_Lon** HCI longitude (degrees)

time-varying

position>longitude

At timestamp. After Fraenz and Harper, PSS, 2002.

**6.3.2.15 HCI\_R** Heliocentric distance (AU)

time-varying

position>radial

At timestamp. After Fraenz and Harper, PSS, 2002.

**6.3.2.16 HET\_A\_HCI** HCI flow direction HETA

Size: 3 time-varying

position>direction

Unit vector, after Fraenz and Harper, PSS, 2002.

**6.3.2.17 HET\_A\_PA** Pitch angle HETA (degree)

time-varying

position>angle

**6.3.2.18 HET\_A\_RTN** RTN flow direction HETA

Size: 3 time-varying

position>direction

Unit vector, after Fraenz and Harper, PSS, 2002.

**6.3.2.19 HET\_A\_SA** Nominal Parker Spiral angle HETA (degree)

time-varying

position>angle

Angle between particle direction and nominal outward Parker Spiral, based on 400km/s solar wind and corotation breakdown at 10Rs.

**6.3.2.20 HET\_B\_HCI** HCI flow direction HETB

Size: 3 time-varying

position>direction

Unit vector, after Fraenz and Harper, PSS, 2002.

**6.3.2.21 HET\_B\_PA** Pitch angle HETB (degree)

time-varying

position>angle

**6.3.2.22 HET\_B\_RTN** RTN flow direction HETB

Size: 3 time-varying

position>direction

Unit vector, after Fraenz and Harper, PSS, 2002.

**6.3.2.23 HET\_B\_SA** Nominal Parker Spiral angle HETB (degree)

time-varying

position>angle

Angle between particle direction and nominal outward Parker Spiral, based on 400km/s solar wind and corotation breakdown at 10Rs.

**6.3.2.24 HGC\_Lat** HGC latitude (degrees)

time-varying

position>latitude

At timestamp. After Fraenz and Harper, PSS, 2002.

**6.3.2.25 HGC\_Lon** HGC longitude (degrees)

time-varying

position>longitude

At timestamp. After Fraenz and Harper, PSS, 2002.

**6.3.2.26 HGC\_R** Heliocentric distance (AU)

time-varying

position>radial

At timestamp. After Fraenz and Harper, PSS, 2002.

### 6.3.3 OTHER SUPPORT

#### 6.3.3.1 **Quality\_Flag** Data-quality flag

Size: 10 time-varying

flag>status

Quality flag number 0 – 9 (10 bins)

## 6.4 PSP\_ISOIS-EPIHI\_L2-HET-RATES300

ISOIS-EPIHI>Integrated Science Investigation of the Sun, Energetic Particle Instrument Hi

L2-HET-rates300>Level 2 HET 5-minute rates

EPI-Hi HET 300 second rates cdf. Time tags indicate midpoint of integration.

Instrument paper: Integrated Science Investigation of the Sun (ISIS): Design of the Energetic Particle Investigation. McComas, D. J. et al (2016). Space Sci. Rev., doi:10.1007/s11214-014-0059-1

1 minute to 1 hour

Cite McComas et al (2016), doi:10.1007/s11214-014-0059-1

### 6.4.1 PRIMARY VARIABLES

#### 6.4.2 OTHER DATA

##### 6.4.2.1 **A\_CNO\_SECT\_Rate** CNO sectored count rate side A (counts s<sup>-1</sup>)

Size: 2 × 25 time-varying

particle\_flux>differential\_directional\_number\_rate

Energy Bins for CNO SECT 35 – 64 MeV/nuc (2 bins)

HET\_R17\_SECTORS 0 – 24 (25 bins)

##### 6.4.2.2 **A\_FeGroup\_SECT\_Rate** FeGroup sectored count rate side A (counts s<sup>-1</sup>)

Size: 1 × 25 time-varying

particle\_flux>differential\_directional\_number\_rate

Energy Bins for FeGroup SECT 76 – 76 MeV/nuc (1 bins)

HET\_R17\_SECTORS 0 – 24 (25 bins)

##### 6.4.2.3 **A\_NetoSi\_SECT\_Rate** NetoS<sub>i</sub> sectored count rate side A (counts s<sup>-1</sup>)

Size: 1 × 25 time-varying

particle\_flux>differential\_directional\_number\_rate

Energy Bins for NetoS<sub>i</sub> SECT 54 – 54 MeV/nuc (1 bins)

HET\_R17\_SECTORS 0 – 24 (25 bins)

**6.4.2.4 B\_CNO\_SECT\_Rate** CNO sectored count rate side B (counts s<sup>-1</sup>)

Size: 2 × 25 time-varying

particle\_flux>differential\_directional\_number\_rate

Energy Bins for CNO SECT 35 – 64 MeV/nuc (2 bins)

HET\_R17\_SECTORS 0 – 24 (25 bins)

**6.4.2.5 B\_FeGroup\_SECT\_Rate** FeGroup sectored count rate side B (counts s<sup>-1</sup>)

Size: 1 × 25 time-varying

particle\_flux>differential\_directional\_number\_rate

Energy Bins for FeGroup SECT 76 – 76 MeV/nuc (1 bins)

HET\_R17\_SECTORS 0 – 24 (25 bins)

**6.4.2.6 B\_NetoSi\_SECT\_Rate** NetoSi sectored count rate side B (counts s<sup>-1</sup>)

Size: 1 × 25 time-varying

particle\_flux>differential\_directional\_number\_rate

Energy Bins for NetoSi SECT 54 – 54 MeV/nuc (1 bins)

HET\_R17\_SECTORS 0 – 24 (25 bins)

**6.4.2.7 HCI\_Lat** HCI latitude (degrees)

time-varying

position>latitude

At timestamp. After Fraenz and Harper, PSS, 2002.

**6.4.2.8 HCI\_Lon** HCI longitude (degrees)

time-varying

position>longitude

At timestamp. After Fraenz and Harper, PSS, 2002.

**6.4.2.9 HCI\_R** Heliocentric distance (AU)

time-varying

position>radial

At timestamp. After Fraenz and Harper, PSS, 2002.

**6.4.2.10 HET\_A\_HCI** HCI flow direction HETA

Size: 3 time-varying

position>direction



Unit vector, after Fraenz and Harper, PSS, 2002.

**6.4.2.11 HET\_A\_PA** Pitch angle HETA (degree)

time-varying

position>angle

**6.4.2.12 HET\_A\_R17\_SECT\_HCI** HCI flow direction HETAR17SECT

Size: 25 × 3 time-varying

position>direction

Unit vector, after Fraenz and Harper, PSS, 2002.

HET\_R17\_SECTORS 0 – 24 (25 bins)

**6.4.2.13 HET\_A\_R17\_SECT\_PA** Pitch angle HETAR17SECT (degree)

Size: 25 time-varying

position>angle

HET\_R17\_SECTORS 0 – 24 (25 bins)

**6.4.2.14 HET\_A\_R17\_SECT\_RTN** RTN flow direction HETAR17SECT

Size: 25 × 3 time-varying

position>direction

Unit vector, after Fraenz and Harper, PSS, 2002.

HET\_R17\_SECTORS 0 – 24 (25 bins)

**6.4.2.15 HET\_A\_R17\_SECT\_SA** Nominal Parker Spiral angle HETAR17SECT (degree)

Size: 25 time-varying

position>angle

Angle between particle direction and nominal outward Parker Spiral, based on 400km/s solar wind and corotation breakdown at 10Rs.

HET\_R17\_SECTORS 0 – 24 (25 bins)

**6.4.2.16 HET\_A\_RTN** RTN flow direction HETA

Size: 3 time-varying

position>direction

Unit vector, after Fraenz and Harper, PSS, 2002.

**6.4.2.17 HET\_A\_SA** Nominal Parker Spiral angle HETA (degree)

time-varying

position>angle

Angle between particle direction and nominal outward Parker Spiral, based on 400km/s solar wind and corotation breakdown at 10Rs.

**6.4.2.18 HET\_B\_HCI** HCI flow direction HETB

Size: 3 time-varying

position>direction

Unit vector, after Fraenz and Harper, PSS, 2002.

**6.4.2.19 HET\_B\_PA** Pitch angle HETB (degree)

time-varying

position>angle

**6.4.2.20 HET\_B\_R17\_SECT\_HCI** HCI flow direction HETBR17SECT

Size: 25 × 3 time-varying

position>direction

Unit vector, after Fraenz and Harper, PSS, 2002.

HET\_R17\_SECTORS 0 – 24 (25 bins)

**6.4.2.21 HET\_B\_R17\_SECT\_PA** Pitch angle HETBR17SECT (degree)

Size: 25 time-varying

position>angle

HET\_R17\_SECTORS 0 – 24 (25 bins)

**6.4.2.22 HET\_B\_R17\_SECT\_RTN** RTN flow direction HETBR17SECT

Size: 25 × 3 time-varying

position>direction

Unit vector, after Fraenz and Harper, PSS, 2002.

HET\_R17\_SECTORS 0 – 24 (25 bins)

**6.4.2.23 HET\_B\_R17\_SECT\_SA** Nominal Parker Spiral angle HETBR17SECT (degree)

Size: 25 time-varying

position>angle

Angle between particle direction and nominal outward Parker Spiral, based on 400km/s solar wind

and corotation breakdown at 10Rs.  
HET\_R17\_SECTORS 0 – 24 (25 bins)

**6.4.2.24 HET\_B\_RTN** RTN flow direction HETB

Size: 3 time-varying

position>direction

Unit vector, after Fraenz and Harper, PSS, 2002.

**6.4.2.25 HET\_B\_SA** Nominal Parker Spiral angle HETB (degree)

time-varying

position>angle

Angle between particle direction and nominal outward Parker Spiral, based on 400km/s solar wind and corotation breakdown at 10Rs.

**6.4.2.26 HGC\_Lat** HGC latitude (degrees)

time-varying

position>latitude

At timestamp. After Fraenz and Harper, PSS, 2002.

**6.4.2.27 HGC\_Lon** HGC longitude (degrees)

time-varying

position>longitude

At timestamp. After Fraenz and Harper, PSS, 2002.

**6.4.2.28 HGC\_R** Heliocentric distance (AU)

time-varying

position>radial

At timestamp. After Fraenz and Harper, PSS, 2002.

**6.4.3 OTHER SUPPORT**

**6.4.3.1 Quality\_Flag** Data-quality flag

Size: 10 time-varying

flag>status

Quality flag number 0 – 9 (10 bins)

## 6.5 PSP\_ISOIS-EPIHI\_L2-HET-RATES3600

ISOIS-EPIHI>Integrated Science Investigation of the Sun, Energetic Particle Instrument Hi  
L2-HET-rates3600>Level 2 HET hourly rates

EPI-Hi HET 3600 second rates cdf. Time tags indicate midpoint of integration.

Instrument paper: Integrated Science Investigation of the Sun (ISIS): Design of the Energetic Particle Investigation. McComas, D. J. et al (2016). Space Sci. Rev., doi:10.1007/s11214-014-0059-1

1 minute to 1 hour

Cite McComas et al (2016), doi:10.1007/s11214-014-0059-1

### 6.5.1 PRIMARY VARIABLES

**6.5.1.1 A\_H\_Flux** H flux side A ( $\text{cm}^{-2}\text{sr}^{-1}\text{sec}^{-1}\text{MeV}^{-1}$ )

Size: 15 time-varying

particle\_flux>differential\_directional\_number

Energy Bins for H 7 – 83 MeV (15 bins)

**6.5.1.2 A\_H\_SECT\_Flux** H sectored flux side A ( $\text{cm}^{-2}\text{sr}^{-1}\text{sec}^{-1}\text{MeV}^{-1}$ )

Size:  $2 \times 25$  time-varying

particle\_flux>differential\_directional\_number

Energy Bins for H SECT 17 – 32 MeV (2 bins)

HET\_R17\_SECTORS 0 – 24 (25 bins)

**6.5.1.3 A\_He\_Flux** He flux side A ( $\text{cm}^{-2}\text{sr}^{-1}\text{sec}^{-1}(\text{MeV}/\text{nuc})^{-1}$ )

Size: 16 time-varying

particle\_flux>differential\_directional\_number

Energy Bins for He 7 – 99 MeV/nuc (16 bins)

**6.5.1.4 A\_He\_SECT\_Flux** He sectored flux side A ( $\text{cm}^{-2}\text{sr}^{-1}\text{sec}^{-1}(\text{MeV}/\text{nuc})^{-1}$ )

Size:  $2 \times 25$  time-varying

particle\_flux>differential\_directional\_number

Energy Bins for He SECT 17 – 32 MeV/nuc (2 bins)

HET\_R17\_SECTORS 0 – 24 (25 bins)

**6.5.1.5 B\_H\_Flux** H flux side B ( $\text{cm}^{-2}\text{sr}^{-1}\text{sec}^{-1}\text{MeV}^{-1}$ )

Size: 15 time-varying

particle\_flux>differential\_directional\_number

Energy Bins for H 7 – 83 MeV (15 bins)

**6.5.1.6 B\_H\_SECT\_Flux** H sectored flux side B ( $\text{cm}^{-2}\text{sr}^{-1}\text{sec}^{-1}\text{MeV}^{-1}$ )

Size:  $2 \times 25$  time-varying

particle\_flux>differential\_directional\_number

Energy Bins for H SECT 17 – 32 MeV (2 bins)

HET\_R17\_SECTORS 0 – 24 (25 bins)

**6.5.1.7 B\_He\_Flux** He flux side B ( $\text{cm}^{-2}\text{sr}^{-1}\text{sec}^{-1}(\text{MeV}/\text{nuc})^{-1}$ )

Size: 16 time-varying

particle\_flux>differential\_directional\_number

Energy Bins for He 7 – 99 MeV/nuc (16 bins)

**6.5.1.8 B\_He\_SECT\_Flux** He sectored flux side B ( $\text{cm}^{-2}\text{sr}^{-1}\text{sec}^{-1}(\text{MeV}/\text{nuc})^{-1}$ )

Size:  $2 \times 25$  time-varying

particle\_flux>differential\_directional\_number

Energy Bins for He SECT 17 – 32 MeV/nuc (2 bins)

HET\_R17\_SECTORS 0 – 24 (25 bins)

**6.5.2 OTHER DATA**

**6.5.2.1 A\_Al** Al counts side A (counts)

Size: 15 time-varying

particle\_flux>differential\_directional\_number\_rate

Energy Bins for Al 21 – 235 MeV/nuc (15 bins)

**6.5.2.2 A\_Al\_Rate** Al count rate side A ( $\text{counts s}^{-1}$ )

Size: 15 time-varying

particle\_flux>differential\_directional\_number\_rate

Energy Bins for Al 21 – 235 MeV/nuc (15 bins)

**6.5.2.3 A\_Ar** Ar counts side A (counts)

Size: 15 time-varying

particle\_flux>differential\_directional\_number\_rate

Energy Bins for Ar 25 – 279 MeV/nuc (15 bins)

**6.5.2.4 A\_Ar\_Rate** Ar count rate side A (counts s<sup>-1</sup>)

Size: 15 time-varying

particle\_flux>differential\_directional\_number\_rate

Energy Bins for Ar 25 – 279 MeV/nuc (15 bins)

**6.5.2.5 A\_C** C counts side A (counts)

Size: 15 time-varying

particle\_flux>differential\_directional\_number\_rate

Energy Bins for C 12 – 140 MeV/nuc (15 bins)

**6.5.2.6 A\_CNO\_SECT\_Rate** CNO sectored count rate side A (counts s<sup>-1</sup>)

Size: 2 × 25 time-varying

particle\_flux>differential\_directional\_number\_rate

Energy Bins for CNO SECT 35 – 64 MeV/nuc (2 bins)

HET\_R17\_SECTORS 0 – 24 (25 bins)

**6.5.2.7 A\_C\_Rate** C count rate side A (counts s<sup>-1</sup>)

Size: 15 time-varying

particle\_flux>differential\_directional\_number\_rate

Energy Bins for C 12 – 140 MeV/nuc (15 bins)

**6.5.2.8 A\_Ca** Ca counts side A (counts)

Size: 15 time-varying

particle\_flux>differential\_directional\_number\_rate

Energy Bins for Ca 25 – 279 MeV/nuc (15 bins)

**6.5.2.9 A\_Ca\_Rate** Ca count rate side A (counts s<sup>-1</sup>)

Size: 15 time-varying

particle\_flux>differential\_directional\_number\_rate

Energy Bins for Ca 25 – 279 MeV/nuc (15 bins)

**6.5.2.10 A\_Cr** Cr counts side A (counts)

Size: 16 time-varying

particle\_flux>differential\_directional\_number\_rate

Energy Bins for Cr 25 – 332 MeV/nuc (16 bins)

**6.5.2.11 A\_Cr\_Rate** Cr count rate side A (counts s<sup>-1</sup>)

Size: 16 time-varying

particle\_flux>differential\_directional\_number\_rate

Energy Bins for Cr 25 – 332 MeV/nuc (16 bins)

**6.5.2.12 A\_Electrons** Electrons counts side A (counts)

Size: 19 time-varying

particle\_flux>differential\_directional\_number\_rate

Energy Bins for Electrons 0 – 10 MeV (19 bins)

**6.5.2.13 A\_Electrons\_Rate** Electrons count rate side A (counts s<sup>-1</sup>)

Size: 19 time-varying

particle\_flux>differential\_directional\_number\_rate

Energy Bins for Electrons 0 – 10 MeV (19 bins)

**6.5.2.14 A\_Electrons\_SECT\_Rate** Electrons sectored count rate side A (counts s<sup>-1</sup>)

Size: 2 × 25 time-varying

particle\_flux>differential\_directional\_number\_rate

Energy Bins for Electrons SECT 1 – 3 MeV (2 bins)

HET\_R17\_SECTORS 0 – 24 (25 bins)

**6.5.2.15 A\_Fe** Fe counts side A (counts)

Size: 15 time-varying

particle\_flux>differential\_directional\_number\_rate

Energy Bins for Fe 29 – 332 MeV/nuc (15 bins)

**6.5.2.16 A\_FeGroup\_SECT\_Rate** FeGroup sectored count rate side A (counts s<sup>-1</sup>)

Size: 1 × 25 time-varying

particle\_flux>differential\_directional\_number\_rate

Energy Bins for FeGroup SECT 76 – 76 MeV/nuc (1 bins)

HET\_R17\_SECTORS 0 – 24 (25 bins)

**6.5.2.17 A\_Fe\_Rate** Fe count rate side A (counts s<sup>-1</sup>)

Size: 15 time-varying

particle\_flux>differential\_directional\_number\_rate

Energy Bins for Fe 29 – 332 MeV/nuc (15 bins)

**6.5.2.18 A\_H** H counts side A (counts)

Size: 15 time-varying

particle\_flux>differential\_directional\_number\_rate

Energy Bins for H 7 – 83 MeV (15 bins)

**6.5.2.19 A\_H\_Rate** H count rate side A (counts s<sup>-1</sup>)

Size: 15 time-varying

particle\_flux>differential\_directional\_number\_rate

Energy Bins for H 7 – 83 MeV (15 bins)

**6.5.2.20 A\_H\_SECT\_Rate** H sectored count rate side A (counts s<sup>-1</sup>)

Size: 2 × 25 time-varying

particle\_flux>differential\_directional\_number\_rate

Energy Bins for H SECT 17 – 32 MeV (2 bins)

HET\_R17\_SECTORS 0 – 24 (25 bins)

**6.5.2.21 A\_He** He counts side A (counts)

Size: 16 time-varying

particle\_flux>differential\_directional\_number\_rate

Energy Bins for He 7 – 99 MeV/nuc (16 bins)

**6.5.2.22 A\_He\_Rate** He count rate side A (counts s<sup>-1</sup>)

Size: 16 time-varying

particle\_flux>differential\_directional\_number\_rate

Energy Bins for He 7 – 99 MeV/nuc (16 bins)

**6.5.2.23 A\_He\_SECT\_Rate** He sectored count rate side A (counts s<sup>-1</sup>)

Size: 2 × 25 time-varying

particle\_flux>differential\_directional\_number\_rate

Energy Bins for He SECT 17 – 32 MeV/nuc (2 bins)

HET\_R17\_SECTORS 0 – 24 (25 bins)



**6.5.2.24 A\_Mg** Mg counts side A (counts)

Size: 15 time-varying

particle\_flux>differential\_directional\_number\_rate

Energy Bins for Mg 21 – 235 MeV/nuc (15 bins)

**6.5.2.25 A\_Mg\_Rate** Mg count rate side A (counts s<sup>-1</sup>)

Size: 15 time-varying

particle\_flux>differential\_directional\_number\_rate

Energy Bins for Mg 21 – 235 MeV/nuc (15 bins)

**6.5.2.26 A\_N** N counts side A (counts)

Size: 15 time-varying

particle\_flux>differential\_directional\_number\_rate

Energy Bins for N 12 – 140 MeV/nuc (15 bins)

**6.5.2.27 A\_N\_Rate** N count rate side A (counts s<sup>-1</sup>)

Size: 15 time-varying

particle\_flux>differential\_directional\_number\_rate

Energy Bins for N 12 – 140 MeV/nuc (15 bins)

**6.5.2.28 A\_Na** Na counts side A (counts)

Size: 15 time-varying

particle\_flux>differential\_directional\_number\_rate

Energy Bins for Na 17 – 197 MeV/nuc (15 bins)

**6.5.2.29 A\_Na\_Rate** Na count rate side A (counts s<sup>-1</sup>)

Size: 15 time-varying

particle\_flux>differential\_directional\_number\_rate

Energy Bins for Na 17 – 197 MeV/nuc (15 bins)

**6.5.2.30 A\_Ne** Ne counts side A (counts)

Size: 15 time-varying

particle\_flux>differential\_directional\_number\_rate

Energy Bins for Ne 17 – 197 MeV/nuc (15 bins)

**6.5.2.31 A\_Ne\_Rate** Ne count rate side A (counts s<sup>-1</sup>)

Size: 15 time-varying

particle\_flux>differential\_directional\_number\_rate

Energy Bins for Ne 17 – 197 MeV/nuc (15 bins)

**6.5.2.32 A\_NetoSi\_SECT\_Rate** NetoSi sectored count rate side A (counts s<sup>-1</sup>)

Size: 1 × 25 time-varying

particle\_flux>differential\_directional\_number\_rate

Energy Bins for NetoSi SECT 54 – 54 MeV/nuc (1 bins)

HET\_R17\_SECTORS 0 – 24 (25 bins)

**6.5.2.33 A\_Ni** Ni counts side A (counts)

Size: 15 time-varying

particle\_flux>differential\_directional\_number\_rate

Energy Bins for Ni 29 – 332 MeV/nuc (15 bins)

**6.5.2.34 A\_Ni\_Rate** Ni count rate side A (counts s<sup>-1</sup>)

Size: 15 time-varying

particle\_flux>differential\_directional\_number\_rate

Energy Bins for Ni 29 – 332 MeV/nuc (15 bins)

**6.5.2.35 A\_O** O counts side A (counts)

Size: 15 time-varying

particle\_flux>differential\_directional\_number\_rate

Energy Bins for O 15 – 166 MeV/nuc (15 bins)

**6.5.2.36 A\_O\_Rate** O count rate side A (counts s<sup>-1</sup>)

Size: 15 time-varying

particle\_flux>differential\_directional\_number\_rate

Energy Bins for O 15 – 166 MeV/nuc (15 bins)

**6.5.2.37 A\_S** S counts side A (counts)

Size: 16 time-varying

particle\_flux>differential\_directional\_number\_rate

Energy Bins for S 21 – 279 MeV/nuc (16 bins)

**6.5.2.38 A\_S\_Rate** S count rate side A (counts s<sup>-1</sup>)

Size: 16 time-varying

particle\_flux>differential\_directional\_number\_rate

Energy Bins for S 21 – 279 MeV/nuc (16 bins)

**6.5.2.39 A\_Si** Si counts side A (counts)

Size: 15 time-varying

particle\_flux>differential\_directional\_number\_rate

Energy Bins for Si 21 – 235 MeV/nuc (15 bins)

**6.5.2.40 A\_Si\_Rate** Si count rate side A (counts s<sup>-1</sup>)

Size: 15 time-varying

particle\_flux>differential\_directional\_number\_rate

Energy Bins for Si 21 – 235 MeV/nuc (15 bins)

**6.5.2.41 B\_Al** Al counts side B (counts)

Size: 15 time-varying

particle\_flux>differential\_directional\_number\_rate

Energy Bins for Al 21 – 235 MeV/nuc (15 bins)

**6.5.2.42 B\_Al\_Rate** Al count rate side B (counts s<sup>-1</sup>)

Size: 15 time-varying

particle\_flux>differential\_directional\_number\_rate

Energy Bins for Al 21 – 235 MeV/nuc (15 bins)

**6.5.2.43 B\_Ar** Ar counts side B (counts)

Size: 15 time-varying

particle\_flux>differential\_directional\_number\_rate

Energy Bins for Ar 25 – 279 MeV/nuc (15 bins)

**6.5.2.44 B\_Ar\_Rate** Ar count rate side B (counts s<sup>-1</sup>)

Size: 15 time-varying

particle\_flux>differential\_directional\_number\_rate

Energy Bins for Ar 25 – 279 MeV/nuc (15 bins)

**6.5.2.45 B\_C** C counts side B (counts)

Size: 15 time-varying

particle\_flux>differential\_directional\_number\_rate

Energy Bins for C 12 – 140 MeV/nuc (15 bins)

**6.5.2.46 B\_CNO\_SECT\_Rate** CNO sectored count rate side B (counts s<sup>-1</sup>)

Size: 2 × 25 time-varying

particle\_flux>differential\_directional\_number\_rate

Energy Bins for CNO SECT 35 – 64 MeV/nuc (2 bins)

HET\_R17\_SECTORS 0 – 24 (25 bins)

**6.5.2.47 B\_C\_Rate** C count rate side B (counts s<sup>-1</sup>)

Size: 15 time-varying

particle\_flux>differential\_directional\_number\_rate

Energy Bins for C 12 – 140 MeV/nuc (15 bins)

**6.5.2.48 B\_Ca** Ca counts side B (counts)

Size: 15 time-varying

particle\_flux>differential\_directional\_number\_rate

Energy Bins for Ca 25 – 279 MeV/nuc (15 bins)

**6.5.2.49 B\_Ca\_Rate** Ca count rate side B (counts s<sup>-1</sup>)

Size: 15 time-varying

particle\_flux>differential\_directional\_number\_rate

Energy Bins for Ca 25 – 279 MeV/nuc (15 bins)

**6.5.2.50 B\_Cr** Cr counts side B (counts)

Size: 16 time-varying

particle\_flux>differential\_directional\_number\_rate

Energy Bins for Cr 25 – 332 MeV/nuc (16 bins)

**6.5.2.51 B\_Cr\_Rate** Cr count rate side B (counts s<sup>-1</sup>)

Size: 16 time-varying

particle\_flux>differential\_directional\_number\_rate

Energy Bins for Cr 25 – 332 MeV/nuc (16 bins)

**6.5.2.52 B\_Electrons** Electrons counts side B (counts)

Size: 19 time-varying

particle\_flux>differential\_directional\_number\_rate

Energy Bins for Electrons 0 – 10 MeV (19 bins)

**6.5.2.53 B\_Electrons\_Rate** Electrons count rate side B (counts s<sup>-1</sup>)

Size: 19 time-varying

particle\_flux>differential\_directional\_number\_rate

Energy Bins for Electrons 0 – 10 MeV (19 bins)

**6.5.2.54 B\_Electrons\_SECT\_Rate** Electrons sectored count rate side B (counts s<sup>-1</sup>)

Size: 2 × 25 time-varying

particle\_flux>differential\_directional\_number\_rate

Energy Bins for Electrons SECT 1 – 3 MeV (2 bins)

HET\_R17\_SECTORS 0 – 24 (25 bins)

**6.5.2.55 B\_Fe** Fe counts side B (counts)

Size: 15 time-varying

particle\_flux>differential\_directional\_number\_rate

Energy Bins for Fe 29 – 332 MeV/nuc (15 bins)

**6.5.2.56 B\_FeGroup\_SECT\_Rate** FeGroup sectored count rate side B (counts s<sup>-1</sup>)

Size: 1 × 25 time-varying

particle\_flux>differential\_directional\_number\_rate

Energy Bins for FeGroup SECT 76 – 76 MeV/nuc (1 bins)

HET\_R17\_SECTORS 0 – 24 (25 bins)

**6.5.2.57 B\_Fe\_Rate** Fe count rate side B (counts s<sup>-1</sup>)

Size: 15 time-varying

particle\_flux>differential\_directional\_number\_rate

Energy Bins for Fe 29 – 332 MeV/nuc (15 bins)

**6.5.2.58 B\_H** H counts side B (counts)

Size: 15 time-varying

particle\_flux>differential\_directional\_number\_rate

Energy Bins for H 7 – 83 MeV (15 bins)

**6.5.2.59 B\_H\_Rate** H count rate side B (counts s<sup>-1</sup>)

Size: 15 time-varying

particle\_flux>differential\_directional\_number\_rate

Energy Bins for H 7 – 83 MeV (15 bins)

**6.5.2.60 B\_H\_SECT\_Rate** H sectored count rate side B (counts s<sup>-1</sup>)

Size: 2 × 25 time-varying

particle\_flux>differential\_directional\_number\_rate

Energy Bins for H SECT 17 – 32 MeV (2 bins)

HET\_R17\_SECTORS 0 – 24 (25 bins)

**6.5.2.61 B\_He** He counts side B (counts)

Size: 16 time-varying

particle\_flux>differential\_directional\_number\_rate

Energy Bins for He 7 – 99 MeV/nuc (16 bins)

**6.5.2.62 B\_He\_Rate** He count rate side B (counts s<sup>-1</sup>)

Size: 16 time-varying

particle\_flux>differential\_directional\_number\_rate

Energy Bins for He 7 – 99 MeV/nuc (16 bins)

**6.5.2.63 B\_He\_SECT\_Rate** He sectored count rate side B (counts s<sup>-1</sup>)

Size: 2 × 25 time-varying

particle\_flux>differential\_directional\_number\_rate

Energy Bins for He SECT 17 – 32 MeV/nuc (2 bins)

HET\_R17\_SECTORS 0 – 24 (25 bins)

**6.5.2.64 B\_Mg** Mg counts side B (counts)

Size: 15 time-varying

particle\_flux>differential\_directional\_number\_rate

Energy Bins for Mg 21 – 235 MeV/nuc (15 bins)

**6.5.2.65 B\_Mg\_Rate** Mg count rate side B (counts s<sup>-1</sup>)

Size: 15 time-varying

particle\_flux>differential\_directional\_number\_rate

Energy Bins for Mg 21 – 235 MeV/nuc (15 bins)

**6.5.2.66 B\_N** N counts side B (counts)

Size: 15 time-varying

particle\_flux>differential\_directional\_number\_rate

Energy Bins for N 12 – 140 MeV/nuc (15 bins)

**6.5.2.67 B\_N\_Rate** N count rate side B (counts s<sup>-1</sup>)

Size: 15 time-varying

particle\_flux>differential\_directional\_number\_rate

Energy Bins for N 12 – 140 MeV/nuc (15 bins)

**6.5.2.68 B\_Na** Na counts side B (counts)

Size: 15 time-varying

particle\_flux>differential\_directional\_number\_rate

Energy Bins for Na 17 – 197 MeV/nuc (15 bins)

**6.5.2.69 B\_Na\_Rate** Na count rate side B (counts s<sup>-1</sup>)

Size: 15 time-varying

particle\_flux>differential\_directional\_number\_rate

Energy Bins for Na 17 – 197 MeV/nuc (15 bins)

**6.5.2.70 B\_Ne** Ne counts side B (counts)

Size: 15 time-varying

particle\_flux>differential\_directional\_number\_rate

Energy Bins for Ne 17 – 197 MeV/nuc (15 bins)

**6.5.2.71 B\_Ne\_Rate** Ne count rate side B (counts s<sup>-1</sup>)

Size: 15 time-varying

particle\_flux>differential\_directional\_number\_rate

Energy Bins for Ne 17 – 197 MeV/nuc (15 bins)

**6.5.2.72 B\_NetoSi\_SECT\_Rate** NetoS<sub>i</sub> sectored count rate side B (counts s<sup>-1</sup>)

Size: 1 × 25 time-varying

particle\_flux>differential\_directional\_number\_rate

Energy Bins for NetoS<sub>i</sub> SECT 54 – 54 MeV/nuc (1 bins)

HET\_R17\_SECTORS 0 – 24 (25 bins)

**6.5.2.73 B\_Ni** Ni counts side B (counts)

Size: 15 time-varying

particle\_flux>differential\_directional\_number\_rate

Energy Bins for Ni 29 – 332 MeV/nuc (15 bins)

**6.5.2.74 B\_Ni\_Rate** Ni count rate side B (counts s<sup>-1</sup>)

Size: 15 time-varying

particle\_flux>differential\_directional\_number\_rate

Energy Bins for Ni 29 – 332 MeV/nuc (15 bins)

**6.5.2.75 B\_O** O counts side B (counts)

Size: 15 time-varying

particle\_flux>differential\_directional\_number\_rate

Energy Bins for O 15 – 166 MeV/nuc (15 bins)

**6.5.2.76 B\_O\_Rate** O count rate side B (counts s<sup>-1</sup>)

Size: 15 time-varying

particle\_flux>differential\_directional\_number\_rate

Energy Bins for O 15 – 166 MeV/nuc (15 bins)

**6.5.2.77 B\_S** S counts side B (counts)

Size: 16 time-varying

particle\_flux>differential\_directional\_number\_rate

Energy Bins for S 21 – 279 MeV/nuc (16 bins)

**6.5.2.78 B\_S\_Rate** S count rate side B (counts s<sup>-1</sup>)

Size: 16 time-varying

particle\_flux>differential\_directional\_number\_rate

Energy Bins for S 21 – 279 MeV/nuc (16 bins)



**6.5.2.79 B\_Si** Si counts side B (counts)

Size: 15 time-varying

particle\_flux>differential\_directional\_number\_rate

Energy Bins for Si 21 – 235 MeV/nuc (15 bins)

**6.5.2.80 B\_Si\_Rate** Si count rate side B (counts s<sup>-1</sup>)

Size: 15 time-varying

particle\_flux>differential\_directional\_number\_rate

Energy Bins for Si 21 – 235 MeV/nuc (15 bins)

**6.5.2.81 HCI\_Lat** HCI latitude (degrees)

time-varying

position>latitude

At timestamp. After Fraenz and Harper, PSS, 2002.

**6.5.2.82 HCI\_Lon** HCI longitude (degrees)

time-varying

position>longitude

At timestamp. After Fraenz and Harper, PSS, 2002.

**6.5.2.83 HCI\_R** Heliocentric distance (AU)

time-varying

position>radial

At timestamp. After Fraenz and Harper, PSS, 2002.

**6.5.2.84 HET\_A\_HCI** HCI flow direction HETA

Size: 3 time-varying

position>direction

Unit vector, after Fraenz and Harper, PSS, 2002.

**6.5.2.85 HET\_A\_PA** Pitch angle HETA (degree)

time-varying

position>angle

**6.5.2.86 HET\_A\_R17\_SECT\_HCI** HCI flow direction HETAR17SECT

Size: 25 × 3 time-varying

position>direction

Unit vector, after Fraenz and Harper, PSS, 2002.

HET\_R17\_SECTORS 0 – 24 (25 bins)

**6.5.2.87 HET\_A\_R17\_SECT\_PA** Pitch angle HETAR17SECT (degree)

Size: 25 time-varying

position>angle

HET\_R17\_SECTORS 0 – 24 (25 bins)

**6.5.2.88 HET\_A\_R17\_SECT\_RTN** RTN flow direction HETAR17SECT

Size: 25 × 3 time-varying

position>direction

Unit vector, after Fraenz and Harper, PSS, 2002.

HET\_R17\_SECTORS 0 – 24 (25 bins)

**6.5.2.89 HET\_A\_R17\_SECT\_SA** Nominal Parker Spiral angle HETAR17SECT (degree)

Size: 25 time-varying

position>angle

Angle between particle direction and nominal outward Parker Spiral, based on 400km/s solar wind and corotation breakdown at 10Rs.

HET\_R17\_SECTORS 0 – 24 (25 bins)

**6.5.2.90 HET\_A\_RTN** RTN flow direction HETA

Size: 3 time-varying

position>direction

Unit vector, after Fraenz and Harper, PSS, 2002.

**6.5.2.91 HET\_A\_SA** Nominal Parker Spiral angle HETA (degree)

time-varying

position>angle

Angle between particle direction and nominal outward Parker Spiral, based on 400km/s solar wind and corotation breakdown at 10Rs.

**6.5.2.92 HET\_B\_HCI** HCI flow direction HETB

Size: 3 time-varying

position>direction

Unit vector, after Fraenz and Harper, PSS, 2002.

**6.5.2.93 HET\_B\_PA** Pitch angle HETB (degree)

time-varying

position>angle

**6.5.2.94 HET\_B\_R17\_SECT\_HCI** HCI flow direction HETBR17SECT

Size: 25 × 3 time-varying

position>direction

Unit vector, after Fraenz and Harper, PSS, 2002.

HET\_R17\_SECTORS 0 – 24 (25 bins)

**6.5.2.95 HET\_B\_R17\_SECT\_PA** Pitch angle HETBR17SECT (degree)

Size: 25 time-varying

position>angle

HET\_R17\_SECTORS 0 – 24 (25 bins)

**6.5.2.96 HET\_B\_R17\_SECT\_RTN** RTN flow direction HETBR17SECT

Size: 25 × 3 time-varying

position>direction

Unit vector, after Fraenz and Harper, PSS, 2002.

HET\_R17\_SECTORS 0 – 24 (25 bins)

**6.5.2.97 HET\_B\_R17\_SECT\_SA** Nominal Parker Spiral angle HETBR17SECT (degree)

Size: 25 time-varying

position>angle

Angle between particle direction and nominal outward Parker Spiral, based on 400km/s solar wind and corotation breakdown at 10Rs.

HET\_R17\_SECTORS 0 – 24 (25 bins)

**6.5.2.98 HET\_B\_RTN** RTN flow direction HETB

Size: 3 time-varying

position>direction

Unit vector, after Fraenz and Harper, PSS, 2002.

**6.5.2.99 HET\_B\_SA** Nominal Parker Spiral angle HETB (degree)

time-varying

position>angle

Angle between particle direction and nominal outward Parker Spiral, based on 400km/s solar wind and corotation breakdown at 10Rs.

**6.5.2.100 HGC\_Lat** HGC latitude (degrees)

time-varying

position>latitude

At timestamp. After Fraenz and Harper, PSS, 2002.

**6.5.2.101 HGC\_Lon** HGC longitude (degrees)

time-varying

position>longitude

At timestamp. After Fraenz and Harper, PSS, 2002.

**6.5.2.102 HGC\_R** Heliocentric distance (AU)

time-varying

position>radial

At timestamp. After Fraenz and Harper, PSS, 2002.

**6.5.2.103 R1A\_He\_BIN** R1A He Rates (counts)

Size:  $5 \times 16$  time-varying

particle\_flux>differential\_directional\_number\_rate

Energy Bins for R1 He BIN 9 – 32 MeV/nuc (5 bins)

R1A\_He\_BIN\_MASS\_BIN 0 – 15 segment (16 bins)

**6.5.2.104 R1A\_Ne\_BIN** R1A Ne Rates (counts)

Size:  $4 \times 8$  time-varying

particle\_flux>differential\_directional\_number\_rate

Energy Bins for R1 Ne BIN 23 – 64 MeV/nuc (4 bins)

R1A\_Ne\_BIN\_MASS\_BIN 0 – 7 segment (8 bins)

**6.5.2.105 R1B\_He\_BIN** R1B He Rates (counts)

Size:  $5 \times 16$  time-varying

particle\_flux>differential\_directional\_number\_rate

Energy Bins for R1 He BIN 9 – 32 MeV/nuc (5 bins)

R1B\_He\_BIN\_MASS\_BIN 0 – 15 segment (16 bins)

**6.5.2.106 R1B\_Ne\_BIN** R1B Ne Rates (counts)

Size:  $4 \times 8$  time-varying

particle\_flux>differential\_directional\_number\_rate

Energy Bins for R1 Ne BIN 23 – 64 MeV/nuc (4 bins)

R1B\_Ne\_BIN\_MASS\_BIN 0 – 7 segment (8 bins)

**6.5.2.107 R2A\_He\_BIN** R2A He Rates (counts)

Size:  $4 \times 16$  time-varying

particle\_flux>differential\_directional\_number\_rate

Energy Bins for R2 He BIN 16 – 45 MeV/nuc (4 bins)

R2A\_He\_BIN\_MASS\_BIN 0 – 15 segment (16 bins)

**6.5.2.108 R2A\_Ne\_BIN** R2A Ne Rates (counts)

Size:  $4 \times 8$  time-varying

particle\_flux>differential\_directional\_number\_rate

Energy Bins for R2 Ne BIN 32 – 91 MeV/nuc (4 bins)

R2A\_Ne\_BIN\_MASS\_BIN 0 – 7 segment (8 bins)

**6.5.2.109 R2B\_He\_BIN** R2B He Rates (counts)

Size:  $4 \times 16$  time-varying

particle\_flux>differential\_directional\_number\_rate

Energy Bins for R2 He BIN 16 – 45 MeV/nuc (4 bins)

R2B\_He\_BIN\_MASS\_BIN 0 – 15 segment (16 bins)

**6.5.2.110 R2B\_Ne\_BIN** R2B Ne Rates (counts)

Size:  $4 \times 8$  time-varying

particle\_flux>differential\_directional\_number\_rate

Energy Bins for R2 Ne BIN 32 – 91 MeV/nuc (4 bins)

R2B\_Ne\_BIN\_MASS\_BIN 0 – 7 segment (8 bins)

**6.5.2.111 R3A\_He\_BIN** R3A He Rates (counts)

Size:  $4 \times 16$  time-varying

particle\_flux>differential\_directional\_number\_rate

Energy Bins for R3 He BIN 23 – 64 MeV/nuc (4 bins)

R3A\_He\_BIN\_MASS\_BIN 0 – 15 segment (16 bins)

**6.5.2.112 R3A\_Ne\_BIN** R3A Ne Rates (counts)

Size:  $4 \times 8$  time-varying

particle\_flux>differential\_directional\_number\_rate

Energy Bins for R3 Ne BIN 45 – 128 MeV/nuc (4 bins)

R3A\_Ne\_BIN\_MASS\_BIN 0 – 7 segment (8 bins)

**6.5.2.113 R3B\_He\_BIN** R3B He Rates (counts)

Size:  $4 \times 16$  time-varying

particle\_flux>differential\_directional\_number\_rate

Energy Bins for R3 He BIN 23 – 64 MeV/nuc (4 bins)

R3B\_He\_BIN\_MASS\_BIN 0 – 15 segment (16 bins)

**6.5.2.114 R3B\_Ne\_BIN** R3B Ne Rates (counts)

Size:  $4 \times 8$  time-varying

particle\_flux>differential\_directional\_number\_rate

Energy Bins for R3 Ne BIN 45 – 128 MeV/nuc (4 bins)

R3B\_Ne\_BIN\_MASS\_BIN 0 – 7 segment (8 bins)

**6.5.2.115 R4A\_He\_BIN** R4A He Rates (counts)

Size:  $3 \times 16$  time-varying

particle\_flux>differential\_directional\_number\_rate

Energy Bins for R4 He BIN 32 – 64 MeV/nuc (3 bins)

R4A\_He\_BIN\_MASS\_BIN 0 – 15 segment (16 bins)

**6.5.2.116 R4A\_Ne\_BIN** R4A Ne Rates (counts)

Size:  $3 \times 8$  time-varying

particle\_flux>differential\_directional\_number\_rate

Energy Bins for R4 Ne BIN 64 – 128 MeV/nuc (3 bins)

R4A\_Ne\_BIN\_MASS\_BIN 0 – 7 segment (8 bins)

**6.5.2.117 R4B\_He\_BIN** R4B He Rates (counts)

Size:  $3 \times 16$  time-varying

particle\_flux>differential\_directional\_number\_rate

Energy Bins for R4 He BIN 32 – 64 MeV/nuc (3 bins)

R4B\_He\_BIN\_MASS\_BIN 0 – 15 segment (16 bins)

**6.5.2.118 R4B\_Ne\_BIN** R4B Ne Rates (counts)

Size:  $3 \times 8$  time-varying

particle\_flux>differential\_directional\_number\_rate

Energy Bins for R4 Ne BIN 64 – 128 MeV/nuc (3 bins)

R4B\_Ne\_BIN\_MASS\_BIN 0 – 7 segment (8 bins)

**6.5.2.119 R5A\_He\_BIN** R5A He Rates (counts)

Size:  $3 \times 16$  time-varying

particle\_flux>differential\_directional\_number\_rate

Energy Bins for R5 He BIN 32 – 64 MeV/nuc (3 bins)

R5A\_He\_BIN\_MASS\_BIN 0 – 15 segment (16 bins)

**6.5.2.120 R5A\_Ne\_BIN** R5A Ne Rates (counts)

Size:  $2 \times 8$  time-varying

particle\_flux>differential\_directional\_number\_rate

Energy Bins for R5 Ne BIN 91 – 128 MeV/nuc (2 bins)

R5A\_Ne\_BIN\_MASS\_BIN 0 – 7 segment (8 bins)

**6.5.2.121 R5B\_He\_BIN** R5B He Rates (counts)

Size:  $3 \times 16$  time-varying

particle\_flux>differential\_directional\_number\_rate

Energy Bins for R5 He BIN 32 – 64 MeV/nuc (3 bins)

R5B\_He\_BIN\_MASS\_BIN 0 – 15 segment (16 bins)

**6.5.2.122 R5B\_Ne\_BIN** R5B Ne Rates (counts)

Size:  $2 \times 8$  time-varying

particle\_flux>differential\_directional\_number\_rate

Energy Bins for R5 Ne BIN 91 – 128 MeV/nuc (2 bins)

R5B\_Ne\_BIN\_MASS\_BIN 0 – 7 segment (8 bins)

**6.5.2.123 R6A\_He\_BIN** R6A He Rates (counts)

Size:  $3 \times 16$  time-varying

particle\_flux>differential\_directional\_number\_rate

Energy Bins for R6 He BIN 32 – 64 MeV/nuc (3 bins)

R6A\_He\_BIN\_MASS\_BIN 0 – 15 segment (16 bins)

**6.5.2.124 R6A\_Ne\_BIN** R6A Ne Rates (counts)

Size:  $3 \times 8$  time-varying

particle\_flux>differential\_directional\_number\_rate

Energy Bins for R6 Ne BIN 91 – 181 MeV/nuc (3 bins)

R6A\_Ne\_BIN\_MASS\_BIN 0 – 7 segment (8 bins)

**6.5.2.125 R6B\_He\_BIN** R6B He Rates (counts)

Size:  $3 \times 16$  time-varying

particle\_flux>differential\_directional\_number\_rate

Energy Bins for R6 He BIN 32 – 64 MeV/nuc (3 bins)

R6B\_He\_BIN\_MASS\_BIN 0 – 15 segment (16 bins)

**6.5.2.126 R6B\_Ne\_BIN** R6B Ne Rates (counts)

Size:  $3 \times 8$  time-varying

particle\_flux>differential\_directional\_number\_rate

Energy Bins for R6 Ne BIN 91 – 181 MeV/nuc (3 bins)

R6B\_Ne\_BIN\_MASS\_BIN 0 – 7 segment (8 bins)

**6.5.2.127 R7A\_He\_BIN** R7A He Rates (counts)

Size:  $2 \times 16$  time-varying

particle\_flux>differential\_directional\_number\_rate

Energy Bins for R7 He BIN 45 – 64 MeV/nuc (2 bins)

R7A\_He\_BIN\_MASS\_BIN 0 – 15 segment (16 bins)

**6.5.2.128 R7A\_Ne\_BIN** R7A Ne Rates (counts)

Size:  $3 \times 8$  time-varying

particle\_flux>differential\_directional\_number\_rate

Energy Bins for R7 Ne BIN 91 – 181 MeV/nuc (3 bins)

R7A\_Ne\_BIN\_MASS\_BIN 0 – 7 segment (8 bins)



**6.5.2.129 R7B\_He\_BIN** R7B He Rates (counts)

Size:  $2 \times 16$  time-varying

particle\_flux>differential\_directional\_number\_rate

Energy Bins for R7 He BIN 45 – 64 MeV/nuc (2 bins)

R7B\_He\_BIN\_MASS\_BIN 0 – 15 segment (16 bins)

**6.5.2.130 R7B\_Ne\_BIN** R7B Ne Rates (counts)

Size:  $3 \times 8$  time-varying

particle\_flux>differential\_directional\_number\_rate

Energy Bins for R7 Ne BIN 91 – 181 MeV/nuc (3 bins)

R7B\_Ne\_BIN\_MASS\_BIN 0 – 7 segment (8 bins)

**6.5.3 OTHER SUPPORT**

**6.5.3.1 Quality\_Flag** Data-quality flag

Size: 10 time-varying

flag>status

Quality flag number 0 – 9 (10 bins)

**6.6 PSP\_ISOIS-EPIHI\_L2-HET-RATES60**

ISOIS-EPIHI>Integrated Science Investigation of the Sun, Energetic Particle Instrument Hi

L2-HET-rates60>Level 2 HET 1-minute rates

EPI-Hi HET 60 second rates cdf. Time tags indicate midpoint of integration.

Instrument paper: Integrated Science Investigation of the Sun (ISIS): Design of the Energetic Particle Investigation. McComas, D. J. et al (2016). Space Sci. Rev., doi:10.1007/s11214-014-0059-1

1 minute to 1 hour

Cite McComas et al (2016), doi:10.1007/s11214-014-0059-1

**6.6.1 PRIMARY VARIABLES**

**6.6.1.1 A\_H\_Flux** H flux side A ( $\text{cm}^{-2}\text{sr}^{-1}\text{sec}^{-1}\text{MeV}^{-1}$ )

Size: 15 time-varying

particle\_flux>differential\_directional\_number

Energy Bins for H 7 – 83 MeV (15 bins)

**6.6.1.2 A\_H\_SECT\_Flux** H sectored flux side A ( $\text{cm}^{-2}\text{sr}^{-1}\text{sec}^{-1}\text{MeV}^{-1}$ )

Size:  $2 \times 25$  time-varying

particle\_flux>differential\_directional\_number

Energy Bins for H SECT 17 – 32 MeV (2 bins)  
HET\_R17\_SECTORS 0 – 24 (25 bins)

**6.6.1.3 A\_He\_Flux** He flux side A ( $\text{cm}^{-2}\text{sr}^{-1}\text{sec}^{-1}(\text{MeV}/\text{nuc})^{-1}$ )  
Size: 16 time-varying  
particle\_flux>differential\_directional\_number  
Energy Bins for He 7 – 99 MeV/nuc (16 bins)

**6.6.1.4 A\_He\_SECT\_Flux** He sectored flux side A ( $\text{cm}^{-2}\text{sr}^{-1}\text{sec}^{-1}(\text{MeV}/\text{nuc})^{-1}$ )  
Size:  $2 \times 25$  time-varying  
particle\_flux>differential\_directional\_number  
Energy Bins for He SECT 17 – 32 MeV/nuc (2 bins)  
HET\_R17\_SECTORS 0 – 24 (25 bins)

**6.6.1.5 B\_H\_Flux** H flux side B ( $\text{cm}^{-2}\text{sr}^{-1}\text{sec}^{-1}\text{MeV}^{-1}$ )  
Size: 15 time-varying  
particle\_flux>differential\_directional\_number  
Energy Bins for H 7 – 83 MeV (15 bins)

**6.6.1.6 B\_H\_SECT\_Flux** H sectored flux side B ( $\text{cm}^{-2}\text{sr}^{-1}\text{sec}^{-1}\text{MeV}^{-1}$ )  
Size:  $2 \times 25$  time-varying  
particle\_flux>differential\_directional\_number  
Energy Bins for H SECT 17 – 32 MeV (2 bins)  
HET\_R17\_SECTORS 0 – 24 (25 bins)

**6.6.1.7 B\_He\_Flux** He flux side B ( $\text{cm}^{-2}\text{sr}^{-1}\text{sec}^{-1}(\text{MeV}/\text{nuc})^{-1}$ )  
Size: 16 time-varying  
particle\_flux>differential\_directional\_number  
Energy Bins for He 7 – 99 MeV/nuc (16 bins)

**6.6.1.8 B\_He\_SECT\_Flux** He sectored flux side B ( $\text{cm}^{-2}\text{sr}^{-1}\text{sec}^{-1}(\text{MeV}/\text{nuc})^{-1}$ )  
Size:  $2 \times 25$  time-varying  
particle\_flux>differential\_directional\_number  
Energy Bins for He SECT 17 – 32 MeV/nuc (2 bins)  
HET\_R17\_SECTORS 0 – 24 (25 bins)

## 6.6.2 OTHER DATA

### 6.6.2.1 A\_Al Al counts side A (counts)

Size: 15 time-varying

particle\_flux>differential\_directional\_number\_rate

Energy Bins for Al 21 – 235 MeV/nuc (15 bins)

### 6.6.2.2 A\_Al\_Rate Al count rate side A (counts s<sup>-1</sup>)

Size: 15 time-varying

particle\_flux>differential\_directional\_number\_rate

Energy Bins for Al 21 – 235 MeV/nuc (15 bins)

### 6.6.2.3 A\_Ar Ar counts side A (counts)

Size: 15 time-varying

particle\_flux>differential\_directional\_number\_rate

Energy Bins for Ar 25 – 279 MeV/nuc (15 bins)

### 6.6.2.4 A\_Ar\_Rate Ar count rate side A (counts s<sup>-1</sup>)

Size: 15 time-varying

particle\_flux>differential\_directional\_number\_rate

Energy Bins for Ar 25 – 279 MeV/nuc (15 bins)

### 6.6.2.5 A\_C C counts side A (counts)

Size: 15 time-varying

particle\_flux>differential\_directional\_number\_rate

Energy Bins for C 12 – 140 MeV/nuc (15 bins)

### 6.6.2.6 A\_C\_Rate C count rate side A (counts s<sup>-1</sup>)

Size: 15 time-varying

particle\_flux>differential\_directional\_number\_rate

Energy Bins for C 12 – 140 MeV/nuc (15 bins)

### 6.6.2.7 A\_Ca Ca counts side A (counts)

Size: 15 time-varying

particle\_flux>differential\_directional\_number\_rate

Energy Bins for Ca 25 – 279 MeV/nuc (15 bins)

**6.6.2.8 A\_Ca\_Rate** Ca count rate side A (counts s<sup>-1</sup>)

Size: 15 time-varying

particle\_flux>differential\_directional\_number\_rate

Energy Bins for Ca 25 – 279 MeV/nuc (15 bins)

**6.6.2.9 A\_Cr** Cr counts side A (counts)

Size: 16 time-varying

particle\_flux>differential\_directional\_number\_rate

Energy Bins for Cr 25 – 332 MeV/nuc (16 bins)

**6.6.2.10 A\_Cr\_Rate** Cr count rate side A (counts s<sup>-1</sup>)

Size: 16 time-varying

particle\_flux>differential\_directional\_number\_rate

Energy Bins for Cr 25 – 332 MeV/nuc (16 bins)

**6.6.2.11 A\_Electrons** Electrons counts side A (counts)

Size: 19 time-varying

particle\_flux>differential\_directional\_number\_rate

Energy Bins for Electrons 0 – 10 MeV (19 bins)

**6.6.2.12 A\_Electrons\_Rate** Electrons count rate side A (counts s<sup>-1</sup>)

Size: 19 time-varying

particle\_flux>differential\_directional\_number\_rate

Energy Bins for Electrons 0 – 10 MeV (19 bins)

**6.6.2.13 A\_Electrons\_SECT\_Rate** Electrons sectored count rate side A (counts s<sup>-1</sup>)

Size: 2 × 25 time-varying

particle\_flux>differential\_directional\_number\_rate

Energy Bins for Electrons SECT 1 – 3 MeV (2 bins)

HET\_R17\_SECTORS 0 – 24 (25 bins)

**6.6.2.14 A\_Fe** Fe counts side A (counts)

Size: 15 time-varying

particle\_flux>differential\_directional\_number\_rate

Energy Bins for Fe 29 – 332 MeV/nuc (15 bins)

**6.6.2.15 A\_Fe\_Rate** Fe count rate side A (counts s<sup>-1</sup>)

Size: 15 time-varying

particle\_flux>differential\_directional\_number\_rate

Energy Bins for Fe 29 – 332 MeV/nuc (15 bins)

**6.6.2.16 A\_H** H counts side A (counts)

Size: 15 time-varying

particle\_flux>differential\_directional\_number\_rate

Energy Bins for H 7 – 83 MeV (15 bins)

**6.6.2.17 A\_H\_Rate** H count rate side A (counts s<sup>-1</sup>)

Size: 15 time-varying

particle\_flux>differential\_directional\_number\_rate

Energy Bins for H 7 – 83 MeV (15 bins)

**6.6.2.18 A\_H\_SECT\_Rate** H sectored count rate side A (counts s<sup>-1</sup>)

Size: 2 × 25 time-varying

particle\_flux>differential\_directional\_number\_rate

Energy Bins for H SECT 17 – 32 MeV (2 bins)

HET\_R17\_SECTORS 0 – 24 (25 bins)

**6.6.2.19 A\_He** He counts side A (counts)

Size: 16 time-varying

particle\_flux>differential\_directional\_number\_rate

Energy Bins for He 7 – 99 MeV/nuc (16 bins)

**6.6.2.20 A\_He\_Rate** He count rate side A (counts s<sup>-1</sup>)

Size: 16 time-varying

particle\_flux>differential\_directional\_number\_rate

Energy Bins for He 7 – 99 MeV/nuc (16 bins)

**6.6.2.21 A\_He\_SECT\_Rate** He sectored count rate side A (counts s<sup>-1</sup>)

Size: 2 × 25 time-varying

particle\_flux>differential\_directional\_number\_rate

Energy Bins for He SECT 17 – 32 MeV/nuc (2 bins)

HET\_R17\_SECTORS 0 – 24 (25 bins)

**6.6.2.22 A\_Mg** Mg counts side A (counts)

Size: 15 time-varying

particle\_flux>differential\_directional\_number\_rate

Energy Bins for Mg 21 – 235 MeV/nuc (15 bins)

**6.6.2.23 A\_Mg\_Rate** Mg count rate side A (counts s<sup>-1</sup>)

Size: 15 time-varying

particle\_flux>differential\_directional\_number\_rate

Energy Bins for Mg 21 – 235 MeV/nuc (15 bins)

**6.6.2.24 A\_N** N counts side A (counts)

Size: 15 time-varying

particle\_flux>differential\_directional\_number\_rate

Energy Bins for N 12 – 140 MeV/nuc (15 bins)

**6.6.2.25 A\_N\_Rate** N count rate side A (counts s<sup>-1</sup>)

Size: 15 time-varying

particle\_flux>differential\_directional\_number\_rate

Energy Bins for N 12 – 140 MeV/nuc (15 bins)

**6.6.2.26 A\_Na** Na counts side A (counts)

Size: 15 time-varying

particle\_flux>differential\_directional\_number\_rate

Energy Bins for Na 17 – 197 MeV/nuc (15 bins)

**6.6.2.27 A\_Na\_Rate** Na count rate side A (counts s<sup>-1</sup>)

Size: 15 time-varying

particle\_flux>differential\_directional\_number\_rate

Energy Bins for Na 17 – 197 MeV/nuc (15 bins)

**6.6.2.28 A\_Ne** Ne counts side A (counts)

Size: 15 time-varying

particle\_flux>differential\_directional\_number\_rate  
Energy Bins for Ne 17 – 197 MeV/nuc (15 bins)

**6.6.2.29 A\_Ne\_Rate** Ne count rate side A (counts s<sup>-1</sup>)

Size: 15 time-varying

particle\_flux>differential\_directional\_number\_rate  
Energy Bins for Ne 17 – 197 MeV/nuc (15 bins)

**6.6.2.30 A\_Ni** Ni counts side A (counts)

Size: 15 time-varying

particle\_flux>differential\_directional\_number\_rate  
Energy Bins for Ni 29 – 332 MeV/nuc (15 bins)

**6.6.2.31 A\_Ni\_Rate** Ni count rate side A (counts s<sup>-1</sup>)

Size: 15 time-varying

particle\_flux>differential\_directional\_number\_rate  
Energy Bins for Ni 29 – 332 MeV/nuc (15 bins)

**6.6.2.32 A\_O** O counts side A (counts)

Size: 15 time-varying

particle\_flux>differential\_directional\_number\_rate  
Energy Bins for O 15 – 166 MeV/nuc (15 bins)

**6.6.2.33 A\_O\_Rate** O count rate side A (counts s<sup>-1</sup>)

Size: 15 time-varying

particle\_flux>differential\_directional\_number\_rate  
Energy Bins for O 15 – 166 MeV/nuc (15 bins)

**6.6.2.34 A\_S** S counts side A (counts)

Size: 16 time-varying

particle\_flux>differential\_directional\_number\_rate  
Energy Bins for S 21 – 279 MeV/nuc (16 bins)

**6.6.2.35 A\_S\_Rate** S count rate side A (counts s<sup>-1</sup>)

Size: 16 time-varying

particle\_flux>differential\_directional\_number\_rate

Energy Bins for S 21 – 279 MeV/nuc (16 bins)

**6.6.2.36 A\_Si** Si counts side A (counts)

Size: 15 time-varying

particle\_flux>differential\_directional\_number\_rate

Energy Bins for Si 21 – 235 MeV/nuc (15 bins)

**6.6.2.37 A\_Si\_Rate** Si count rate side A (counts s<sup>-1</sup>)

Size: 15 time-varying

particle\_flux>differential\_directional\_number\_rate

Energy Bins for Si 21 – 235 MeV/nuc (15 bins)

**6.6.2.38 B\_Al** Al counts side B (counts)

Size: 15 time-varying

particle\_flux>differential\_directional\_number\_rate

Energy Bins for Al 21 – 235 MeV/nuc (15 bins)

**6.6.2.39 B\_Al\_Rate** Al count rate side B (counts s<sup>-1</sup>)

Size: 15 time-varying

particle\_flux>differential\_directional\_number\_rate

Energy Bins for Al 21 – 235 MeV/nuc (15 bins)

**6.6.2.40 B\_Ar** Ar counts side B (counts)

Size: 15 time-varying

particle\_flux>differential\_directional\_number\_rate

Energy Bins for Ar 25 – 279 MeV/nuc (15 bins)

**6.6.2.41 B\_Ar\_Rate** Ar count rate side B (counts s<sup>-1</sup>)

Size: 15 time-varying

particle\_flux>differential\_directional\_number\_rate

Energy Bins for Ar 25 – 279 MeV/nuc (15 bins)



**6.6.2.42 B\_C** C counts side B (counts)

Size: 15 time-varying

particle\_flux>differential\_directional\_number\_rate

Energy Bins for C 12 – 140 MeV/nuc (15 bins)

**6.6.2.43 B\_C\_Rate** C count rate side B (counts s<sup>-1</sup>)

Size: 15 time-varying

particle\_flux>differential\_directional\_number\_rate

Energy Bins for C 12 – 140 MeV/nuc (15 bins)

**6.6.2.44 B\_Ca** Ca counts side B (counts)

Size: 15 time-varying

particle\_flux>differential\_directional\_number\_rate

Energy Bins for Ca 25 – 279 MeV/nuc (15 bins)

**6.6.2.45 B\_Ca\_Rate** Ca count rate side B (counts s<sup>-1</sup>)

Size: 15 time-varying

particle\_flux>differential\_directional\_number\_rate

Energy Bins for Ca 25 – 279 MeV/nuc (15 bins)

**6.6.2.46 B\_Cr** Cr counts side B (counts)

Size: 16 time-varying

particle\_flux>differential\_directional\_number\_rate

Energy Bins for Cr 25 – 332 MeV/nuc (16 bins)

**6.6.2.47 B\_Cr\_Rate** Cr count rate side B (counts s<sup>-1</sup>)

Size: 16 time-varying

particle\_flux>differential\_directional\_number\_rate

Energy Bins for Cr 25 – 332 MeV/nuc (16 bins)

**6.6.2.48 B\_Electrons** Electrons counts side B (counts)

Size: 19 time-varying

particle\_flux>differential\_directional\_number\_rate

Energy Bins for Electrons 0 – 10 MeV (19 bins)

**6.6.2.49 B\_Electrons\_Rate** Electrons count rate side B (counts s<sup>-1</sup>)

Size: 19 time-varying

particle\_flux>differential\_directional\_number\_rate

Energy Bins for Electrons 0 – 10 MeV (19 bins)

**6.6.2.50 B\_Electrons\_SECT\_Rate** Electrons sectored count rate side B (counts s<sup>-1</sup>)

Size: 2 × 25 time-varying

particle\_flux>differential\_directional\_number\_rate

Energy Bins for Electrons SECT 1 – 3 MeV (2 bins)

HET\_R17\_SECTORS 0 – 24 (25 bins)

**6.6.2.51 B\_Fe** Fe counts side B (counts)

Size: 15 time-varying

particle\_flux>differential\_directional\_number\_rate

Energy Bins for Fe 29 – 332 MeV/nuc (15 bins)

**6.6.2.52 B\_Fe\_Rate** Fe count rate side B (counts s<sup>-1</sup>)

Size: 15 time-varying

particle\_flux>differential\_directional\_number\_rate

Energy Bins for Fe 29 – 332 MeV/nuc (15 bins)

**6.6.2.53 B\_H** H counts side B (counts)

Size: 15 time-varying

particle\_flux>differential\_directional\_number\_rate

Energy Bins for H 7 – 83 MeV (15 bins)

**6.6.2.54 B\_H\_Rate** H count rate side B (counts s<sup>-1</sup>)

Size: 15 time-varying

particle\_flux>differential\_directional\_number\_rate

Energy Bins for H 7 – 83 MeV (15 bins)

**6.6.2.55 B\_H\_SECT\_Rate** H sectored count rate side B (counts s<sup>-1</sup>)

Size: 2 × 25 time-varying

particle\_flux>differential\_directional\_number\_rate

Energy Bins for H SECT 17 – 32 MeV (2 bins)

HET\_R17\_SECTORS 0 – 24 (25 bins)

**6.6.2.56 B\_He** He counts side B (counts)

Size: 16 time-varying

particle\_flux>differential\_directional\_number\_rate

Energy Bins for He 7 – 99 MeV/nuc (16 bins)

**6.6.2.57 B\_He\_Rate** He count rate side B (counts s<sup>-1</sup>)

Size: 16 time-varying

particle\_flux>differential\_directional\_number\_rate

Energy Bins for He 7 – 99 MeV/nuc (16 bins)

**6.6.2.58 B\_He\_SECT\_Rate** He sectored count rate side B (counts s<sup>-1</sup>)

Size: 2 × 25 time-varying

particle\_flux>differential\_directional\_number\_rate

Energy Bins for He SECT 17 – 32 MeV/nuc (2 bins)

HET\_R17\_SECTORS 0 – 24 (25 bins)

**6.6.2.59 B\_Mg** Mg counts side B (counts)

Size: 15 time-varying

particle\_flux>differential\_directional\_number\_rate

Energy Bins for Mg 21 – 235 MeV/nuc (15 bins)

**6.6.2.60 B\_Mg\_Rate** Mg count rate side B (counts s<sup>-1</sup>)

Size: 15 time-varying

particle\_flux>differential\_directional\_number\_rate

Energy Bins for Mg 21 – 235 MeV/nuc (15 bins)

**6.6.2.61 B\_N** N counts side B (counts)

Size: 15 time-varying

particle\_flux>differential\_directional\_number\_rate

Energy Bins for N 12 – 140 MeV/nuc (15 bins)

**6.6.2.62 B\_N\_Rate** N count rate side B (counts s<sup>-1</sup>)

Size: 15 time-varying

particle\_flux>differential\_directional\_number\_rate

Energy Bins for N 12 – 140 MeV/nuc (15 bins)

**6.6.2.63 B\_Na** Na counts side B (counts)

Size: 15 time-varying

particle\_flux>differential\_directional\_number\_rate

Energy Bins for Na 17 – 197 MeV/nuc (15 bins)

**6.6.2.64 B\_Na\_Rate** Na count rate side B (counts s<sup>-1</sup>)

Size: 15 time-varying

particle\_flux>differential\_directional\_number\_rate

Energy Bins for Na 17 – 197 MeV/nuc (15 bins)

**6.6.2.65 B\_Ne** Ne counts side B (counts)

Size: 15 time-varying

particle\_flux>differential\_directional\_number\_rate

Energy Bins for Ne 17 – 197 MeV/nuc (15 bins)

**6.6.2.66 B\_Ne\_Rate** Ne count rate side B (counts s<sup>-1</sup>)

Size: 15 time-varying

particle\_flux>differential\_directional\_number\_rate

Energy Bins for Ne 17 – 197 MeV/nuc (15 bins)

**6.6.2.67 B\_Ni** Ni counts side B (counts)

Size: 15 time-varying

particle\_flux>differential\_directional\_number\_rate

Energy Bins for Ni 29 – 332 MeV/nuc (15 bins)

**6.6.2.68 B\_Ni\_Rate** Ni count rate side B (counts s<sup>-1</sup>)

Size: 15 time-varying

particle\_flux>differential\_directional\_number\_rate

Energy Bins for Ni 29 – 332 MeV/nuc (15 bins)

**6.6.2.69 B\_O** O counts side B (counts)

Size: 15 time-varying

particle\_flux>differential\_directional\_number\_rate

Energy Bins for O 15 – 166 MeV/nuc (15 bins)

**6.6.2.70 B\_O\_Rate** O count rate side B (counts s<sup>-1</sup>)

Size: 15 time-varying

particle\_flux>differential\_directional\_number\_rate

Energy Bins for O 15 – 166 MeV/nuc (15 bins)

**6.6.2.71 B\_S** S counts side B (counts)

Size: 16 time-varying

particle\_flux>differential\_directional\_number\_rate

Energy Bins for S 21 – 279 MeV/nuc (16 bins)

**6.6.2.72 B\_S\_Rate** S count rate side B (counts s<sup>-1</sup>)

Size: 16 time-varying

particle\_flux>differential\_directional\_number\_rate

Energy Bins for S 21 – 279 MeV/nuc (16 bins)

**6.6.2.73 B\_Si** Si counts side B (counts)

Size: 15 time-varying

particle\_flux>differential\_directional\_number\_rate

Energy Bins for Si 21 – 235 MeV/nuc (15 bins)

**6.6.2.74 B\_Si\_Rate** Si count rate side B (counts s<sup>-1</sup>)

Size: 15 time-varying

particle\_flux>differential\_directional\_number\_rate

Energy Bins for Si 21 – 235 MeV/nuc (15 bins)

**6.6.2.75 HCI\_Lat** HCI latitude (degrees)

time-varying

position>latitude

At timestamp. After Fraenz and Harper, PSS, 2002.

**6.6.2.76 HCI\_Lon** HCI longitude (degrees)  
time-varying  
position>longitude  
At timestamp. After Fraenz and Harper, PSS, 2002.

**6.6.2.77 HCI\_R** Heliocentric distance (AU)  
time-varying  
position>radial  
At timestamp. After Fraenz and Harper, PSS, 2002.

**6.6.2.78 HET\_A\_HCI** HCI flow direction HETA  
Size: 3 time-varying  
position>direction  
Unit vector, after Fraenz and Harper, PSS, 2002.

**6.6.2.79 HET\_A\_PA** Pitch angle HETA (degree)  
time-varying  
position>angle

**6.6.2.80 HET\_A\_R17\_SECT\_HCI** HCI flow direction HETAR17SECT  
Size: 25 × 3 time-varying  
position>direction  
Unit vector, after Fraenz and Harper, PSS, 2002.  
HET\_R17\_SECTORS 0 – 24 (25 bins)

**6.6.2.81 HET\_A\_R17\_SECT\_PA** Pitch angle HETAR17SECT (degree)  
Size: 25 time-varying  
position>angle  
HET\_R17\_SECTORS 0 – 24 (25 bins)

**6.6.2.82 HET\_A\_R17\_SECT\_RTN** RTN flow direction HETAR17SECT  
Size: 25 × 3 time-varying  
position>direction  
Unit vector, after Fraenz and Harper, PSS, 2002.  
HET\_R17\_SECTORS 0 – 24 (25 bins)

**6.6.2.83 HET\_A\_R17\_SECT\_SA** Nominal Parker Spiral angle HETAR17SECT (degree)

Size: 25 time-varying

position>angle

Angle between particle direction and nominal outward Parker Spiral, based on 400km/s solar wind and corotation breakdown at 10Rs.

HET\_R17\_SECTORS 0 – 24 (25 bins)

**6.6.2.84 HET\_A\_RTN** RTN flow direction HETA

Size: 3 time-varying

position>direction

Unit vector, after Fraenz and Harper, PSS, 2002.

**6.6.2.85 HET\_A\_SA** Nominal Parker Spiral angle HETA (degree)

time-varying

position>angle

Angle between particle direction and nominal outward Parker Spiral, based on 400km/s solar wind and corotation breakdown at 10Rs.

**6.6.2.86 HET\_B\_HCI** HCI flow direction HETB

Size: 3 time-varying

position>direction

Unit vector, after Fraenz and Harper, PSS, 2002.

**6.6.2.87 HET\_B\_PA** Pitch angle HETB (degree)

time-varying

position>angle

**6.6.2.88 HET\_B\_R17\_SECT\_HCI** HCI flow direction HETBR17SECT

Size: 25 × 3 time-varying

position>direction

Unit vector, after Fraenz and Harper, PSS, 2002.

HET\_R17\_SECTORS 0 – 24 (25 bins)

**6.6.2.89 HET\_B\_R17\_SECT\_PA** Pitch angle HETBR17SECT (degree)

Size: 25 time-varying

position>angle

HET\_R17\_SECTORS 0 – 24 (25 bins)

**6.6.2.90 HET\_B\_R17\_SECT\_RTN** RTN flow direction HETBR17SECT

Size: 25 × 3 time-varying

position>direction

Unit vector, after Fraenz and Harper, PSS, 2002.

HET\_R17\_SECTORS 0 – 24 (25 bins)

**6.6.2.91 HET\_B\_R17\_SECT\_SA** Nominal Parker Spiral angle HETBR17SECT (degree)

Size: 25 time-varying

position>angle

Angle between particle direction and nominal outward Parker Spiral, based on 400km/s solar wind and corotation breakdown at 10Rs.

HET\_R17\_SECTORS 0 – 24 (25 bins)

**6.6.2.92 HET\_B\_RTN** RTN flow direction HETB

Size: 3 time-varying

position>direction

Unit vector, after Fraenz and Harper, PSS, 2002.

**6.6.2.93 HET\_B\_SA** Nominal Parker Spiral angle HETB (degree)

time-varying

position>angle

Angle between particle direction and nominal outward Parker Spiral, based on 400km/s solar wind and corotation breakdown at 10Rs.

**6.6.2.94 HGC\_Lat** HGC latitude (degrees)

time-varying

position>latitude

At timestamp. After Fraenz and Harper, PSS, 2002.

**6.6.2.95 HGC\_Lon** HGC longitude (degrees)

time-varying

position>longitude

At timestamp. After Fraenz and Harper, PSS, 2002.



**6.6.2.96 HGC\_R** Heliocentric distance (AU)

time-varying

position>radial

At timestamp. After Fraenz and Harper, PSS, 2002.

**6.6.3 OTHER SUPPORT**

**6.6.3.1 Quality\_Flag** Data-quality flag

Size: 10 time-varying

flag>status

Quality flag number 0 – 9 (10 bins)

**6.7 PSP\_ISOIS-EPIHI\_L2-LET1-RATES10**

ISOIS-EPIHI>Integrated Science Investigation of the Sun, Energetic Particle Instrument Hi

L2-LET1-rates10>Level 2 LET1 10-second rates

EPI-Hi 10 second rates cdf. Time tags indicate midpoint of integration.

Instrument paper: Integrated Science Investigation of the Sun (ISIS): Design of the Energetic Particle Investigation. McComas, D. J. et al (2016). Space Sci. Rev., doi:10.1007/s11214-014-0059-1

1 minute to 1 hour

Cite McComas et al (2016), doi:10.1007/s11214-014-0059-1

**6.7.1 PRIMARY VARIABLES**

**6.7.1.1 A\_H\_Flux** H flux side A ( $\text{cm}^{-2}\text{sr}^{-1}\text{sec}^{-1}\text{MeV}^{-1}$ )

Size: 18 time-varying

particle\_flux>differential\_directional\_number

Energy Bins for H 1 – 15 MeV (18 bins)

**6.7.1.2 A\_He\_Flux** He flux side A ( $\text{cm}^{-2}\text{sr}^{-1}\text{sec}^{-1}(\text{MeV}/\text{nuc})^{-1}$ )

Size: 22 time-varying

particle\_flux>differential\_directional\_number

Energy Bins for He 1 – 29 MeV/nuc (22 bins)

**6.7.1.3 B\_H\_Flux** H flux side B ( $\text{cm}^{-2}\text{sr}^{-1}\text{sec}^{-1}\text{MeV}^{-1}$ )

Size: 18 time-varying

particle\_flux>differential\_directional\_number

Energy Bins for H 1 – 15 MeV (18 bins)

**6.7.1.4 B\_He\_Flux** He flux side B ( $\text{cm}^{-2}\text{sr}^{-1}\text{sec}^{-1}(\text{MeV}/\text{nuc})^{-1}$ )

Size: 22 time-varying

particle\_flux>differential\_directional\_number

Energy Bins for He 1 – 29 MeV/nuc (22 bins)

**6.7.2 OTHER DATA**

**6.7.2.1 A\_Electrons** Electrons counts side A (counts)

Size: 14 time-varying

particle\_flux>differential\_directional\_number\_rate

Energy Bins for Electrons 1 – 5 MeV (14 bins)

**6.7.2.2 A\_Electrons\_Rate** Electrons count rate side A ( $\text{counts s}^{-1}$ )

Size: 14 time-varying

particle\_flux>differential\_directional\_number\_rate

Energy Bins for Electrons 1 – 5 MeV (14 bins)

**6.7.2.3 A\_H** H counts side A (counts)

Size: 18 time-varying

particle\_flux>differential\_directional\_number\_rate

Energy Bins for H 1 – 15 MeV (18 bins)

**6.7.2.4 A\_H\_Rate** H count rate side A ( $\text{counts s}^{-1}$ )

Size: 18 time-varying

particle\_flux>differential\_directional\_number\_rate

Energy Bins for H 1 – 15 MeV (18 bins)

**6.7.2.5 A\_He** He counts side A (counts)

Size: 22 time-varying

particle\_flux>differential\_directional\_number\_rate

Energy Bins for He 1 – 29 MeV/nuc (22 bins)

**6.7.2.6 A\_He\_Rate** He count rate side A ( $\text{counts s}^{-1}$ )

Size: 22 time-varying

particle\_flux>differential\_directional\_number\_rate

Energy Bins for He 1 – 29 MeV/nuc (22 bins)

**6.7.2.7 B\_Electrons** Electrons counts side B (counts)

Size: 14 time-varying

particle\_flux>differential\_directional\_number\_rate

Energy Bins for Electrons 1 – 5 MeV (14 bins)

**6.7.2.8 B\_Electrons\_Rate** Electrons count rate side B (counts s<sup>-1</sup>)

Size: 14 time-varying

particle\_flux>differential\_directional\_number\_rate

Energy Bins for Electrons 1 – 5 MeV (14 bins)

**6.7.2.9 B\_H** H counts side B (counts)

Size: 18 time-varying

particle\_flux>differential\_directional\_number\_rate

Energy Bins for H 1 – 15 MeV (18 bins)

**6.7.2.10 B\_H\_Rate** H count rate side B (counts s<sup>-1</sup>)

Size: 18 time-varying

particle\_flux>differential\_directional\_number\_rate

Energy Bins for H 1 – 15 MeV (18 bins)

**6.7.2.11 B\_He** He counts side B (counts)

Size: 22 time-varying

particle\_flux>differential\_directional\_number\_rate

Energy Bins for He 1 – 29 MeV/nuc (22 bins)

**6.7.2.12 B\_He\_Rate** He count rate side B (counts s<sup>-1</sup>)

Size: 22 time-varying

particle\_flux>differential\_directional\_number\_rate

Energy Bins for He 1 – 29 MeV/nuc (22 bins)

**6.7.2.13 HCI\_Lat** HCI latitude (degrees)

time-varying

position>latitude

At timestamp. After Fraenz and Harper, PSS, 2002.

**6.7.2.14 HCI\_Lon** HCI longitude (degrees)  
time-varying  
position>longitude  
At timestamp. After Fraenz and Harper, PSS, 2002.

**6.7.2.15 HCI\_R** Heliocentric distance (AU)  
time-varying  
position>radial  
At timestamp. After Fraenz and Harper, PSS, 2002.

**6.7.2.16 HGC\_Lat** HGC latitude (degrees)  
time-varying  
position>latitude  
At timestamp. After Fraenz and Harper, PSS, 2002.

**6.7.2.17 HGC\_Lon** HGC longitude (degrees)  
time-varying  
position>longitude  
At timestamp. After Fraenz and Harper, PSS, 2002.

**6.7.2.18 HGC\_R** Heliocentric distance (AU)  
time-varying  
position>radial  
At timestamp. After Fraenz and Harper, PSS, 2002.

**6.7.2.19 LET1\_A\_HCI** HCI flow direction LET1A  
Size: 3 time-varying  
position>direction  
Unit vector, after Fraenz and Harper, PSS, 2002.

**6.7.2.20 LET1\_A\_PA** Pitch angle LET1A (degree)  
time-varying  
position>angle

**6.7.2.21 LET1\_A\_RTN** RTN flow direction LET1A

Size: 3 time-varying

position>direction

Unit vector, after Fraenz and Harper, PSS, 2002.

**6.7.2.22 LET1\_A\_SA** Nominal Parker Spiral angle LET1A (degree)

time-varying

position>angle

Angle between particle direction and nominal outward Parker Spiral, based on 400km/s solar wind and corotation breakdown at 10Rs.

**6.7.2.23 LET1\_B\_HCI** HCI flow direction LET1B

Size: 3 time-varying

position>direction

Unit vector, after Fraenz and Harper, PSS, 2002.

**6.7.2.24 LET1\_B\_PA** Pitch angle LET1B (degree)

time-varying

position>angle

**6.7.2.25 LET1\_B\_RTN** RTN flow direction LET1B

Size: 3 time-varying

position>direction

Unit vector, after Fraenz and Harper, PSS, 2002.

**6.7.2.26 LET1\_B\_SA** Nominal Parker Spiral angle LET1B (degree)

time-varying

position>angle

Angle between particle direction and nominal outward Parker Spiral, based on 400km/s solar wind and corotation breakdown at 10Rs.

### 6.7.3 OTHER SUPPORT

**6.7.3.1 Quality\_Flag** Data-quality flag

Size: 10 time-varying

flag>status

Quality flag number 0 – 9 (10 bins)

## 6.8 PSP\_ISOIS-EPIHI\_L2-LET1-RATES300

ISOIS-EPIHI>Integrated Science Investigation of the Sun, Energetic Particle Instrument Hi  
L2-LET1-rates300>Level 2 LET1 5-minute rates

EPI-Hi LET1 300 second rates cdf. Time tags indicate midpoint of integration.

Instrument paper: Integrated Science Investigation of the Sun (ISIS): Design of the Energetic Particle Investigation. McComas, D. J. et al (2016). Space Sci. Rev., doi:10.1007/s11214-014-0059-1

1 minute to 1 hour

Cite McComas et al (2016), doi:10.1007/s11214-014-0059-1

### 6.8.1 PRIMARY VARIABLES

#### 6.8.2 OTHER DATA

##### 6.8.2.1 HCI\_Lat HCI latitude (degrees)

time-varying

position>latitude

At timestamp. After Fraenz and Harper, PSS, 2002.

##### 6.8.2.2 HCI\_Lon HCI longitude (degrees)

time-varying

position>longitude

At timestamp. After Fraenz and Harper, PSS, 2002.

##### 6.8.2.3 HCI\_R Heliocentric distance (AU)

time-varying

position>radial

At timestamp. After Fraenz and Harper, PSS, 2002.

##### 6.8.2.4 HGC\_Lat HGC latitude (degrees)

time-varying

position>latitude

At timestamp. After Fraenz and Harper, PSS, 2002.

##### 6.8.2.5 HGC\_Lon HGC longitude (degrees)

time-varying

position>longitude

At timestamp. After Fraenz and Harper, PSS, 2002.

**6.8.2.6 HGC\_R** Heliocentric distance (AU)

time-varying

position>radial

At timestamp. After Fraenz and Harper, PSS, 2002.

**6.8.2.7 LET1\_A\_HCI** HCI flow direction LET1A

Size: 3 time-varying

position>direction

Unit vector, after Fraenz and Harper, PSS, 2002.

**6.8.2.8 LET1\_A\_PA** Pitch angle LET1A (degree)

time-varying

position>angle

**6.8.2.9 LET1\_A\_R1\_SECT\_HCI** HCI flow direction LET1AR1SECT

Size:  $9 \times 3$  time-varying

position>direction

Unit vector, after Fraenz and Harper, PSS, 2002.

LET1\_R1\_SECTORS 0 – 8 (9 bins)

**6.8.2.10 LET1\_A\_R1\_SECT\_PA** Pitch angle LET1AR1SECT (degree)

Size: 9 time-varying

position>angle

LET1\_R1\_SECTORS 0 – 8 (9 bins)

**6.8.2.11 LET1\_A\_R1\_SECT\_RTN** RTN flow direction LET1AR1SECT

Size:  $9 \times 3$  time-varying

position>direction

Unit vector, after Fraenz and Harper, PSS, 2002.

LET1\_R1\_SECTORS 0 – 8 (9 bins)

**6.8.2.12 LET1\_A\_R1\_SECT\_SA** Nominal Parker Spiral angle LET1AR1SECT (degree)

Size: 9 time-varying

position>angle

Angle between particle direction and nominal outward Parker Spiral, based on 400km/s solar wind and corotation breakdown at 10Rs.

LET1\_R1\_SECTORS 0 – 8 (9 bins)

**6.8.2.13 LET1\_A\_R26\_SECT\_HCI** HCI flow direction LET1AR26SECT

Size: 25 × 3 time-varying

position>direction

Unit vector, after Fraenz and Harper, PSS, 2002.

LET1\_R26\_SECTORS 0 – 24 (25 bins)

**6.8.2.14 LET1\_A\_R26\_SECT\_PA** Pitch angle LET1AR26SECT (degree)

Size: 25 time-varying

position>angle

LET1\_R26\_SECTORS 0 – 24 (25 bins)

**6.8.2.15 LET1\_A\_R26\_SECT\_RTN** RTN flow direction LET1AR26SECT

Size: 25 × 3 time-varying

position>direction

Unit vector, after Fraenz and Harper, PSS, 2002.

LET1\_R26\_SECTORS 0 – 24 (25 bins)

**6.8.2.16 LET1\_A\_R26\_SECT\_SA** Nominal Parker Spiral angle LET1AR26SECT (degree)

Size: 25 time-varying

position>angle

Angle between particle direction and nominal outward Parker Spiral, based on 400km/s solar wind and corotation breakdown at 10Rs.

LET1\_R26\_SECTORS 0 – 24 (25 bins)

**6.8.2.17 LET1\_A\_RTN** RTN flow direction LET1A

Size: 3 time-varying

position>direction

Unit vector, after Fraenz and Harper, PSS, 2002.



**6.8.2.18 LET1\_A\_SA** Nominal Parker Spiral angle LET1A (degree)

time-varying

position>angle

Angle between particle direction and nominal outward Parker Spiral, based on 400km/s solar wind and corotation breakdown at 10Rs.

**6.8.2.19 LET1\_B\_HCI** HCI flow direction LET1B

Size: 3 time-varying

position>direction

Unit vector, after Fraenz and Harper, PSS, 2002.

**6.8.2.20 LET1\_B\_PA** Pitch angle LET1B (degree)

time-varying

position>angle

**6.8.2.21 LET1\_B\_R1\_SECT\_HCI** HCI flow direction LET1BR1SECT

Size:  $9 \times 3$  time-varying

position>direction

Unit vector, after Fraenz and Harper, PSS, 2002.

LET1\_R1\_SECTORS 0 – 8 (9 bins)

**6.8.2.22 LET1\_B\_R1\_SECT\_PA** Pitch angle LET1BR1SECT (degree)

Size: 9 time-varying

position>angle

LET1\_R1\_SECTORS 0 – 8 (9 bins)

**6.8.2.23 LET1\_B\_R1\_SECT\_RTN** RTN flow direction LET1BR1SECT

Size:  $9 \times 3$  time-varying

position>direction

Unit vector, after Fraenz and Harper, PSS, 2002.

LET1\_R1\_SECTORS 0 – 8 (9 bins)

**6.8.2.24 LET1\_B\_R1\_SECT\_SA** Nominal Parker Spiral angle LET1BR1SECT (degree)

Size: 9 time-varying

position>angle

Angle between particle direction and nominal outward Parker Spiral, based on 400km/s solar wind

and corotation breakdown at 10Rs.

LET1\_R1\_SECTORS 0 – 8 (9 bins)

**6.8.2.25 LET1\_B\_R26\_SECT\_HCI** HCI flow direction LET1BR26SECT

Size: 25 × 3 time-varying

position>direction

Unit vector, after Fraenz and Harper, PSS, 2002.

LET1\_R26\_SECTORS 0 – 24 (25 bins)

**6.8.2.26 LET1\_B\_R26\_SECT\_PA** Pitch angle LET1BR26SECT (degree)

Size: 25 time-varying

position>angle

LET1\_R26\_SECTORS 0 – 24 (25 bins)

**6.8.2.27 LET1\_B\_R26\_SECT\_RTN** RTN flow direction LET1BR26SECT

Size: 25 × 3 time-varying

position>direction

Unit vector, after Fraenz and Harper, PSS, 2002.

LET1\_R26\_SECTORS 0 – 24 (25 bins)

**6.8.2.28 LET1\_B\_R26\_SECT\_SA** Nominal Parker Spiral angle LET1BR26SECT (degree)

Size: 25 time-varying

position>angle

Angle between particle direction and nominal outward Parker Spiral, based on 400km/s solar wind and corotation breakdown at 10Rs.

LET1\_R26\_SECTORS 0 – 24 (25 bins)

**6.8.2.29 LET1\_B\_RTN** RTN flow direction LET1B

Size: 3 time-varying

position>direction

Unit vector, after Fraenz and Harper, PSS, 2002.

**6.8.2.30 LET1\_B\_SA** Nominal Parker Spiral angle LET1B (degree)

time-varying

position>angle

Angle between particle direction and nominal outward Parker Spiral, based on 400km/s solar wind

and corotation breakdown at 10Rs.

**6.8.2.31 R1A\_CNO\_SECT\_Rate** CNO sectored count rate R1A (counts s<sup>-1</sup>)

Size: 1 × 9 time-varying

particle\_flux>differential\_directional\_number\_rate

Energy Bins for R1 CNO SECT 3 – 3 MeV/nuc (1 bins)

LET1\_R1\_SECTORS 0 – 8 (9 bins)

**6.8.2.32 R1A\_FeGroup\_SECT\_Rate** FeGroup sectored count rate R1A (counts s<sup>-1</sup>)

Size: 1 × 9 time-varying

particle\_flux>differential\_directional\_number\_rate

Energy Bins for R1 FeGroup SECT 3 – 3 MeV/nuc (1 bins)

LET1\_R1\_SECTORS 0 – 8 (9 bins)

**6.8.2.33 R1A\_NetoSi\_SECT\_Rate** NetoS<sub>i</sub> sectored count rate R1A (counts s<sup>-1</sup>)

Size: 1 × 9 time-varying

particle\_flux>differential\_directional\_number\_rate

Energy Bins for R1 NetoS<sub>i</sub> SECT 3 – 3 MeV/nuc (1 bins)

LET1\_R1\_SECTORS 0 – 8 (9 bins)

**6.8.2.34 R1B\_CNO\_SECT\_Rate** CNO sectored count rate R1B (counts s<sup>-1</sup>)

Size: 1 × 9 time-varying

particle\_flux>differential\_directional\_number\_rate

Energy Bins for R1 CNO SECT 3 – 3 MeV/nuc (1 bins)

LET1\_R1\_SECTORS 0 – 8 (9 bins)

**6.8.2.35 R1B\_FeGroup\_SECT\_Rate** FeGroup sectored count rate R1B (counts s<sup>-1</sup>)

Size: 1 × 9 time-varying

particle\_flux>differential\_directional\_number\_rate

Energy Bins for R1 FeGroup SECT 3 – 3 MeV/nuc (1 bins)

LET1\_R1\_SECTORS 0 – 8 (9 bins)

**6.8.2.36 R1B\_NetoSi\_SECT\_Rate** NetoS<sub>i</sub> sectored count rate R1B (counts s<sup>-1</sup>)

Size: 1 × 9 time-varying

particle\_flux>differential\_directional\_number\_rate

Energy Bins for R1 NetoS<sub>i</sub> SECT 3 – 3 MeV/nuc (1 bins)

LET1\_R1\_SECTORS 0 – 8 (9 bins)

**6.8.2.37 R26A\_CNO\_SECT\_Rate** CNO sectored count rate R26A (counts s<sup>-1</sup>)

Size: 3 × 25 time-varying

particle\_flux>differential\_directional\_number\_rate

Energy Bins for R26 CNO SECT 6 – 23 MeV/nuc (3 bins)

LET1\_R26\_SECTORS 0 – 24 (25 bins)

**6.8.2.38 R26A\_FeGroup\_SECT\_Rate** FeGroup sectored count rate R26A (counts s<sup>-1</sup>)

Size: 3 × 25 time-varying

particle\_flux>differential\_directional\_number\_rate

Energy Bins for R26 FeGroup SECT 6 – 23 MeV/nuc (3 bins)

LET1\_R26\_SECTORS 0 – 24 (25 bins)

**6.8.2.39 R26A\_NetoSi\_SECT\_Rate** NetoS<sub>i</sub> sectored count rate R26A (counts s<sup>-1</sup>)

Size: 3 × 25 time-varying

particle\_flux>differential\_directional\_number\_rate

Energy Bins for R26 NetoS<sub>i</sub> SECT 6 – 23 MeV/nuc (3 bins)

LET1\_R26\_SECTORS 0 – 24 (25 bins)

**6.8.2.40 R26B\_CNO\_SECT\_Rate** CNO sectored count rate R26B (counts s<sup>-1</sup>)

Size: 3 × 25 time-varying

particle\_flux>differential\_directional\_number\_rate

Energy Bins for R26 CNO SECT 6 – 23 MeV/nuc (3 bins)

LET1\_R26\_SECTORS 0 – 24 (25 bins)

**6.8.2.41 R26B\_FeGroup\_SECT\_Rate** FeGroup sectored count rate R26B (counts s<sup>-1</sup>)

Size: 3 × 25 time-varying

particle\_flux>differential\_directional\_number\_rate

Energy Bins for R26 FeGroup SECT 6 – 23 MeV/nuc (3 bins)

LET1\_R26\_SECTORS 0 – 24 (25 bins)

**6.8.2.42 R26B\_NetoSi\_SECT\_Rate** NetoS<sub>i</sub> sectored count rate R26B (counts s<sup>-1</sup>)

Size: 3 × 25 time-varying

particle\_flux>differential\_directional\_number\_rate

Energy Bins for R26 NetoS<sub>i</sub> SECT 6 – 23 MeV/nuc (3 bins)

LET1\_R26\_SECTORS 0 – 24 (25 bins)

### 6.8.3 OTHER SUPPORT

#### 6.8.3.1 Quality\_Flag Data-quality flag

Size: 10 time-varying

flag>status

Quality flag number 0 – 9 (10 bins)

## 6.9 PSP\_ISOIS-EPIHI\_L2-LET1-RATES3600

ISOIS-EPIHI>Integrated Science Investigation of the Sun, Energetic Particle Instrument Hi

L2-LET1-rates3600>Level 2 LET1 hourly rates

EPI-Hi 3600 seconds rates cdf. Time tags indicate midpoint of integration.

Instrument paper: Integrated Science Investigation of the Sun (ISIS): Design of the Energetic Particle Investigation. McComas, D. J. et al (2016). Space Sci. Rev., doi:10.1007/s11214-014-0059-1

1 minute to 1 hour

Cite McComas et al (2016), doi:10.1007/s11214-014-0059-1

### 6.9.1 PRIMARY VARIABLES

#### 6.9.1.1 A\_H\_Flux H flux side A ( $\text{cm}^{-2}\text{sr}^{-1}\text{sec}^{-1}\text{MeV}^{-1}$ )

Size: 25 time-varying

particle\_flux>differential\_directional\_number

Energy Bins for H 1 – 41 MeV (25 bins)

#### 6.9.1.2 A\_He\_Flux He flux side A ( $\text{cm}^{-2}\text{sr}^{-1}\text{sec}^{-1}(\text{MeV}/\text{nuc})^{-1}$ )

Size: 26 time-varying

particle\_flux>differential\_directional\_number

Energy Bins for He 1 – 49 MeV/nuc (26 bins)

#### 6.9.1.3 B\_H\_Flux H flux side B ( $\text{cm}^{-2}\text{sr}^{-1}\text{sec}^{-1}\text{MeV}^{-1}$ )

Size: 25 time-varying

particle\_flux>differential\_directional\_number

Energy Bins for H 1 – 41 MeV (25 bins)

#### 6.9.1.4 B\_He\_Flux He flux side B ( $\text{cm}^{-2}\text{sr}^{-1}\text{sec}^{-1}(\text{MeV}/\text{nuc})^{-1}$ )

Size: 26 time-varying

particle\_flux>differential\_directional\_number  
Energy Bins for He 1 – 49 MeV/nuc (26 bins)

**6.9.1.5 R1A\_H\_SECT\_Flux** H sectored flux R1A ( $\text{cm}^{-2}\text{sr}^{-1}\text{sec}^{-1}\text{MeV}^{-1}$ )

Size:  $1 \times 9$  time-varying

particle\_flux>differential\_directional\_number  
Energy Bins for R1 H SECT 1 – 1 MeV (1 bins)  
LET1\_R1\_SECTORS 0 – 8 (9 bins)

**6.9.1.6 R1A\_He\_SECT\_Flux** He sectored flux R1A ( $\text{cm}^{-2}\text{sr}^{-1}\text{sec}^{-1}(\text{MeV}/\text{nuc})^{-1}$ )

Size:  $1 \times 9$  time-varying

particle\_flux>differential\_directional\_number  
Energy Bins for R1 He SECT 1 – 1 MeV/nuc (1 bins)  
LET1\_R1\_SECTORS 0 – 8 (9 bins)

**6.9.1.7 R1B\_H\_SECT\_Flux** H sectored flux R1B ( $\text{cm}^{-2}\text{sr}^{-1}\text{sec}^{-1}\text{MeV}^{-1}$ )

Size:  $1 \times 9$  time-varying

particle\_flux>differential\_directional\_number  
Energy Bins for R1 H SECT 1 – 1 MeV (1 bins)  
LET1\_R1\_SECTORS 0 – 8 (9 bins)

**6.9.1.8 R1B\_He\_SECT\_Flux** He sectored flux R1B ( $\text{cm}^{-2}\text{sr}^{-1}\text{sec}^{-1}(\text{MeV}/\text{nuc})^{-1}$ )

Size:  $1 \times 9$  time-varying

particle\_flux>differential\_directional\_number  
Energy Bins for R1 He SECT 1 – 1 MeV/nuc (1 bins)  
LET1\_R1\_SECTORS 0 – 8 (9 bins)

**6.9.1.9 R26A\_H\_SECT\_Flux** H sectored flux R26A ( $\text{cm}^{-2}\text{sr}^{-1}\text{sec}^{-1}\text{MeV}^{-1}$ )

Size:  $3 \times 25$  time-varying

particle\_flux>differential\_directional\_number  
Energy Bins for R26 H SECT 3 – 11 MeV (3 bins)  
LET1\_R26\_SECTORS 0 – 24 (25 bins)

**6.9.1.10 R26A\_He\_SECT\_Flux** He sectored flux R26A ( $\text{cm}^{-2}\text{sr}^{-1}\text{sec}^{-1}(\text{MeV}/\text{nuc})^{-1}$ )

Size:  $3 \times 25$  time-varying

particle\_flux>differential\_directional\_number

Energy Bins for R26 He SECT 3 – 11 MeV/nuc (3 bins)  
LET1\_R26\_SECTORS 0 – 24 (25 bins)

**6.9.1.11 R26B\_H\_SECT\_Flux** H sectored flux R26B ( $\text{cm}^{-2}\text{sr}^{-1}\text{sec}^{-1}\text{MeV}^{-1}$ )  
Size:  $3 \times 25$  time-varying  
particle\_flux>differential\_directional\_number  
Energy Bins for R26 H SECT 3 – 11 MeV (3 bins)  
LET1\_R26\_SECTORS 0 – 24 (25 bins)

**6.9.1.12 R26B\_He\_SECT\_Flux** He sectored flux R26B ( $\text{cm}^{-2}\text{sr}^{-1}\text{sec}^{-1}(\text{MeV}/\text{nuc})^{-1}$ )  
Size:  $3 \times 25$  time-varying  
particle\_flux>differential\_directional\_number  
Energy Bins for R26 He SECT 3 – 11 MeV/nuc (3 bins)  
LET1\_R26\_SECTORS 0 – 24 (25 bins)

## 6.9.2 OTHER DATA

**6.9.2.1 A\_Al** Al counts side A (counts)  
Size: 28 time-varying  
particle\_flux>differential\_directional\_number\_rate  
Energy Bins for Al 1 – 117 MeV/nuc (28 bins)

**6.9.2.2 A\_Al\_Rate** Al count rate side A ( $\text{counts s}^{-1}$ )  
Size: 28 time-varying  
particle\_flux>differential\_directional\_number\_rate  
Energy Bins for Al 1 – 117 MeV/nuc (28 bins)

**6.9.2.3 A\_Ar** Ar counts side A (counts)  
Size: 29 time-varying  
particle\_flux>differential\_directional\_number\_rate  
Energy Bins for Ar 1 – 140 MeV/nuc (29 bins)

**6.9.2.4 A\_Ar\_Rate** Ar count rate side A ( $\text{counts s}^{-1}$ )  
Size: 29 time-varying  
particle\_flux>differential\_directional\_number\_rate  
Energy Bins for Ar 1 – 140 MeV/nuc (29 bins)

**6.9.2.5 A\_C** C counts side A (counts)

Size: 27 time-varying

particle\_flux>differential\_directional\_number\_rate

Energy Bins for C 1 – 99 MeV/nuc (27 bins)

**6.9.2.6 A\_C\_Rate** C count rate side A (counts s<sup>-1</sup>)

Size: 27 time-varying

particle\_flux>differential\_directional\_number\_rate

Energy Bins for C 1 – 99 MeV/nuc (27 bins)

**6.9.2.7 A\_Ca** Ca counts side A (counts)

Size: 30 time-varying

particle\_flux>differential\_directional\_number\_rate

Energy Bins for Ca 1 – 140 MeV/nuc (30 bins)

**6.9.2.8 A\_Ca\_Rate** Ca count rate side A (counts s<sup>-1</sup>)

Size: 30 time-varying

particle\_flux>differential\_directional\_number\_rate

Energy Bins for Ca 1 – 140 MeV/nuc (30 bins)

**6.9.2.9 A\_Cr** Cr counts side A (counts)

Size: 31 time-varying

particle\_flux>differential\_directional\_number\_rate

Energy Bins for Cr 1 – 140 MeV/nuc (31 bins)

**6.9.2.10 A\_Cr\_Rate** Cr count rate side A (counts s<sup>-1</sup>)

Size: 31 time-varying

particle\_flux>differential\_directional\_number\_rate

Energy Bins for Cr 1 – 140 MeV/nuc (31 bins)

**6.9.2.11 A\_Electrons** Electrons counts side A (counts)

Size: 16 time-varying

particle\_flux>differential\_directional\_number\_rate

Energy Bins for Electrons 0 – 6 MeV (16 bins)



**6.9.2.12 A\_Electrons\_Rate** Electrons count rate side A (counts s<sup>-1</sup>)

Size: 16 time-varying

particle\_flux>differential\_directional\_number\_rate

Energy Bins for Electrons 0 – 6 MeV (16 bins)

**6.9.2.13 A\_Fe** Fe counts side A (counts)

Size: 32 time-varying

particle\_flux>differential\_directional\_number\_rate

Energy Bins for Fe 1 – 166 MeV/nuc (32 bins)

**6.9.2.14 A\_Fe\_Rate** Fe count rate side A (counts s<sup>-1</sup>)

Size: 32 time-varying

particle\_flux>differential\_directional\_number\_rate

Energy Bins for Fe 1 – 166 MeV/nuc (32 bins)

**6.9.2.15 A\_H** H counts side A (counts)

Size: 25 time-varying

particle\_flux>differential\_directional\_number\_rate

Energy Bins for H 1 – 41 MeV (25 bins)

**6.9.2.16 A\_H\_Rate** H count rate side A (counts s<sup>-1</sup>)

Size: 25 time-varying

particle\_flux>differential\_directional\_number\_rate

Energy Bins for H 1 – 41 MeV (25 bins)

**6.9.2.17 A\_He** He counts side A (counts)

Size: 26 time-varying

particle\_flux>differential\_directional\_number\_rate

Energy Bins for He 1 – 49 MeV/nuc (26 bins)

**6.9.2.18 A\_He\_Rate** He count rate side A (counts s<sup>-1</sup>)

Size: 26 time-varying

particle\_flux>differential\_directional\_number\_rate

Energy Bins for He 1 – 49 MeV/nuc (26 bins)

**6.9.2.19 A\_Mg** Mg counts side A (counts)

Size: 28 time-varying

particle\_flux>differential\_directional\_number\_rate

Energy Bins for Mg 1 – 117 MeV/nuc (28 bins)

**6.9.2.20 A\_Mg\_Rate** Mg count rate side A (counts s<sup>-1</sup>)

Size: 28 time-varying

particle\_flux>differential\_directional\_number\_rate

Energy Bins for Mg 1 – 117 MeV/nuc (28 bins)

**6.9.2.21 A\_N** N counts side A (counts)

Size: 27 time-varying

particle\_flux>differential\_directional\_number\_rate

Energy Bins for N 1 – 99 MeV/nuc (27 bins)

**6.9.2.22 A\_N\_Rate** N count rate side A (counts s<sup>-1</sup>)

Size: 27 time-varying

particle\_flux>differential\_directional\_number\_rate

Energy Bins for N 1 – 99 MeV/nuc (27 bins)

**6.9.2.23 A\_Na** Na counts side A (counts)

Size: 28 time-varying

particle\_flux>differential\_directional\_number\_rate

Energy Bins for Na 1 – 117 MeV/nuc (28 bins)

**6.9.2.24 A\_Na\_Rate** Na count rate side A (counts s<sup>-1</sup>)

Size: 28 time-varying

particle\_flux>differential\_directional\_number\_rate

Energy Bins for Na 1 – 117 MeV/nuc (28 bins)

**6.9.2.25 A\_Ne** Ne counts side A (counts)

Size: 28 time-varying

particle\_flux>differential\_directional\_number\_rate

Energy Bins for Ne 1 – 117 MeV/nuc (28 bins)

**6.9.2.26 A\_Ne\_Rate** Ne count rate side A (counts s<sup>-1</sup>)

Size: 28 time-varying

particle\_flux>differential\_directional\_number\_rate

Energy Bins for Ne 1 – 117 MeV/nuc (28 bins)

**6.9.2.27 A\_Ni** Ni counts side A (counts)

Size: 33 time-varying

particle\_flux>differential\_directional\_number\_rate

Energy Bins for Ni 1 – 197 MeV/nuc (33 bins)

**6.9.2.28 A\_Ni\_Rate** Ni count rate side A (counts s<sup>-1</sup>)

Size: 33 time-varying

particle\_flux>differential\_directional\_number\_rate

Energy Bins for Ni 1 – 197 MeV/nuc (33 bins)

**6.9.2.29 A\_O** O counts side A (counts)

Size: 28 time-varying

particle\_flux>differential\_directional\_number\_rate

Energy Bins for O 1 – 117 MeV/nuc (28 bins)

**6.9.2.30 A\_O\_Rate** O count rate side A (counts s<sup>-1</sup>)

Size: 28 time-varying

particle\_flux>differential\_directional\_number\_rate

Energy Bins for O 1 – 117 MeV/nuc (28 bins)

**6.9.2.31 A\_S** S counts side A (counts)

Size: 29 time-varying

particle\_flux>differential\_directional\_number\_rate

Energy Bins for S 1 – 140 MeV/nuc (29 bins)

**6.9.2.32 A\_S\_Rate** S count rate side A (counts s<sup>-1</sup>)

Size: 29 time-varying

particle\_flux>differential\_directional\_number\_rate

Energy Bins for S 1 – 140 MeV/nuc (29 bins)

**6.9.2.33 A\_Si** Si counts side A (counts)

Size: 29 time-varying

particle\_flux>differential\_directional\_number\_rate

Energy Bins for Si 1 – 140 MeV/nuc (29 bins)

**6.9.2.34 A\_Si\_Rate** Si count rate side A (counts s<sup>-1</sup>)

Size: 29 time-varying

particle\_flux>differential\_directional\_number\_rate

Energy Bins for Si 1 – 140 MeV/nuc (29 bins)

**6.9.2.35 B\_Al** Al counts side B (counts)

Size: 28 time-varying

particle\_flux>differential\_directional\_number\_rate

Energy Bins for Al 1 – 117 MeV/nuc (28 bins)

**6.9.2.36 B\_Al\_Rate** Al count rate side B (counts s<sup>-1</sup>)

Size: 28 time-varying

particle\_flux>differential\_directional\_number\_rate

Energy Bins for Al 1 – 117 MeV/nuc (28 bins)

**6.9.2.37 B\_Ar** Ar counts side B (counts)

Size: 29 time-varying

particle\_flux>differential\_directional\_number\_rate

Energy Bins for Ar 1 – 140 MeV/nuc (29 bins)

**6.9.2.38 B\_Ar\_Rate** Ar count rate side B (counts s<sup>-1</sup>)

Size: 29 time-varying

particle\_flux>differential\_directional\_number\_rate

Energy Bins for Ar 1 – 140 MeV/nuc (29 bins)

**6.9.2.39 B\_C** C counts side B (counts)

Size: 27 time-varying

particle\_flux>differential\_directional\_number\_rate

Energy Bins for C 1 – 99 MeV/nuc (27 bins)

**6.9.2.40 B\_C\_Rate** C count rate side B (counts s<sup>-1</sup>)

Size: 27 time-varying

particle\_flux>differential\_directional\_number\_rate

Energy Bins for C 1 – 99 MeV/nuc (27 bins)

**6.9.2.41 B\_Ca** Ca counts side B (counts)

Size: 30 time-varying

particle\_flux>differential\_directional\_number\_rate

Energy Bins for Ca 1 – 140 MeV/nuc (30 bins)

**6.9.2.42 B\_Ca\_Rate** Ca count rate side B (counts s<sup>-1</sup>)

Size: 30 time-varying

particle\_flux>differential\_directional\_number\_rate

Energy Bins for Ca 1 – 140 MeV/nuc (30 bins)

**6.9.2.43 B\_Cr** Cr counts side B (counts)

Size: 31 time-varying

particle\_flux>differential\_directional\_number\_rate

Energy Bins for Cr 1 – 140 MeV/nuc (31 bins)

**6.9.2.44 B\_Cr\_Rate** Cr count rate side B (counts s<sup>-1</sup>)

Size: 31 time-varying

particle\_flux>differential\_directional\_number\_rate

Energy Bins for Cr 1 – 140 MeV/nuc (31 bins)

**6.9.2.45 B\_Electrons** Electrons counts side B (counts)

Size: 16 time-varying

particle\_flux>differential\_directional\_number\_rate

Energy Bins for Electrons 0 – 6 MeV (16 bins)

**6.9.2.46 B\_Electrons\_Rate** Electrons count rate side B (counts s<sup>-1</sup>)

Size: 16 time-varying

particle\_flux>differential\_directional\_number\_rate

Energy Bins for Electrons 0 – 6 MeV (16 bins)

**6.9.2.47 B\_Fe** Fe counts side B (counts)

Size: 32 time-varying

particle\_flux>differential\_directional\_number\_rate

Energy Bins for Fe 1 – 166 MeV/nuc (32 bins)

**6.9.2.48 B\_Fe\_Rate** Fe count rate side B (counts s<sup>-1</sup>)

Size: 32 time-varying

particle\_flux>differential\_directional\_number\_rate

Energy Bins for Fe 1 – 166 MeV/nuc (32 bins)

**6.9.2.49 B\_H** H counts side B (counts)

Size: 25 time-varying

particle\_flux>differential\_directional\_number\_rate

Energy Bins for H 1 – 41 MeV (25 bins)

**6.9.2.50 B\_H\_Rate** H count rate side B (counts s<sup>-1</sup>)

Size: 25 time-varying

particle\_flux>differential\_directional\_number\_rate

Energy Bins for H 1 – 41 MeV (25 bins)

**6.9.2.51 B\_He** He counts side B (counts)

Size: 26 time-varying

particle\_flux>differential\_directional\_number\_rate

Energy Bins for He 1 – 49 MeV/nuc (26 bins)

**6.9.2.52 B\_He\_Rate** He count rate side B (counts s<sup>-1</sup>)

Size: 26 time-varying

particle\_flux>differential\_directional\_number\_rate

Energy Bins for He 1 – 49 MeV/nuc (26 bins)

**6.9.2.53 B\_Mg** Mg counts side B (counts)

Size: 28 time-varying

particle\_flux>differential\_directional\_number\_rate

Energy Bins for Mg 1 – 117 MeV/nuc (28 bins)

**6.9.2.54 B\_Mg\_Rate** Mg count rate side B (counts s<sup>-1</sup>)

Size: 28 time-varying

particle\_flux>differential\_directional\_number\_rate

Energy Bins for Mg 1 – 117 MeV/nuc (28 bins)

**6.9.2.55 B\_N** N counts side B (counts)

Size: 27 time-varying

particle\_flux>differential\_directional\_number\_rate

Energy Bins for N 1 – 99 MeV/nuc (27 bins)

**6.9.2.56 B\_N\_Rate** N count rate side B (counts s<sup>-1</sup>)

Size: 27 time-varying

particle\_flux>differential\_directional\_number\_rate

Energy Bins for N 1 – 99 MeV/nuc (27 bins)

**6.9.2.57 B\_Na** Na counts side B (counts)

Size: 28 time-varying

particle\_flux>differential\_directional\_number\_rate

Energy Bins for Na 1 – 117 MeV/nuc (28 bins)

**6.9.2.58 B\_Na\_Rate** Na count rate side B (counts s<sup>-1</sup>)

Size: 28 time-varying

particle\_flux>differential\_directional\_number\_rate

Energy Bins for Na 1 – 117 MeV/nuc (28 bins)

**6.9.2.59 B\_Ne** Ne counts side B (counts)

Size: 28 time-varying

particle\_flux>differential\_directional\_number\_rate

Energy Bins for Ne 1 – 117 MeV/nuc (28 bins)

**6.9.2.60 B\_Ne\_Rate** Ne count rate side B (counts s<sup>-1</sup>)

Size: 28 time-varying

particle\_flux>differential\_directional\_number\_rate

Energy Bins for Ne 1 – 117 MeV/nuc (28 bins)

**6.9.2.61 B\_Ni** Ni counts side B (counts)

Size: 33 time-varying

particle\_flux>differential\_directional\_number\_rate

Energy Bins for Ni 1 – 197 MeV/nuc (33 bins)

**6.9.2.62 B\_Ni\_Rate** Ni count rate side B (counts s<sup>-1</sup>)

Size: 33 time-varying

particle\_flux>differential\_directional\_number\_rate

Energy Bins for Ni 1 – 197 MeV/nuc (33 bins)

**6.9.2.63 B\_O** O counts side B (counts)

Size: 28 time-varying

particle\_flux>differential\_directional\_number\_rate

Energy Bins for O 1 – 117 MeV/nuc (28 bins)

**6.9.2.64 B\_O\_Rate** O count rate side B (counts s<sup>-1</sup>)

Size: 28 time-varying

particle\_flux>differential\_directional\_number\_rate

Energy Bins for O 1 – 117 MeV/nuc (28 bins)

**6.9.2.65 B\_S** S counts side B (counts)

Size: 29 time-varying

particle\_flux>differential\_directional\_number\_rate

Energy Bins for S 1 – 140 MeV/nuc (29 bins)

**6.9.2.66 B\_S\_Rate** S count rate side B (counts s<sup>-1</sup>)

Size: 29 time-varying

particle\_flux>differential\_directional\_number\_rate

Energy Bins for S 1 – 140 MeV/nuc (29 bins)

**6.9.2.67 B\_Si** Si counts side B (counts)

Size: 29 time-varying

particle\_flux>differential\_directional\_number\_rate

Energy Bins for Si 1 – 140 MeV/nuc (29 bins)



**6.9.2.68 B\_Si\_Rate** Si count rate side B (counts s<sup>-1</sup>)

Size: 29 time-varying

particle\_flux>differential\_directional\_number\_rate

Energy Bins for Si 1 – 140 MeV/nuc (29 bins)

**6.9.2.69 HCI\_Lat** HCI latitude (degrees)

time-varying

position>latitude

At timestamp. After Fraenz and Harper, PSS, 2002.

**6.9.2.70 HCI\_Lon** HCI longitude (degrees)

time-varying

position>longitude

At timestamp. After Fraenz and Harper, PSS, 2002.

**6.9.2.71 HCI\_R** Heliocentric distance (AU)

time-varying

position>radial

At timestamp. After Fraenz and Harper, PSS, 2002.

**6.9.2.72 HGC\_Lat** HGC latitude (degrees)

time-varying

position>latitude

At timestamp. After Fraenz and Harper, PSS, 2002.

**6.9.2.73 HGC\_Lon** HGC longitude (degrees)

time-varying

position>longitude

At timestamp. After Fraenz and Harper, PSS, 2002.

**6.9.2.74 HGC\_R** Heliocentric distance (AU)

time-varying

position>radial

At timestamp. After Fraenz and Harper, PSS, 2002.

**6.9.2.75 LET1\_A\_HCI** HCI flow direction LET1A

Size: 3 time-varying

position>direction

Unit vector, after Fraenz and Harper, PSS, 2002.

**6.9.2.76 LET1\_A\_PA** Pitch angle LET1A (degree)

time-varying

position>angle

**6.9.2.77 LET1\_A\_R1\_SECT\_HCI** HCI flow direction LET1AR1SECT

Size:  $9 \times 3$  time-varying

position>direction

Unit vector, after Fraenz and Harper, PSS, 2002.

LET1\_R1\_SECTORS 0 – 8 (9 bins)

**6.9.2.78 LET1\_A\_R1\_SECT\_PA** Pitch angle LET1AR1SECT (degree)

Size: 9 time-varying

position>angle

LET1\_R1\_SECTORS 0 – 8 (9 bins)

**6.9.2.79 LET1\_A\_R1\_SECT\_RTN** RTN flow direction LET1AR1SECT

Size:  $9 \times 3$  time-varying

position>direction

Unit vector, after Fraenz and Harper, PSS, 2002.

LET1\_R1\_SECTORS 0 – 8 (9 bins)

**6.9.2.80 LET1\_A\_R1\_SECT\_SA** Nominal Parker Spiral angle LET1AR1SECT (degree)

Size: 9 time-varying

position>angle

Angle between particle direction and nominal outward Parker Spiral, based on 400km/s solar wind and corotation breakdown at 10Rs.

LET1\_R1\_SECTORS 0 – 8 (9 bins)

**6.9.2.81 LET1\_A\_R26\_SECT\_HCI** HCI flow direction LET1AR26SECT

Size:  $25 \times 3$  time-varying

position>direction

Unit vector, after Fraenz and Harper, PSS, 2002.

LET1\_R26\_SECTORS 0 – 24 (25 bins)

**6.9.2.82 LET1\_A\_R26\_SECT\_PA** Pitch angle LET1AR26SECT (degree)

Size: 25 time-varying

position>angle

LET1\_R26\_SECTORS 0 – 24 (25 bins)

**6.9.2.83 LET1\_A\_R26\_SECT\_RTN** RTN flow direction LET1AR26SECT

Size: 25 × 3 time-varying

position>direction

Unit vector, after Fraenz and Harper, PSS, 2002.

LET1\_R26\_SECTORS 0 – 24 (25 bins)

**6.9.2.84 LET1\_A\_R26\_SECT\_SA** Nominal Parker Spiral angle LET1AR26SECT (degree)

Size: 25 time-varying

position>angle

Angle between particle direction and nominal outward Parker Spiral, based on 400km/s solar wind and corotation breakdown at 10Rs.

LET1\_R26\_SECTORS 0 – 24 (25 bins)

**6.9.2.85 LET1\_A\_RTN** RTN flow direction LET1A

Size: 3 time-varying

position>direction

Unit vector, after Fraenz and Harper, PSS, 2002.

**6.9.2.86 LET1\_A\_SA** Nominal Parker Spiral angle LET1A (degree)

time-varying

position>angle

Angle between particle direction and nominal outward Parker Spiral, based on 400km/s solar wind and corotation breakdown at 10Rs.

**6.9.2.87 LET1\_B\_HCI** HCI flow direction LET1B

Size: 3 time-varying

position>direction

Unit vector, after Fraenz and Harper, PSS, 2002.

**6.9.2.88 LET1\_B\_PA** Pitch angle LET1B (degree)

time-varying

position>angle

**6.9.2.89 LET1\_B\_R1\_SECT\_HCI** HCI flow direction LET1BR1SECT

Size:  $9 \times 3$  time-varying

position>direction

Unit vector, after Fraenz and Harper, PSS, 2002.

LET1\_R1\_SECTORS 0 – 8 (9 bins)

**6.9.2.90 LET1\_B\_R1\_SECT\_PA** Pitch angle LET1BR1SECT (degree)

Size: 9 time-varying

position>angle

LET1\_R1\_SECTORS 0 – 8 (9 bins)

**6.9.2.91 LET1\_B\_R1\_SECT\_RTN** RTN flow direction LET1BR1SECT

Size:  $9 \times 3$  time-varying

position>direction

Unit vector, after Fraenz and Harper, PSS, 2002.

LET1\_R1\_SECTORS 0 – 8 (9 bins)

**6.9.2.92 LET1\_B\_R1\_SECT\_SA** Nominal Parker Spiral angle LET1BR1SECT (degree)

Size: 9 time-varying

position>angle

Angle between particle direction and nominal outward Parker Spiral, based on 400km/s solar wind and corotation breakdown at 10Rs.

LET1\_R1\_SECTORS 0 – 8 (9 bins)

**6.9.2.93 LET1\_B\_R26\_SECT\_HCI** HCI flow direction LET1BR26SECT

Size:  $25 \times 3$  time-varying

position>direction

Unit vector, after Fraenz and Harper, PSS, 2002.

LET1\_R26\_SECTORS 0 – 24 (25 bins)

**6.9.2.94 LET1\_B\_R26\_SECT\_PA** Pitch angle LET1BR26SECT (degree)

Size: 25 time-varying

position>angle

LET1\_R26\_SECTORS 0 – 24 (25 bins)

**6.9.2.95 LET1\_B\_R26\_SECT\_RTN** RTN flow direction LET1BR26SECT

Size: 25 × 3 time-varying

position>direction

Unit vector, after Fraenz and Harper, PSS, 2002.

LET1\_R26\_SECTORS 0 – 24 (25 bins)

**6.9.2.96 LET1\_B\_R26\_SECT\_SA** Nominal Parker Spiral angle LET1BR26SECT (degree)

Size: 25 time-varying

position>angle

Angle between particle direction and nominal outward Parker Spiral, based on 400km/s solar wind and corotation breakdown at 10Rs.

LET1\_R26\_SECTORS 0 – 24 (25 bins)

**6.9.2.97 LET1\_B\_RTN** RTN flow direction LET1B

Size: 3 time-varying

position>direction

Unit vector, after Fraenz and Harper, PSS, 2002.

**6.9.2.98 LET1\_B\_SA** Nominal Parker Spiral angle LET1B (degree)

time-varying

position>angle

Angle between particle direction and nominal outward Parker Spiral, based on 400km/s solar wind and corotation breakdown at 10Rs.

**6.9.2.99 R1A\_CNO\_SECT\_Rate** CNO sectored count rate R1A (counts s<sup>-1</sup>)

Size: 1 × 9 time-varying

particle\_flux>differential\_directional\_number\_rate

Energy Bins for R1 CNO SECT 3 – 3 MeV/nuc (1 bins)

LET1\_R1\_SECTORS 0 – 8 (9 bins)

**6.9.2.100 R1A\_FeGroup\_SECT\_Rate** FeGroup sectored count rate R1A (counts s<sup>-1</sup>)

Size: 1 × 9 time-varying

particle\_flux>differential\_directional\_number\_rate

Energy Bins for R1 FeGroup SECT 3 – 3 MeV/nuc (1 bins)

LET1\_R1\_SECTORS 0 – 8 (9 bins)

**6.9.2.101 R1A\_H\_SECT\_Rate** H sectored count rate R1A (counts s<sup>-1</sup>)

Size: 1 × 9 time-varying

particle\_flux>differential\_directional\_number\_rate

Energy Bins for R1 H SECT 1 – 1 MeV (1 bins)

LET1\_R1\_SECTORS 0 – 8 (9 bins)

**6.9.2.102 R1A\_He\_BIN** R1A He Rates (counts)

Size: 5 × 16 time-varying

particle\_flux>differential\_directional\_number\_rate

Energy Bins for R1 He BIN 1 – 3 MeV/nuc (5 bins)

R1A\_He\_BIN\_MASS\_BIN 0 – 15 segment (16 bins)

**6.9.2.103 R1A\_He\_SECT\_Rate** He sectored count rate R1A (counts s<sup>-1</sup>)

Size: 1 × 9 time-varying

particle\_flux>differential\_directional\_number\_rate

Energy Bins for R1 He SECT 1 – 1 MeV/nuc (1 bins)

LET1\_R1\_SECTORS 0 – 8 (9 bins)

**6.9.2.104 R1A\_Ne\_BIN** R1A Ne Rates (counts)

Size: 5 × 8 time-varying

particle\_flux>differential\_directional\_number\_rate

Energy Bins for R1 Ne BIN 1 – 6 MeV/nuc (5 bins)

R1A\_Ne\_BIN\_MASS\_BIN 0 – 7 segment (8 bins)

**6.9.2.105 R1A\_NetoSi\_SECT\_Rate** NetoS<sub>i</sub> sectored count rate R1A (counts s<sup>-1</sup>)

Size: 1 × 9 time-varying

particle\_flux>differential\_directional\_number\_rate

Energy Bins for R1 NetoS<sub>i</sub> SECT 3 – 3 MeV/nuc (1 bins)

LET1\_R1\_SECTORS 0 – 8 (9 bins)

**6.9.2.106 R1B\_CNO\_SECT\_Rate** CNO sectored count rate R1B (counts s<sup>-1</sup>)

Size: 1 × 9 time-varying

particle\_flux>differential\_directional\_number\_rate

Energy Bins for R1 CNO SECT 3 – 3 MeV/nuc (1 bins)

LET1\_R1\_SECTORS 0 – 8 (9 bins)

**6.9.2.107 R1B\_FeGroup\_SECT\_Rate** FeGroup sectored count rate R1B (counts s<sup>-1</sup>)

Size: 1 × 9 time-varying

particle\_flux>differential\_directional\_number\_rate

Energy Bins for R1 FeGroup SECT 3 – 3 MeV/nuc (1 bins)

LET1\_R1\_SECTORS 0 – 8 (9 bins)

**6.9.2.108 R1B\_H\_SECT\_Rate** H sectored count rate R1B (counts s<sup>-1</sup>)

Size: 1 × 9 time-varying

particle\_flux>differential\_directional\_number\_rate

Energy Bins for R1 H SECT 1 – 1 MeV (1 bins)

LET1\_R1\_SECTORS 0 – 8 (9 bins)

**6.9.2.109 R1B\_He\_BIN** R1B He Rates (counts)

Size: 5 × 16 time-varying

particle\_flux>differential\_directional\_number\_rate

Energy Bins for R1 He BIN 1 – 3 MeV/nuc (5 bins)

R1B\_He\_BIN\_MASS\_BIN 0 – 15 segment (16 bins)

**6.9.2.110 R1B\_He\_SECT\_Rate** He sectored count rate R1B (counts s<sup>-1</sup>)

Size: 1 × 9 time-varying

particle\_flux>differential\_directional\_number\_rate

Energy Bins for R1 He SECT 1 – 1 MeV/nuc (1 bins)

LET1\_R1\_SECTORS 0 – 8 (9 bins)

**6.9.2.111 R1B\_Ne\_BIN** R1B Ne Rates (counts)

Size: 5 × 8 time-varying

particle\_flux>differential\_directional\_number\_rate

Energy Bins for R1 Ne BIN 1 – 6 MeV/nuc (5 bins)

R1B\_Ne\_BIN\_MASS\_BIN 0 – 7 segment (8 bins)

**6.9.2.112 R1B\_NetoSi\_SECT\_Rate** NetoS $i$  sectored count rate R1B (counts s $^{-1}$ )

Size: 1  $\times$  9 time-varying

particle\_flux>differential\_directional\_number\_rate

Energy Bins for R1 NetoS $i$  SECT 3 – 3 MeV/nuc (1 bins)

LET1\_R1\_SECTORS 0 – 8 (9 bins)

**6.9.2.113 R26A\_CNO\_SECT\_Rate** CNO sectored count rate R26A (counts s $^{-1}$ )

Size: 3  $\times$  25 time-varying

particle\_flux>differential\_directional\_number\_rate

Energy Bins for R26 CNO SECT 6 – 23 MeV/nuc (3 bins)

LET1\_R26\_SECTORS 0 – 24 (25 bins)

**6.9.2.114 R26A\_FeGroup\_SECT\_Rate** FeGroup sectored count rate R26A (counts s $^{-1}$ )

Size: 3  $\times$  25 time-varying

particle\_flux>differential\_directional\_number\_rate

Energy Bins for R26 FeGroup SECT 6 – 23 MeV/nuc (3 bins)

LET1\_R26\_SECTORS 0 – 24 (25 bins)

**6.9.2.115 R26A\_H\_SECT\_Rate** H sectored count rate R26A (counts s $^{-1}$ )

Size: 3  $\times$  25 time-varying

particle\_flux>differential\_directional\_number\_rate

Energy Bins for R26 H SECT 3 – 11 MeV (3 bins)

LET1\_R26\_SECTORS 0 – 24 (25 bins)

**6.9.2.116 R26A\_He\_SECT\_Rate** He sectored count rate R26A (counts s $^{-1}$ )

Size: 3  $\times$  25 time-varying

particle\_flux>differential\_directional\_number\_rate

Energy Bins for R26 He SECT 3 – 11 MeV/nuc (3 bins)

LET1\_R26\_SECTORS 0 – 24 (25 bins)

**6.9.2.117 R26A\_NetoSi\_SECT\_Rate** NetoS $i$  sectored count rate R26A (counts s $^{-1}$ )

Size: 3  $\times$  25 time-varying

particle\_flux>differential\_directional\_number\_rate

Energy Bins for R26 NetoS $i$  SECT 6 – 23 MeV/nuc (3 bins)

LET1\_R26\_SECTORS 0 – 24 (25 bins)



**6.9.2.118 R26B\_CNO\_SECT\_Rate** CNO sectored count rate R26B (counts s<sup>-1</sup>)

Size: 3 × 25 time-varying

particle\_flux>differential\_directional\_number\_rate

Energy Bins for R26 CNO SECT 6 – 23 MeV/nuc (3 bins)

LET1\_R26\_SECTORS 0 – 24 (25 bins)

**6.9.2.119 R26B\_FeGroup\_SECT\_Rate** FeGroup sectored count rate R26B (counts s<sup>-1</sup>)

Size: 3 × 25 time-varying

particle\_flux>differential\_directional\_number\_rate

Energy Bins for R26 FeGroup SECT 6 – 23 MeV/nuc (3 bins)

LET1\_R26\_SECTORS 0 – 24 (25 bins)

**6.9.2.120 R26B\_H\_SECT\_Rate** H sectored count rate R26B (counts s<sup>-1</sup>)

Size: 3 × 25 time-varying

particle\_flux>differential\_directional\_number\_rate

Energy Bins for R26 H SECT 3 – 11 MeV (3 bins)

LET1\_R26\_SECTORS 0 – 24 (25 bins)

**6.9.2.121 R26B\_He\_SECT\_Rate** He sectored count rate R26B (counts s<sup>-1</sup>)

Size: 3 × 25 time-varying

particle\_flux>differential\_directional\_number\_rate

Energy Bins for R26 He SECT 3 – 11 MeV/nuc (3 bins)

LET1\_R26\_SECTORS 0 – 24 (25 bins)

**6.9.2.122 R26B\_NetoSi\_SECT\_Rate** NetoS<sub>i</sub> sectored count rate R26B (counts s<sup>-1</sup>)

Size: 3 × 25 time-varying

particle\_flux>differential\_directional\_number\_rate

Energy Bins for R26 NetoS<sub>i</sub> SECT 6 – 23 MeV/nuc (3 bins)

LET1\_R26\_SECTORS 0 – 24 (25 bins)

**6.9.2.123 R2A\_He\_BIN** R2A He Rates (counts)

Size: 7 × 16 time-varying

particle\_flux>differential\_directional\_number\_rate

Energy Bins for R2 He BIN 2 – 16 MeV/nuc (7 bins)

R2A\_He\_BIN\_MASS\_BIN 0 – 15 segment (16 bins)

**6.9.2.124 R2A\_Ne\_BIN** R2A Ne Rates (counts)

Size:  $8 \times 8$  time-varying

particle\_flux>differential\_directional\_number\_rate

Energy Bins for R2 Ne BIN 3 – 32 MeV/nuc (8 bins)

R2A\_Ne\_BIN\_MASS\_BIN 0 – 7 segment (8 bins)

**6.9.2.125 R2B\_He\_BIN** R2B He Rates (counts)

Size:  $7 \times 16$  time-varying

particle\_flux>differential\_directional\_number\_rate

Energy Bins for R2 He BIN 2 – 16 MeV/nuc (7 bins)

R2B\_He\_BIN\_MASS\_BIN 0 – 15 segment (16 bins)

**6.9.2.126 R2B\_Ne\_BIN** R2B Ne Rates (counts)

Size:  $8 \times 8$  time-varying

particle\_flux>differential\_directional\_number\_rate

Energy Bins for R2 Ne BIN 3 – 32 MeV/nuc (8 bins)

R2B\_Ne\_BIN\_MASS\_BIN 0 – 7 segment (8 bins)

**6.9.2.127 R3A\_He\_BIN** R3A He Rates (counts)

Size:  $5 \times 16$  time-varying

particle\_flux>differential\_directional\_number\_rate

Energy Bins for R3 He BIN 8 – 32 MeV/nuc (5 bins)

R3A\_He\_BIN\_MASS\_BIN 0 – 15 segment (16 bins)

**6.9.2.128 R3A\_Ne\_BIN** R3A Ne Rates (counts)

Size:  $6 \times 8$  time-varying

particle\_flux>differential\_directional\_number\_rate

Energy Bins for R3 Ne BIN 16 – 91 MeV/nuc (6 bins)

R3A\_Ne\_BIN\_MASS\_BIN 0 – 7 segment (8 bins)

**6.9.2.129 R3B\_He\_BIN** R3B He Rates (counts)

Size:  $5 \times 16$  time-varying

particle\_flux>differential\_directional\_number\_rate

Energy Bins for R3 He BIN 8 – 32 MeV/nuc (5 bins)

R3B\_He\_BIN\_MASS\_BIN 0 – 15 segment (16 bins)

**6.9.2.130 R3B\_Ne\_BIN** R3B Ne Rates (counts)

Size:  $6 \times 8$  time-varying

particle\_flux>differential\_directional\_number\_rate

Energy Bins for R3 Ne BIN 16 – 91 MeV/nuc (6 bins)

R3B\_Ne\_BIN\_MASS\_BIN 0 – 7 segment (8 bins)

**6.9.2.131 R45A\_He\_BIN** R45A He Rates (counts)

Size:  $5 \times 16$  time-varying

particle\_flux>differential\_directional\_number\_rate

Energy Bins for R45 He BIN 8 – 32 MeV/nuc (5 bins)

R45A\_He\_BIN\_MASS\_BIN 0 – 15 segment (16 bins)

**6.9.2.132 R45A\_Ne\_BIN** R45A Ne Rates (counts)

Size:  $6 \times 8$  time-varying

particle\_flux>differential\_directional\_number\_rate

Energy Bins for R45 Ne BIN 16 – 91 MeV/nuc (6 bins)

R45A\_Ne\_BIN\_MASS\_BIN 0 – 7 segment (8 bins)

**6.9.2.133 R45B\_He\_BIN** R45B He Rates (counts)

Size:  $5 \times 16$  time-varying

particle\_flux>differential\_directional\_number\_rate

Energy Bins for R45 He BIN 8 – 32 MeV/nuc (5 bins)

R45B\_He\_BIN\_MASS\_BIN 0 – 15 segment (16 bins)

**6.9.2.134 R45B\_Ne\_BIN** R45B Ne Rates (counts)

Size:  $6 \times 8$  time-varying

particle\_flux>differential\_directional\_number\_rate

Energy Bins for R45 Ne BIN 16 – 91 MeV/nuc (6 bins)

R45B\_Ne\_BIN\_MASS\_BIN 0 – 7 segment (8 bins)

**6.9.2.135 R6A\_He\_BIN** R6A He Rates (counts)

Size:  $3 \times 16$  time-varying

particle\_flux>differential\_directional\_number\_rate

Energy Bins for R6 He BIN 23 – 45 MeV/nuc (3 bins)

R6A\_He\_BIN\_MASS\_BIN 0 – 15 segment (16 bins)

**6.9.2.136 R6A\_Ne\_BIN** R6A Ne Rates (counts)

Size:  $3 \times 8$  time-varying

particle\_flux>differential\_directional\_number\_rate

Energy Bins for R6 Ne BIN 45 – 91 MeV/nuc (3 bins)

R6A\_Ne\_BIN\_MASS\_BIN 0 – 7 segment (8 bins)

**6.9.2.137 R6B\_He\_BIN** R6B He Rates (counts)

Size:  $3 \times 16$  time-varying

particle\_flux>differential\_directional\_number\_rate

Energy Bins for R6 He BIN 23 – 45 MeV/nuc (3 bins)

R6B\_He\_BIN\_MASS\_BIN 0 – 15 segment (16 bins)

**6.9.2.138 R6B\_Ne\_BIN** R6B Ne Rates (counts)

Size:  $3 \times 8$  time-varying

particle\_flux>differential\_directional\_number\_rate

Energy Bins for R6 Ne BIN 45 – 91 MeV/nuc (3 bins)

R6B\_Ne\_BIN\_MASS\_BIN 0 – 7 segment (8 bins)

**6.9.3 OTHER SUPPORT**

**6.9.3.1 Quality\_Flag** Data-quality flag

Size: 10 time-varying

flag>status

Quality flag number 0 – 9 (10 bins)

**6.10 PSP\_ISOIS-EPIHI\_L2-LET1-RATES60**

ISOIS-EPIHI>Integrated Science Investigation of the Sun, Energetic Particle Instrument Hi

L2-LET1-rates60>Level 2 LET1 1-minute rates

EPI-Hi LET1 60 second rates cdf. Time tags indicate midpoint of integration.

Instrument paper: Integrated Science Investigation of the Sun (ISIS): Design of the Energetic Particle Investigation. McComas, D. J. et al (2016). Space Sci. Rev., doi:10.1007/s11214-014-0059-1

1 minute to 1 hour

Cite McComas et al (2016), doi:10.1007/s11214-014-0059-1

**6.10.1 PRIMARY VARIABLES**

**6.10.1.1 A\_H\_Flux** H flux side A ( $\text{cm}^{-2}\text{sr}^{-1}\text{sec}^{-1}\text{MeV}^{-1}$ )

Size: 25 time-varying

particle\_flux>differential\_directional\_number  
Energy Bins for H 1 – 41 MeV (25 bins)

**6.10.1.2 A\_He\_Flux** He flux side A ( $\text{cm}^{-2}\text{sr}^{-1}\text{sec}^{-1}(\text{MeV}/\text{nuc})^{-1}$ )  
Size: 26 time-varying

particle\_flux>differential\_directional\_number  
Energy Bins for He 1 – 49 MeV/nuc (26 bins)

**6.10.1.3 B\_H\_Flux** H flux side B ( $\text{cm}^{-2}\text{sr}^{-1}\text{sec}^{-1}\text{MeV}^{-1}$ )  
Size: 25 time-varying

particle\_flux>differential\_directional\_number  
Energy Bins for H 1 – 41 MeV (25 bins)

**6.10.1.4 B\_He\_Flux** He flux side B ( $\text{cm}^{-2}\text{sr}^{-1}\text{sec}^{-1}(\text{MeV}/\text{nuc})^{-1}$ )  
Size: 26 time-varying

particle\_flux>differential\_directional\_number  
Energy Bins for He 1 – 49 MeV/nuc (26 bins)

**6.10.1.5 R1A\_H\_SECT\_Flux** H sectored flux R1A ( $\text{cm}^{-2}\text{sr}^{-1}\text{sec}^{-1}\text{MeV}^{-1}$ )  
Size:  $1 \times 9$  time-varying

particle\_flux>differential\_directional\_number  
Energy Bins for R1 H SECT 1 – 1 MeV (1 bins)  
LET1\_R1\_SECTORS 0 – 8 (9 bins)

**6.10.1.6 R1A\_He\_SECT\_Flux** He sectored flux R1A ( $\text{cm}^{-2}\text{sr}^{-1}\text{sec}^{-1}(\text{MeV}/\text{nuc})^{-1}$ )  
Size:  $1 \times 9$  time-varying

particle\_flux>differential\_directional\_number  
Energy Bins for R1 He SECT 1 – 1 MeV/nuc (1 bins)  
LET1\_R1\_SECTORS 0 – 8 (9 bins)

**6.10.1.7 R1B\_H\_SECT\_Flux** H sectored flux R1B ( $\text{cm}^{-2}\text{sr}^{-1}\text{sec}^{-1}\text{MeV}^{-1}$ )  
Size:  $1 \times 9$  time-varying

particle\_flux>differential\_directional\_number  
Energy Bins for R1 H SECT 1 – 1 MeV (1 bins)  
LET1\_R1\_SECTORS 0 – 8 (9 bins)

**6.10.1.8 R1B\_He\_SECT\_Flux** He sectored flux R1B ( $\text{cm}^{-2}\text{sr}^{-1}\text{sec}^{-1}(\text{MeV}/\text{nuc})^{-1}$ )

Size:  $1 \times 9$  time-varying

particle\_flux>differential\_directional\_number

Energy Bins for R1 He SECT 1 – 1 MeV/nuc (1 bins)

LET1\_R1\_SECTORS 0 – 8 (9 bins)

**6.10.1.9 R26A\_H\_SECT\_Flux** H sectored flux R26A ( $\text{cm}^{-2}\text{sr}^{-1}\text{sec}^{-1}\text{MeV}^{-1}$ )

Size:  $3 \times 25$  time-varying

particle\_flux>differential\_directional\_number

Energy Bins for R26 H SECT 3 – 11 MeV (3 bins)

LET1\_R26\_SECTORS 0 – 24 (25 bins)

**6.10.1.10 R26A\_He\_SECT\_Flux** He sectored flux R26A ( $\text{cm}^{-2}\text{sr}^{-1}\text{sec}^{-1}(\text{MeV}/\text{nuc})^{-1}$ )

Size:  $3 \times 25$  time-varying

particle\_flux>differential\_directional\_number

Energy Bins for R26 He SECT 3 – 11 MeV/nuc (3 bins)

LET1\_R26\_SECTORS 0 – 24 (25 bins)

**6.10.1.11 R26B\_H\_SECT\_Flux** H sectored flux R26B ( $\text{cm}^{-2}\text{sr}^{-1}\text{sec}^{-1}\text{MeV}^{-1}$ )

Size:  $3 \times 25$  time-varying

particle\_flux>differential\_directional\_number

Energy Bins for R26 H SECT 3 – 11 MeV (3 bins)

LET1\_R26\_SECTORS 0 – 24 (25 bins)

**6.10.1.12 R26B\_He\_SECT\_Flux** He sectored flux R26B ( $\text{cm}^{-2}\text{sr}^{-1}\text{sec}^{-1}(\text{MeV}/\text{nuc})^{-1}$ )

Size:  $3 \times 25$  time-varying

particle\_flux>differential\_directional\_number

Energy Bins for R26 He SECT 3 – 11 MeV/nuc (3 bins)

LET1\_R26\_SECTORS 0 – 24 (25 bins)

**6.10.2 OTHER DATA**

**6.10.2.1 A\_Al** Al counts side A (counts)

Size: 28 time-varying

particle\_flux>differential\_directional\_number\_rate

Energy Bins for Al 1 – 117 MeV/nuc (28 bins)

**6.10.2.2 A\_Al\_Rate** Al count rate side A (counts s<sup>-1</sup>)

Size: 28 time-varying

particle\_flux>differential\_directional\_number\_rate

Energy Bins for Al 1 – 117 MeV/nuc (28 bins)

**6.10.2.3 A\_Ar** Ar counts side A (counts)

Size: 29 time-varying

particle\_flux>differential\_directional\_number\_rate

Energy Bins for Ar 1 – 140 MeV/nuc (29 bins)

**6.10.2.4 A\_Ar\_Rate** Ar count rate side A (counts s<sup>-1</sup>)

Size: 29 time-varying

particle\_flux>differential\_directional\_number\_rate

Energy Bins for Ar 1 – 140 MeV/nuc (29 bins)

**6.10.2.5 A\_C** C counts side A (counts)

Size: 27 time-varying

particle\_flux>differential\_directional\_number\_rate

Energy Bins for C 1 – 99 MeV/nuc (27 bins)

**6.10.2.6 A\_C\_Rate** C count rate side A (counts s<sup>-1</sup>)

Size: 27 time-varying

particle\_flux>differential\_directional\_number\_rate

Energy Bins for C 1 – 99 MeV/nuc (27 bins)

**6.10.2.7 A\_Ca** Ca counts side A (counts)

Size: 30 time-varying

particle\_flux>differential\_directional\_number\_rate

Energy Bins for Ca 1 – 140 MeV/nuc (30 bins)

**6.10.2.8 A\_Ca\_Rate** Ca count rate side A (counts s<sup>-1</sup>)

Size: 30 time-varying

particle\_flux>differential\_directional\_number\_rate

Energy Bins for Ca 1 – 140 MeV/nuc (30 bins)

**6.10.2.9 A\_Cr** Cr counts side A (counts)

Size: 31 time-varying

particle\_flux>differential\_directional\_number\_rate

Energy Bins for Cr 1 – 140 MeV/nuc (31 bins)

**6.10.2.10 A\_Cr\_Rate** Cr count rate side A (counts s<sup>-1</sup>)

Size: 31 time-varying

particle\_flux>differential\_directional\_number\_rate

Energy Bins for Cr 1 – 140 MeV/nuc (31 bins)

**6.10.2.11 A\_Electrons** Electrons counts side A (counts)

Size: 16 time-varying

particle\_flux>differential\_directional\_number\_rate

Energy Bins for Electrons 0 – 6 MeV (16 bins)

**6.10.2.12 A\_Electrons\_Rate** Electrons count rate side A (counts s<sup>-1</sup>)

Size: 16 time-varying

particle\_flux>differential\_directional\_number\_rate

Energy Bins for Electrons 0 – 6 MeV (16 bins)

**6.10.2.13 A\_Fe** Fe counts side A (counts)

Size: 32 time-varying

particle\_flux>differential\_directional\_number\_rate

Energy Bins for Fe 1 – 166 MeV/nuc (32 bins)

**6.10.2.14 A\_Fe\_Rate** Fe count rate side A (counts s<sup>-1</sup>)

Size: 32 time-varying

particle\_flux>differential\_directional\_number\_rate

Energy Bins for Fe 1 – 166 MeV/nuc (32 bins)

**6.10.2.15 A\_H** H counts side A (counts)

Size: 25 time-varying

particle\_flux>differential\_directional\_number\_rate

Energy Bins for H 1 – 41 MeV (25 bins)



**6.10.2.16 A\_H\_Rate** H count rate side A (counts s<sup>-1</sup>)

Size: 25 time-varying

particle\_flux>differential\_directional\_number\_rate

Energy Bins for H 1 – 41 MeV (25 bins)

**6.10.2.17 A\_He** He counts side A (counts)

Size: 26 time-varying

particle\_flux>differential\_directional\_number\_rate

Energy Bins for He 1 – 49 MeV/nuc (26 bins)

**6.10.2.18 A\_He\_Rate** He count rate side A (counts s<sup>-1</sup>)

Size: 26 time-varying

particle\_flux>differential\_directional\_number\_rate

Energy Bins for He 1 – 49 MeV/nuc (26 bins)

**6.10.2.19 A\_Mg** Mg counts side A (counts)

Size: 28 time-varying

particle\_flux>differential\_directional\_number\_rate

Energy Bins for Mg 1 – 117 MeV/nuc (28 bins)

**6.10.2.20 A\_Mg\_Rate** Mg count rate side A (counts s<sup>-1</sup>)

Size: 28 time-varying

particle\_flux>differential\_directional\_number\_rate

Energy Bins for Mg 1 – 117 MeV/nuc (28 bins)

**6.10.2.21 A\_N** N counts side A (counts)

Size: 27 time-varying

particle\_flux>differential\_directional\_number\_rate

Energy Bins for N 1 – 99 MeV/nuc (27 bins)

**6.10.2.22 A\_N\_Rate** N count rate side A (counts s<sup>-1</sup>)

Size: 27 time-varying

particle\_flux>differential\_directional\_number\_rate

Energy Bins for N 1 – 99 MeV/nuc (27 bins)

**6.10.2.23 A\_Na** Na counts side A (counts)

Size: 28 time-varying

particle\_flux>differential\_directional\_number\_rate

Energy Bins for Na 1 – 117 MeV/nuc (28 bins)

**6.10.2.24 A\_Na\_Rate** Na count rate side A (counts s<sup>-1</sup>)

Size: 28 time-varying

particle\_flux>differential\_directional\_number\_rate

Energy Bins for Na 1 – 117 MeV/nuc (28 bins)

**6.10.2.25 A\_Ne** Ne counts side A (counts)

Size: 28 time-varying

particle\_flux>differential\_directional\_number\_rate

Energy Bins for Ne 1 – 117 MeV/nuc (28 bins)

**6.10.2.26 A\_Ne\_Rate** Ne count rate side A (counts s<sup>-1</sup>)

Size: 28 time-varying

particle\_flux>differential\_directional\_number\_rate

Energy Bins for Ne 1 – 117 MeV/nuc (28 bins)

**6.10.2.27 A\_Ni** Ni counts side A (counts)

Size: 33 time-varying

particle\_flux>differential\_directional\_number\_rate

Energy Bins for Ni 1 – 197 MeV/nuc (33 bins)

**6.10.2.28 A\_Ni\_Rate** Ni count rate side A (counts s<sup>-1</sup>)

Size: 33 time-varying

particle\_flux>differential\_directional\_number\_rate

Energy Bins for Ni 1 – 197 MeV/nuc (33 bins)

**6.10.2.29 A\_O** O counts side A (counts)

Size: 28 time-varying

particle\_flux>differential\_directional\_number\_rate

Energy Bins for O 1 – 117 MeV/nuc (28 bins)

**6.10.2.30 A\_O\_Rate** O count rate side A (counts s<sup>-1</sup>)

Size: 28 time-varying

particle\_flux>differential\_directional\_number\_rate

Energy Bins for O 1 – 117 MeV/nuc (28 bins)

**6.10.2.31 A\_S** S counts side A (counts)

Size: 29 time-varying

particle\_flux>differential\_directional\_number\_rate

Energy Bins for S 1 – 140 MeV/nuc (29 bins)

**6.10.2.32 A\_S\_Rate** S count rate side A (counts s<sup>-1</sup>)

Size: 29 time-varying

particle\_flux>differential\_directional\_number\_rate

Energy Bins for S 1 – 140 MeV/nuc (29 bins)

**6.10.2.33 A\_Si** Si counts side A (counts)

Size: 29 time-varying

particle\_flux>differential\_directional\_number\_rate

Energy Bins for Si 1 – 140 MeV/nuc (29 bins)

**6.10.2.34 A\_Si\_Rate** Si count rate side A (counts s<sup>-1</sup>)

Size: 29 time-varying

particle\_flux>differential\_directional\_number\_rate

Energy Bins for Si 1 – 140 MeV/nuc (29 bins)

**6.10.2.35 B\_Al** Al counts side B (counts)

Size: 28 time-varying

particle\_flux>differential\_directional\_number\_rate

Energy Bins for Al 1 – 117 MeV/nuc (28 bins)

**6.10.2.36 B\_Al\_Rate** Al count rate side B (counts s<sup>-1</sup>)

Size: 28 time-varying

particle\_flux>differential\_directional\_number\_rate

Energy Bins for Al 1 – 117 MeV/nuc (28 bins)

**6.10.2.37 B\_Ar** Ar counts side B (counts)

Size: 29 time-varying

particle\_flux>differential\_directional\_number\_rate

Energy Bins for Ar 1 – 140 MeV/nuc (29 bins)

**6.10.2.38 B\_Ar\_Rate** Ar count rate side B (counts s<sup>-1</sup>)

Size: 29 time-varying

particle\_flux>differential\_directional\_number\_rate

Energy Bins for Ar 1 – 140 MeV/nuc (29 bins)

**6.10.2.39 B\_C** C counts side B (counts)

Size: 27 time-varying

particle\_flux>differential\_directional\_number\_rate

Energy Bins for C 1 – 99 MeV/nuc (27 bins)

**6.10.2.40 B\_C\_Rate** C count rate side B (counts s<sup>-1</sup>)

Size: 27 time-varying

particle\_flux>differential\_directional\_number\_rate

Energy Bins for C 1 – 99 MeV/nuc (27 bins)

**6.10.2.41 B\_Ca** Ca counts side B (counts)

Size: 30 time-varying

particle\_flux>differential\_directional\_number\_rate

Energy Bins for Ca 1 – 140 MeV/nuc (30 bins)

**6.10.2.42 B\_Ca\_Rate** Ca count rate side B (counts s<sup>-1</sup>)

Size: 30 time-varying

particle\_flux>differential\_directional\_number\_rate

Energy Bins for Ca 1 – 140 MeV/nuc (30 bins)

**6.10.2.43 B\_Cr** Cr counts side B (counts)

Size: 31 time-varying

particle\_flux>differential\_directional\_number\_rate

Energy Bins for Cr 1 – 140 MeV/nuc (31 bins)

**6.10.2.44 B\_Cr\_Rate** Cr count rate side B (counts s<sup>-1</sup>)

Size: 31 time-varying

particle\_flux>differential\_directional\_number\_rate

Energy Bins for Cr 1 – 140 MeV/nuc (31 bins)

**6.10.2.45 B\_Electrons** Electrons counts side B (counts)

Size: 16 time-varying

particle\_flux>differential\_directional\_number\_rate

Energy Bins for Electrons 0 – 6 MeV (16 bins)

**6.10.2.46 B\_Electrons\_Rate** Electrons count rate side B (counts s<sup>-1</sup>)

Size: 16 time-varying

particle\_flux>differential\_directional\_number\_rate

Energy Bins for Electrons 0 – 6 MeV (16 bins)

**6.10.2.47 B\_Fe** Fe counts side B (counts)

Size: 32 time-varying

particle\_flux>differential\_directional\_number\_rate

Energy Bins for Fe 1 – 166 MeV/nuc (32 bins)

**6.10.2.48 B\_Fe\_Rate** Fe count rate side B (counts s<sup>-1</sup>)

Size: 32 time-varying

particle\_flux>differential\_directional\_number\_rate

Energy Bins for Fe 1 – 166 MeV/nuc (32 bins)

**6.10.2.49 B\_H** H counts side B (counts)

Size: 25 time-varying

particle\_flux>differential\_directional\_number\_rate

Energy Bins for H 1 – 41 MeV (25 bins)

**6.10.2.50 B\_H\_Rate** H count rate side B (counts s<sup>-1</sup>)

Size: 25 time-varying

particle\_flux>differential\_directional\_number\_rate

Energy Bins for H 1 – 41 MeV (25 bins)

**6.10.2.51 B\_He** He counts side B (counts)

Size: 26 time-varying

particle\_flux>differential\_directional\_number\_rate

Energy Bins for He 1 – 49 MeV/nuc (26 bins)

**6.10.2.52 B\_He\_Rate** He count rate side B (counts s<sup>-1</sup>)

Size: 26 time-varying

particle\_flux>differential\_directional\_number\_rate

Energy Bins for He 1 – 49 MeV/nuc (26 bins)

**6.10.2.53 B\_Mg** Mg counts side B (counts)

Size: 28 time-varying

particle\_flux>differential\_directional\_number\_rate

Energy Bins for Mg 1 – 117 MeV/nuc (28 bins)

**6.10.2.54 B\_Mg\_Rate** Mg count rate side B (counts s<sup>-1</sup>)

Size: 28 time-varying

particle\_flux>differential\_directional\_number\_rate

Energy Bins for Mg 1 – 117 MeV/nuc (28 bins)

**6.10.2.55 B\_N** N counts side B (counts)

Size: 27 time-varying

particle\_flux>differential\_directional\_number\_rate

Energy Bins for N 1 – 99 MeV/nuc (27 bins)

**6.10.2.56 B\_N\_Rate** N count rate side B (counts s<sup>-1</sup>)

Size: 27 time-varying

particle\_flux>differential\_directional\_number\_rate

Energy Bins for N 1 – 99 MeV/nuc (27 bins)

**6.10.2.57 B\_Na** Na counts side B (counts)

Size: 28 time-varying

particle\_flux>differential\_directional\_number\_rate

Energy Bins for Na 1 – 117 MeV/nuc (28 bins)

**6.10.2.58 B\_Na\_Rate** Na count rate side B (counts s<sup>-1</sup>)

Size: 28 time-varying

particle\_flux>differential\_directional\_number\_rate

Energy Bins for Na 1 – 117 MeV/nuc (28 bins)

**6.10.2.59 B\_Ne** Ne counts side B (counts)

Size: 28 time-varying

particle\_flux>differential\_directional\_number\_rate

Energy Bins for Ne 1 – 117 MeV/nuc (28 bins)

**6.10.2.60 B\_Ne\_Rate** Ne count rate side B (counts s<sup>-1</sup>)

Size: 28 time-varying

particle\_flux>differential\_directional\_number\_rate

Energy Bins for Ne 1 – 117 MeV/nuc (28 bins)

**6.10.2.61 B\_Ni** Ni counts side B (counts)

Size: 33 time-varying

particle\_flux>differential\_directional\_number\_rate

Energy Bins for Ni 1 – 197 MeV/nuc (33 bins)

**6.10.2.62 B\_Ni\_Rate** Ni count rate side B (counts s<sup>-1</sup>)

Size: 33 time-varying

particle\_flux>differential\_directional\_number\_rate

Energy Bins for Ni 1 – 197 MeV/nuc (33 bins)

**6.10.2.63 B\_O** O counts side B (counts)

Size: 28 time-varying

particle\_flux>differential\_directional\_number\_rate

Energy Bins for O 1 – 117 MeV/nuc (28 bins)

**6.10.2.64 B\_O\_Rate** O count rate side B (counts s<sup>-1</sup>)

Size: 28 time-varying

particle\_flux>differential\_directional\_number\_rate

Energy Bins for O 1 – 117 MeV/nuc (28 bins)

**6.10.2.65 B\_S** S counts side B (counts)

Size: 29 time-varying

particle\_flux>differential\_directional\_number\_rate

Energy Bins for S 1 – 140 MeV/nuc (29 bins)

**6.10.2.66 B\_S\_Rate** S count rate side B (counts s<sup>-1</sup>)

Size: 29 time-varying

particle\_flux>differential\_directional\_number\_rate

Energy Bins for S 1 – 140 MeV/nuc (29 bins)

**6.10.2.67 B\_Si** Si counts side B (counts)

Size: 29 time-varying

particle\_flux>differential\_directional\_number\_rate

Energy Bins for Si 1 – 140 MeV/nuc (29 bins)

**6.10.2.68 B\_Si\_Rate** Si count rate side B (counts s<sup>-1</sup>)

Size: 29 time-varying

particle\_flux>differential\_directional\_number\_rate

Energy Bins for Si 1 – 140 MeV/nuc (29 bins)

**6.10.2.69 HCI\_Lat** HCI latitude (degrees)

time-varying

position>latitude

At timestamp. After Fraenz and Harper, PSS, 2002.

**6.10.2.70 HCI\_Lon** HCI longitude (degrees)

time-varying

position>longitude

At timestamp. After Fraenz and Harper, PSS, 2002.

**6.10.2.71 HCI\_R** Heliocentric distance (AU)

time-varying

position>radial

At timestamp. After Fraenz and Harper, PSS, 2002.



**6.10.2.72 HGC\_Lat** HGC latitude (degrees)  
time-varying  
position>latitude  
At timestamp. After Fraenz and Harper, PSS, 2002.

**6.10.2.73 HGC\_Lon** HGC longitude (degrees)  
time-varying  
position>longitude  
At timestamp. After Fraenz and Harper, PSS, 2002.

**6.10.2.74 HGC\_R** Heliocentric distance (AU)  
time-varying  
position>radial  
At timestamp. After Fraenz and Harper, PSS, 2002.

**6.10.2.75 LET1\_A\_HCI** HCI flow direction LET1A  
Size: 3 time-varying  
position>direction  
Unit vector, after Fraenz and Harper, PSS, 2002.

**6.10.2.76 LET1\_A\_PA** Pitch angle LET1A (degree)  
time-varying  
position>angle

**6.10.2.77 LET1\_A\_R1\_SECT\_HCI** HCI flow direction LET1AR1SECT  
Size:  $9 \times 3$  time-varying  
position>direction  
Unit vector, after Fraenz and Harper, PSS, 2002.  
LET1\_R1\_SECTORS 0 – 8 (9 bins)

**6.10.2.78 LET1\_A\_R1\_SECT\_PA** Pitch angle LET1AR1SECT (degree)  
Size: 9 time-varying  
position>angle  
LET1\_R1\_SECTORS 0 – 8 (9 bins)

**6.10.2.79 LET1\_A\_R1\_SECT\_RTN** RTN flow direction LET1AR1SECT

Size:  $9 \times 3$  time-varying

position>direction

Unit vector, after Fraenz and Harper, PSS, 2002.

LET1\_R1\_SECTORS 0 – 8 (9 bins)

**6.10.2.80 LET1\_A\_R1\_SECT\_SA** Nominal Parker Spiral angle LET1AR1SECT (degree)

Size: 9 time-varying

position>angle

Angle between particle direction and nominal outward Parker Spiral, based on 400km/s solar wind and corotation breakdown at 10Rs.

LET1\_R1\_SECTORS 0 – 8 (9 bins)

**6.10.2.81 LET1\_A\_R26\_SECT\_HCI** HCI flow direction LET1AR26SECT

Size:  $25 \times 3$  time-varying

position>direction

Unit vector, after Fraenz and Harper, PSS, 2002.

LET1\_R26\_SECTORS 0 – 24 (25 bins)

**6.10.2.82 LET1\_A\_R26\_SECT\_PA** Pitch angle LET1AR26SECT (degree)

Size: 25 time-varying

position>angle

LET1\_R26\_SECTORS 0 – 24 (25 bins)

**6.10.2.83 LET1\_A\_R26\_SECT\_RTN** RTN flow direction LET1AR26SECT

Size:  $25 \times 3$  time-varying

position>direction

Unit vector, after Fraenz and Harper, PSS, 2002.

LET1\_R26\_SECTORS 0 – 24 (25 bins)

**6.10.2.84 LET1\_A\_R26\_SECT\_SA** Nominal Parker Spiral angle LET1AR26SECT (degree)

Size: 25 time-varying

position>angle

Angle between particle direction and nominal outward Parker Spiral, based on 400km/s solar wind and corotation breakdown at 10Rs.

LET1\_R26\_SECTORS 0 – 24 (25 bins)

**6.10.2.85 LET1\_A\_RTN** RTN flow direction LET1A

Size: 3 time-varying

position>direction

Unit vector, after Fraenz and Harper, PSS, 2002.

**6.10.2.86 LET1\_A\_SA** Nominal Parker Spiral angle LET1A (degree)

time-varying

position>angle

Angle between particle direction and nominal outward Parker Spiral, based on 400km/s solar wind and corotation breakdown at 10Rs.

**6.10.2.87 LET1\_B\_HCI** HCI flow direction LET1B

Size: 3 time-varying

position>direction

Unit vector, after Fraenz and Harper, PSS, 2002.

**6.10.2.88 LET1\_B\_PA** Pitch angle LET1B (degree)

time-varying

position>angle

**6.10.2.89 LET1\_B\_R1\_SECT\_HCI** HCI flow direction LET1BR1SECT

Size:  $9 \times 3$  time-varying

position>direction

Unit vector, after Fraenz and Harper, PSS, 2002.

LET1\_R1\_SECTORS 0 – 8 (9 bins)

**6.10.2.90 LET1\_B\_R1\_SECT\_PA** Pitch angle LET1BR1SECT (degree)

Size: 9 time-varying

position>angle

LET1\_R1\_SECTORS 0 – 8 (9 bins)

**6.10.2.91 LET1\_B\_R1\_SECT\_RTN** RTN flow direction LET1BR1SECT

Size:  $9 \times 3$  time-varying

position>direction

Unit vector, after Fraenz and Harper, PSS, 2002.

LET1\_R1\_SECTORS 0 – 8 (9 bins)

**6.10.2.92 LET1\_B\_R1\_SECT\_SA** Nominal Parker Spiral angle LET1BR1SECT (degree)

Size: 9 time-varying

position>angle

Angle between particle direction and nominal outward Parker Spiral, based on 400km/s solar wind and corotation breakdown at 10Rs.

LET1\_R1\_SECTORS 0 – 8 (9 bins)

**6.10.2.93 LET1\_B\_R26\_SECT\_HCI** HCI flow direction LET1BR26SECT

Size: 25  $\times$  3 time-varying

position>direction

Unit vector, after Fraenz and Harper, PSS, 2002.

LET1\_R26\_SECTORS 0 – 24 (25 bins)

**6.10.2.94 LET1\_B\_R26\_SECT\_PA** Pitch angle LET1BR26SECT (degree)

Size: 25 time-varying

position>angle

LET1\_R26\_SECTORS 0 – 24 (25 bins)

**6.10.2.95 LET1\_B\_R26\_SECT\_RTN** RTN flow direction LET1BR26SECT

Size: 25  $\times$  3 time-varying

position>direction

Unit vector, after Fraenz and Harper, PSS, 2002.

LET1\_R26\_SECTORS 0 – 24 (25 bins)

**6.10.2.96 LET1\_B\_R26\_SECT\_SA** Nominal Parker Spiral angle LET1BR26SECT (degree)

Size: 25 time-varying

position>angle

Angle between particle direction and nominal outward Parker Spiral, based on 400km/s solar wind and corotation breakdown at 10Rs.

LET1\_R26\_SECTORS 0 – 24 (25 bins)

**6.10.2.97 LET1\_B\_RTN** RTN flow direction LET1B

Size: 3 time-varying

position>direction

Unit vector, after Fraenz and Harper, PSS, 2002.

**6.10.2.98 LET1\_B\_SA** Nominal Parker Spiral angle LET1B (degree)

time-varying

position>angle

Angle between particle direction and nominal outward Parker Spiral, based on 400km/s solar wind and corotation breakdown at 10Rs.

**6.10.2.99 R1A\_H\_SECT\_Rate** H sectored count rate R1A (counts s<sup>-1</sup>)

Size: 1 × 9 time-varying

particle\_flux>differential\_directional\_number\_rate

Energy Bins for R1 H SECT 1 – 1 MeV (1 bins)

LET1\_R1\_SECTORS 0 – 8 (9 bins)

**6.10.2.100 R1A\_He\_SECT\_Rate** He sectored count rate R1A (counts s<sup>-1</sup>)

Size: 1 × 9 time-varying

particle\_flux>differential\_directional\_number\_rate

Energy Bins for R1 He SECT 1 – 1 MeV/nuc (1 bins)

LET1\_R1\_SECTORS 0 – 8 (9 bins)

**6.10.2.101 R1B\_H\_SECT\_Rate** H sectored count rate R1B (counts s<sup>-1</sup>)

Size: 1 × 9 time-varying

particle\_flux>differential\_directional\_number\_rate

Energy Bins for R1 H SECT 1 – 1 MeV (1 bins)

LET1\_R1\_SECTORS 0 – 8 (9 bins)

**6.10.2.102 R1B\_He\_SECT\_Rate** He sectored count rate R1B (counts s<sup>-1</sup>)

Size: 1 × 9 time-varying

particle\_flux>differential\_directional\_number\_rate

Energy Bins for R1 He SECT 1 – 1 MeV/nuc (1 bins)

LET1\_R1\_SECTORS 0 – 8 (9 bins)

**6.10.2.103 R26A\_H\_SECT\_Rate** H sectored count rate R26A (counts s<sup>-1</sup>)

Size: 3 × 25 time-varying

particle\_flux>differential\_directional\_number\_rate

Energy Bins for R26 H SECT 3 – 11 MeV (3 bins)

LET1\_R26\_SECTORS 0 – 24 (25 bins)

**6.10.2.104 R26A\_He\_SECT\_Rate** He sectored count rate R26A (counts s<sup>-1</sup>)

Size: 3 × 25 time-varying

particle\_flux>differential\_directional\_number\_rate

Energy Bins for R26 He SECT 3 – 11 MeV/nuc (3 bins)

LET1\_R26\_SECTORS 0 – 24 (25 bins)

**6.10.2.105 R26B\_H\_SECT\_Rate** H sectored count rate R26B (counts s<sup>-1</sup>)

Size: 3 × 25 time-varying

particle\_flux>differential\_directional\_number\_rate

Energy Bins for R26 H SECT 3 – 11 MeV (3 bins)

LET1\_R26\_SECTORS 0 – 24 (25 bins)

**6.10.2.106 R26B\_He\_SECT\_Rate** He sectored count rate R26B (counts s<sup>-1</sup>)

Size: 3 × 25 time-varying

particle\_flux>differential\_directional\_number\_rate

Energy Bins for R26 He SECT 3 – 11 MeV/nuc (3 bins)

LET1\_R26\_SECTORS 0 – 24 (25 bins)

### 6.10.3 OTHER SUPPORT

**6.10.3.1 Quality\_Flag** Data-quality flag

Size: 10 time-varying

flag>status

Quality flag number 0 – 9 (10 bins)

## 6.11 PSP\_ISOIS-EPIHI\_L2-LET2-RATES10

ISOIS-EPIHI>Integrated Science Investigation of the Sun, Energetic Particle Instrument Hi

L2-LET2-rates10>Level 2 LET2 10-second rates

EPI-Hi 10 second rates cdf. Time tags indicate midpoint of integration.

Instrument paper: Integrated Science Investigation of the Sun (ISIS): Design of the Energetic Particle Investigation. McComas, D. J. et al (2016). Space Sci. Rev., doi:10.1007/s11214-014-0059-1

1 minute to 1 hour

Cite McComas et al (2016), doi:10.1007/s11214-014-0059-1

### 6.11.1 PRIMARY VARIABLES

**6.11.1.1 C\_H\_Flux** H flux side C ( $\text{cm}^{-2}\text{sr}^{-1}\text{sec}^{-1}\text{MeV}^{-1}$ )

Size: 18 time-varying

particle\_flux>differential\_directional\_number

Energy Bins for H 1 – 15 MeV (18 bins)

**6.11.1.2 C\_He\_Flux** He flux side C ( $\text{cm}^{-2}\text{sr}^{-1}\text{sec}^{-1}(\text{MeV}/\text{nuc})^{-1}$ )

Size: 22 time-varying

particle\_flux>differential\_directional\_number

Energy Bins for He 1 – 29 MeV/nuc (22 bins)

### 6.11.2 OTHER DATA

**6.11.2.1 C\_Electrons** Electrons counts side C (counts)

Size: 13 time-varying

particle\_flux>differential\_directional\_number\_rate

Energy Bins for Electrons 1 – 4 MeV (13 bins)

**6.11.2.2 C\_Electrons\_Rate** Electrons count rate side C ( $\text{counts s}^{-1}$ )

Size: 13 time-varying

particle\_flux>differential\_directional\_number\_rate

Energy Bins for Electrons 1 – 4 MeV (13 bins)

**6.11.2.3 C\_H** H counts side C (counts)

Size: 18 time-varying

particle\_flux>differential\_directional\_number\_rate

Energy Bins for H 1 – 15 MeV (18 bins)

**6.11.2.4 C\_H\_Rate** H count rate side C ( $\text{counts s}^{-1}$ )

Size: 18 time-varying

particle\_flux>differential\_directional\_number\_rate

Energy Bins for H 1 – 15 MeV (18 bins)

**6.11.2.5 C\_He** He counts side C (counts)

Size: 22 time-varying

particle\_flux>differential\_directional\_number\_rate

Energy Bins for He 1 – 29 MeV/nuc (22 bins)

**6.11.2.6 C\_He\_Rate** He count rate side C (counts s<sup>-1</sup>)

Size: 22 time-varying

particle\_flux>differential\_directional\_number\_rate

Energy Bins for He 1 – 29 MeV/nuc (22 bins)

**6.11.2.7 HCI\_Lat** HCI latitude (degrees)

time-varying

position>latitude

At timestamp. After Fraenz and Harper, PSS, 2002.

**6.11.2.8 HCI\_Lon** HCI longitude (degrees)

time-varying

position>longitude

At timestamp. After Fraenz and Harper, PSS, 2002.

**6.11.2.9 HCI\_R** Heliocentric distance (AU)

time-varying

position>radial

At timestamp. After Fraenz and Harper, PSS, 2002.

**6.11.2.10 HGC\_Lat** HGC latitude (degrees)

time-varying

position>latitude

At timestamp. After Fraenz and Harper, PSS, 2002.

**6.11.2.11 HGC\_Lon** HGC longitude (degrees)

time-varying

position>longitude

At timestamp. After Fraenz and Harper, PSS, 2002.

**6.11.2.12 HGC\_R** Heliocentric distance (AU)

time-varying



position>radial

At timestamp. After Fraenz and Harper, PSS, 2002.

#### **6.11.2.13 LET2\_C\_HCI** HCI flow direction LET2C

Size: 3 time-varying

position>direction

Unit vector, after Fraenz and Harper, PSS, 2002.

#### **6.11.2.14 LET2\_C\_PA** Pitch angle LET2C (degree)

time-varying

position>angle

#### **6.11.2.15 LET2\_C\_RTN** RTN flow direction LET2C

Size: 3 time-varying

position>direction

Unit vector, after Fraenz and Harper, PSS, 2002.

#### **6.11.2.16 LET2\_C\_SA** Nominal Parker Spiral angle LET2C (degree)

time-varying

position>angle

Angle between particle direction and nominal outward Parker Spiral, based on 400km/s solar wind and corotation breakdown at 10Rs.

### **6.11.3 OTHER SUPPORT**

#### **6.11.3.1 Quality\_Flag** Data-quality flag

Size: 10 time-varying

flag>status

Quality flag number 0 – 9 (10 bins)

## **6.12 PSP\_ISOIS-EPIHI\_L2-LET2-RATES300**

ISOIS-EPIHI>Integrated Science Investigation of the Sun, Energetic Particle Instrument Hi

L2-LET2-rates300>Level 2 LET2 5-minute rates

EPI-Hi LET2 300 second rates cdf. Time tags indicate midpoint of integration.

Instrument paper: Integrated Science Investigation of the Sun (ISIS): Design of the Energetic Particle Investigation. McComas, D. J. et al (2016). Space Sci. Rev., doi:10.1007/s11214-014-0059-1

1 minute to 1 hour

Cite McComas et al (2016), doi:10.1007/s11214-014-0059-1

## **6.12.1 PRIMARY VARIABLES**

### **6.12.2 OTHER DATA**

#### **6.12.2.1 HCI\_Lat** HCI latitude (degrees)

time-varying

position>latitude

At timestamp. After Fraenz and Harper, PSS, 2002.

#### **6.12.2.2 HCI\_Lon** HCI longitude (degrees)

time-varying

position>longitude

At timestamp. After Fraenz and Harper, PSS, 2002.

#### **6.12.2.3 HCI\_R** Heliocentric distance (AU)

time-varying

position>radial

At timestamp. After Fraenz and Harper, PSS, 2002.

#### **6.12.2.4 HGC\_Lat** HGC latitude (degrees)

time-varying

position>latitude

At timestamp. After Fraenz and Harper, PSS, 2002.

#### **6.12.2.5 HGC\_Lon** HGC longitude (degrees)

time-varying

position>longitude

At timestamp. After Fraenz and Harper, PSS, 2002.

#### **6.12.2.6 HGC\_R** Heliocentric distance (AU)

time-varying

position>radial

At timestamp. After Fraenz and Harper, PSS, 2002.

**6.12.2.7 LET2\_C\_HCI** HCI flow direction LET2C

Size: 3 time-varying

position>direction

Unit vector, after Fraenz and Harper, PSS, 2002.

**6.12.2.8 LET2\_C\_PA** Pitch angle LET2C (degree)

time-varying

position>angle

**6.12.2.9 LET2\_C\_R1\_SECT\_HCI** HCI flow direction LET2CR1SECT

Size:  $9 \times 3$  time-varying

position>direction

Unit vector, after Fraenz and Harper, PSS, 2002.

LET2\_R1\_SECTORS 0 – 8 (9 bins)

**6.12.2.10 LET2\_C\_R1\_SECT\_PA** Pitch angle LET2CR1SECT (degree)

Size: 9 time-varying

position>angle

LET2\_R1\_SECTORS 0 – 8 (9 bins)

**6.12.2.11 LET2\_C\_R1\_SECT\_RTN** RTN flow direction LET2CR1SECT

Size:  $9 \times 3$  time-varying

position>direction

Unit vector, after Fraenz and Harper, PSS, 2002.

LET2\_R1\_SECTORS 0 – 8 (9 bins)

**6.12.2.12 LET2\_C\_R1\_SECT\_SA** Nominal Parker Spiral angle LET2CR1SECT (degree)

Size: 9 time-varying

position>angle

Angle between particle direction and nominal outward Parker Spiral, based on 400km/s solar wind and corotation breakdown at 10Rs.

LET2\_R1\_SECTORS 0 – 8 (9 bins)

**6.12.2.13 LET2\_C\_R25\_SECT\_HCI** HCI flow direction LET2CR25SECT

Size:  $25 \times 3$  time-varying

position>direction

Unit vector, after Fraenz and Harper, PSS, 2002.  
LET2\_R25\_SECTORS 0 – 24 (25 bins)

**6.12.2.14 LET2\_C\_R25\_SECT\_PA** Pitch angle LET2CR25SECT (degree)  
Size: 25 time-varying  
position>angle  
LET2\_R25\_SECTORS 0 – 24 (25 bins)

**6.12.2.15 LET2\_C\_R25\_SECT\_RTN** RTN flow direction LET2CR25SECT  
Size: 25 × 3 time-varying  
position>direction  
Unit vector, after Fraenz and Harper, PSS, 2002.  
LET2\_R25\_SECTORS 0 – 24 (25 bins)

**6.12.2.16 LET2\_C\_R25\_SECT\_SA** Nominal Parker Spiral angle LET2CR25SECT (degree)  
Size: 25 time-varying  
position>angle  
Angle between particle direction and nominal outward Parker Spiral, based on 400km/s solar wind and corotation breakdown at 10Rs.  
LET2\_R25\_SECTORS 0 – 24 (25 bins)

**6.12.2.17 LET2\_C\_RTN** RTN flow direction LET2C  
Size: 3 time-varying  
position>direction  
Unit vector, after Fraenz and Harper, PSS, 2002.

**6.12.2.18 LET2\_C\_SA** Nominal Parker Spiral angle LET2C (degree)  
time-varying  
position>angle  
Angle between particle direction and nominal outward Parker Spiral, based on 400km/s solar wind and corotation breakdown at 10Rs.

**6.12.2.19 R1C\_CNO\_SECT\_Rate** CNO sectored count rate R1C (counts s<sup>-1</sup>)  
Size: 1 × 9 time-varying  
particle\_flux>differential\_directional\_number\_rate  
Energy Bins for R1 CNO SECT 3 – 3 MeV/nuc (1 bins)

LET2\_R1\_SECTORS 0 – 8 (9 bins)

**6.12.2.20 R1C\_FeGroup\_SECT\_Rate** FeGroup sectored count rate R1C (counts s<sup>-1</sup>)

Size: 1 × 9 time-varying

particle\_flux>differential\_directional\_number\_rate

Energy Bins for R1 FeGroup SECT 3 – 3 MeV/nuc (1 bins)

LET2\_R1\_SECTORS 0 – 8 (9 bins)

**6.12.2.21 R1C\_NetoSi\_SECT\_Rate** NetoS<sub>i</sub> sectored count rate R1C (counts s<sup>-1</sup>)

Size: 1 × 9 time-varying

particle\_flux>differential\_directional\_number\_rate

Energy Bins for R1 NetoS<sub>i</sub> SECT 3 – 3 MeV/nuc (1 bins)

LET2\_R1\_SECTORS 0 – 8 (9 bins)

**6.12.2.22 R25C\_CNO\_SECT\_Rate** CNO sectored count rate R25C (counts s<sup>-1</sup>)

Size: 3 × 25 time-varying

particle\_flux>differential\_directional\_number\_rate

Energy Bins for R25 CNO SECT 6 – 23 MeV/nuc (3 bins)

LET2\_R25\_SECTORS 0 – 24 (25 bins)

**6.12.2.23 R25C\_FeGroup\_SECT\_Rate** FeGroup sectored count rate R25C (counts s<sup>-1</sup>)

Size: 3 × 25 time-varying

particle\_flux>differential\_directional\_number\_rate

Energy Bins for R25 FeGroup SECT 6 – 23 MeV/nuc (3 bins)

LET2\_R25\_SECTORS 0 – 24 (25 bins)

**6.12.2.24 R25C\_NetoSi\_SECT\_Rate** NetoS<sub>i</sub> sectored count rate R25C (counts s<sup>-1</sup>)

Size: 3 × 25 time-varying

particle\_flux>differential\_directional\_number\_rate

Energy Bins for R25 NetoS<sub>i</sub> SECT 6 – 23 MeV/nuc (3 bins)

LET2\_R25\_SECTORS 0 – 24 (25 bins)

### 6.12.3 OTHER SUPPORT

**6.12.3.1 Quality\_Flag** Data-quality flag

Size: 10 time-varying

flag>status

Quality flag number 0 – 9 (10 bins)

### 6.13 PSP\_ISOIS-EPIHI\_L2-LET2-RATES3600

ISOIS-EPIHI>Integrated Science Investigation of the Sun, Energetic Particle Instrument Hi  
L2-LET2-rates3600>Level 2 LET2 hourly rates

EPI-Hi LET2 3600 second rates cdf. Time tags indicate midpoint of integration.

Instrument paper: Integrated Science Investigation of the Sun (ISIS): Design of the Energetic Particle Investigation. McComas, D. J. et al (2016). Space Sci. Rev., doi:10.1007/s11214-014-0059-1

1 minute to 1 hour

Cite McComas et al (2016), doi:10.1007/s11214-014-0059-1

#### 6.13.1 PRIMARY VARIABLES

##### 6.13.1.1 C\_H\_Flux H flux side C ( $\text{cm}^{-2}\text{sr}^{-1}\text{sec}^{-1}\text{MeV}^{-1}$ )

Size: 24 time-varying

particle\_flux>differential\_directional\_number

Energy Bins for H 1 – 35 MeV (24 bins)

##### 6.13.1.2 C\_He\_Flux He flux side C ( $\text{cm}^{-2}\text{sr}^{-1}\text{sec}^{-1}(\text{MeV}/\text{nuc})^{-1}$ )

Size: 25 time-varying

particle\_flux>differential\_directional\_number

Energy Bins for He 1 – 41 MeV/nuc (25 bins)

##### 6.13.1.3 R1C\_H\_SECT\_Flux H sectored flux R1C ( $\text{cm}^{-2}\text{sr}^{-1}\text{sec}^{-1}\text{MeV}^{-1}$ )

Size:  $1 \times 9$  time-varying

particle\_flux>differential\_directional\_number

Energy Bins for R1 H SECT 1 – 1 MeV (1 bins)

LET2\_R1\_SECTORS 0 – 8 (9 bins)

##### 6.13.1.4 R1C\_He\_SECT\_Flux He sectored flux R1C ( $\text{cm}^{-2}\text{sr}^{-1}\text{sec}^{-1}(\text{MeV}/\text{nuc})^{-1}$ )

Size:  $1 \times 9$  time-varying

particle\_flux>differential\_directional\_number

Energy Bins for R1 He SECT 1 – 1 MeV/nuc (1 bins)

LET2\_R1\_SECTORS 0 – 8 (9 bins)

**6.13.1.5 R25C\_H\_SECT\_Flux** H sectored flux R25C ( $\text{cm}^{-2}\text{sr}^{-1}\text{sec}^{-1}\text{MeV}^{-1}$ )

Size:  $3 \times 25$  time-varying

particle\_flux>differential\_directional\_number

Energy Bins for R25 H SECT 3 – 11 MeV (3 bins)

LET2\_R25\_SECTORS 0 – 24 (25 bins)

**6.13.1.6 R25C\_He\_SECT\_Flux** He sectored flux R25C ( $\text{cm}^{-2}\text{sr}^{-1}\text{sec}^{-1}(\text{MeV}/\text{nuc})^{-1}$ )

Size:  $3 \times 25$  time-varying

particle\_flux>differential\_directional\_number

Energy Bins for R25 He SECT 3 – 11 MeV/nuc (3 bins)

LET2\_R25\_SECTORS 0 – 24 (25 bins)

**6.13.2 OTHER DATA**

**6.13.2.1 C\_Al** Al counts side C (counts)

Size: 27 time-varying

particle\_flux>differential\_directional\_number\_rate

Energy Bins for Al 1 – 99 MeV/nuc (27 bins)

**6.13.2.2 C\_Al\_Rate** Al count rate side C ( $\text{counts s}^{-1}$ )

Size: 27 time-varying

particle\_flux>differential\_directional\_number\_rate

Energy Bins for Al 1 – 99 MeV/nuc (27 bins)

**6.13.2.3 C\_Ar** Ar counts side C (counts)

Size: 28 time-varying

particle\_flux>differential\_directional\_number\_rate

Energy Bins for Ar 1 – 117 MeV/nuc (28 bins)

**6.13.2.4 C\_Ar\_Rate** Ar count rate side C ( $\text{counts s}^{-1}$ )

Size: 28 time-varying

particle\_flux>differential\_directional\_number\_rate

Energy Bins for Ar 1 – 117 MeV/nuc (28 bins)

**6.13.2.5 C\_C** C counts side C (counts)

Size: 25 time-varying

particle\_flux>differential\_directional\_number\_rate

Energy Bins for C 1 – 70 MeV/nuc (25 bins)

**6.13.2.6 C\_C\_Rate** C count rate side C (counts s<sup>-1</sup>)

Size: 25 time-varying

particle\_flux>differential\_directional\_number\_rate

Energy Bins for C 1 – 70 MeV/nuc (25 bins)

**6.13.2.7 C\_Ca** Ca counts side C (counts)

Size: 30 time-varying

particle\_flux>differential\_directional\_number\_rate

Energy Bins for Ca 1 – 140 MeV/nuc (30 bins)

**6.13.2.8 C\_Ca\_Rate** Ca count rate side C (counts s<sup>-1</sup>)

Size: 30 time-varying

particle\_flux>differential\_directional\_number\_rate

Energy Bins for Ca 1 – 140 MeV/nuc (30 bins)

**6.13.2.9 C\_Cr** Cr counts side C (counts)

Size: 31 time-varying

particle\_flux>differential\_directional\_number\_rate

Energy Bins for Cr 1 – 140 MeV/nuc (31 bins)

**6.13.2.10 C\_Cr\_Rate** Cr count rate side C (counts s<sup>-1</sup>)

Size: 31 time-varying

particle\_flux>differential\_directional\_number\_rate

Energy Bins for Cr 1 – 140 MeV/nuc (31 bins)

**6.13.2.11 C\_Electrons** Electrons counts side C (counts)

Size: 16 time-varying

particle\_flux>differential\_directional\_number\_rate

Energy Bins for Electrons 0 – 6 MeV (16 bins)

**6.13.2.12 C\_Electrons\_Rate** Electrons count rate side C (counts s<sup>-1</sup>)

Size: 16 time-varying



particle\_flux>differential\_directional\_number\_rate  
Energy Bins for Electrons 0 – 6 MeV (16 bins)

**6.13.2.13 C\_Fe** Fe counts side C (counts)

Size: 31 time-varying

particle\_flux>differential\_directional\_number\_rate  
Energy Bins for Fe 1 – 140 MeV/nuc (31 bins)

**6.13.2.14 C\_Fe\_Rate** Fe count rate side C (counts s<sup>-1</sup>)

Size: 31 time-varying

particle\_flux>differential\_directional\_number\_rate  
Energy Bins for Fe 1 – 140 MeV/nuc (31 bins)

**6.13.2.15 C\_H** H counts side C (counts)

Size: 24 time-varying

particle\_flux>differential\_directional\_number\_rate  
Energy Bins for H 1 – 35 MeV (24 bins)

**6.13.2.16 C\_H\_Rate** H count rate side C (counts s<sup>-1</sup>)

Size: 24 time-varying

particle\_flux>differential\_directional\_number\_rate  
Energy Bins for H 1 – 35 MeV (24 bins)

**6.13.2.17 C\_He** He counts side C (counts)

Size: 25 time-varying

particle\_flux>differential\_directional\_number\_rate  
Energy Bins for He 1 – 41 MeV/nuc (25 bins)

**6.13.2.18 C\_He\_Rate** He count rate side C (counts s<sup>-1</sup>)

Size: 25 time-varying

particle\_flux>differential\_directional\_number\_rate  
Energy Bins for He 1 – 41 MeV/nuc (25 bins)

**6.13.2.19 C\_Mg** Mg counts side C (counts)

Size: 27 time-varying

particle\_flux>differential\_directional\_number\_rate

Energy Bins for Mg 1 – 99 MeV/nuc (27 bins)

**6.13.2.20 C\_Mg\_Rate** Mg count rate side C (counts s<sup>-1</sup>)

Size: 27 time-varying

particle\_flux>differential\_directional\_number\_rate

Energy Bins for Mg 1 – 99 MeV/nuc (27 bins)

**6.13.2.21 C\_N** N counts side C (counts)

Size: 25 time-varying

particle\_flux>differential\_directional\_number\_rate

Energy Bins for N 1 – 70 MeV/nuc (25 bins)

**6.13.2.22 C\_N\_Rate** N count rate side C (counts s<sup>-1</sup>)

Size: 25 time-varying

particle\_flux>differential\_directional\_number\_rate

Energy Bins for N 1 – 70 MeV/nuc (25 bins)

**6.13.2.23 C\_Na** Na counts side C (counts)

Size: 27 time-varying

particle\_flux>differential\_directional\_number\_rate

Energy Bins for Na 1 – 99 MeV/nuc (27 bins)

**6.13.2.24 C\_Na\_Rate** Na count rate side C (counts s<sup>-1</sup>)

Size: 27 time-varying

particle\_flux>differential\_directional\_number\_rate

Energy Bins for Na 1 – 99 MeV/nuc (27 bins)

**6.13.2.25 C\_Ne** Ne counts side C (counts)

Size: 27 time-varying

particle\_flux>differential\_directional\_number\_rate

Energy Bins for Ne 1 – 99 MeV/nuc (27 bins)

**6.13.2.26 C\_Ne\_Rate** Ne count rate side C (counts s<sup>-1</sup>)

Size: 27 time-varying

particle\_flux>differential\_directional\_number\_rate

Energy Bins for Ne 1 – 99 MeV/nuc (27 bins)

**6.13.2.27 C\_Ni** Ni counts side C (counts)

Size: 32 time-varying

particle\_flux>differential\_directional\_number\_rate

Energy Bins for Ni 1 – 166 MeV/nuc (32 bins)

**6.13.2.28 C\_Ni\_Rate** Ni count rate side C (counts s<sup>-1</sup>)

Size: 32 time-varying

particle\_flux>differential\_directional\_number\_rate

Energy Bins for Ni 1 – 166 MeV/nuc (32 bins)

**6.13.2.29 C\_O** O counts side C (counts)

Size: 26 time-varying

particle\_flux>differential\_directional\_number\_rate

Energy Bins for O 1 – 83 MeV/nuc (26 bins)

**6.13.2.30 C\_O\_Rate** O count rate side C (counts s<sup>-1</sup>)

Size: 26 time-varying

particle\_flux>differential\_directional\_number\_rate

Energy Bins for O 1 – 83 MeV/nuc (26 bins)

**6.13.2.31 C\_S** S counts side C (counts)

Size: 28 time-varying

particle\_flux>differential\_directional\_number\_rate

Energy Bins for S 1 – 117 MeV/nuc (28 bins)

**6.13.2.32 C\_S\_Rate** S count rate side C (counts s<sup>-1</sup>)

Size: 28 time-varying

particle\_flux>differential\_directional\_number\_rate

Energy Bins for S 1 – 117 MeV/nuc (28 bins)

**6.13.2.33 C\_Si** Si counts side C (counts)

Size: 28 time-varying

particle\_flux>differential\_directional\_number\_rate

Energy Bins for Si 1 – 117 MeV/nuc (28 bins)

**6.13.2.34 C\_Si\_Rate** Si count rate side C (counts s<sup>-1</sup>)

Size: 28 time-varying

particle\_flux>differential\_directional\_number\_rate

Energy Bins for Si 1 – 117 MeV/nuc (28 bins)

**6.13.2.35 HCI\_Lat** HCI latitude (degrees)

time-varying

position>latitude

At timestamp. After Fraenz and Harper, PSS, 2002.

**6.13.2.36 HCI\_Lon** HCI longitude (degrees)

time-varying

position>longitude

At timestamp. After Fraenz and Harper, PSS, 2002.

**6.13.2.37 HCI\_R** Heliocentric distance (AU)

time-varying

position>radial

At timestamp. After Fraenz and Harper, PSS, 2002.

**6.13.2.38 HGC\_Lat** HGC latitude (degrees)

time-varying

position>latitude

At timestamp. After Fraenz and Harper, PSS, 2002.

**6.13.2.39 HGC\_Lon** HGC longitude (degrees)

time-varying

position>longitude

At timestamp. After Fraenz and Harper, PSS, 2002.

**6.13.2.40 HGC\_R** Heliocentric distance (AU)

time-varying

position>radial

At timestamp. After Fraenz and Harper, PSS, 2002.

**6.13.2.41 LET2\_C\_HCI** HCI flow direction LET2C

Size: 3 time-varying

position>direction

Unit vector, after Fraenz and Harper, PSS, 2002.

**6.13.2.42 LET2\_C\_PA** Pitch angle LET2C (degree)

time-varying

position>angle

**6.13.2.43 LET2\_C\_R1\_SECT\_HCI** HCI flow direction LET2CR1SECT

Size:  $9 \times 3$  time-varying

position>direction

Unit vector, after Fraenz and Harper, PSS, 2002.

LET2\_R1\_SECTORS 0 – 8 (9 bins)

**6.13.2.44 LET2\_C\_R1\_SECT\_PA** Pitch angle LET2CR1SECT (degree)

Size: 9 time-varying

position>angle

LET2\_R1\_SECTORS 0 – 8 (9 bins)

**6.13.2.45 LET2\_C\_R1\_SECT\_RTN** RTN flow direction LET2CR1SECT

Size:  $9 \times 3$  time-varying

position>direction

Unit vector, after Fraenz and Harper, PSS, 2002.

LET2\_R1\_SECTORS 0 – 8 (9 bins)

**6.13.2.46 LET2\_C\_R1\_SECT\_SA** Nominal Parker Spiral angle LET2CR1SECT (degree)

Size: 9 time-varying

position>angle

Angle between particle direction and nominal outward Parker Spiral, based on 400km/s solar wind and corotation breakdown at 10Rs.

LET2\_R1\_SECTORS 0 – 8 (9 bins)

**6.13.2.47 LET2\_C\_R25\_SECT\_HCI** HCI flow direction LET2CR25SECT

Size: 25 × 3 time-varying

position>direction

Unit vector, after Fraenz and Harper, PSS, 2002.

LET2\_R25\_SECTORS 0 – 24 (25 bins)

**6.13.2.48 LET2\_C\_R25\_SECT\_PA** Pitch angle LET2CR25SECT (degree)

Size: 25 time-varying

position>angle

LET2\_R25\_SECTORS 0 – 24 (25 bins)

**6.13.2.49 LET2\_C\_R25\_SECT\_RTN** RTN flow direction LET2CR25SECT

Size: 25 × 3 time-varying

position>direction

Unit vector, after Fraenz and Harper, PSS, 2002.

LET2\_R25\_SECTORS 0 – 24 (25 bins)

**6.13.2.50 LET2\_C\_R25\_SECT\_SA** Nominal Parker Spiral angle LET2CR25SECT (degree)

Size: 25 time-varying

position>angle

Angle between particle direction and nominal outward Parker Spiral, based on 400km/s solar wind and corotation breakdown at 10Rs.

LET2\_R25\_SECTORS 0 – 24 (25 bins)

**6.13.2.51 LET2\_C\_RTN** RTN flow direction LET2C

Size: 3 time-varying

position>direction

Unit vector, after Fraenz and Harper, PSS, 2002.

**6.13.2.52 LET2\_C\_SA** Nominal Parker Spiral angle LET2C (degree)

time-varying

position>angle

Angle between particle direction and nominal outward Parker Spiral, based on 400km/s solar wind

and corotation breakdown at 10Rs.

**6.13.2.53 R1C\_CNO\_SECT\_Rate** CNO sectored count rate R1C (counts s<sup>-1</sup>)

Size: 1 × 9 time-varying

particle\_flux>differential\_directional\_number\_rate

Energy Bins for R1 CNO SECT 3 – 3 MeV/nuc (1 bins)

LET2\_R1\_SECTORS 0 – 8 (9 bins)

**6.13.2.54 R1C\_FeGroup\_SECT\_Rate** FeGroup sectored count rate R1C (counts s<sup>-1</sup>)

Size: 1 × 9 time-varying

particle\_flux>differential\_directional\_number\_rate

Energy Bins for R1 FeGroup SECT 3 – 3 MeV/nuc (1 bins)

LET2\_R1\_SECTORS 0 – 8 (9 bins)

**6.13.2.55 R1C\_H\_SECT\_Rate** H sectored count rate R1C (counts s<sup>-1</sup>)

Size: 1 × 9 time-varying

particle\_flux>differential\_directional\_number\_rate

Energy Bins for R1 H SECT 1 – 1 MeV (1 bins)

LET2\_R1\_SECTORS 0 – 8 (9 bins)

**6.13.2.56 R1C\_He\_BIN** R1C He Rates (counts)

Size: 5 × 16 time-varying

particle\_flux>differential\_directional\_number\_rate

Energy Bins for R1 He BIN 1 – 3 MeV/nuc (5 bins)

R1C\_He\_BIN\_MASS\_BIN 0 – 15 segment (16 bins)

**6.13.2.57 R1C\_He\_SECT\_Rate** He sectored count rate R1C (counts s<sup>-1</sup>)

Size: 1 × 9 time-varying

particle\_flux>differential\_directional\_number\_rate

Energy Bins for R1 He SECT 1 – 1 MeV/nuc (1 bins)

LET2\_R1\_SECTORS 0 – 8 (9 bins)

**6.13.2.58 R1C\_Ne\_BIN** R1C Ne Rates (counts)

Size: 5 × 8 time-varying

particle\_flux>differential\_directional\_number\_rate

Energy Bins for R1 Ne BIN 1 – 6 MeV/nuc (5 bins)

R1C\_Ne\_BIN\_MASS\_BIN 0 – 7 segment (8 bins)

**6.13.2.59 R1C\_NetoSi\_SECT\_Rate** NetoS<sub>i</sub> sectored count rate R1C (counts s<sup>-1</sup>)

Size: 1 × 9 time-varying

particle\_flux>differential\_directional\_number\_rate

Energy Bins for R1 NetoS<sub>i</sub> SECT 3 – 3 MeV/nuc (1 bins)

LET2\_R1\_SECTORS 0 – 8 (9 bins)

**6.13.2.60 R25C\_CNO\_SECT\_Rate** CNO sectored count rate R25C (counts s<sup>-1</sup>)

Size: 3 × 25 time-varying

particle\_flux>differential\_directional\_number\_rate

Energy Bins for R25 CNO SECT 6 – 23 MeV/nuc (3 bins)

LET2\_R25\_SECTORS 0 – 24 (25 bins)

**6.13.2.61 R25C\_FeGroup\_SECT\_Rate** FeGroup sectored count rate R25C (counts s<sup>-1</sup>)

Size: 3 × 25 time-varying

particle\_flux>differential\_directional\_number\_rate

Energy Bins for R25 FeGroup SECT 6 – 23 MeV/nuc (3 bins)

LET2\_R25\_SECTORS 0 – 24 (25 bins)

**6.13.2.62 R25C\_H\_SECT\_Rate** H sectored count rate R25C (counts s<sup>-1</sup>)

Size: 3 × 25 time-varying

particle\_flux>differential\_directional\_number\_rate

Energy Bins for R25 H SECT 3 – 11 MeV (3 bins)

LET2\_R25\_SECTORS 0 – 24 (25 bins)

**6.13.2.63 R25C\_He\_SECT\_Rate** He sectored count rate R25C (counts s<sup>-1</sup>)

Size: 3 × 25 time-varying

particle\_flux>differential\_directional\_number\_rate

Energy Bins for R25 He SECT 3 – 11 MeV/nuc (3 bins)

LET2\_R25\_SECTORS 0 – 24 (25 bins)

**6.13.2.64 R25C\_NetoSi\_SECT\_Rate** NetoS<sub>i</sub> sectored count rate R25C (counts s<sup>-1</sup>)

Size: 3 × 25 time-varying

particle\_flux>differential\_directional\_number\_rate

Energy Bins for R25 NetoS<sub>i</sub> SECT 6 – 23 MeV/nuc (3 bins)



LET2\_R25\_SECTORS 0 – 24 (25 bins)

**6.13.2.65 R2C\_He\_BIN** R2C He Rates (counts)

Size:  $7 \times 16$  time-varying

particle\_flux>differential\_directional\_number\_rate

Energy Bins for R2 He BIN 2 – 16 MeV/nuc (7 bins)

R2C\_He\_BIN\_MASS\_BIN 0 – 15 segment (16 bins)

**6.13.2.66 R2C\_Ne\_BIN** R2C Ne Rates (counts)

Size:  $8 \times 8$  time-varying

particle\_flux>differential\_directional\_number\_rate

Energy Bins for R2 Ne BIN 3 – 32 MeV/nuc (8 bins)

R2C\_Ne\_BIN\_MASS\_BIN 0 – 7 segment (8 bins)

**6.13.2.67 R3C\_He\_BIN** R3C He Rates (counts)

Size:  $5 \times 16$  time-varying

particle\_flux>differential\_directional\_number\_rate

Energy Bins for R3 He BIN 8 – 32 MeV/nuc (5 bins)

R3C\_He\_BIN\_MASS\_BIN 0 – 15 segment (16 bins)

**6.13.2.68 R3C\_Ne\_BIN** R3C Ne Rates (counts)

Size:  $6 \times 8$  time-varying

particle\_flux>differential\_directional\_number\_rate

Energy Bins for R3 Ne BIN 16 – 91 MeV/nuc (6 bins)

R3C\_Ne\_BIN\_MASS\_BIN 0 – 7 segment (8 bins)

**6.13.2.69 R45C\_He\_BIN** R45C He Rates (counts)

Size:  $5 \times 16$  time-varying

particle\_flux>differential\_directional\_number\_rate

Energy Bins for R45 He BIN 8 – 32 MeV/nuc (5 bins)

R45C\_He\_BIN\_MASS\_BIN 0 – 15 segment (16 bins)

**6.13.2.70 R45C\_Ne\_BIN** R45C Ne Rates (counts)

Size:  $6 \times 8$  time-varying

particle\_flux>differential\_directional\_number\_rate

Energy Bins for R45 Ne BIN 16 – 91 MeV/nuc (6 bins)

R45C\_Ne\_BIN\_MASS\_BIN 0 – 7 segment (8 bins)

### 6.13.3 OTHER SUPPORT

#### 6.13.3.1 Quality\_Flag Data-quality flag

Size: 10 time-varying

flag>status

Quality flag number 0 – 9 (10 bins)

## 6.14 PSP\_ISOIS-EPIHI\_L2-LET2-RATES60

ISOIS-EPIHI>Integrated Science Investigation of the Sun, Energetic Particle Instrument Hi  
L2-LET2-rates60>Level 2 LET2 1-minute rates

EPI-Hi LET2 60 second rates cdf. Time tags indicate midpoint of integration.

Instrument paper: Integrated Science Investigation of the Sun (ISIS): Design of the Energetic Particle Investigation. McComas, D. J. et al (2016). Space Sci. Rev., doi:10.1007/s11214-014-0059-1

1 minute to 1 hour

Cite McComas et al (2016), doi:10.1007/s11214-014-0059-1

### 6.14.1 PRIMARY VARIABLES

#### 6.14.1.1 C\_H\_Flux H flux side C ( $\text{cm}^{-2}\text{sr}^{-1}\text{sec}^{-1}\text{MeV}^{-1}$ )

Size: 24 time-varying

particle\_flux>differential\_directional\_number

Energy Bins for H 1 – 35 MeV (24 bins)

#### 6.14.1.2 C\_He\_Flux He flux side C ( $\text{cm}^{-2}\text{sr}^{-1}\text{sec}^{-1}(\text{MeV}/\text{nuc})^{-1}$ )

Size: 25 time-varying

particle\_flux>differential\_directional\_number

Energy Bins for He 1 – 41 MeV/nuc (25 bins)

#### 6.14.1.3 R1C\_H\_SECT\_Flux H sector flux R1C ( $\text{cm}^{-2}\text{sr}^{-1}\text{sec}^{-1}\text{MeV}^{-1}$ )

Size:  $1 \times 9$  time-varying

particle\_flux>differential\_directional\_number

Energy Bins for R1 H SECT 1 – 1 MeV (1 bins)

LET2\_R1\_SECTORS 0 – 8 (9 bins)

**6.14.1.4 R1C\_He\_SECT\_Flux** He sectored flux R1C ( $\text{cm}^{-2}\text{sr}^{-1}\text{sec}^{-1}(\text{MeV}/\text{nuc})^{-1}$ )

Size:  $1 \times 9$  time-varying

particle\_flux>differential\_directional\_number

Energy Bins for R1 He SECT 1 – 1 MeV/nuc (1 bins)

LET2\_R1\_SECTORS 0 – 8 (9 bins)

**6.14.1.5 R25C\_H\_SECT\_Flux** H sectored flux R25C ( $\text{cm}^{-2}\text{sr}^{-1}\text{sec}^{-1}\text{MeV}^{-1}$ )

Size:  $3 \times 25$  time-varying

particle\_flux>differential\_directional\_number

Energy Bins for R25 H SECT 3 – 11 MeV (3 bins)

LET2\_R25\_SECTORS 0 – 24 (25 bins)

**6.14.1.6 R25C\_He\_SECT\_Flux** He sectored flux R25C ( $\text{cm}^{-2}\text{sr}^{-1}\text{sec}^{-1}(\text{MeV}/\text{nuc})^{-1}$ )

Size:  $3 \times 25$  time-varying

particle\_flux>differential\_directional\_number

Energy Bins for R25 He SECT 3 – 11 MeV/nuc (3 bins)

LET2\_R25\_SECTORS 0 – 24 (25 bins)

**6.14.2 OTHER DATA**

**6.14.2.1 C\_Al** Al counts side C (counts)

Size: 27 time-varying

particle\_flux>differential\_directional\_number\_rate

Energy Bins for Al 1 – 99 MeV/nuc (27 bins)

**6.14.2.2 C\_Al\_Rate** Al count rate side C ( $\text{counts s}^{-1}$ )

Size: 27 time-varying

particle\_flux>differential\_directional\_number\_rate

Energy Bins for Al 1 – 99 MeV/nuc (27 bins)

**6.14.2.3 C\_Ar** Ar counts side C (counts)

Size: 28 time-varying

particle\_flux>differential\_directional\_number\_rate

Energy Bins for Ar 1 – 117 MeV/nuc (28 bins)

**6.14.2.4 C\_Ar\_Rate** Ar count rate side C ( $\text{counts s}^{-1}$ )

Size: 28 time-varying

particle\_flux>differential\_directional\_number\_rate  
Energy Bins for Ar 1 – 117 MeV/nuc (28 bins)

**6.14.2.5 C\_C** C counts side C (counts)

Size: 25 time-varying

particle\_flux>differential\_directional\_number\_rate  
Energy Bins for C 1 – 70 MeV/nuc (25 bins)

**6.14.2.6 C\_C\_Rate** C count rate side C (counts s<sup>-1</sup>)

Size: 25 time-varying

particle\_flux>differential\_directional\_number\_rate  
Energy Bins for C 1 – 70 MeV/nuc (25 bins)

**6.14.2.7 C\_Ca** Ca counts side C (counts)

Size: 30 time-varying

particle\_flux>differential\_directional\_number\_rate  
Energy Bins for Ca 1 – 140 MeV/nuc (30 bins)

**6.14.2.8 C\_Ca\_Rate** Ca count rate side C (counts s<sup>-1</sup>)

Size: 30 time-varying

particle\_flux>differential\_directional\_number\_rate  
Energy Bins for Ca 1 – 140 MeV/nuc (30 bins)

**6.14.2.9 C\_Cr** Cr counts side C (counts)

Size: 31 time-varying

particle\_flux>differential\_directional\_number\_rate  
Energy Bins for Cr 1 – 140 MeV/nuc (31 bins)

**6.14.2.10 C\_Cr\_Rate** Cr count rate side C (counts s<sup>-1</sup>)

Size: 31 time-varying

particle\_flux>differential\_directional\_number\_rate  
Energy Bins for Cr 1 – 140 MeV/nuc (31 bins)

**6.14.2.11 C\_Electrons** Electrons counts side C (counts)

Size: 16 time-varying

particle\_flux>differential\_directional\_number\_rate

Energy Bins for Electrons 0 – 6 MeV (16 bins)

**6.14.2.12 C\_Electrons\_Rate** Electrons count rate side C (counts s<sup>-1</sup>)

Size: 16 time-varying

particle\_flux>differential\_directional\_number\_rate

Energy Bins for Electrons 0 – 6 MeV (16 bins)

**6.14.2.13 C\_Fe** Fe counts side C (counts)

Size: 31 time-varying

particle\_flux>differential\_directional\_number\_rate

Energy Bins for Fe 1 – 140 MeV/nuc (31 bins)

**6.14.2.14 C\_Fe\_Rate** Fe count rate side C (counts s<sup>-1</sup>)

Size: 31 time-varying

particle\_flux>differential\_directional\_number\_rate

Energy Bins for Fe 1 – 140 MeV/nuc (31 bins)

**6.14.2.15 C\_H** H counts side C (counts)

Size: 24 time-varying

particle\_flux>differential\_directional\_number\_rate

Energy Bins for H 1 – 35 MeV (24 bins)

**6.14.2.16 C\_H\_Rate** H count rate side C (counts s<sup>-1</sup>)

Size: 24 time-varying

particle\_flux>differential\_directional\_number\_rate

Energy Bins for H 1 – 35 MeV (24 bins)

**6.14.2.17 C\_He** He counts side C (counts)

Size: 25 time-varying

particle\_flux>differential\_directional\_number\_rate

Energy Bins for He 1 – 41 MeV/nuc (25 bins)

**6.14.2.18 C\_He\_Rate** He count rate side C (counts s<sup>-1</sup>)

Size: 25 time-varying

particle\_flux>differential\_directional\_number\_rate

Energy Bins for He 1 – 41 MeV/nuc (25 bins)

**6.14.2.19 C\_Mg** Mg counts side C (counts)

Size: 27 time-varying

particle\_flux>differential\_directional\_number\_rate

Energy Bins for Mg 1 – 99 MeV/nuc (27 bins)

**6.14.2.20 C\_Mg\_Rate** Mg count rate side C (counts s<sup>-1</sup>)

Size: 27 time-varying

particle\_flux>differential\_directional\_number\_rate

Energy Bins for Mg 1 – 99 MeV/nuc (27 bins)

**6.14.2.21 C\_N** N counts side C (counts)

Size: 25 time-varying

particle\_flux>differential\_directional\_number\_rate

Energy Bins for N 1 – 70 MeV/nuc (25 bins)

**6.14.2.22 C\_N\_Rate** N count rate side C (counts s<sup>-1</sup>)

Size: 25 time-varying

particle\_flux>differential\_directional\_number\_rate

Energy Bins for N 1 – 70 MeV/nuc (25 bins)

**6.14.2.23 C\_Na** Na counts side C (counts)

Size: 27 time-varying

particle\_flux>differential\_directional\_number\_rate

Energy Bins for Na 1 – 99 MeV/nuc (27 bins)

**6.14.2.24 C\_Na\_Rate** Na count rate side C (counts s<sup>-1</sup>)

Size: 27 time-varying

particle\_flux>differential\_directional\_number\_rate

Energy Bins for Na 1 – 99 MeV/nuc (27 bins)

**6.14.2.25 C\_Ne** Ne counts side C (counts)

Size: 27 time-varying

particle\_flux>differential\_directional\_number\_rate

Energy Bins for Ne 1 – 99 MeV/nuc (27 bins)

**6.14.2.26 C\_Ne\_Rate** Ne count rate side C (counts s<sup>-1</sup>)

Size: 27 time-varying

particle\_flux>differential\_directional\_number\_rate

Energy Bins for Ne 1 – 99 MeV/nuc (27 bins)

**6.14.2.27 C\_Ni** Ni counts side C (counts)

Size: 32 time-varying

particle\_flux>differential\_directional\_number\_rate

Energy Bins for Ni 1 – 166 MeV/nuc (32 bins)

**6.14.2.28 C\_Ni\_Rate** Ni count rate side C (counts s<sup>-1</sup>)

Size: 32 time-varying

particle\_flux>differential\_directional\_number\_rate

Energy Bins for Ni 1 – 166 MeV/nuc (32 bins)

**6.14.2.29 C\_O** O counts side C (counts)

Size: 26 time-varying

particle\_flux>differential\_directional\_number\_rate

Energy Bins for O 1 – 83 MeV/nuc (26 bins)

**6.14.2.30 C\_O\_Rate** O count rate side C (counts s<sup>-1</sup>)

Size: 26 time-varying

particle\_flux>differential\_directional\_number\_rate

Energy Bins for O 1 – 83 MeV/nuc (26 bins)

**6.14.2.31 C\_S** S counts side C (counts)

Size: 28 time-varying

particle\_flux>differential\_directional\_number\_rate

Energy Bins for S 1 – 117 MeV/nuc (28 bins)

**6.14.2.32 C\_S\_Rate** S count rate side C (counts s<sup>-1</sup>)

Size: 28 time-varying

particle\_flux>differential\_directional\_number\_rate

Energy Bins for S 1 – 117 MeV/nuc (28 bins)

**6.14.2.33 C\_Si** Si counts side C (counts)

Size: 28 time-varying

particle\_flux>differential\_directional\_number\_rate

Energy Bins for Si 1 – 117 MeV/nuc (28 bins)

**6.14.2.34 C\_Si\_Rate** Si count rate side C (counts s<sup>-1</sup>)

Size: 28 time-varying

particle\_flux>differential\_directional\_number\_rate

Energy Bins for Si 1 – 117 MeV/nuc (28 bins)

**6.14.2.35 HCI\_Lat** HCI latitude (degrees)

time-varying

position>latitude

At timestamp. After Fraenz and Harper, PSS, 2002.

**6.14.2.36 HCI\_Lon** HCI longitude (degrees)

time-varying

position>longitude

At timestamp. After Fraenz and Harper, PSS, 2002.

**6.14.2.37 HCI\_R** Heliocentric distance (AU)

time-varying

position>radial

At timestamp. After Fraenz and Harper, PSS, 2002.

**6.14.2.38 HGC\_Lat** HGC latitude (degrees)

time-varying

position>latitude

At timestamp. After Fraenz and Harper, PSS, 2002.



**6.14.2.39 HGC\_Lon** HGC longitude (degrees)

time-varying

position>longitude

At timestamp. After Fraenz and Harper, PSS, 2002.

**6.14.2.40 HGC\_R** Heliocentric distance (AU)

time-varying

position>radial

At timestamp. After Fraenz and Harper, PSS, 2002.

**6.14.2.41 LET2\_C\_HCI** HCI flow direction LET2C

Size: 3 time-varying

position>direction

Unit vector, after Fraenz and Harper, PSS, 2002.

**6.14.2.42 LET2\_C\_PA** Pitch angle LET2C (degree)

time-varying

position>angle

**6.14.2.43 LET2\_C\_R1\_SECT\_HCI** HCI flow direction LET2CR1SECT

Size:  $9 \times 3$  time-varying

position>direction

Unit vector, after Fraenz and Harper, PSS, 2002.

LET2\_R1\_SECTORS 0 – 8 (9 bins)

**6.14.2.44 LET2\_C\_R1\_SECT\_PA** Pitch angle LET2CR1SECT (degree)

Size: 9 time-varying

position>angle

LET2\_R1\_SECTORS 0 – 8 (9 bins)

**6.14.2.45 LET2\_C\_R1\_SECT\_RTN** RTN flow direction LET2CR1SECT

Size:  $9 \times 3$  time-varying

position>direction

Unit vector, after Fraenz and Harper, PSS, 2002.

LET2\_R1\_SECTORS 0 – 8 (9 bins)

**6.14.2.46 LET2\_C\_R1\_SECT\_SA** Nominal Parker Spiral angle LET2CR1SECT (degree)

Size: 9 time-varying

position>angle

Angle between particle direction and nominal outward Parker Spiral, based on 400km/s solar wind and corotation breakdown at 10Rs.

LET2\_R1\_SECTORS 0 – 8 (9 bins)

**6.14.2.47 LET2\_C\_R25\_SECT\_HCI** HCI flow direction LET2CR25SECT

Size: 25 × 3 time-varying

position>direction

Unit vector, after Fraenz and Harper, PSS, 2002.

LET2\_R25\_SECTORS 0 – 24 (25 bins)

**6.14.2.48 LET2\_C\_R25\_SECT\_PA** Pitch angle LET2CR25SECT (degree)

Size: 25 time-varying

position>angle

LET2\_R25\_SECTORS 0 – 24 (25 bins)

**6.14.2.49 LET2\_C\_R25\_SECT\_RTN** RTN flow direction LET2CR25SECT

Size: 25 × 3 time-varying

position>direction

Unit vector, after Fraenz and Harper, PSS, 2002.

LET2\_R25\_SECTORS 0 – 24 (25 bins)

**6.14.2.50 LET2\_C\_R25\_SECT\_SA** Nominal Parker Spiral angle LET2CR25SECT (degree)

Size: 25 time-varying

position>angle

Angle between particle direction and nominal outward Parker Spiral, based on 400km/s solar wind and corotation breakdown at 10Rs.

LET2\_R25\_SECTORS 0 – 24 (25 bins)

**6.14.2.51 LET2\_C\_RTN** RTN flow direction LET2C

Size: 3 time-varying

position>direction

Unit vector, after Fraenz and Harper, PSS, 2002.

**6.14.2.52 LET2\_C\_SA** Nominal Parker Spiral angle LET2C (degree)

time-varying

position>angle

Angle between particle direction and nominal outward Parker Spiral, based on 400km/s solar wind and corotation breakdown at 10Rs.

**6.14.2.53 RIC\_H\_SECT\_Rate** H sectored count rate RIC (counts s<sup>-1</sup>)

Size: 1 × 9 time-varying

particle\_flux>differential\_directional\_number\_rate

Energy Bins for R1 H SECT 1 – 1 MeV (1 bins)

LET2\_R1\_SECTORS 0 – 8 (9 bins)

**6.14.2.54 RIC\_He\_SECT\_Rate** He sectored count rate RIC (counts s<sup>-1</sup>)

Size: 1 × 9 time-varying

particle\_flux>differential\_directional\_number\_rate

Energy Bins for R1 He SECT 1 – 1 MeV/nuc (1 bins)

LET2\_R1\_SECTORS 0 – 8 (9 bins)

**6.14.2.55 R25C\_H\_SECT\_Rate** H sectored count rate R25C (counts s<sup>-1</sup>)

Size: 3 × 25 time-varying

particle\_flux>differential\_directional\_number\_rate

Energy Bins for R25 H SECT 3 – 11 MeV (3 bins)

LET2\_R25\_SECTORS 0 – 24 (25 bins)

**6.14.2.56 R25C\_He\_SECT\_Rate** He sectored count rate R25C (counts s<sup>-1</sup>)

Size: 3 × 25 time-varying

particle\_flux>differential\_directional\_number\_rate

Energy Bins for R25 He SECT 3 – 11 MeV/nuc (3 bins)

LET2\_R25\_SECTORS 0 – 24 (25 bins)

**6.14.3 OTHER SUPPORT**

**6.14.3.1 Quality\_Flag** Data-quality flag

Size: 10 time-varying

flag>status

Quality flag number 0 – 9 (10 bins)

## 6.15 PSP\_ISOIS-EPIHI\_L2-SECOND-RATES

ISOIS-EPIHI>Integrated Science Investigation of the Sun, Energetic Particle Instrument Hi  
L2-second-rates>Level 2 one-second rates

EPI-Hi second rates cdf. Time tags indicate time of collection.

Instrument paper: Integrated Science Investigation of the Sun (ISIS): Design of the Energetic Particle Investigation. McComas, D. J. et al (2016). Space Sci. Rev., doi:10.1007/s11214-014-0059-1

1 minute to 1 hour

Cite McComas et al (2016), doi:10.1007/s11214-014-0059-1

### 6.15.1 PRIMARY VARIABLES

#### 6.15.2 OTHER DATA

##### 6.15.2.1 HCI\_Lat HCI latitude (degrees)

time-varying

position>latitude

At timestamp. After Fraenz and Harper, PSS, 2002.

##### 6.15.2.2 HCI\_Lon HCI longitude (degrees)

time-varying

position>longitude

At timestamp. After Fraenz and Harper, PSS, 2002.

##### 6.15.2.3 HCI\_R Heliocentric distance (AU)

time-varying

position>radial

At timestamp. After Fraenz and Harper, PSS, 2002.

##### 6.15.2.4 HET\_A\_Electrons HET A-side electron rates (counts)

Size: 3 time-varying

particle\_flux>differential\_directional\_number\_rate

Energy Bins for HET Electrons 1 – 3 MeV (3 bins)

##### 6.15.2.5 HET\_A\_Electrons\_Rate Electrons rate HET A (counts s<sup>-1</sup>)

Size: 3 time-varying

particle\_flux>differential\_directional\_number\_rate

Energy Bins for HET Electrons 1 – 3 MeV (3 bins)

**6.15.2.6 HET\_A\_H** HET A-side hydrogen rates (counts)

Size: 2 time-varying

particle\_flux>differential\_directional\_number\_rate

Energy Bins for HET H 12 – 23 MeV (2 bins)

**6.15.2.7 HET\_A\_HCI** HCI flow direction HETA

Size: 3 time-varying

position>direction

Unit vector, after Fraenz and Harper, PSS, 2002.

**6.15.2.8 HET\_A\_H\_Rate** H rate HET A (counts s<sup>-1</sup>)

Size: 2 time-varying

particle\_flux>differential\_directional\_number\_rate

Energy Bins for HET H 12 – 23 MeV (2 bins)

**6.15.2.9 HET\_A\_PA** Pitch angle HETA (degree)

time-varying

position>angle

**6.15.2.10 HET\_A\_RTN** RTN flow direction HETA

Size: 3 time-varying

position>direction

Unit vector, after Fraenz and Harper, PSS, 2002.

**6.15.2.11 HET\_A\_SA** Nominal Parker Spiral angle HETA (degree)

time-varying

position>angle

Angle between particle direction and nominal outward Parker Spiral, based on 400km/s solar wind and corotation breakdown at 10Rs.

**6.15.2.12 HET\_B\_Electrons** HET B-side electron rates (counts)

Size: 3 time-varying

particle\_flux>differential\_directional\_number\_rate

Energy Bins for HET Electrons 1 – 3 MeV (3 bins)

**6.15.2.13 HET\_B\_Electrons\_Rate** Electrons rate HET B (counts s<sup>-1</sup>)

Size: 3 time-varying

particle\_flux>differential\_directional\_number\_rate

Energy Bins for HET Electrons 1 – 3 MeV (3 bins)

**6.15.2.14 HET\_B\_H** HET B-side hydrogen rates (counts)

Size: 2 time-varying

particle\_flux>differential\_directional\_number\_rate

Energy Bins for HET H 12 – 23 MeV (2 bins)

**6.15.2.15 HET\_B\_HCI** HCl flow direction HETB

Size: 3 time-varying

position>direction

Unit vector, after Fraenz and Harper, PSS, 2002.

**6.15.2.16 HET\_B\_H\_Rate** H rate HET B (counts s<sup>-1</sup>)

Size: 2 time-varying

particle\_flux>differential\_directional\_number\_rate

Energy Bins for HET H 12 – 23 MeV (2 bins)

**6.15.2.17 HET\_B\_PA** Pitch angle HETB (degree)

time-varying

position>angle

**6.15.2.18 HET\_B\_RTN** RTN flow direction HETB

Size: 3 time-varying

position>direction

Unit vector, after Fraenz and Harper, PSS, 2002.

**6.15.2.19 HET\_B\_SA** Nominal Parker Spiral angle HETB (degree)

time-varying

position>angle

Angle between particle direction and nominal outward Parker Spiral, based on 400km/s solar wind and corotation breakdown at 10Rs.

**6.15.2.20 HGC\_Lat** HGC latitude (degrees)  
time-varying  
position>latitude  
At timestamp. After Fraenz and Harper, PSS, 2002.

**6.15.2.21 HGC\_Lon** HGC longitude (degrees)  
time-varying  
position>longitude  
At timestamp. After Fraenz and Harper, PSS, 2002.

**6.15.2.22 HGC\_R** Heliocentric distance (AU)  
time-varying  
position>radial  
At timestamp. After Fraenz and Harper, PSS, 2002.

**6.15.2.23 LET1\_A\_Electrons** LET1 A-side electron rates (counts)  
Size: 2 time-varying  
particle\_flux>differential\_directional\_number\_rate  
Energy Bins for LET Electrons 1 – 1 MeV (2 bins)

**6.15.2.24 LET1\_A\_Electrons\_Rate** Electrons rate LET1 A (counts s<sup>-1</sup>)  
Size: 2 time-varying  
particle\_flux>differential\_directional\_number\_rate  
Energy Bins for LET Electrons 1 – 1 MeV (2 bins)

**6.15.2.25 LET1\_A\_H** LET1 A-side hydrogen rates (counts)  
Size: 3 time-varying  
particle\_flux>differential\_directional\_number\_rate  
Energy Bins for LET H 2 – 10 MeV (3 bins)

**6.15.2.26 LET1\_A\_HCI** HCI flow direction LET1A  
Size: 3 time-varying  
position>direction  
Unit vector, after Fraenz and Harper, PSS, 2002.

**6.15.2.27 LET1\_A\_H\_Rate** H rate LET1 A (counts s<sup>-1</sup>)

Size: 3 time-varying

particle\_flux>differential\_directional\_number\_rate

Energy Bins for LET H 2 – 10 MeV (3 bins)

**6.15.2.28 LET1\_A\_PA** Pitch angle LET1A (degree)

time-varying

position>angle

**6.15.2.29 LET1\_A\_RTN** RTN flow direction LET1A

Size: 3 time-varying

position>direction

Unit vector, after Fraenz and Harper, PSS, 2002.

**6.15.2.30 LET1\_A\_SA** Nominal Parker Spiral angle LET1A (degree)

time-varying

position>angle

Angle between particle direction and nominal outward Parker Spiral, based on 400km/s solar wind and corotation breakdown at 10Rs.

**6.15.2.31 LET1\_B\_Electrons** LET1 B-side electron rates (counts)

Size: 2 time-varying

particle\_flux>differential\_directional\_number\_rate

Energy Bins for LET Electrons 1 – 1 MeV (2 bins)

**6.15.2.32 LET1\_B\_Electrons\_Rate** Electrons rate LET1 B (counts s<sup>-1</sup>)

Size: 2 time-varying

particle\_flux>differential\_directional\_number\_rate

Energy Bins for LET Electrons 1 – 1 MeV (2 bins)

**6.15.2.33 LET1\_B\_H** LET1 B-side hydrogen rates (counts)

Size: 3 time-varying

particle\_flux>differential\_directional\_number\_rate

Energy Bins for LET H 2 – 10 MeV (3 bins)



**6.15.2.34 LET1\_B\_HCI** HCI flow direction LET1B

Size: 3 time-varying

position>direction

Unit vector, after Fraenz and Harper, PSS, 2002.

**6.15.2.35 LET1\_B\_H\_Rate** H rate LET1 B (counts s<sup>-1</sup>)

Size: 3 time-varying

particle\_flux>differential\_directional\_number\_rate

Energy Bins for LET H 2 – 10 MeV (3 bins)

**6.15.2.36 LET1\_B\_PA** Pitch angle LET1B (degree)

time-varying

position>angle

**6.15.2.37 LET1\_B\_RTN** RTN flow direction LET1B

Size: 3 time-varying

position>direction

Unit vector, after Fraenz and Harper, PSS, 2002.

**6.15.2.38 LET1\_B\_SA** Nominal Parker Spiral angle LET1B (degree)

time-varying

position>angle

Angle between particle direction and nominal outward Parker Spiral, based on 400km/s solar wind and corotation breakdown at 10Rs.

**6.15.2.39 LET2\_C\_Electrons** LET2 C-side electron rates (counts)

Size: 2 time-varying

particle\_flux>differential\_directional\_number\_rate

Energy Bins for LET Electrons 1 – 1 MeV (2 bins)

**6.15.2.40 LET2\_C\_Electrons\_Rate** Electrons rate LET2 C (counts s<sup>-1</sup>)

Size: 2 time-varying

particle\_flux>differential\_directional\_number\_rate

Energy Bins for LET Electrons 1 – 1 MeV (2 bins)

**6.15.2.41 LET2\_C\_H** LET2 C-side hydrogen rates (counts)

Size: 3 time-varying

particle\_flux>differential\_directional\_number\_rate

Energy Bins for LET H 2 – 10 MeV (3 bins)

**6.15.2.42 LET2\_C\_HCI** HCI flow direction LET2C

Size: 3 time-varying

position>direction

Unit vector, after Fraenz and Harper, PSS, 2002.

**6.15.2.43 LET2\_C\_H\_Rate** H rate LET2 C (counts s<sup>-1</sup>)

Size: 3 time-varying

particle\_flux>differential\_directional\_number\_rate

Energy Bins for LET H 2 – 10 MeV (3 bins)

**6.15.2.44 LET2\_C\_PA** Pitch angle LET2C (degree)

time-varying

position>angle

**6.15.2.45 LET2\_C\_RTN** RTN flow direction LET2C

Size: 3 time-varying

position>direction

Unit vector, after Fraenz and Harper, PSS, 2002.

**6.15.2.46 LET2\_C\_SA** Nominal Parker Spiral angle LET2C (degree)

time-varying

position>angle

Angle between particle direction and nominal outward Parker Spiral, based on 400km/s solar wind and corotation breakdown at 10Rs.

**6.15.3 OTHER SUPPORT**

**6.15.3.1 Quality\_Flag** Data-quality flag

Size: 10 time-varying

flag>status

Quality flag number 0 – 9 (10 bins)

## 6.16 PSP\_ISOIS\_L2-EPHEM

ISOIS>Integrated Science Investigation of the Sun

L2-ephem>Level 2 ephem

Instrument paper: Integrated Science Investigation of the Sun (ISIS): Design of the Energetic Particle Investigation. McComas, D. J. et al (2016). Space Sci. Rev., doi:10.1007/s11214-014-0059-1

1 minute to 1 hour

Cite McComas et al (2016), doi:10.1007/s11214-014-0059-1

### 6.16.1 PRIMARY VARIABLES

#### 6.16.2 OTHER DATA

**6.16.2.1 Clock\_Angle** angle of off-pointing from ecliptic north when not in encounter (degrees)

time-varying

position>angle

Angle (around +R axis) between SC +Z projected into the TN plane and +N axis. Nominally zero (roughly ecliptic north). Ascends CCW (right-handed) despite the name, so positive values are toward -T (opposite ram) and negative towards +T (into ram). Undefined (fill) if Sun Angle is small.

**6.16.2.2 HCI\_Lat** HCI latitude (degrees)

time-varying

position>latitude

At timestamp. After Fraenz and Harper, PSS, 2002.

**6.16.2.3 HCI\_Lon** HCI longitude (degrees)

time-varying

position>longitude

At timestamp. After Fraenz and Harper, PSS, 2002.

**6.16.2.4 HCI\_R** Heliocentric distance (AU)

time-varying

position>radial

At timestamp. After Fraenz and Harper, PSS, 2002.

**6.16.2.5 HGC\_Lat** HGC latitude (degrees)

time-varying

position>latitude

At timestamp. After Fraenz and Harper, PSS, 2002.

**6.16.2.6 HGC\_Lon** HGC longitude (degrees)

time-varying

position>longitude

At timestamp. After Fraenz and Harper, PSS, 2002.

**6.16.2.7 HGC\_R** Heliocentric distance (AU)

time-varying

position>radial

At timestamp. After Fraenz and Harper, PSS, 2002.

**6.16.2.8 Ram\_Pointing** Spacecraft is ram pointing

time-varying

flag>status

1 if roll angle is small, and either sun angle or clock angle are small (pointing into ram).

**6.16.2.9 Roll\_Angle** Angle between nominal ram and actual ram, 0 in encounter (degrees)

time-varying

position>angle

Angle between s/c +X and RTN +T. Positive if s/c +X is towards +N (roughly ecliptic north); right-handed in RTN.

**6.16.2.10 Spiral\_HETA** HETA look angle with nominal parker spiral (degrees)

time-varying

position>angle

Angle between +Z HETA frame and nominal parker spiral assuming constant 400 km/s solar wind speed and a corotation boundary of 20 solar radii

**6.16.2.11 Spiral\_LET1A** LET1A look angle with nominal parker spiral (degrees)

time-varying

position>angle

Angle between +Z LET1A frame and nominal parker spiral assuming constant 400 km/s solar wind speed and a corotation boundary of 20 solar radii

**6.16.2.12 Spiral\_LET2C** LET2C look angle with nominal parker spiral (degrees)

time-varying

position>angle

Angle between +Z LET2C frame and nominal parker spiral assuming constant 400 km/s solar wind speed and a corotation boundary of 20 solar radii

**6.16.2.13 Spiral\_Lo** Lo look angle with nominal parker spiral (degrees)

time-varying

position>angle

Angle between +Z Lo frame (look directions x9) and nominal parker spiral assuming constant 400 km/s solar wind speed and a corotation boundry of 20 solar radii

**6.16.2.14 Sun\_Angle** Angle between TPS and Sun, 0 in encounter (degrees)

time-varying

position>angle

Angle between s/c +Z and RTN -R. Always positive.

**6.16.2.15 Umbra\_Pointing** Spacecraft is umbra pointing

time-varying

flag>status

1 (nominal for encounter) if Sun angle = 0 else 0

**6.16.3 OTHER SUPPORT**

**6.17 PSP\_ISOIS\_L2-SUMMARY**

ISOIS>Integrated Science Investigation of the Sun

L2-Summary>level 2 summary

EPI-Hi HET 3600 second rates cdf. Time tags indicate midpoint of integration.

Instrument paper: Integrated Science Investigation of the Sun (ISIS): Design of the Energetic Particle Investigation. McComas, D. J. et al (2016). Space Sci. Rev., doi:10.1007/s11214-014-0059-1

EPI-Hi 3600 seconds rates cdf. Time tags indicate midpoint of integration.

EPI-Lo, Ion Composition mode.

EPI-Lo, Particle Energy mode.

1 minute to 1 hour

Cite McComas et al (2016), doi:10.1007/s11214-014-0059-1

### 6.17.1 PRIMARY VARIABLES

#### 6.17.2 OTHER DATA

**6.17.2.1 A\_H\_Rate\_TS** H count rate side A 2-10MeV (counts s<sup>-1</sup>)

time-varying

particle\_flux>differential\_directional\_number\_rate

**6.17.2.2 A\_Heavy\_Rate\_TS** Heavy (6<=z<=28) ion count rate side A 4-40 MeV/nuc (counts s<sup>-1</sup>)

time-varying

particle\_flux>differential\_directional\_number\_rate

**6.17.2.3 Electron\_CountRate\_ChanE** Electron count rate channel E (HiResElectrons) (counts/sec)

Size: 48 time-varying

particle\_flux>differential\_directional\_number\_rate

Particle Energy mode. Corrected for deadtime. May contain substantial non-electron background.

Electron\_ChanE\_Energy 12 – 9065 keV (32 bins)

**6.17.2.4 HET\_A\_Electrons\_Rate\_TS** HET Electrons count rate side A 1-5MeV (counts s<sup>-1</sup>)

time-varying

particle\_flux>differential\_directional\_number\_rate

**6.17.2.5 HET\_A\_H\_Rate\_TS** HET H count rate side A 10-50MeV (counts s<sup>-1</sup>)

time-varying

particle\_flux>differential\_directional\_number\_rate

**6.17.2.6 H\_CountRate\_ChanP\_SP** H count rate channel P (HiResProtons) (counts/sec)

Size: 48 time-varying

particle\_flux>differential\_directional\_number\_rate

Ion Composition mode. Corrected for deadtime.

H\_ChanP\_Energy 70 – 9464 keV (39 bins)

### 6.17.3 OTHER SUPPORT

## 7 ACRONYMS

For detailed information on the various [coordinate systems](#), refer to [Franz and Harper \(2002\)](#).

**ApID:** Application Identifier  
**EPI-Lo:** Energetic Particle Instrument - Low Energy  
**EPI-Hi:** Energetic Particle - High Energy  
**FOV:** Field of View  
**GSE:** Geocentric Solar Ecliptic  
**GSM:** Geocentric Solar Magnetospheric  
**HGC:** Heliographic Coordinates  
**HAE:** Heliocentric Aries Ecliptic  
**HCI:** Heliocentric Inertial  
**HEE:** Heliocentric Earth Ecliptic  
**HEEQ:** Heliocentric Earth Equatorial  
**IC:** Ion Composition  
**IE:** Ion Energy  
**IS $\odot$ IS:** Integrated Science Investigations of the Sun  
**PC:** Particle Composition  
**PE:** Particle Energy  
**PSP:** Parker Solar Probe  
**RTN:** Heliocentric  
**TAI:** International Atomic Time, defined by SI seconds  
**TOF:** Time of Flight  
**TPS:** Thermal Protection System  
**UTC:** Coordinated Universal Time

## REFERENCES

- McComas, D., et al. (2016). Integrated science Investigation of the Sun (ISIS): Design of the Energetic Particle Investigation. *SSRv*, 204:187–256. DOI 10.1007/s11214-014-0059-1.
- Hill, M., et al. (2019). in preparation.
- Szalay, J., et al. (2019). in preparation.
- Franz, M. and D. Harper (2002). Heliospheric Coordinate Systems. *Plan.Space Sci.*, 50, 217–233.